

Department of Biomedical Sciences  
University of Veterinary Medicine Vienna

Institute of Pharmacology and Toxicology  
Head: Univ.-Prof. Dr.med.univ. Veronika Sexl

# Novel functions of Cyclin-dependent kinase 8 (CDK8) in Tumorigenesis and Tumor Immune Surveillance

PhD thesis submitted for the fulfilment of the requirements for the degree of

**DOCTOR OF PHILOSOPHY (PhD)**

University of Veterinary Medicine Vienna

submitted by

**Vanessa-Maria Knab, MSc.**

Vienna, March 2022

## **PhD committee**

### **1<sup>st</sup> PhD Advisor**

**Mag.rer.nat. Priv.-Doz<sup>in</sup> Andrea Hölbl-Kovacic, PhD**

Department of Biomedical Sciences  
Institute of Pharmacology and Toxicology  
University of Veterinary Medicine Vienna

### **2<sup>nd</sup> PhD Advisor**

**Mag.rer.nat. Dr.rer.nat. Birgit Strobl**

Department of Biomedical Sciences  
Institute of Animal Breeding and Genetics  
University of Veterinary Medicine Vienna

### **1<sup>st</sup> PhD Advisor from 2016 to 2019**

***Ass.-Prof. Dr.med.vet. Priv.-Doz<sup>in</sup> Daniela FUX***

*Department of Biomedical Sciences  
Institute of Pharmacology and Toxicology  
University of Veterinary Medicine Vienna*

### **Additional Supervisor**

**Univ.-Prof. Dr.med.univ. Veronika SEXL**

Department of Biomedical Sciences  
Institute of Pharmacology and Toxicology  
University of Veterinary Medicine Vienna

## Publication List

**Knab VM**, Gotthardt D, Klein K, Menzl I, Prinz D, Trifinopoulos J, List J, Fux D, Witalisz-Siepracka A, Sexl V. Triple-negative breast cancer cells rely on kinase-independent functions of CDK8 to evade NK-cell-mediated tumor surveillance. *Cell Death & Disease* (2021) Oct 23;12(11):991. doi: 10.1038/s41419-021-04279-2. Impact factor: 8.469

Menzl I, Zhang T, Berger-Becvar A, Grausenburger R, Heller G, Prchal-Murphy M, Edlinger L, **Knab VM**, Uras IZ, Grunderschober E, Bauer K, Roth M, Skucha A, Liu Y, Hatcher JM, Liang Y, Kwiatkowski NP, Fux D, Hoelbl-Kovacic A, Kubicek S, Melo JV, Valent P, Weichhart T, Grebien F, Zuber J, Gray NS, Sexl V. A kinase-independent role for CDK8 in BCR-ABL1<sup>+</sup> leukemia. *Nature Communications* (2019) Oct 18;10(1):4741. doi: 10.1038/s41467-019-12656-x. Impact Factor: 14.919

### List of publications not included in this PhD thesis:

Schmalzbauer BS, Thondanpillil T, Heller G, Schirripa A, Sperl CM, Mayer IM, **Knab VM**, Nebenfuhr S, Mueller AC, Fontaine F, Zojer M, Klampfl T, Sexl V, Kollmann K. CDK6 degradation is counteracted by p16<sup>INK4A</sup> and p18<sup>INK4C</sup> in AML. *Cancers* (2022) *accepted*. Impact Factor: 6.639

Kollmann S, Grausenburger R, Klampfl T, Prchal-Murphy M, Bastl K, Pisa H, **Knab VM**, Brandstoetter T, Doma E, Sperr WR, Lagger S, Farlik M, Moriggl RH, Valent P, Halbritter F, Kollmann K, Heller G, Maurer B, Sexl V. A STAT5B-CD9 axis determines self-renewal in hematopoietic and leukemic stem cells. *Blood* (2021) Jul 28:blood.2021010980. doi: 10.1182/blood.2021010980. Impact Factor: 22.113

Klein K, Witalisz-Siepracka A, Gotthardt D, Agerer B, Locker F, Grausenburger R, **Knab VM**, Bergthaler A, Sexl V. T Cell-Intrinsic CDK6 Is Dispensable for Anti-Viral and Anti-Tumor Responses *In Vivo*. *Frontiers in Immunology* (2021) Jun 24;12:650977. doi: 10.3389/fimmu.2021.650977. Impact Factor: 6.429

Tripolt S, Neubauer HA, **Knab VM**, Elmer DP, Aberger F, Moriggl R, Fux DA. Opioids drive breast cancer metastasis through the  $\delta$ -opioid receptor and oncogenic STAT3. *Neoplasia* (2021) 23, 270-279. Impact Factor: 5.715

Prinz D, Klein K, List J, **Knab VM**, Menzl I, Leidenfrost N, Heller G, Polic B, Putz EM, Witalisz-Siepracka A, Sexl V, Gotthardt D. Loss of NKG2D in murine NK cells leads to increased perforin production upon long-term stimulation with IL-2. *European Journal of Immunology* (2020) Jun;50(6):880-890. doi: 10.1002/eji.201948222. Impact Factor 2019: 4.225

Schoos A, **Knab VM**, Cordula G, Tripolt S, Wagner D, Bauder B, Url A, Fux D. In-vitro study to assess the efficacy of CDK4/6 inhibitor Palbociclib (PD-0332991) for treating canine mammary tumours. *Veterinary and Comparative Oncology* (2019) Dec;17(4):507-521. doi: 10.1111/vco.12514. Impact Factor: 2.107

Schoos A, Gabriel C, **Knab VM**, Fux DA. Activation of HIF-1 $\alpha$  by  $\delta$ -Opioid Receptors Induces COX-2 Expression in Breast Cancer Cells and Leads to Paracrine Activation of Vascular Endothelial Cells. *The Journal of Pharmacology and Experimental Therapeutics* (2019) Sep;370(3):480-489. doi: 10.1124/jpet.119.257501. Impact Factor: 3.594



## **Acknowledgments**

First and foremost, I would like to thank Veronika Sexl for the opportunity to work on such an interesting project, for always challenging me and for constant support which helped me a lot to improve my scientific skills. I would also like to acknowledge my supervisor Daniela Fux for her great support and supervision during the first years of my PhD.

Great thanks go to my PhD committee members Andrea Hölbl-Kovacic and Birgit Strobl for their scientific input and discussion and to all the co-authors for their support.

I also want to thank all the current and former colleagues within the Sexl group. It was always a pleasure to work in such a friendly and motivating atmosphere and I am grateful for all the scientific and technical help as well as for our funny after-work activities.

My very special thanks go to my boyfriend Dominik for being always there to listen, support me and to cheer me up. Finally, I want to thank my family and friends for their support.

## **Declaration**

I, Vanessa Maria Knab, declare that I performed and authored the PhD thesis entitled “Novel functions of Cyclin-dependent kinase 8 (CDK8) in Tumorigenesis and Tumor Immune Surveillance” independently, following the guidelines of good scientific practice.

The majority of experiments presented in this thesis were performed at the University of Veterinary Medicine, Institute of Pharmacology and Toxicology (Veterinaerplatz 1, 1210 Vienna, Austria). Contributions of others, ethics approvals and funding are indicated clearly in the manuscripts arising from this thesis (chapter 2).

## **Copyright**

Copyrights and license agreements for the figures used in this thesis were obtained via Copyright Clearance Center and license numbers are depicted in the figure legends. Otherwise, permission is granted for fair use by the Creative Commons Attribution License.

## Table of contents

<b>PUBLICATION LIST</b> .....	<b>III</b>
<b>ACKNOWLEDGMENTS</b> .....	<b>V</b>
<b>DECLARATION</b> .....	<b>VI</b>
<b>COPYRIGHT</b> .....	<b>VI</b>
<b>TABLE OF CONTENTS</b> .....	<b>VII</b>
<b>LIST OF FIGURES</b> .....	<b>IX</b>
<b>LIST OF TABLES</b> .....	<b>IX</b>
<b>SUMMARY</b> .....	<b>X</b>
<b>ZUSAMMENFASSUNG</b> .....	<b>XI</b>
<b>ABBREVIATIONS</b> .....	<b>XIII</b>
<b>1. INTRODUCTION</b> .....	<b>1</b>
1.1. Cyclin-dependent kinases (CDKs).....	1
1.1.1. Cell cycle regulation by CDKs.....	2
1.1.2. Transcriptional regulation by CDKs.....	4
1.1.3. Cyclin-dependent kinase 8 (CDK8).....	5
CDK8 in solid tumors.....	8
CDK8 in leukemia.....	11
CDK8 in tumor surveillance.....	12
CDK8/CDK19-specific inhibitors.....	14
1.2. Breast cancer.....	16
1.2.1. Classification.....	16
1.2.2. Treatment.....	18
Non-metastatic breast cancer.....	18
Metastatic breast cancer.....	20
1.2.3. Triple-negative breast cancer (TNBC).....	21

Tumorigenesis .....	22
1.3. Philadelphia Chromosome-Positive Leukemia .....	24
1.3.1. Chronic myeloid leukemia (CML) .....	25
1.3.2. Acute lymphoblastic leukemia (ALL) .....	26
1.3.3. Treatment .....	27
ATP-competitive inhibitors .....	27
Allosteric inhibitors.....	29
1.4. Tumor immune surveillance .....	31
1.4.1. Cancer immunoediting .....	32
1.4.2. The innate and adaptive immune system .....	35
Recognition of cancer cells .....	36
1.4.3. Natural killer (NK) cell mediated tumor immune surveillance .....	37
1.4.4. NK cells in the immunosurveillance of metastasis .....	40
<b>2.    MANUSCRIPTS.....</b>	<b>43</b>
2.1. Prologue .....	43
2.1.1. Triple-negative breast cancer cells rely on kinase-independent functions of CDK8 to evade NK-cell-mediated tumor surveillance .....	44
2.2. Prologue .....	61
2.2.1. A kinase-independent role for CDK8 in BCR-ABL1 <sup>+</sup> leukemia.....	62
<b>3.    DISCUSSION AND CONCLUSION .....</b>	<b>87</b>
<b>4.    REFERENCES .....</b>	<b>92</b>

## List of Figures

Figure 1: Biological functions of CDK complexes. ....	1
Figure 2: Human CDK subfamilies and their evolutionary relationship. ....	2
Figure 3: Cell cycle progression by CDKs. ....	3
Figure 4: Regulation of transcription by CDKs.....	4
Figure 5: The Mediator complex. ....	6
Figure 6: CDK8 regulates metastatic growth in the liver. ....	11
Figure 7: Physiological and pathological functions of CDK8.....	14
Figure 8: WHO statistics on Cancer worldwide. ....	16
Figure 9: Molecular subtypes of triple-negative breast cancer.....	21
Figure 10: Main signal transduction pathways in TNBC tumorigenesis. ....	22
Figure 11: Chromosomal translocation and BCR-ABL protein isotypes.....	24
Figure 12: The triphasic course of CML. ....	26
Figure 13: BCR-ABL inhibition strategies. ....	27
Figure 14: List of approved ATP-competitive inhibitors. ....	28
Figure 15: Cancer immunoediting. ....	34
Figure 16: The innate and adaptive immune response.....	35
Figure 17: Mechanisms of cancer recognition by the innate and adaptive immune system. .	37
Figure 18: Biological functions of natural killer cells. ....	38
Figure 19: NK cell effector functions. ....	39
Figure 20: Immunosurveillance of Metastasis by NK Cells. ....	42

## List of Tables

Table 1: Clinical trials using CDK8/CDK19 inhibitors.....	15
Table 2: Overview of different molecular subtypes of breast cancer.....	17
Table 3: Therapeutic options for different breast cancer subtypes. ....	19

## Summary

Cyclin-dependent kinases (CDKs) are serine/threonine kinases that are frequently deregulated in cancer and represent promising therapeutic targets. CDK8 and its close homolog CDK19 were initially reported to exert transcriptional functions, relying on binding of cyclin C for kinase activity and subsequent binding to the mediator complex. Over the last decades we learned that CDK8 has a lot more functions. The CDK8 submodule can directly phosphorylate signaling molecules including members of the JAK-STAT pathway, TGF- $\beta$  and BMP receptor signaling. In tumorigenesis, CDK8 has been identified as an oncogenic driver in various cancer types, including colorectal cancer, melanoma, breast cancer and hematological malignancies. In contrast, tumor suppressing roles were identified, so its functions seem to be divergent and highly context-dependent.

In this thesis, novel functions of CDK8 in the tumorigenesis of triple-negative breast cancer and BCR-ABL-positive leukemia have been studied and identified.

We demonstrate an essential role for CDK8 in regulating the invasiveness and metastatic capacity of highly aggressive and metastatic triple-negative breast cancer cells, as observed in *in vivo* experiments and differential gene expression analysis. Our *in vitro* and *in vivo* experiments further uncovered an essential function of CDK8 in tumor immune surveillance. In TNBC cells, we found that CDK8 is a crucial regulator of natural killer (NK)-cell-mediated immune evasion by regulating crucial immune checkpoints including the expression of PD-L1. We pioneered and uncovered a CDK8-PD-L1 axis.

In the second part, we could assign a critical role to CDK8 in BCR-ABL-positive leukemia and provide a potential therapeutic point of attack for acute lymphoblastic leukemia (ALL). Our findings identify CDK8 as a key mediator of leukemia maintenance. Transcriptomic and correlation analyses in human datasets identified a connection of CDK8 and the mTOR signaling pathway and led us to apply a small molecule, which inhibits mTOR and simultaneously degrades the CDK8 protein. We showed successful reduction of viability of human leukemic cell lines and primary patient cells upon treatment with this small molecule, suggesting a new promising treatment avenue.

In summary, my studies add novel and highly relevant pieces to the big puzzle on finding candidates for targeted therapies and allow us to closer understand functions and mechanisms of CDK8-driven tumorigenesis and tumor immune surveillance. The studies further

demonstrate CDK8 as a new promising drug target, which might in future help us to cure fatal diseases.

## Zusammenfassung

Cyclin-abhängige Kinasen (CDKs) sind Serin/Threonin-Proteinkinasen, die häufig in Krebserkrankungen dereguliert sind und vielversprechende therapeutische Ansatzpunkte darstellen. CDK8 wurde als erkrankungsinduzierendes Onkogen in einer Reihe von Tumorarten beschrieben (u.a. Kolorektalkrebs, Melanom, Brustkrebs und hämatologischen Krebserkrankungen). Konträr dazu, wurden auch Funktionen als Tumorsuppressor identifiziert. Die Funktionen von CDK8 scheinen somit divergent und stark kontextabhängig zu sein.

CDK8 und ihr Homolog CDK19 wurden ursprünglich in der Regulation der Transkription beschrieben. Sie benötigen die Bindung von Cyclin C um ihre Funktion als Kinase auszuüben und in einem weiteren Schritt den Mediator Komplex zu binden. In den letzten Jahren wurde zunehmend bekannt, dass CDK8 jedoch deutlich vielfältigere Funktionen besitzt. Das CDK8-Untermolekül kann direkt Signalmoleküle phosphorylieren, unter anderem im JAK-STAT, TGF- $\beta$  und BMP Rezeptor Signalweg.

Diese Dissertation fokussiert auf triple-negativen Brustkrebs und BCR-ABL positive Leukämie und analysiert, identifiziert und bewertet neue Funktionen von CDK8 in der Tumorentstehung.

Anhand von *in vivo* Experimenten und differentieller Genexpressionsanalyse zeigen wir eine essenzielle Rolle von CDK8 in der Regulation der Invasivität und der metastatischen Fähigkeit von hoch-aggressivem und metastatischem triple-negativem Brustkrebs auf. Unsere Ergebnisse aus *in vitro* und *in vivo* Experimenten enthüllen kritische Funktionen von CDK8 in der Immunüberwachung des Tumors. In triple-negativem Brustkrebs erweist sich CDK8 als Modulator der Immunevasion vor natürlichen Killerzellen (NK-Zellen). Diese Evasion erfolgt, indem CDK8 wesentliche Immuncheckpoints reguliert, unter anderem PD-L1. Wir konnten somit erstmals eine CDK8-PD-L1 Achse identifizieren.

In dem zweiten Teil dieser Dissertation finden wir eine essentielle Rolle für CDK8 in BCR-ABL positiven Leukämien und zeigen einen neuen therapeutischen Ansatz für die Behandlung von ALL Patienten auf. Unsere Ergebnisse ordnen CDK8 eine Schlüsselrolle in der Aufrechterhaltung der Leukämien zu. Analysen des Transkriptom und Korrelationen mit humanen Datensätzen zeigen einen Zusammenhang zwischen CDK8 und dem mTOR

Signalweg auf. Basierend auf dieser Erkenntnis, bedienen wir uns eines „small molecules“, welches mTOR hemmt und gleichzeitig den Abbau des CDK8 Proteins induziert. Wir beweisen, dass die Behandlung von humanen Leukämie Zelllinien und primären Patientenproben zur Reduktion der Viabilität führt.

Zusammenfassend stellen meine Ergebnisse neue und wesentliche Teile eines größeren Puzzles dar, welches darauf abzielt passende Kandidaten für zielgerichtete Therapieansätze aufzuzeigen. Sie helfen uns Funktionen und Mechanismen zu verstehen, wie CDK8 zur Krebsentstehung und Immunüberwachung des Tumors beiträgt. Wir demonstrieren, dass es sich bei CDK8 um einen vielversprechenden Ansatzpunkt handelt, der uns eventuell in der Zukunft helfen kann, fatale Erkrankungen zu heilen.



**Abbreviations**

AP	accelerated phase
ALL	acute lymphoblastic leukemia
AML	acute myeloid leukemia
ALND	axillary lymph node dissection
BP	blastic phase
BMP	bone morphogenetic protein
CTD	C-terminal domain
CKIs	CDK inhibitors
CAK	CDK-activating kinase
CNS	Central nervous system
CHIPseq	chromatin immunoprecipitation followed by sequencing
CML	chronic myeloid leukemia
CP	chronic phase
CRC	colorectal cancer
CA	cortistatin A
CDK	Cyclin-dependent kinase
CTLs	cytotoxic lymphocytes
DC	dendritic cells
DSIF	DRB sensitivity-inducing factor
EGF	epidermal growth factor
EMT	epithelial-to-mesenchymal transition
ER	estrogen receptor
EAE	experimental autoimmune encephalomyelitis
FGF	fibroblastic growth factor
GIST	gastrointestinal sarcoma
GO	Gene Ontology
GTF	general transcription factor
HSPs	Heat-shock proteins
HDR	homologous recombination deficiency
IDC-NST	infiltrating duct carcinomas and no special type
ILC	innate lymphoid cells
IFN	interferon

ICD	intracellular domain
JAK	Janus kinase
Kd	dissociation constant
KIRs	killer cell immunoglobulin-like receptors
mH2A	MacroH2A
MHC	major histocompatibility complex
MMP	matrix metalloproteinase
MAPK	mitogen-activated protein kinases
mAbs	monoclonal antibodies
MPNs	myeloproliferative neoplasms
NK	natural killer cells
NKT	natural killer T cells
NELF	negative elongation factor
NOTCH	neurogenic locus notch homolog protein
NGS	Next generation sequencing
NKARs	NK activating receptors
NKIRs	NK inhibitory receptors
Ph	Philadelphia chromosome
Pten	phosphatase and tensin homolog
PVR	poliovirus receptor
PcG	Polycomb group
p-TEFb	positive transcription elongation factor b
PIC	preinitiation complex
PR	progesterone receptor
Treg	regulatory T cells
RB	retinoblastoma protein
RNAPII	RNA polymerase II
ROCK	Rho-associated, coiled-coil containing protein kinase
SERD	selective estrogen receptor down-regulators
STAT	signal transducer and activator of transcription
SE	super-enhancers
TAD	transactivation domain
TFs	transcription factors
TGF- $\beta$	transforming growth factor- $\beta$

TNBC	triple-negative breast cancers
TILs	tumor-infiltrating lymphocytes
TSA	tumor-specific antigens
TKI	tyrosine kinase inhibitor
VEGF	vascular endothelial growth factor
WNT	wingless-related integration site
WT	wildtype
Zeb2	zinc finger E-box binding homeobox 2

## 1. Introduction

### 1.1. Cyclin-dependent kinases (CDKs)

Cyclin-dependent kinases (CDKs) are a family of serine/ threonine kinases consisting of 21 members. Their catalytic activity is modulated by interacting with cyclins and CDK inhibitors (CKIs) (Lim and Kaldis, 2013). Studies were mainly performed in yeast and resulted in the identification of the CDKs and their binding partner cyclins, a finding which was awarded the Nobel Prize in 2001. Interaction of CDKs, cyclins and CKIs is necessary for orderly progression through the cell cycle. Deregulation of cell cycle control leading to sustained proliferation is recognized as one of the key hallmarks of cancer (Hanahan and Weinberg, 2011; Whittaker et al., 2017). Beside cell cycle regulation, CDKs have indispensable roles in other important processes, such as transcriptional regulation, epigenetic regulation, metabolism, stem cell self-renewal, neuronal functions and spermatogenesis. CDKs and their corresponding binding partner involved in cell cycle (green), transcription (blue) and neuronal functions (red) are depicted in Figure 1. Tasks can be accomplished with or without the need for CDK/cyclin complex formation or kinase activity (Lim and Kaldis, 2013).

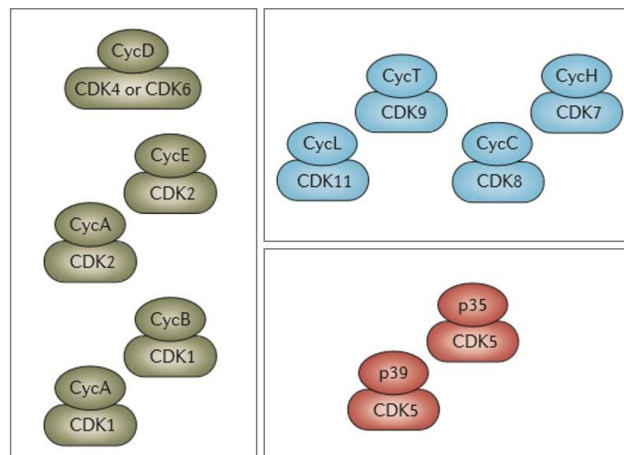


Figure 1: Biological functions of CDK complexes.

CDK-Cyc complexes, involved in cell cycle progression (in green), transcriptional processes (in blue) and in control of neuronal viability (in red); modified from (Asghar et al., 2015). (Copyright permission obtained by Copyright Clearance Center, License number: 5240841255637).

Phylogenetic analysis identified evolutionary relationships between CDK subfamilies – dividing them into direct and indirect regulators of the cell cycle (CDKs 1-6, 11 and 14-18) as well as transcriptional regulators (CDKs 7-13, 19 and 20) (Figure 2). CDKs have a conserved catalytic core containing an ATP-binding pocket, a cyclin subunit-binding domain and activating T-loop motif. They are constitutively expressed but typically need association with a cyclin subunit to

get active, as associated cyclins are shown in Figure 2 (right part) (Malumbres, 2014; Malumbres et al., 2009).

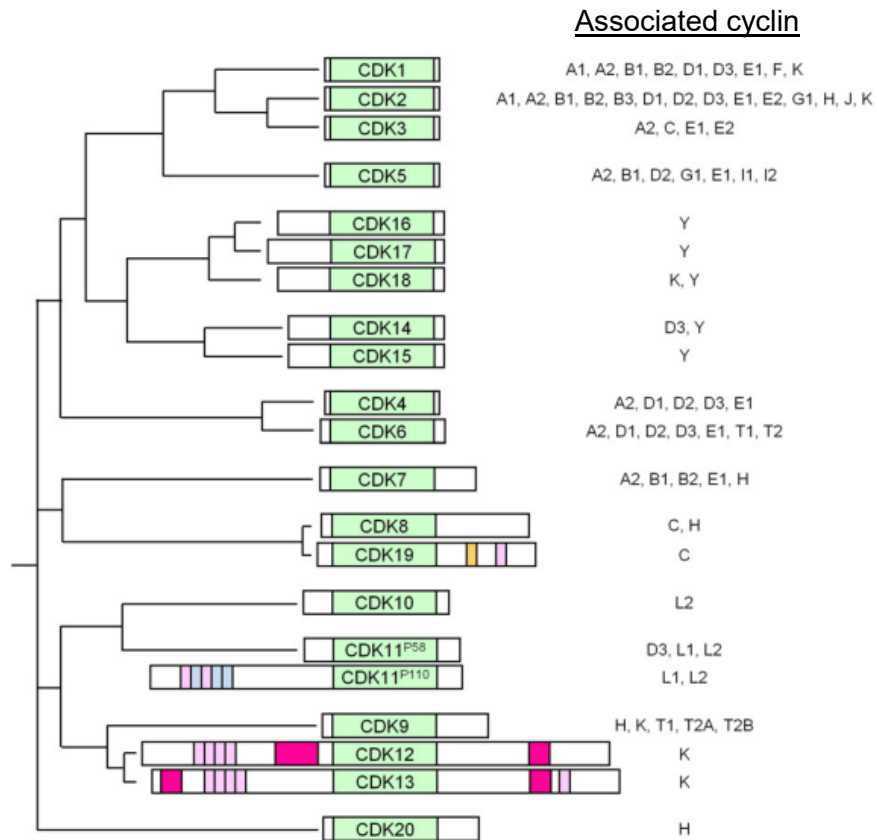


Figure 2: Human CDK subfamilies and their evolutionary relationship.

The color-code describes conserved domains: green, kinase domain; associated cyclins required for activation of CDKs are listed right; modified from (Whittaker et al., 2017). (Copyright permission obtained by Copyright Clearance Center, License number: 5240840838308).

### 1.1.1. Cell cycle regulation by CDKs

The cell cycle consists of five phases. In G1 and G2 phases, cells have the capacity to grow, in S phase they replicate their DNA, divide by mitosis in M phase and stop to proliferate and enter quiescence once they reach G0 phase. Progression through the cell cycle is regulated by activities of different CDKs and interaction with their corresponding regulatory cyclin partner (Asghar et al., 2015; Whittaker et al., 2017).

Entry into cell cycle happens in normal cells by stimulation of growth factor receptors by mitogenic signals. These different signals stimulate CDK4 and CDK6. Mitogenic signals in contrast can also activate antiproliferative checkpoints that directly inhibit CDK4/6 or induce for example the CDK4/6 inhibitor p16<sup>INK4A</sup>. CDK4 and CDK6 associate with D-type cyclins, thereby forming the active kinase complex which then phosphorylates key substrates, including the retinoblastoma protein (RB). This leads to the dissociation of HDAC1 and E2F

transcription factors allowing histone acetylation and starting a gene expression program (Figure 3, big blue box). CDK4 and CDK6 further initiate the stability of E-type and A-type cyclins and subsequent CDK2 transcription (Figure 3) (Blais and Dynlacht, 2007). The CDK2/cyclin E complexes phosphorylate RB - leading to a hyper-phosphorylated RB, which permits cell cycle progression by initiation of DNA replication. RB remains phosphorylated throughout the cell cycle S, G2 and M phases. At the end of mitosis RB is dephosphorylated by protein phosphatase-1 (Malumbres and Barbacid, 2009). Again, other checkpoints can directly inhibit CDK2 activity or induce inhibitors of CDK2/cyclin complexes (e.g. p21<sup>CIP1</sup> and p27<sup>KIP1</sup>). Once the DNA replication is completed, CDK1-cycA and CDK1-cycB complexes form and phosphorylate targets in G2 phase. This promotes expression of genes involved in mitotic progression. Repeatedly, potent checkpoints can limit CDK1 activity. Subsequent Cyclin B is degraded, which is required for anaphase progression and the production of two daughter cells in G1 phase of the cell cycle. RB gets dephosphorylated and the cell cycle is responsive to new signals again (Figure 3) (Asghar et al., 2015; Whittaker et al., 2017).

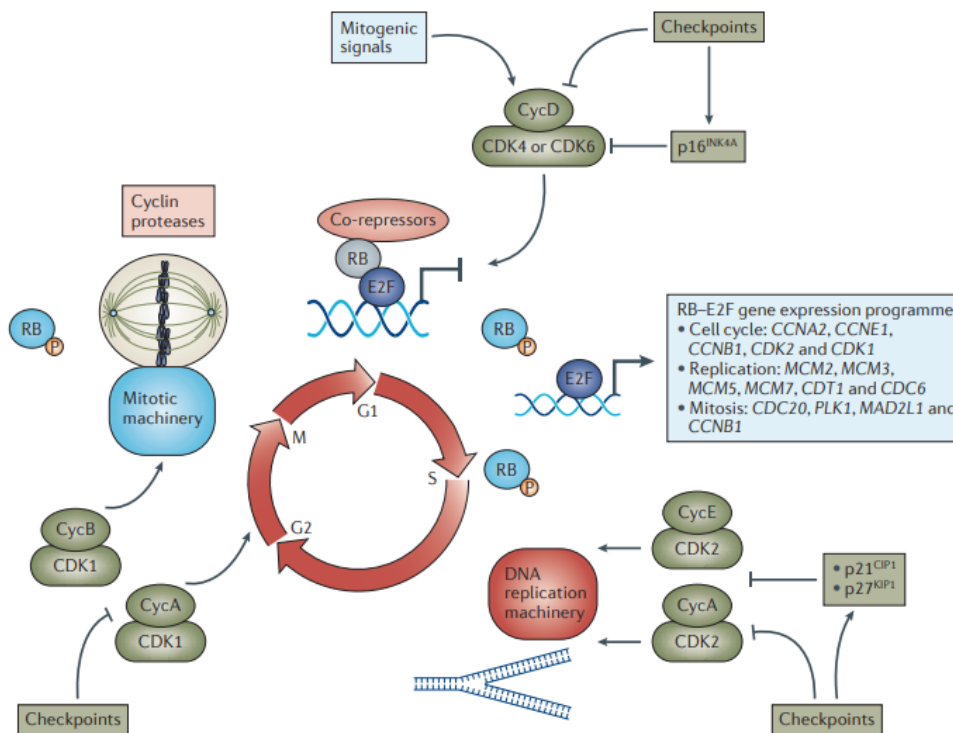


Figure 3: Cell cycle progression by CDKs.

CDK-Cyc complexes and their inhibitory checkpoints (in green) acting in different phases of cell cycle progression (Asghar et al., 2015). (Copyright permission obtained by Copyright Clearance Center, License number: 5240841255637).

### 1.1.2. Transcriptional regulation by CDKs

The RNA polymerase II (RNAPII) is responsible for transcribing all protein-coding genes in eukaryotes. It is recruited to the promoter of genes where it initiates productive transcription. The C-terminal domain (CTD) of RNAPII (the DNA-directed RNAPII subunit (RPB1)) contains multiple heptapeptide repeats which can be targeted and phosphorylated by transcription-associated CDKs, including CDK7, CDK8, CDK9, CDK12, CDK13 bound to their respective cyclin. Changes in the phosphorylation pattern of the CTD are important in the timing of its polymerase activity and the sequential recruitment of co-regulators (Jeronimo et al., 2013, 2016; Lim and Kaldis, 2013). As described for cell cycle control, in the regulation of transcriptional control, different CDK/cyclin complexes and their activities are restricted to different phases of the transcriptional cycle. This is important to drive the stepwise progression from pre-initiation, initiation, elongation to termination (Figure 4).

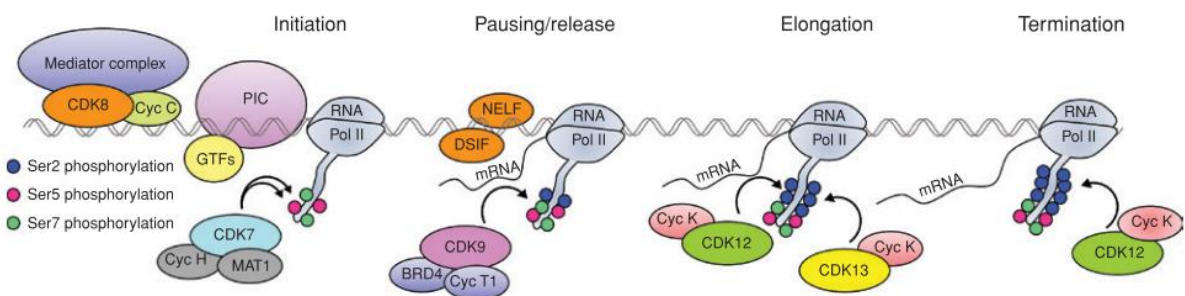


Figure 4: Regulation of transcription by CDKs.

The stepwise progression of transcriptional regulation, consisting of initiation, pausing/release, elongation and the termination phase (Chou et al., 2020). (Copyright permission obtained by Copyright Clearance Center, License number: 5240850038948).

The ablation of CDK7, CDK8, CDK11, cyclin H, cyclin T2 and cyclin K causes embryonic lethality, showing that their functions are non-redundant (Lim and Kaldis, 2013).

In the transcriptional process (Figure 4) a coactivator complex, namely the Mediator complex transmits signals from transcription factors to RNAPII. CDK8 binds to cyclin C, MED12 and MED13 and thereby forms the CDK8 module, which associates with the Mediator complex (Allen and Taatjes, 2015; Tassan et al., 1995). Further, the preinitiation complex (PIC) needs to assemble to facilitate DNA entry at the active site of RNAPII and start the process. Different general transcription factors (GTFs) are recruited, among them the final GTF TFIIH, which includes CDK7 (Compe and Egly, 2012). The CDK8-cycC complex can phosphorylate CDK7, which binds cyclin H and an accessory protein MAT1, a CDK-activating kinase (CAK). Its general role is the phosphorylation of the CTD at Ser5, thereby regulating the initiation of transcription and promoter escape. However, the precise role of CDK7 remains controversial

(Chou et al., 2020). A recent study showed that selective CDK7 inhibition primarily inhibited E2F-driven gene expression, causing a G1-S cell cycle arrest, and did not significantly inhibit phosphorylation of the CTD or global gene expression (Olson et al., 2019). Additionally, CDK7 may indirectly regulate transcription by phosphorylating TFs, such as the estrogen or androgen receptor, which are important in hormone-driven cancers (Chou et al., 2020).

By association of the CDK7/CAK complex with core TFIIH complex, CDK9 gets activated and serves as a control for the switch of initiation to elongation. CDK9 itself binds cyclin T or cyclin K for its kinase activity. CDK9-cycT is called the “positive transcription elongation factor b (p-TEFb)” and phosphorylates the CTD of RNAPII as well as other factors including DRB sensitivity-inducing factor (DSIF) and negative elongation factor (NELF) to relieve promoter pausing and promote transcription elongation (Wang and Fischer, 2008). CDK12 and CDK13 represent further transcriptional CDKs. They are closely related, share 50% amino acid homology overall and even 92% identity in their kinase domains. Shared and non-overlapping functions have been described (Chou et al., 2020). Both phosphorylate RNAPII’s CTD at Ser2 and Ser5 and regulate its elongation phase, CDK12 also regulates transcriptional termination. Further, CDK10 and CDK11 have roles in transcription. CDK10 partners with cyclin M and has been described as a tumor-suppressor in estrogen-driven tumors. CDK11 associates with L-type cyclins and acts on the splicing machinery and on proteins involved in transcriptional initiation and elongation. It is highly expressed in triple-negative breast cancer, multiple myeloma and liposarcoma (Chou et al., 2020).

The remaining CDKs are rather poorly studied yet. CDK3 appears to be important for cell cycle control. However, other studies suggest that CDK3’s function can be compensated. CDK5 was initially found as a “neuronal” kinase although more recent data from thyroid cancer models suggest a similar role to CDK4 and CDK2 in cell cycle control. Last but not least, CDK20 and its binding partner cyclin H were thought to phosphorylate and activate CDK2 – this still remains controversial in literature and needs further studies. Additional data suggest that CDK20 rather functions as an activating kinase for intestinal cell kinase (ICK), a regulator of cell cycle progression of intestinal epithelial cells (Whittaker et al., 2017).

### **1.1.3. Cyclin-dependent kinase 8 (CDK8)**

CDK8 is part of the transcriptional group of CDKs. It exists in a CDK8 module, together with cyclin C, MED12 and MED13. This module either binds the Mediator complex, in a reversible, but stable association or interacts directly with transcription factors (Malik and Roeder, 2005;



Menzl et al., 2019a). The interaction between the CDK8 module and core mediator occurs via MED13 (Knuesel et al., 2009; Tsai et al., 2013).

In vertebrates, CDK8 has a paralogue, CDK19, which appears to assemble in a “CDK19 module”, together with cyclin C, MED12 and MED13 (Daniels et al., 2013). Additionally, also paralogues for MED12 and MED13 exist: “MED12-like” and “MED13-like” (MED12L, MED13L), respectively. CDK8 and CDK19 share 83 % sequence homology, whereas MED12 and MED13 share only 59 % and 53 % identity with their paralogues. Different constellations and thereby functional specialization can occur as the paralogues bind mutually exclusively to the CDK8 module (Fant and Taatjes, 2019).

The core mediator complex consists of 26 submodules and has a head, middle and tail structure (Figure 5). Once bound to the CDK8 module it builds a bridge for transcription factors, chromatin modifiers, promoters and enhancers to RNAPII and is crucial during transcription (described in chapter 1.1.2). CDK8 can either repress or activate gene transcription. It represses transcription on the one hand by phosphorylating cyclin H, leading to inactivation of TFIIF and on the other hand by phosphorylating the CTD of RNAPII to preclude its recruitment to promoter DNA and to inhibit the assembly of the PIC in the initiation step of transcription (Lim and Kaldis, 2013). CDK8-mediator can support transcription by cooperating with the positive transcription elongation factor b (p-TEFb), which releases RNAPII for active transcription (Ebmeier and Taatjes, 2010).

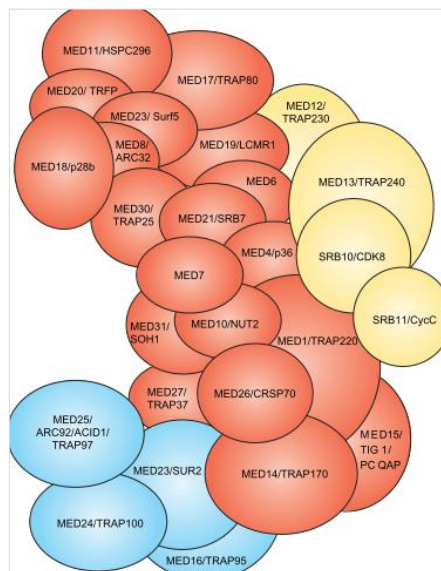


Figure 5: The Mediator complex.

It consists of a head and middle region (red) plus a tail (blue) which bind the CDK8 module (yellow) (Malik and Roeder, 2005). (Copyright permission obtained by Copyright Clearance Center, License number: 5240850379920).

The CDK8 module also acts independently of the mediator complex by directly interacting with transcription factors. Thereby it can regulate different signaling pathways, as NOTCH-dependent signaling, signal transducer and activator of transcription (STAT) signaling and transforming growth factor- $\beta$  (TGF- $\beta$ ) and bone morphogenetic protein (BMP) receptor signaling.

The neurogenic locus notch homolog protein (NOTCH) signaling pathway is important for inter-cellular communication, T-cell differentiation and neuronal development. Once a ligand (p.e. Delta) binds the extracellular domain, the intracellular NOTCH domain gets proteolytically cleaved, which releases the NOTCH receptor intracellular domain (ICD). ICD shuttles to the nucleus, where it activates transcription of NOTCH target genes (Kopan, 2012). CDK8-cycC phosphorylates the ICD thereby enhancing its activity, but also priming the ICD for ubiquitination and subsequent degradation (Fryer et al., 2004).

The Janus kinase (JAK) - signal transducer and activator of transcription (STAT) signaling pathway controls cytokine-mediated communication in the immune system. Upon ligand binding of the cell surface receptor, cytokine-receptor-associated JAKs phosphorylate a tyrosine at STAT homodimers, inducing dimerization and translocation to the nucleus, where DNA binding and transcription of target genes can occur. STATs can be posttranslationally modified, as described by phosphorylation of serine in the C-terminal transactivation domain (TAD). The CDK8 module phosphorylates regulatory sites within the TADs of STAT1, STAT3 and STAT5. In the interferon (IFN) signaling pathway CDK8 phosphorylates STAT1 at serine 727, making it a key regulator of anti-viral responses and NK cell anti-tumor responses (Bancerek et al., 2013; Putz et al., 2014; Staab et al., 2013).

Transforming growth factor  $\beta$  (TGF- $\beta$ ) and bone morphogenetic protein (BMP) signaling pathways propagate signaling through SMAD2, SMAD3 and SMAD1, SMAD5, SMAD8, respectively. Upon ligand binding to heteromeric serine/threonine kinase receptor complexes SMADs get phosphorylated at C-terminal tails. This leads to accumulation of SMADs in the nucleus and subsequent assembly of transcriptional complexes and regulation of target genes (Massagué, 2012). SMAD linker phosphorylation in the nucleus controls transcriptional activity. Antagonistic signals, such as fibroblastic growth factor (FGF), epidermal growth factor (EGF) and stress signals acting through mitogen-activated protein kinases (MAPKs) signaling lead to cytoplasmic retention and proteasomal degradation. CDK8 and CDK9, in contrast, have been shown to act as agonists and phosphorylate the linker regions before assembly of transcriptional complexes. This fully activates SMAD-dependent transcription, at the same time it also primes SMAD proteins for degradation (Alarcón et al., 2010; Aragón et al., 2011).

CDK8 is required for embryonic development. A complete *Cdk8* knockout in mice leads to embryonic lethality on day 2.5 to 3 due to a preimplantation defect (Westerling et al., 2007). In adult mice, it is dispensable for adult tissue homeostasis. A conditional and inducible deletion of *Cdk8* showed no gross abnormalities (McClelland et al., 2015). The physiological role of its paralogue CDK19 is still unclear. *Cdk19* knockout mice have a normal phenotype of the nervous, reproductive or cardiovascular systems. However, further studies are needed to unravel the physiological functions of CDK19 (Wu et al., 2021).

### **CDK8 in solid tumors**

Most of the previously described CDK8-dependent pathways are deregulated in cancer. There is accumulating evidence that CDK8 contributes to tumor development in different steps and cancer entities.

First indications for a role of CDK8 as a proto-oncogene came from data of colorectal cancer patients (CRC). The *CDK8* gene is amplified in 47 % of 123 CRC patient samples (Firestein et al., 2008) and a negative correlation could be shown between CDK8 expression and survival of patients with CRC (Firestein et al., 2010). Further, CDK8 is even higher expressed in advanced stages III and IV and contributes to disease progression from colorectal adenoma to carcinoma (Seo et al., 2010). In almost all CRCs an abnormal activation of the wingless-related integration site (WNT)/  $\beta$ -catenin pathway was found, contributing to growth, invasion and survival (Bienz and Clevers, 2000). To have a full malignant transformation, additional genetic perturbations are required - CDK8 was identified to contribute. The kinase function of CDK8 interacts with the Wnt pathway, it is essential to promote  $\beta$ -catenin-dependent transcription and transformation by phosphorylating  $\beta$ -catenin target genes. CDK8 additionally phosphorylates E2F1 on serine 375, thereby hindering the suppressive effect of E2F1 on  $\beta$ -catenin. Upon loss of CDK8, cell proliferation is reduced and the numbers of cells in G1 and S-phase are diminished (Firestein et al., 2008). In contrast, a study shows that CDK8 suppresses tumor growth in an *in vivo* model of *Apc<sup>Min</sup>* colon cancer. An inducible deletion of *Cdk8* increased tumor size and accelerated growth due to a reduction in histone H3K27 trimethylation and an increase of Polycomb group (PcG)-regulated genes which are relevant for oncogenic signaling (McClelland et al., 2015). This emphasizes that CDK8's functions are highly context specific.

MacroH2A (mH2A) is another epigenetic factor. It is a histone variant which replaces conventional histones and has unique biological functions. In malignant melanoma it suppresses tumor progression. Loss of mH2A increases the malignant phenotype. Knockdown

of mH2A led to increased proliferation and migration *in vitro* and accelerated growth and metastasis *in vivo*. To a certain extent, these tumor promoting functions result from direct transcriptional upregulation of CDK8. Further, CDK8 was found to have an inverse correlation with mH2A in 36 melanoma patient samples. It is therefore speculated that CDK8 drives melanoma progression by upregulating cell growth and migration (Kapoor et al., 2010).

In breast cancer, CDK8 appears to play an essential part. Analysis of transcriptome data of 968 breast cancer patients revealed increased levels of CDK8/CDK19, cyclin C and MED13 compared to normal mammary tissue or benign/ hyperplastic breast cancer. Further, high levels of CDK8 correlate with worse recurrence free survival in breast cancer patients (Broude et al., 2015; Roninson et al., 2019). Functions of CDK19 have not been verified yet. However, functions of CDK8 have been reported. The Skp2-mH2A1-CDK8 axis appears to be a critical pathway in breast cancer development. Skp2 is a F-box protein which forms a E3 ligase complex (SCF complex) together with Skp1 and Cullin-1. It was found as a novel E3 ligase, triggering ubiquitination and degradation of the histone variant mH2A1, which is low expressed in breast cancer. Skp2 induced mH2A1 degradation leads to gene and protein expression of CDK8. CDK8 itself can serve as a kinase for p27 or lead to promoting p27 ubiquitination and degradation mediated by Skp2. This may contribute to cell growth and migration, polyploidy, G2/M arrest and tumorigenesis, dependently and independently of p27 regulation (Xu et al., 2015a). A further function of CDK8 was observed in estrogen receptor positive breast cancer. Estrogen-induced transcription depends on CDK8 kinase activity, with CDK8 acting downstream of the estrogen receptor. These effects could be recapitulated with a specific CDK8/CDK19 inhibitor, Senexin A. Further, inhibitor treatment resulted in diminished tumor growth but failed to induce apoptosis in mouse models. Synergistic effects with an ER antagonist fulvestrant (belonging to selective estrogen receptor down-regulators – SERD) were reported, without any apparent toxicity in mice (McDermott et al., 2017).

Further, pancreatic cancer studies showed that CDK8 has a role in epithelial-to-mesenchymal transition (EMT) – a process important in the metastatic and invasive potential of cells. Dependent on the status of K-RAS mutation, pancreatic cancer samples had higher expression of CDK8. High levels of CDK8 and mutated K-RAS trigger invasion and migration of cells via WNT/  $\beta$ -catenin signaling by increasing the EMT-associated transcription factors (TFs) Snai1 and ZEB1 (Xu et al., 2015b). Further evidence for a correlation between CDK8/CDK19 expression and EMT-associated TFs is provided by studies in ovarian, pancreatic and breast cancer cell lines. The BMP signaling pathway induces invasion of pancreatic cancer. In detail, BMP-induced SMAD1 drives the upregulation of matrix metalloproteinase (MMP)-2. Activation

of this pathway depends on the kinase activity of CDK8 as described in the previous chapter. Upon CDK8/CDK19 inhibition or knockdown of CDK8 or CDK19, BMP4-induced EMT was shown to be suppressed in ovarian and pancreatic cancer cell lines. Furthermore, CDK8/CDK19 inhibition abrogated muscle invasion *in vivo* in a murine breast cancer model, using Py2T cells, mimicking a HER2-enriched cell line. Mechanistically this goes together with an upregulation of E-cadherin and downregulation of EMT-associated TFs Snai1 and Snai2. RNA-seq data of 293 high-grade serous ovarian tumors additionally provided evidence for a positive correlation of CDK8 and CDK19 with EMT markers in patients (Serrao et al., 2018). In addition, a study revealed that high levels of CDK8 promote angiogenesis in pancreatic cancer via activating the CDK8- $\beta$ -catenin-KLF2 signaling pathway, consequently leading to upregulation of vascular endothelial growth factor (VEGF), VEGFR2, MMP-9, c-myc and cyclin D1. This thereby supports the metastatic potential of cells as confirmed in a nude mice xenograft model (Wei et al., 2018).

In colorectal cancer (CRC), CDK8 has a specific role as it interacts with two signaling pathways which are important in formation of hepatic metastasis (Figure 6). Hepatic metastases are often unresectable, unresponsive to therapies and a major cause of lethality in colon cancer patients (Liang et al., 2018). Using human and mouse colon cancer cells, CDK8 knockdown or inhibition of CDK8/CDK19 resulted in only little effects on colon cancer cell growth but suppressed the metastatic growth in the liver. By interacting with two different signaling pathways, CDK8 enables the metastatic growth in the liver. It downregulates the matrix metalloproteinase (MMP) inhibitor TIMP3 via TGF- $\beta$ / SMAD-driven expression of the microRNA miR-181b, which targets TIMP3. In CRC TIMP3 is a well described suppressor of invasion, angiogenesis and metastasis (Lin et al., 2012). Additionally, CDK8 induces *Mmp3* in murine and *MMP9* in human colon cancer cells, via WNT/  $\beta$ -catenin-driven transcription (Figure 6) (Liang et al., 2018). MMPs do as well have a major role in tumor progression. Aside from matrix degradation, they have key roles in growth factor receptor signaling, cell adhesion, angiogenesis and apoptosis (Duarte et al., 2015).

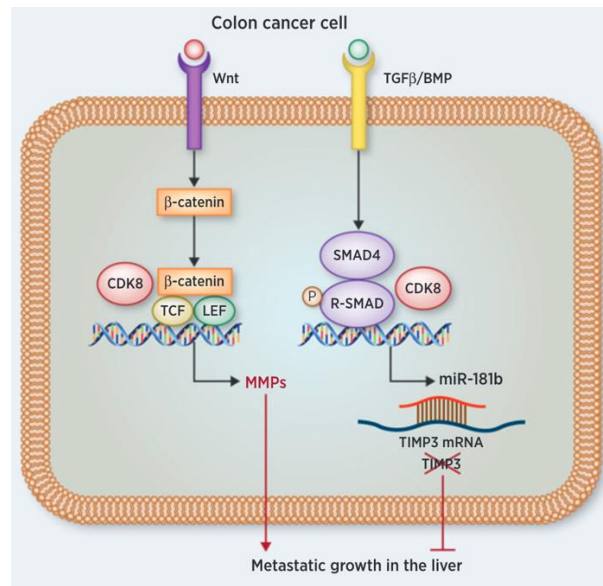


Figure 6: CDK8 regulates metastatic growth in the liver.

CDK8 regulates two different pathways (WNT/  $\beta$ -catenin and TGF- $\beta$ / SMAD), important in formation of hepatic metastasis in colorectal cancer (Liang et al., 2018). (Copyright permission obtained by Copyright Clearance Center, License number: 5240850642860).

### CDK8 in leukemia

In leukemia, key roles of CDK8 have been proposed. A study found a role of both, CDK8 and CDK19 in acute myeloid leukemia (AML) on super-enhancers (SE) – regions/ clusters composed of multiple enhancers loaded with Mediator complex, transcription factors and chromatin regulators. In a CDK8-chromatin immunoprecipitation followed by sequencing (CHIPseq) experiment in the AML cell line MOLM-14, CDK8 was found on SE, associated with binding of MED1 and BRD4. Gene Ontology (GO) terms hematopoiesis, transcription and cellular differentiation were found among the CDK8-occupied SE-associated genes. In MOLM-14 cells BRD4 supports SE-mediated transcription, CDK8 and CDK19 inhibit SE-associated genes. Using the natural product Cortistatin A (CA), CDK8 and CDK19 could be selectively inhibited, leading to diminished cell proliferation of MOLM-14 cells *in vitro*, reduced AML progression in mice bearing MV4-11 leukemic cells and even more enhanced transcription of SE-associated genes in sensitive AML cells (Pelish et al., 2015). A further study reported that CA treatment inhibited growth of AML cells with a hyper-activated JAK-STAT signaling, in part by blocking STAT1-S727 phosphorylation. Myeloproliferative neoplasms (MPNs) can progress to an AML in up to 20% of MPN patients, called “post-MPN AML”. Post-MPN AML is characterized by constitutive JAK-STAT signaling, often induced by an activating somatic mutation in the JAK2 kinase (V617F). The JAK1/2 inhibitor Ruxolitinib was approved as targeted therapy for a subset of MPN patients, reducing STAT tyrosine phosphorylation,

without being curative alone. CA was found to act different, perturbing the STAT1 serine phosphorylation, thereby inducing growth arrest and differentiation in JAK2-mutated AML cells. In contrast, Ruxolitinib only induced apoptosis. A combination treatment of CA and Ruxolitinib enhanced growth suppression *in vitro* and in patient samples, may representing a new therapeutic approach (Nitulescu et al., 2017). SEL120-34A, another CDK8/CDK19 inhibitor, reducing the CDK8 targets STAT1-S727 and STAT5-S726 phosphorylation, was also tested on AML cells. Treatment of cells with high levels of STAT1 and STAT5 phosphorylation and high expression of hematopoietic progenitor markers showed anti-proliferative effects. Results could be recapitulated with other CDK8/CDK19 inhibitors SEL129-34A, Senexin B and CCT251545 (Rzymiski et al., 2017). In addition, a study in T-cell acute lymphoblastic leukemia (T-ALL) described a tumor-suppressive function of the CDK8/cyclin C axis. Activation of CDK8 by cyclin C enhances ICN1 degradation within the NOTCH signaling pathway. A significant fraction of human T-ALLs have reduced cyclin C levels due to a heterozygously deleted *CCNC* gene (encoding cyclin C). Deficiency of cyclin C increases ICN 1 oncogene levels and thereby accelerates T-ALL disease progression (Li et al., 2014).

A hallmark of cancer cells is aerobic glycolysis, also named the Warburg effect. Cancer cells require high levels of ATP to be able to proliferate fast, which is provided by increased glucose consumption and high rates of glycolysis. HIF1 $\alpha$  acts together with CDK8 to affect gene expression and is a master transcriptional regulator of glycolytic enzymes. A role for CDK8 in the expression of glycolytic genes has been described in colorectal cancer cell lines using the CDK8/CDK19 inhibitor Senexin A. Transcriptome analysis revealed that CDK8 kinase activity regulates parts of the glycolytic cascade. CDK8/CDK19 inhibition lowered glucose transporters and uptake, the glycolytic capacity and diminished cell proliferation and anchorage-independent growth in normoxia and hypoxia (Galbraith et al., 2017).

### **CDK8 in tumor surveillance**

CDK8 also plays an important part in the immune system. For natural killer (NK) cells it has been described that CDK8 acts upstream of STAT1, modulating NK-cell anti-tumor responses. Mice with a point mutation in the CDK8 phosphorylation site of STAT1, (serine 727 to alanine; STAT1-S727A), showed enhanced NK cell cytotoxicity against a range of NK cell-surveilled tumor cell lines, together with increased expression of granzyme B and perforin. It translates *in vivo* into a later disease onset in different cancer models, such as melanoma, leukemia, and metastasizing breast cancer in STAT1-S727A mice. This could be attributed to enhanced cytotoxic potential of STAT1-S727A NK cells (Putz et al., 2013). Deletion of CDK8 in the NK

cell compartment, in *Cdk8<sup>fl/fl</sup>Ncr1Cre* transgenic mice revealed a normal development and maturation of NK cells but increased expression of the lytic molecule perforin. This translates into enhanced NK cell cytotoxicity *in vitro* and improved NK cell-mediated tumor surveillance of melanoma, lymphoma and leukemia mouse models *in vivo*, describing a suppressive effect of CDK8 on NK cell activity. Unexpectedly, CDK8-deficient NK cells have unaltered STAT1-S727 phosphorylation, probably due to a compensatory effect of CDK19 (Witalisz-Siepracka et al., 2018). On top, a recent study described a newly developed CDK8/CDK19 inhibitor BI-1347. Treatment of NK cells with the inhibitor decreased STAT1-S727 phosphorylation and increased perforin and granzyme B production. Functionally, NK cell lysis of primary leukemia cells was increased and inhibitor treatment *in vivo* showed prolonged survival of mice with melanoma xenografts. Combination treatments with either PD-1 monoclonal antibodies in a colorectal cancer model or SMAC mimetic in a breast cancer model increased survival of mice and provides evidence for new therapeutic combinations (Hofmann et al., 2020).

A novel role of CDK8/CDK19 was also reported in the adaptive immune system, in *Foxp3* expressing regulatory T (Treg) cells. CDK8/CDK19 inhibitors induced the differentiation of Treg cells and expression of Treg signature genes, such as *Foxp3*. Inhibitor treatment led to a sensitized TGF- $\beta$  signaling together with decreased IFN $\gamma$ -STAT1 signaling and enhanced Smad2/3 phosphorylation. *In vivo* this translated into an increased Treg population and dampened autoimmune symptoms in an experimental autoimmune encephalomyelitis (EAE) model upon inhibitor treatment (Guo et al., 2019).

Figure 7 summarizes all previously described physiological and pathological functions of CDK8. It illustrates the context-specific roles of CDK8 which are not yet fully understood and demand further research, but also harbor a lot of novel treatment options.



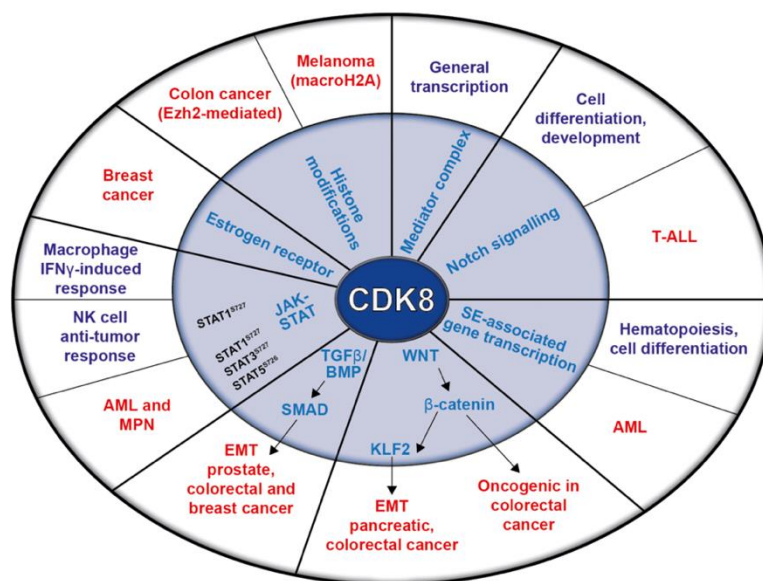


Figure 7: Physiological and pathological functions of CDK8.

Functions of CDK8 in transcription and signaling (depicted in the inner circle) and their relation to physiological (violet) and pathological (red) conditions (depicted in the outer circle) (Menzl et al., 2019a). (Copyright permission obtained by Creative Common CC BY license).

### CDK8/CDK19-specific inhibitors

The functions of CDK8 and CDK19 are context dependent, making them important drug targets and a high number of inhibitors have been developed to date. Due to their high degree of structural similarity, they inhibit not only CDK8 but also the kinase function of CDK19. The compounds are reversible inhibitors which bind competitively with ATP. For measuring kinase activity, CDK8 needs to be tested as an active kinase, which it is when associated with cyclin C. Association with cyclin C and MED12 increases CDK8 activity about 30-fold (Fant and Taatjes, 2019).

In the beginning of inhibitor development, several known kinase inhibitors were found to bind CDK8 when evaluated against a panel of human protein kinases. Selectivity of these compounds is very different - reaching from low (e.g. Flavopyridol, a pan-CDK inhibitor) to medium and high for only one compound (Rzymiski et al., 2015). In 2009, Cortistatin A was reported, showing a high level of selectivity to CDK8 and binding it with high affinity, with a dissociation constant ( $K_d$ ) of 17 nM. It is a steroidal alkaloid, isolated from a marine sponge *Corticium simplex*. It is also described as a high affinity ligand for CDK19 ( $K_d$ = 10 nM) and Rho-associated, coiled-coil containing protein kinases (ROCK) with  $K_d$  for ROCK I of 250 nM and for ROCK II of 220 nM (Cee et al., 2009). In 2012, SNX2-class compounds were revealed as selective inhibitors of CDK8 and its isoform CDK19. These compounds were discovered in a high-throughput screening and subsequent structure optimization resulted in the detection

of Senexin A, an inhibitor with  $K_d = 0.83 \mu\text{M}$  and  $K_d = 0.31 \mu\text{M}$  for CDK8 and CDK19, respectively. CDK8 kinase activity is inhibited with an  $\text{IC}_{50}$  of  $0.28 \mu\text{M}$  (Porter et al., 2012). Improvement of solubility and potency led to the development of a new generation compound, called Senexin B. It strongly binds to CDK8 and CDK19 with  $K_d$  values of  $140 \text{ nM}$  and  $80 \text{ nM}$ , respectively and CDK8 kinase inhibition reveal  $\text{IC}_{50}$  values from  $24$  to  $50 \text{ nM}$  in different assays. The compound further was investigated in pharmacokinetic studies, using mice and rats with positive outcome. In 2014 novel CDK8 inhibitors were reported by three companies and screening revealed highly selective inhibitors for CDK8. Among, the company Selvita identified a clinical candidate molecule, SEL120-34, which made it to clinical trials (Rzymiski et al., 2015).

Further studies modified structures and developed different CDK8/CDK19 inhibitors, as e.g. BI-1347 (Hofmann et al., 2020), compound 2, compound 20 and many more with having different  $\text{IC}_{50}$  values and varying levels of off-target effects and off-target kinase inhibition (Fant and Taatjes, 2019). Described functions of promising inhibitors were reviewed in the previous chapter.

Most important, two inhibitors made it to a Phase I clinical trial, with only one – SEL120 – being currently ongoing and recruiting in an early-phase clinical trial for treatment of hematologic malignancies (Table 1).

Number	Status	Drug	Condition	Start	Completion
NCT04021368	Recruiting	RVU120 (SEL120)	<ul style="list-style-type: none"> <li>○ Acute Myeloid Leukemia</li> <li>○ High-risk Myelodysplastic Syndrome</li> </ul>	Sept 2019	Dec 2022
NCT03065010	Completed	BCD-115	<ul style="list-style-type: none"> <li>○ ER+ HER2- local advanced and metastatic Breast Cancer</li> </ul>	Nov 2016	March 2018

Table 1: Clinical trials using CDK8/CDK19 inhibitors.

<https://clinicaltrials.gov/ct2/results?cond=&term=cdk8&cntry=&state=&city=&dist=> (access 20220110)

The first clinical trial with BCD-115 treatment in breast cancer was discontinued after 90 days due to adverse events. Dual CDK8/CDK19-targeting compounds at therapeutic dose levels may be too toxic. Combinations of CDK8 inhibitors with drugs targeting alternative pathways are the way to go and may generate synergy and lead to tolerable levels of CDK8 inhibitors, as some studies already described such synergies (Chou et al., 2020).

## 1.2. Breast cancer

Breast cancer represents a major public-health issue. It is among the most common cancer entities and the most common causes of cancer deaths worldwide (Veronesi et al., 2005). According to WHO statistics the estimated number of new cases in 2020 was over 2 million breast cancer cases worldwide, including both sexes and all ages (Figure 8 left panel). Statistics revealed almost 700,000 deaths and a 6.9% mortality rate in breast cancer cases worldwide (Figure 8 right panel).

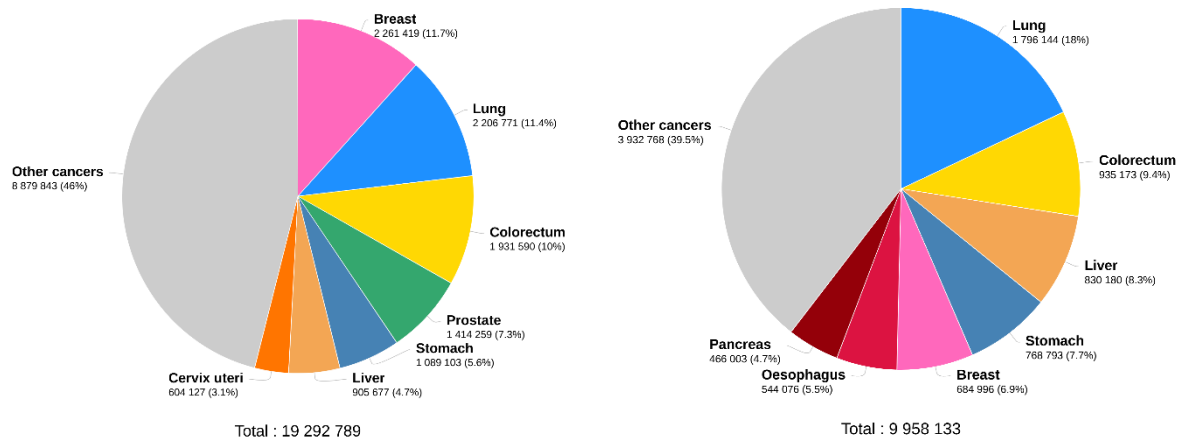


Figure 8: WHO statistics on Cancer worldwide.

Estimated number of new cases (left) and estimated number of deaths in 2020 (right), worldwide, both sexes and all ages. <https://gco.iarc.fr> (access 20210219)

### 1.2.1. Classification

Breast cancer is a heterogenous disease with different morphologic and biological features. The traditional classification and routine assessment are based on histologic typing, grading, tumor staging and hormonal receptor expression analysis (Tsang and Tse, 2020). Histologic subtypes are based on the pathologic growth pattern. There are over 20 different types of invasive breast cancer with the most common being infiltrating duct carcinomas and no special type (IDC-NST) comprising 70-80%. Criteria for classification include tumor cell type, extracellular secretion, architectural features and immunohistochemical profile (Tan et al., 2020). The Nottingham modification of the Scarff-Bloom Richardson grading evaluates tumor grade. The scoring system takes microscopic assessment of histologic differentiation into account, analyzing tubule formation, nuclear pleomorphism and proliferation, stating a mitotic index (Mook et al., 2009). Tumor staging is based on tumor size (T), status of regional lymph nodes (N) and distant metastasis formation (M), referred to as "TNM staging". It uses both, clinical and aforementioned pathologic information and distinguishes 5 stages (0, I, II, III, IV)

(Weiss et al., 2018). Latest, also the hormonal receptor status was incorporated into tumor staging. Routine assessment includes defining the status of the two nuclear sex steroid receptors estrogen receptor (ER) and progesterone receptor (PR) and analysis of HER2 (=ERBB2) expression. Determination is crucial in prediction for hormonal and anti-HER2 targeted therapy response. The majority, ~75% of breast cancer cases express ER and PR and are usually low grade and less aggressive (Hammond et al., 2010). HER2 is overexpressed in 15% of all cases, showing an amplification of the corresponding gene at 17q12 (Slamon et al., 1987). They show an aggressive clinical course and poor prognosis. Nevertheless, they respond to anti-HER2 targeted treatments. Remaining 10-15% of breast cancer cases belong to the group of triple-negative breast cancers (TNBC). They are high grade, have a poor prognosis and no targeted therapies are available to date (Tsang and Tse, 2020).

With emerging high-throughput technologies paradigms in breast cancer biology changed. By performing global gene expression profiling 5 intrinsic subtypes were identified performing hierarchical clustering - namely luminal A, luminal B, HER2-overexpressing, basal-like (BLBC) and normal-like tumors (Table 2) (Perou et al., 2000).

<b>Intrinsic Subtype</b>	<b>Gene Profile</b>	<b>IHC Phenotype</b>
Luminal A	High expression of <ul style="list-style-type: none"> <li>- luminal epithelial genes</li> <li>- ER-related genes</li> </ul>	ER <sup>+</sup> , PR $\geq$ 20%, HER2 <sup>-</sup> , Ki67 <sup>low</sup>
Luminal B	Lower expression of <ul style="list-style-type: none"> <li>- Luminal epithelium</li> <li>- ER-related genes</li> </ul> Higher level of <ul style="list-style-type: none"> <li>- HER2-related genes</li> </ul>	ER <sup>+</sup> , PR <20% or HER2 <sup>+/</sup> or Ki67 <sup>high</sup>
HER2-overexpression	High expression of <ul style="list-style-type: none"> <li>- HER2-related genes</li> </ul> Low expression of <ul style="list-style-type: none"> <li>- ER-related genes</li> </ul>	ER <sup>-</sup> , PR <sup>-</sup> , HER2 <sup>+</sup>
Basal-like	High expression of <ul style="list-style-type: none"> <li>- Basal epithelial and proliferation genes</li> </ul> Low expression of <ul style="list-style-type: none"> <li>- HER2-related genes</li> <li>- ER-related genes</li> </ul>	ER <sup>-</sup> , PR <sup>-</sup> , HER2 <sup>-</sup>

Table 2: Overview of different molecular subtypes of breast cancer.

(Tsang and Tse, 2020); IHC: immunohistochemical

For daily clinical practice these methods are too costly and technically complex, therefore immunohistochemistry of ER, PR, HER2 and Ki67 are state-of-the-art (Goldhirsch et al., 2013). Consequently, some discrepancies exist. Only 80% of TNBC belong to the intrinsic basal-like BC group, only 65% of HER2<sup>+</sup> patients belong to the HER2-overexpressing group and the cutoff for Ki67 is still a matter of debate (Cheang et al., 2015; Morigi, 2017; Prat et al., 2014). Further clustering was reported by the Molecular Taxonomy of Breast Cancer International Consortium (METABRIC) including intrinsic subtyping and genomic heterogeneity - assigning ten integrative clusters (IntClust 1 to 10) (Curtis et al., 2012). Next generation sequencing (NGS) identified 40 driver mutations. TP53, PIK3CA and GATA3 are the most common driver genes with incidences over 10%, showing that generally mutations are rare in breast cancer (Koboldt et al., 2012) and are found across subtypes. The Cancer Genome Atlas Network (TCGA) performed a multiomics approach combining six different platforms and in the end could show the existence of four main breast cancer classes, which correlated well with the subtypes shown in Table 2.

### **1.2.2. Treatment**

Treatment approaches and strategies are based on the categorization of breast cancer into 3 major subtypes (hormone receptor positive/ HER2 negative, HER2 positive and triple-negative) and into nonmetastatic or metastatic disease. The majority of cases (>90 %) are non-metastatic at time of diagnosis. Therapeutic goals are primarily eradication of the tumor and secondly the prevention of metastatic recurrence, which happens more likely in triple-negative breast cancer. Metastatic breast cancer is incurable. Therapy aims are prolonging life and alleviating symptoms (Waks and Winer, 2019). The median overall survival for metastatic hormone receptor positive and HER2 positive breast cancer is five years and for triple-negative breast cancer it is one year (Waks and Winer, 2019).

#### **Non-metastatic breast cancer**

The two main therapeutic opportunities for treating non-metastatic breast cancer are systemic and local therapy. Dependent on breast cancer subclass, there are different systemic treatment options summarized in Table 3.

	<b>Hormone receptor positive/ HER2 negative</b>	<b>HER2 positive</b>	<b>Triple-negative</b>
% of breast cancer cases	70	15-20	15
Typical systemic therapy for <u>non-metastatic</u> disease	Endocrine therapy (all patients) Chemotherapy (some patients)	Chemotherapy + HER2-targeted therapy (all patients) Endocrine therapy (if also HR+)	Chemotherapy (all patients)
Systemic therapy for <u>metastatic</u> disease	Initial: Aromatase inhibitors + CDK4/6 inhibitor Later: Hormonal and/or targeted therapy	Initial: taxane+ trastuzumab+ pertuzumab Endocrine therapy+ HER2-targeted therapy Ado-trastuzumab emtansine Later: HER2-targeted therapy+ chemotherapy or endocrine therapy (if HR+)	Initial: single-agent chemotherapy Later: single-agent chemotherapy

Table 3: Therapeutic options for different breast cancer subtypes.

Hormone receptor positive breast cancer is the most common subclass, with around 70 % of cases (Howlader et al., 2014). All patients receive endocrine therapy, which consists of oral antiestrogen medication. Tamoxifen is a selective estrogen receptor inhibitor, which inhibits the binding of estrogen to its receptor and therefore downstream signaling. It is taken daily for 5 years and is effective in pre- and postmenopausal women (Abe et al., 2011). Aromatase inhibitors (anastrozole, exemestane and letrozole) are effective in postmenopausal woman as well and inhibit the conversion of androgens to estrogen, lowering circulating levels of estrogen (Joshi and Press, 2018). Adjunct to endocrine therapy, chemotherapy remains as an essential treatment option in HR<sup>+</sup> tumors, as it has been shown that higher-risk tumors are associated with greater absolute benefit from chemotherapy (Albain et al., 2012). Chemotherapy regimens contain anthracycline (e.g. adriamycin) in combination with taxane (such as adriamycine/cyclophosphamide followed by taxane) for high-risk patients (Blum et al., 2017) and are administered by intravenous therapy for 12-20 weeks. In the treatment of HER2<sup>+</sup> (ERBB2) breast cancer big progress has been made by developing HER2-targeted therapy.

The monoclonal antibody trastuzumab targets the extracellular domain of ERBB2. It is now standard of care treatment to add one year of this monoclonal antibody to 12-20 weeks of chemotherapy, in the combination paclitaxel/ trastuzumab, in patients with small, node-negative HER2<sup>+</sup> tumors (Piccart-Gebhart et al., 2005; Romond et al., 2005; Slamon et al., 2011). Patients with higher-risk tumors further receive the agents pertuzumab, a monoclonal antibody targeting the ERBB2 dimerization domain or neratinib, an oral small-molecule tyrosine kinase inhibitor of multiple HER family members (Martin et al., 2017; Von Minckwitz et al., 2018). Dependent on the hormonal status of HER2<sup>+</sup> patients, additional endocrine therapy is administered. For treatment of non-metastatic triple-negative breast cancer, the only FDA approved drugs are chemotherapeutic agents. All patients with breast tumors larger than 5 mm receive intravenous therapy for 12-20 weeks with aforementioned combinations of chemotherapeutic drugs. One single evidence-based adjuvant strategy available for patients with TNBC is single-agent capecitabine (Masuda et al., 2017).

Local therapy of non-metastatic breast cancer is another treatment approach consisting of two methods – surgery and radiation therapy. There are two standard surgical procedures, either a total mastectomy or an excision plus radiation, assuming clear margins between cancerous and healthy tissue. Separately, axillary lymph node dissection (ALND) needs to be considered, both as a diagnostic tool, as well as for a therapeutic purpose to remove cancerous cells (Ernard et al., 2002). Radiation therapy can be delivered to a portion of the breast or the whole breast, to the chest wall (after mastectomy) and the regional lymph nodes (Maughan et al., 2010; Waks and Winer, 2019).

### **Metastatic breast cancer**

Almost all deaths of patients with metastatic breast cancer are due to metastatic disease (National Institutes of Health). Different factors are relevant to prognosis as visceral metastasis, brain metastasis and multiple metastatic sites claim worse prognosis and younger age, bone-only metastasis and longer disease-free interval between diagnosis and metastasis development give improved prognosis (Waks and Winer, 2019). In the systemic treatment of metastatic breast cancer there is an early and later treatment regiment, summarized in Table 3. Dependent on the subclass of breast cancer there are principles, which are followed. In hormone receptor positive/ HER2 negative breast cancer, early treatment is endocrine therapy usually in corporation with a CDK4/6 inhibitor (abemaciclib, palbociclib or ribociclib) in the first or second line (Finn et al., 2016; Goetz et al., 2017; Hortobagyi et al., 2016). After resistance, there is a transition to chemotherapy, as a single-agent sequential chemotherapy. In HER2

positive cases first-line therapy includes a taxane plus trastuzumab and pertuzumab and second-line the antibody-drug conjugate trastuzumab emtansine (Von Minckwitz et al., 2009). For metastatic triple-negative breast cancer cytotoxic chemotherapy is the only therapeutic option available in patients not harboring BRCA1/2 mutations. If they do so, targeted inhibitors of PARP enzymes are approved (Litton et al., 2018; Robson et al., 2017). Also, a phase 3 clinical trial showed improved progression-free survival upon treatment with chemotherapy and immunotherapy combination, like nab-paclitaxel plus PD-L1 inhibitor atezolizumab for pretreated metastatic triple-negative breast cancer patients (Schmid et al., 2018) but still, there is an urgent need to discover new, targeted therapies.

### 1.2.3. Triple-negative breast cancer (TNBC)

As aforementioned 10-15% of all breast cancer cases are classified as triple-negative breast cancer, defined by the lack of ER, PR and HER2 expression. TNBC is more common among specific ethnicities as Latin, African and African-American (Lund et al., 2009). It is characterized by an aggressive behavior, early relapse, metastatic spread to lung, liver and central nervous system and a poor survival (Dent et al., 2007). Although it is a defined breast cancer subclass, it is very heterogeneous showing diverse response rates to therapies. Genomic expression profile assays were used to define “molecular fingerprints” to be able to propose seven molecular subtypes (Lehmann et al., 2011). A refinement was performed including clinical trial datasets summarizing the groups into four, which are in use as prognostic and predictive tool, summarized in Figure 9 (Burstein et al., 2015; Lehmann et al., 2016; Lopes Da Silva et al., 2020).

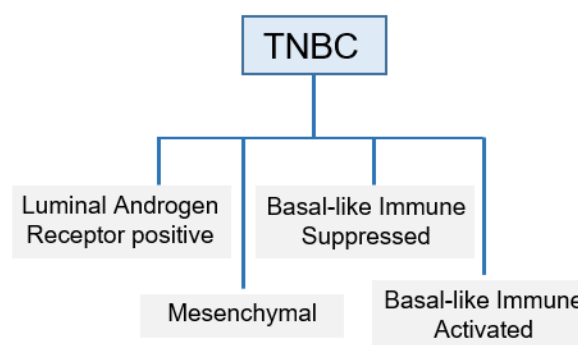


Figure 9: Molecular subtypes of triple-negative breast cancer.

(Lopes Da Silva et al., 2020)

TNBC do express neither hormone receptors, nor HER2 and therefore therapeutic approaches as mentioned in chapter 1.2.2. are not an option. No targeted therapies are available hence



specific molecular subtypes and biological factors, important in TNBC tumorigenesis are of utmost interest in the discovery of new drugs and biomarkers.

## Tumorigenesis

Several studies identified main signal transduction pathways important in tumorigenesis of TNBC, summarized in Figure 10.

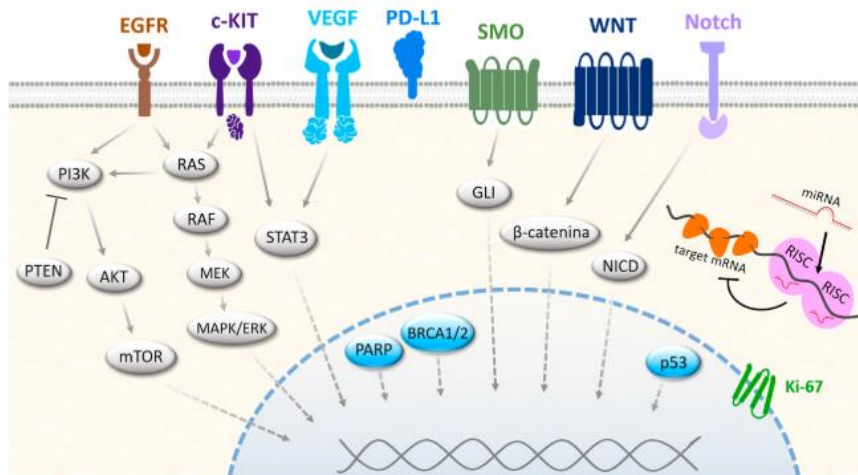


Figure 10: Main signal transduction pathways in TNBC tumorigenesis.

Different signaling pathways found to be important in tumorigenesis of TNBC (Lopes Da Silva et al., 2020).  
(Copyright permission obtained by Copyright Clearance Center, License number: 5240851033309).

Among them is the p53 protein, a transcription factor important in cellular response to DNA damage. The p53 gene is mutated in 75-80 % of patients with TNBC, harboring either missense mutations with high p53 protein expression or deletion mutations with no expression of the protein (Yemelyanova et al., 2011). Ki67, a cell membrane antigen, important in determination of cell proliferation is a prognostic marker, however in TNBC it is an uncertain value (Viale et al., 2008). The EGF receptor is part of a transmembrane glycoprotein family with a tyrosine kinase domain and activates pathways important in cell proliferation and apoptosis inhibition. The prevalence of overexpression in TNBC is controversial and ranges from 13-78 %. Targeted therapies do exist, however data from TNBC patients are controversial and EGFR is no confirmed prognostic marker (Gumuskaya et al., 2010). C-KIT (CD117) protein expression is detected in 50 % of patients. It has an important role in cell transformation and differentiation and is particularly interesting because targeted therapy (via imatinib) is a well-established approach in the treatment of other cancer entities such as chronic myeloid leukemia or solid tumors like Gastrointestinal Stromal Tumors (Lopes Da Silva et al., 2020). Angiogenesis signaling is mediated by vascular endothelial growth factors (VEGFs) and is important in the growth and tumor spreading. VEGF is highly expressed in 30-60 % of TNBC

patients (Linderholm et al., 2009) and efficacy of bevacizumab, the humanized monoclonal antibody of VEGF-A has been studied in TNBC. It failed to show improvements in overall survival in phase 3 studies (Miller et al., 2007; Robert et al., 2011). Germline mutations of *BRCA1* and *BRCA2* genes occur in 14-20 % of patients and even more patients have been reported to harbor homologous recombination deficiency (HDR). Both are important in DNA-double strand break repair, which is important in all cells of the body that undergo constant external damage to the DNA apparatus (Jasin and Rothstein, 2013; Sharma et al., 2014; Telli et al., 2016). The tumors are likely to be more sensitive to platinum chemotherapy and PARP inhibitors, like Olaparib (Underhill et al., 2011).

Normal breast tissue usually does not contain immune cells, whereas tumor tissue and surrounding stroma consists of higher levels of immune cell infiltrates (Degnim et al., 2014). TNBC is considered to be one of the most immunogenic breast cancer types and tumor-infiltrating lymphocytes (TILs) are highly expressed in around 20 % of cases (DeNardo and Coussens, 2007; Schmidt et al., 2008). Both, the innate and adaptive immune system are important in the defense against non-self-cells or tumor antigens. Breast cancer cells do express many antigens on the cell membrane, which can activate and stimulate immune cells and thereby induce an immune response. PD-L1 has been reported to be expressed on 15.8-30 % of TNBC cases (Beckers et al., 2016; Ghebeh et al., 2006). It can be measured on tumor cells or on tumor infiltrating immune cells and can be used as a predictive biomarker (Schalper et al., 2014). As described in chapter 1.2.2. large phase 3 clinical studies evaluated the combination of atezolizumab, a PD-L1 inhibitor and nab-paclitaxel as first-line therapy in TNBC showing improvements in overall survival for PD-L1 positive tumors (Impassion130 Trial) (Emens et al., 2021).

Among described signaling pathways, targeted therapies do exist for some of them, however for patients with TNBC cytotoxic chemotherapy remains the mainstay of therapy. PARP inhibitors and checkpoint inhibitors show promising results in clinical trials for TNBC and have been recently incorporated in therapy in some settings (Lopes Da Silva et al., 2020). Nevertheless, a more comprehensive understanding of the disease is needed for the development of more targeted and effective treatment options.

### 1.3. Philadelphia Chromosome-Positive Leukemia

Leukemia is a malignant disease and one of the most common types of cancer worldwide with 250,000 new cases per year. Among children up to 15 years, it makes up 30 % of cancer cases (Avelino et al., 2017). Leukemia is characterized by an abnormal expansion of white blood cells, which are produced in the bone marrow. In rare cases, erythroid precursors can give rise to leukemia as well, the so called acute erythroid leukemia. Cells can spread to other organs like spleen, brain, lymph nodes and other tissues and due to the rise of abnormal cells, healthy cells are diminished (Inamdar and Bueso-Ramos, 2007).

Important biomarkers in leukemia are BCR/ABL (=BCR-ABL1) fusion genes. They are found in all cases of chronic myeloid leukemia (CML) and in up to 30 % of acute lymphoblastic leukemia (ALL). The formation of the fusion gene is a molecular consequence of the Philadelphia (Ph) chromosome, a shortened chromosome 22 resulting from a translocation between long arms of chromosome 9 and 22 in hematopoietic stem cells (presented as  $t(9;22)(q34;q11)$  - shown in the upper panel of figure 5) (Avelino et al., 2017). The Philadelphia chromosome is found in 90 % of CML patients (Rowley, 1973).

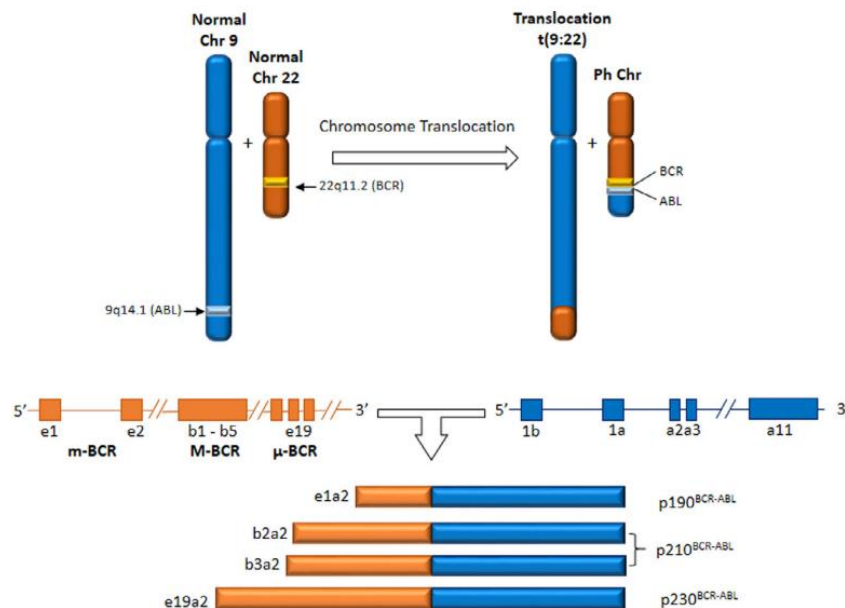


Figure 11: Chromosomal translocation and BCR-ABL protein isoatypes.

(Avelino et al., 2017) (Copyright permission obtained by Creative Common CC BY license).

The resulting BCR/ABL protein is located in the cytoplasm and has a deregulated tyrosine kinase function. Three main isoatypes of the protein with abnormal activity are produced –  $p230^{BCR/ABL}$ ,  $p210^{BCR/ABL}$  and  $p190^{BCR/ABL}$  (=p185) (Figure 11).  $p210^{BCR/ABL}$  is expressed in 95 % of CML cases during stable phase of the disease and in some ALL and AML cases; the p190

is present in 70 % of Ph<sup>+</sup> B-ALL patients and p230 is rarely found (Komorowski et al., 2020; Melo, 1996; Winter et al., 1999). The native ABL1 has a tightly regulated kinase activity, serving as a key hub to control cell cycle and apoptosis. The malignant transformation by BCR/ABL shows constitutive activation of the protein because it loses the N-terminal “cap” – a region with critical autoregulatory domain. Two major mechanisms have been implicated in the transformation of BCR/ABL<sup>+</sup> cells. First, an altered adhesion to bone marrow stroma cells and the extracellular matrix and second, the constitutively active mitogenic signaling and reduced apoptosis (Sattler and Griffin, 2003). In the promotion of CML, pathways like the RAS/RAF/MEK/ERK pathway, the JAK2/STAT pathway and the PI3K/AKT/mTOR pathway are hijacked by BCR/ABL (Mughal et al., 2016; Soverini et al., 2018). Interestingly, the slightly different isoforms (p190 versus p210) show differences in their interactomes, signaling networks and the subcellular localization, although both isoforms contain an intact ABL1-derived kinase domain and show the same autophosphorylation and kinase activation (Cutler et al., 2017; Komorowski et al., 2020; Reckel et al., 2017).

### **1.3.1. Chronic myeloid leukemia (CML)**

CML is a rare disease with 1-2 cases per 100,000 per year and it makes up 15-20 % of all leukemia cases in adults (Hehlmann, 2020; Sawyers, 1999). It was the first human malignancy that could be associated with a chromosomal abnormality, the Philadelphia chromosome, resulting in the deregulated activity of BCR/ABL thereby inducing leukemia. In clinics, patients harbor a leukocytosis, a left shift in the differential count and splenomegaly. The disease has a natural course of 3 phases, namely the initial chronic phase (CP), the intermediate accelerated phase (AP) and the final, fatal blastic phase (BP) (Figure 12). The first chronic phase (CP) lasts for several years and leads to expansion of the myeloid cell compartment; however the cells retain their capacity to differentiate and function normal. Patients have mild symptoms and often are asymptomatic. In the accelerated phase (AP) more immature cells are in the blood. Patients have symptoms and response to therapy is less favorable. This phase can last from weeks to years. The final stage is the blast phase (BP), where immature cells are predominant and survival is measured only in months. There is an increase in genetic instability, either in BCR/ABL itself or in other genes/chromosomes leading to accumulation of genetic/ cytogenetic defects (depicted as “X”, “Y” or “Z” in Figure 12) and the possibility for drug resistance increases substantially (Soverini et al., 2018).

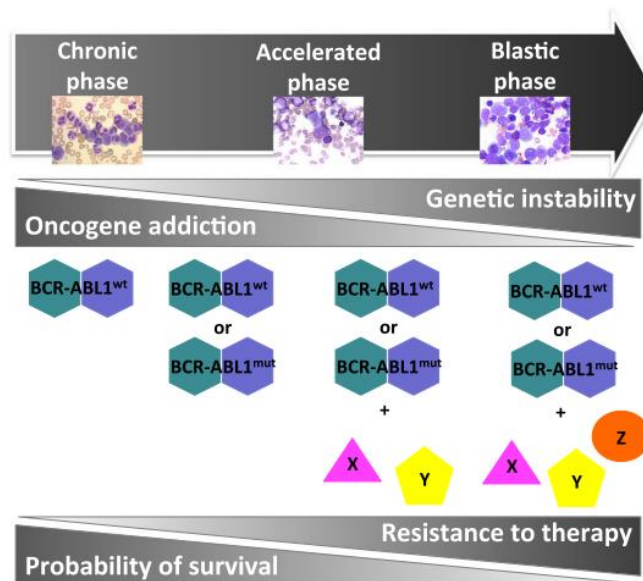


Figure 12: The triphasic course of CML.

The course of CML consists of chronic phase, accelerated phase and blastic phase (Soverini et al., 2018).  
(Copyright permission obtained by Creative Common CC BY license).

### 1.3.2. Acute lymphoblastic leukemia (ALL)

ALL is a rare malignancy of lymphoid T- or B-cell progenitor cells in the bone marrow, blood and extramedullary sites. 75 % of ALL cases develop from B-cell lineage. There is a bimodal distribution with one peak of ALL cases developing in childhood and representing the most common pediatric malignancy and a second peak occurring in patients around 50 years of age. Most of cases, around 80 % develop in children. Treatment of childhood ALL represents a success story with traditional chemotherapy and clinical trial methods leading nowadays to cure rates exceeding 90 %. The prognosis for adults is far worse with an ongoing decline in survival with higher age from adolescence and poor prognosis for all patients with relapse (Salvaris and Fedele, 2021; Terwilliger and Abdul-Hay, 2017). A wide range of genetic lesions have been identified in ALL patients. Among different genetic subtypes for B-ALL is the BCR/ABL fusion gene and Philadelphia chromosome. The prevalence of this subtype is least in Children (with 2-4 %) < AYA (adolescent and young adult) < Adults – where 20-30 % of adult ALL patients harbor it. The prognosis is poor but improved with tyrosine kinase inhibitor (TKI) as a standard therapy (Byun et al., 2017; Salvaris and Fedele, 2021).

In clinics, ALL manifests as an accumulation of malignant poorly differentiated lymphoid cells. Typical symptoms include “B symptoms” (weight loss, fever and night sweats), easy bruising and bleeding, dyspnea, fatigue and infections. Extramedullary sites can be involved leading to lymphadenopathy, splenomegaly or hepatomegaly. Central nervous system (CNS)

involvement may occur as well. As a diagnostic marker the presence of 20 % or more lymphoblasts in blood or bone marrow is established (Terwilliger and Abdul-Hay, 2017).

### 1.3.3. Treatment

Two different strategies are applied to inhibit BCR/ABL, namely ATP-competitive inhibitors and allosteric inhibitors (Figure 13).

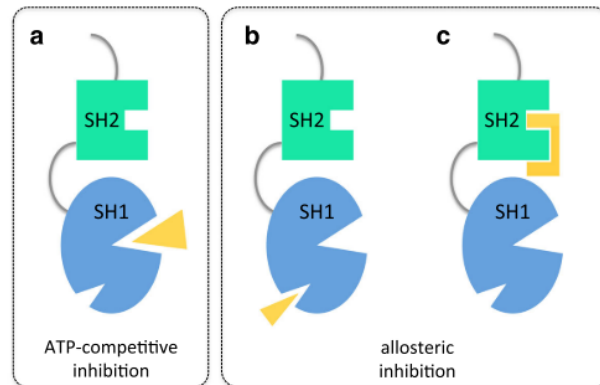


Figure 13: BCR-ABL inhibition strategies.

The two different BCR-ABL inhibition strategies are ATP-competitive and allosteric inhibition (green: SH2 domain, blue: SH1/ kinase domain, yellow: inhibitor) (Soverini et al., 2018). (Copyright permission obtained by Creative Common CC BY license).

ATP-competitive inhibitors bind the kinase domain of the protein, in the cleft between the N-lobe and the C-lobe, where the ATP-binding site is located (Figure 13a). Allosteric inhibitors in contrast, bind to other sites that are important in regulation of the kinase activity. There are small molecules that bind to the hydrophobic pocket in the C-lobe (Figure 13b) or proteins (monobodies) that bind the SH2-kinase interface (Figure 13c) (Soverini et al., 2018).

#### ATP-competitive inhibitors

Imatinib is a 2-phenyl-amino-pyrimidine that was originally named “signal transduction inhibitor 571” (STI571). Its discovery was a big breakthrough – it is a potent ABL1 inhibitor, although it also inhibits other kinases as the PDGFR family and c-KIT (Soverini et al., 2008). Kinases have different activation states. They are either in an active (“open”) or an inactive (“closed”) conformation. The activation usually happens by phosphorylation of a key serine/threonine or tyrosine residue – in the case of ABL1 Tyrosine 393 is phosphorylated allowing substrates to bind. Imatinib selectively binds to the inactive conformation of the kinase (type 2 inhibitor). Thereby it can trap the deregulated BCR/ABL oncoprotein, which results in inhibition of BCR/ABL autophosphorylation and substrate phosphorylation and subsequent in blocking proliferation and inducing apoptosis (Druker et al., 1996; Gambacorti-Passerini et al., 1997).

Compared to prior IFN- $\alpha$  therapy, side effects are minimal, including nausea, myalgia, edema and skin rash. Hematologic and cytogenetic responses are remarkable. Imatinib appears to be a safe and effective therapy and got approved by the FDA in May 2001 and in December 2002 it was approved for first-line use in newly diagnosed CML patients (Johnson et al., 2003).

The problem of drug resistance and still detectable BCR/ABL transcripts in the blood and bone marrow in some patients led to the development of second and third generation tyrosine kinase inhibitors (TKIs). Intrinsic and acquired resistance mechanisms against TKIs are still an issue and can be divided in mutational (ABL1 kinase domain mutations) or non-mutational (BCR-ABL1 independent) changes in leukemic cells. Most studies are based on data received from CML patients. It was found that most common mutational changes are point mutations in T315 of *ABL1* (T315I), also known as the gatekeeper residue. It limits TKI binding and confers resistance to first and second-generation TKIs. On top, the switch to other TKIs can have disadvantages in causing selective pressure on leukemic cells which leads to multi-TKIs resistance. For example, concomitant mutations of T315I, such as D276G or F359V lead to resistance of third generation TKIs (ponatinib) as well. Regarding non-mutational changes, alternative activation of BCR/ABL1 downstream pathways (p.e. JAK/STAT, SRC, MAPK or PI3K) are likely to account for and seem crucial in mediating resistance. Similar mechanisms were also found in Ph<sup>+</sup> B-ALL, as was reported for e.g. RAF/MAPK and AKT/mTOR signaling in conferring imatinib resistance. Additionally, non-mutational TKIs resistance are likely to be mediated by the leukemic microenvironment as e.g. by mesenchymal stem cells (Komorowski et al., 2020).

Of second and third-generation TKIs only four were successful and made it up to FDA and EMA approval (Figure 14) (Soverini et al., 2018).

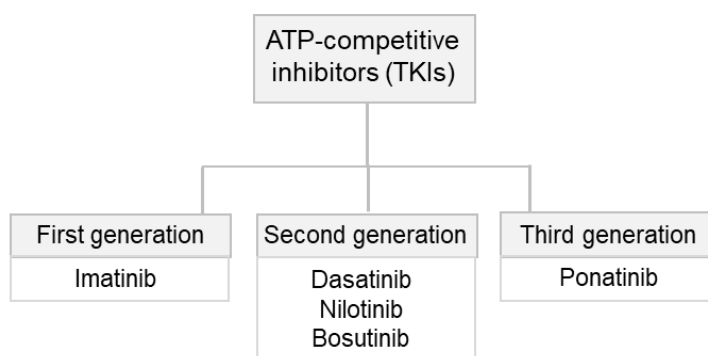


Figure 14: List of approved ATP-competitive inhibitors.

Three generations of TKIs and corresponding members (TKIs: tyrosine kinase inhibitors).

Dasatinib, nilotinib and bosutinib are second generation TKIs. Dasatinib is a thiazolylamino-pyrimidine and in addition to potently inhibiting ABL1 and some other kinases, it inhibits the SRC family kinases. It is around 300-fold more potent against BCR/ABL compared to imatinib and is also able to bind the open kinase conformation (type 1 inhibitor) (Shah et al., 2004). Nilotinib is a phenylamino-pyrimidine derivative, structurally close to imatinib and also binds the inactive conformation of the kinase. It is 20- to 30-fold more potent than imatinib and highly selective for BCR/ABL (Weisberg et al., 2006). Bosutinib, together with dasatinib, belongs to the dual BCR/ABL1 kinase inhibitors and has an *in vitro* 1-log greater potency compared to imatinib (Rensing Rix et al., 2009). Taken together, second-generation TKIs can induce deeper and faster molecular responses and cases who progress from CP to BP can be reduced. However, no significant differences in overall survival could be observed. Using nilotinib and dasatinib, more severe adverse effects and serious complications have been reported. Both are used as a first-line and second or subsequent-line of treatment, bosutinib in contrast as a third-line treatment is only administered in cases where other first and second-generation inhibitors are not appropriate (Soverini et al., 2018).

As a second/ subsequent line of treatment in patients harboring the highly resistant T315I mutation, a third-generation TKI was developed namely ponatinib. It is a type 2 inhibitor that binds its targets in the inactive state. It is active against SRC kinases, indicating medium-range specificity. In contrast to first and second generation TKIs it can bind the kinase domain irrespective of mutations. However, severe complications like thrombosis and heart failure have been reported (Zhou et al., 2011).

### **Allosteric inhibitors**

Several allosteric regions have been identified in the BCR/ABL molecule and are potentially “drugable”. The two compounds GNF-2 and GNF-5 can mimic myristate binding, which is a conformational change in the C-terminal lobe important in keeping the kinase inactive. This region is lost in BCR/ABL, making it a potential drug target. GNF-2 development dropped because of inefficacy against the T315I mutant and GNF-5 (renamed ABL001 or asciminib) reached advanced clinical development including combination studies with nilotinib (Wylie et al., 2017). As a second key regulatory region, the SH2-kinase interface has been identified having a stimulatory effect on kinase activity. Studies tested and synthesized monobodies – single-domain proteins that can bind to a bait protein of interest with very high affinity. Using monobodies binding to the SH2 domain led to inhibition of BCR/ABL kinase activity *in vitro*



and *ex vivo* and furthermore to induction of cell death in CML cell lines – however *in vivo* delivery of monobodies remain a big challenge (Grebien et al., 2011).

Taken together targeting the BCR/ABL oncoprotein is a showcase example for a successful therapeutic avenue towards a fusion kinase. Treatment with TKIs are promising, leading to stable responses with some patients who can discontinue the treatment and are considered cured. However, most of the patients need life-long TKI treatment. Point mutations in the tumor cells facilitate tumor escape mechanisms. These mutations frequently lead to an impairment of TKI binding. The search for novel inhibitors or inhibitory approaches is still of high relevance and ongoing (Soverini et al., 2018).

#### 1.4. Tumor immune surveillance

During cellular division, the DNA replication machinery may make mistakes thereby supporting cancer formation. Luckily, there are numerous **intrinsic and extrinsic tumor-suppressor mechanisms** that prevent the development of cancer cells (Chang and Beatty, 2020; Vesely et al., 2011).

**Intrinsic** tumor-suppressor mechanisms happen within healthy cells and trigger senescence, repair or apoptosis aiming at establishing a potent barrier and preventing transformation (Figure 15, upper part). Cellular senescence can be induced by numerous cellular proteins (e.g. p53) that sense genomic disorders caused by mutagenic insults and also by activated oncogenes. Other mechanisms, including p53 can sense the activity of oncogenes and initiate the programmed cell death machinery. Cell death can as well be triggered in response to cellular stress, injury, lack of survival signals and so on, which results in release of proapoptotic effectors and activates executioner caspases. There are alternative cell death pathways known, such as necrosis, autophagy and mitotic catastrophe that may halt the transformation process of healthy cells (Vesely et al., 2011).

On the other hand, **extrinsic** tumor-suppressor mechanisms of nontransformed cells exist, with the goal to restrict the growth of cancerous cells. There are three commonly accepted **extrinsic** tumor-suppressor mechanisms by which cells and their adjacent tissues sense the presence of cancerous cells and prevent them from invading and spreading to other tissues in the host, as first, disruption of epithelial cell-extracellular matrix association results in cell death. Second, the dysregulation of polarity genes, that control cellular junctions, protect the cell and prevents it from progressing the cell cycle. And last, effector leukocytes of the immune system limit transformation or tumor cell growth (Vesely et al., 2011).

The **immune system** has three roles in the prevention of tumors. First, it eliminates and suppresses viral infections and protects from virus-induced tumors. Further, it eliminates pathogens and dissolves inflammation, preventing an inflammatory environment which would support tumorigenesis. Finally, the immune system can specifically identify and eliminate tumor cells on basis of tumor-specific antigens (TSAs) expressed on tumor cells. This process is called “cancer immunosurveillance” and occurs when the immune system identifies transformed cells that have escaped cell-intrinsic tumor-suppressor mechanisms and eliminates them before they can establish malignancy (Zitvogel et al., 2006). The innate and adaptive immune cell types, effector molecules and pathways collectively act together, each of them having a specific mechanism of action to control tumor targets.

Observations in cancer mouse models and patients revealed that the immune system not only protects the host against malignant formation, but also edits tumor immunogenicity. This concept is called “cancer immunoediting” and is a refinement of the cancer immunosurveillance concept, considering that immunity is a dynamic process with dual host-protective and tumor-sculpting actions. Cancer immunoediting is composed of 3 phases: elimination, equilibrium, and escape, described in detail in the following chapter (Dunn et al., 2002; Schreiber et al., 2011).

#### 1.4.1. Cancer immunoediting

The first phase of cancer immunoediting is the **elimination phase**. Molecules and cells of both innate and adaptive immunity work together to locate, recognize and directly destroy nascent transformed cells and prevent the development of malignancy. Involved immune cells include natural killer (NK) cells, T cells, natural killer T (NKT) cells,  $\gamma\delta$  T cells, macrophages, and dendritic cells (DC), along with effector molecules, including TRAIL and perforin and cytokines IFN- $\gamma$ , IL-12 and type I IFNs (Figure 15). Knowledge is inferred from studies in mouse models which are deficient for certain cytokines, molecules, or immune cell subsets. They revealed earlier onset of disease or a higher penetrance of neoplasia. This was mainly done in gene-targeted mice or by using neutralizing monoclonal antibodies (mAbs) (Schreiber et al., 2011; Shankaran et al., 2001; Swann and Smyth, 2007; Vesely et al., 2011).

If the antitumor immunity of the host is unable to completely eliminate transformed cells, there is progress into the next phase – the **equilibrium phase** or cancer persistence/ dormancy – the longest of the immunoediting phases. Historically, the term “tumor dormancy” described the status of a latent tumor, which is present in patients for decades and may be re-occur as a local lesion or distant metastases (Aguirre-Ghiso, 2007). The tumor cells in the equilibrium phase are still controlled by components of the immune system. Studies support that the adaptive immunity (but not the innate immunity) is responsible in this phase. Tumor cells and the immune system are in a dynamic balance in the host – an antitumor immunity is present but fails to fully eradicate the transformed cells. Some of the tumor cells become capable of evading the immune system, a heterogenous population of tumor cells arises. The selective pressure provided by the immune system selects for tumor cells with the most immune-evasive mutations. Eventually, these cells initiate the disease outbreak. The last phase of immunoediting, the **escape phase** (Figure 15) has started. Tumor cells can grow in an immunological unrestricted manner as the immune system fails to either eliminate or control transformed cells. Additionally, cancer cells undergo genetic and epigenetic changes to

circumvent both, the innate and adaptive immune system, which in turn also contributes in selecting more aggressive tumor variants. A lot of escape mechanisms exist and can be categorized in two groups. On the one hand there are cell-autonomous modifications of tumor cells to directly evade immune recognition and elimination, or on the other hand, tumor cells effect immune cells and modify them to generate an immunosuppressive surrounding (Chang and Beatty, 2020; Schreiber et al., 2011; Vesely and Schreiber, 2013; Vesely et al., 2011). The concept of cancer immunoediting is graphically illustrated in Figure 15.

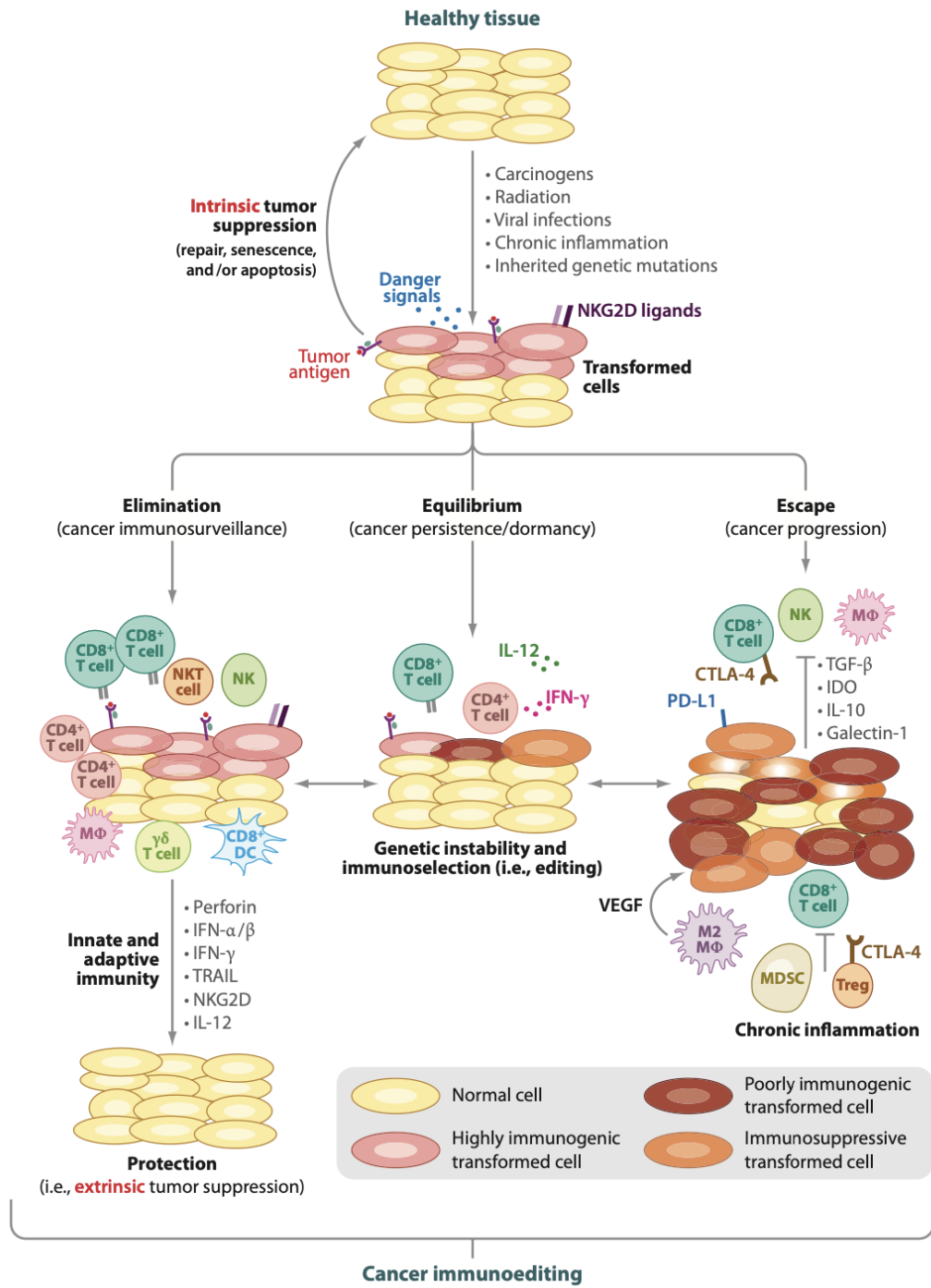


Figure 15: Cancer immunoediting.

The different phases of cancer immunoediting and involved immune cell subsets (Vesely et al., 2011). (Copyright permission obtained by Copyright Clearance Center, License number: 1184904).

### 1.4.2. The innate and adaptive immune system

The immune system can be roughly divided into the innate and adaptive part with an extensive crosstalk between them. The **innate immune system** serves as a first line of defense against infections by having germ-line encoded pattern-recognition receptors and other cell-surface molecules allowing to quickly detect microbial components and thereby orchestrating inflammation (Dranoff, 2004). It includes soluble factors, such as complement proteins – plasma proteins, which are activated as a proteolytic cascade. They function to coat the surface of microbes which leads to their lysis or phagocytosis. Further the innate part consists of several cellular effectors, such as granulocytes, mast cells, macrophages, dendritic cells (DCs), natural killer (NK) cells and the recently discovered family of innate lymphoid cells (ILC) 1-3 (Figure 16) (Mariotti et al., 2019).

The **adaptive immune system**, by contrast consists of B cells, producing antibodies and T cells, consisting of CD4<sup>+</sup>, CD8<sup>+</sup> and regulatory T cells. Its development is more time-consuming, as it first requires the expansion of rare lymphocytes that have somatically rearranged a T-cell receptor or immunoglobulin molecules that are highly specific for either microbial-derived proteins or processed peptides presented via major histocompatibility complex (MHC) molecules. There are further two cell types, natural killer T (NKT) cells and  $\gamma\delta$  T cells that function at the intersection of both parts of the immune system (Figure 16) (Dranoff, 2004).

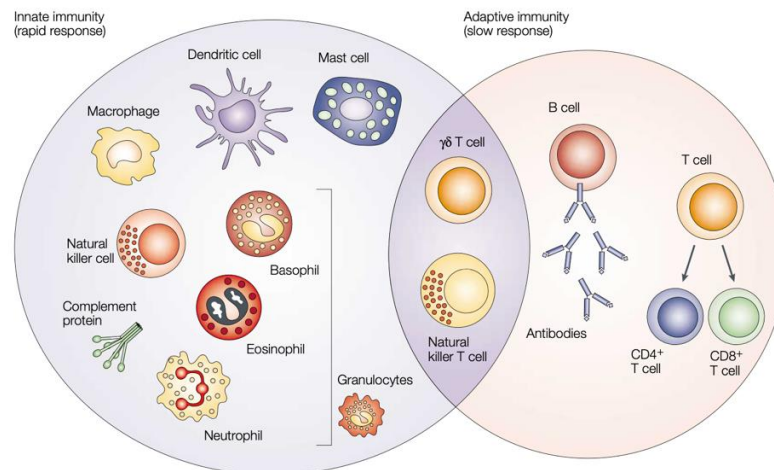


Figure 16: The innate and adaptive immune response.

Summary of innate and adaptive immunity and involved immune cell subsets (Dranoff, 2004). (Copyright permission obtained by Copyright Clearance Center, License number: 5240860203036).

**Recognition of cancer cells**

Two main mechanisms are involved in the recognition of cancer cells (Figure 17). First, innate immune cells use pattern-recognition receptors or other cell-surface molecules to directly detect tumor cells. Cancer cells often express stress-related genes, such as MICA and MICB (in humans) – ligands for NKG2D receptors on NK cells, cytotoxic lymphocytes (CTLs) and phagocytes (Diefenbach and Raulet, 2002). DCs can use integrins and CD36 to bind and phagocyte apoptotic tumor cells. Macrophages and DCs can also use scavenger receptors and CD91 to ingest complexes of heat-shock proteins (HSPs) with tumor-derived peptides. HSPs are released from necrotic cancer cells (Figure 17a). Secondly and in contrast, adaptive immune cells use an indirect pathway of cancer recognition, called cross-priming by DCs (Figure 17b). Co-stimulatory signals for T-cell activation are not expressed by tumor cells, therefore DCs need to stimulate them. Tumor cells or debris are usually captured by DCs, subsequently they migrate to regional lymph nodes and process the material onto CD1D for presentation to NKT cells and onto MHC class I and MHC class II molecules for presentation to CD8<sup>+</sup> and CD4<sup>+</sup> T cells. Further DCs express co-stimulatory molecules B7-1 and B7-2 to boost T-cell activation and secrete IL-12 and IL-18 to activate T helper 1 (TH1), CD4<sup>+</sup> T-cell responses and cytotoxic CD8<sup>+</sup> T cells. DC maturation gets stimulated through CD40 signaling, the CD40 ligand in turn, is expressed on activated CD4<sup>+</sup> T cells and NKT cells. B cells produce antibodies that are reactive with tumor proteins and get triggered among others by CD4<sup>+</sup> T cells and DCs (Figure 17b) (Dranoff, 2004).

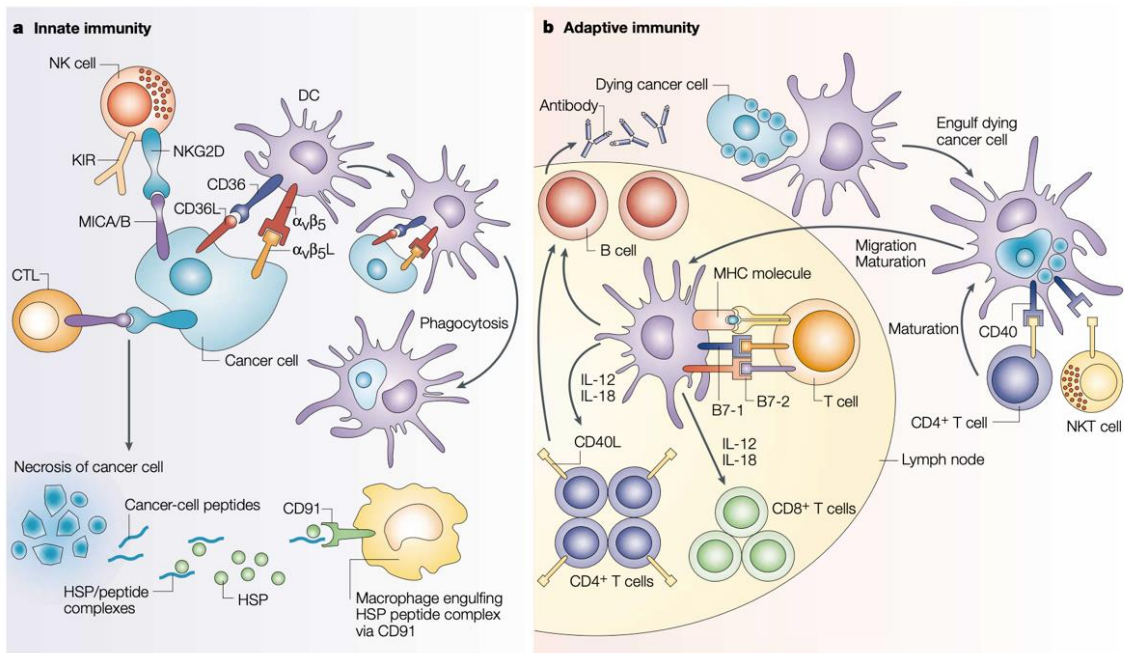


Figure 17: Mechanisms of cancer recognition by the innate and adaptive immune system.

(Dranoff, 2004) (Copyright permission obtained by Copyright Clearance Center, License number: 5240860203036).

### 1.4.3. Natural killer (NK) cell mediated tumor immune surveillance

On basis of their morphology, expression of lymphoid markers and their origin from the common lymphoid progenitor cell in the bone marrow NK cells are classified as lymphocytes. They are components of the innate immune system because of their constitutive cytolytic function and lack of antigen-specific cell surface receptors. In mice and humans NK cells participate in the early control against virus infections and in tumor immunosurveillance (Smyth et al., 2002). Additionally, they contribute to embryonal development, as they have the special capacity to invade the uterus (Moffett-King, 2002).

As cytolytic effector lymphocytes NK cells directly induce death of virus-infected cells and tumor cells. They produce various cytokines and chemokines which are important to crosstalk with other hematopoietic cells. NK cells are major producer of cytokines such as  $IFN\gamma$  in physiological and pathological settings. This helps to shape T-cell responses in lymph nodes by a direct interaction of naïve T cells and NK cells, which then migrate to lymphoid organs or by indirect effects on DCs (Figure 18) (Martín-Fontecha et al., 2004). Further, NK cells produce proinflammatory and immunosuppressive cytokines, such as  $TNF\alpha$  or IL-10. In many conditions NK cells are biased to produce  $IFN\gamma$ , however there are situations of systemic or chronic inflammation that promote IL-10 secretion. The subsequent immune response gets



shaped – NK cells either dampen or boost T-cell and macrophage responses through these cytokines (Figure 18, IFN $\gamma$ -green or IL10-red arrows). Additionally, NK cells produce growth factors, such as GM-CSF, G-CSF and IL-3 and secrete chemokines such as CCL2-5, XCL1, CXCL8 (IL-8). They are important for NK cells to colocalize with other cells, such as DCs in inflammation (Bottino et al., 2005; Walzer et al., 2005).

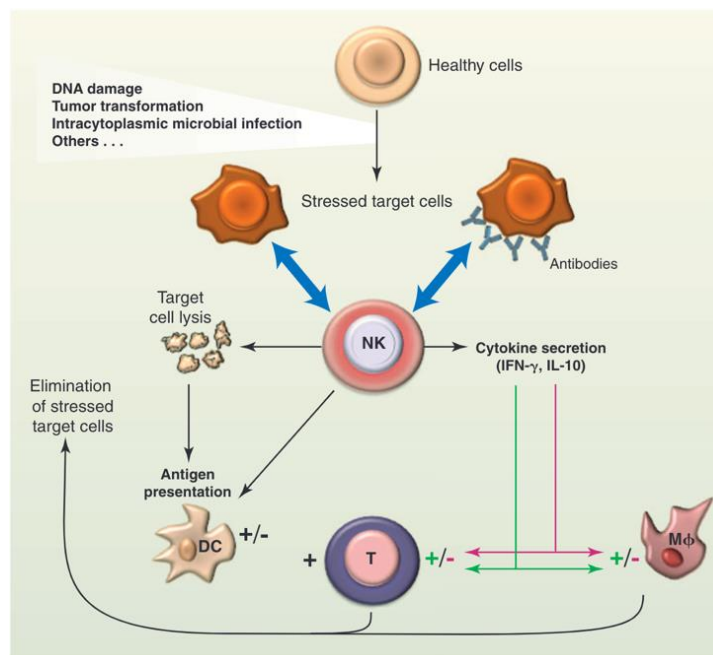


Figure 18: Biological functions of natural killer cells.

(Vivier et al., 2011) (Copyright permission obtained by Copyright Clearance Center, License number: 1184916).

NK cell-mediated cytotoxicity and cytokine production impacts other cell types, equipping NK cells also with regulatory functions. These interactions between NK cells and other immune response components are tightly regulated. To achieve full effector potential, NK cells vice versa require priming by different factors, such as IL-15, which is presented by macrophages or DCs, IL12 or IL-18 (Chaix et al., 2008; Guia et al., 2008; Lucas et al., 2007; Mortier et al., 2009). Summarized, NK cells participate in immunity in many different ways and they undergo a process of functional maturation to achieve all of their functions.

Regulation of NK cells occurs via a plethora of receptors, which are either **activating receptors**, stimulating NK cell reactivity, or **inhibitory receptors** that dampen the NK cell activity (Bottino et al., 2005; Bryceson et al., 2006; Vivier et al., 2004). The group of activating receptors include surface proteins that interact with soluble ligands such as cytokines or other cell surface molecules. Cytokine receptors such as IL-15R, IL-2R and IL-21R are involved in NK cell development and effector functions. Especially IL-15 is important for maturation and

survival, and IL-1R in humans/ IL-18R in mouse for maturation of NK cells (Chaix et al., 2008; Hughes et al., 2010).

In conditions of cellular stress self-molecules can be induced, such as ligands for NKG2D. They are expressed at low levels in some tissues, most normal cells, however, do not express substantial levels of NKG2D ligands on their cell surface. Upon cellular distress, for example after the initiation of the DNA damage response, their surface expression is enhanced. Furthermore, most tumor cell lines express one or more ligands for NKG2D and many primary human tumors. The activating receptor NKG2D on NK cells interacts with those ligands (Raulet and Guerra, 2009). NK cells also detect a lack of MHC class I molecules, called “missing self”, which occurs when cells are perturbed by transformation or infection. They express MHC class I-specific inhibitory receptors, like killer cell immunoglobulin-like receptors (KIRs) in humans, lectin-like Ly49 molecules and CD94/NKG2A heterodimers in both, humans and mice, by which they recognize the lack of MHC class I molecules. Taken together, NK cells sense the density of different cell surface molecules that are expressed on the surface of interacting cells. Healthy cells do express MHC class I molecules and low amount of stress-induced self-molecules – therefore NK cells repress them (Figure 19A). They selectively kill target cells which are “in distress” by downregulating MHC class I molecules or upregulating NKG2D ligands (Figure 19B) (Raulet and Guerra, 2009).

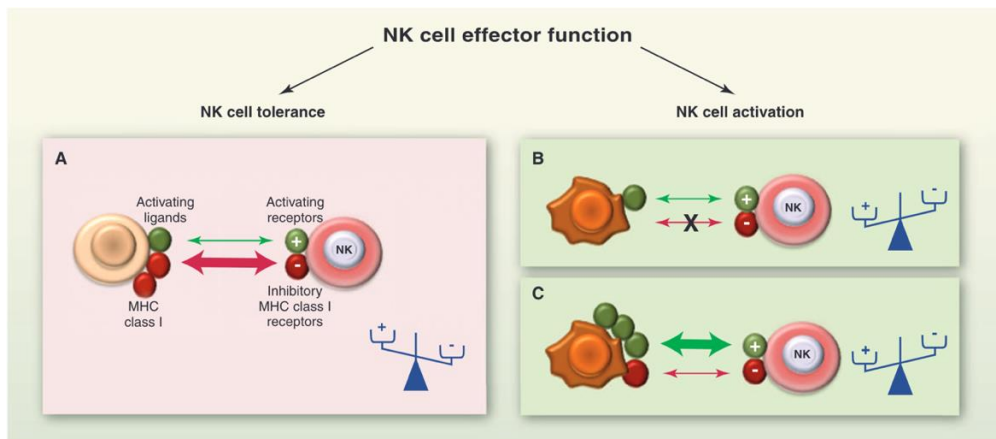


Figure 19: NK cell effector functions.

NK cell effector functions are dynamically regulated, leading to NK cell tolerance (left) or NK cell activation (right) (Vivier et al., 2011). (Copyright permission obtained by Copyright Clearance Center, License number: 1184916).

#### 1.4.4. NK cells in the immunosurveillance of metastasis

Metastatic spread of malignant cells is governed by cancer-cell-intrinsic mechanisms which allow for epithelial-to-mesenchymal transition (EMT). This process includes a series of events summarized as the “metastatic cascade”. Briefly, this includes invasion of the local microenvironment, reaching the circulation and colonizing distant anatomical sites. Importantly, considerable influence comes from microenvironmental and systemic processes. Further, immune cells - and in particular NK cells - control metastatic dissemination (Cerwenka and Lanier, 2016; Guillerey et al., 2016; Peinado et al., 2017). Human and mouse metastatic melanoma cells are killed by NK cells *in vitro* and *in vivo* due to their overexpression of ligands for NKp44, NKp46 and DNAM-1, (Lakshmikanth et al., 2009). In line, EMT has been linked to upregulation of different NKG2D ligands coupled to the loss of ligands for NK cell inhibitory receptors (NKIR) such as E-cadherin, rendering metastatic cells susceptible to recognition and elimination by NK cells (Li et al., 2009; Lopez-Soto et al., 2013).

Extensive preclinical literature further linked an increase in metastatic colonization with a decrease in NK cell number or level of activity, as concluded from studies in different engineered mouse models harboring molecular defects or the use of pharmacological agents. Vice versa, robust protection against metastasis have been shown upon interventions that boost NK cell effector functions. For example, mice with a selective deletion of *Mcl1* in NKp46<sup>+</sup> NK cells (leading to a loss of circulating and tissue-infiltrating NK cells) rapidly develop pulmonary, bone and hepatic metastasis upon challenge with B16F10 melanoma cells. Their wildtype (wt) counterparts accumulate no metastasis at all (Sathe et al., 2014). Adoptive transfer of *Cish*<sup>-/-</sup> NK cells (displaying a hyperactive phenotype) efficiently rescues such an increased sensitivity of mice (Putz et al., 2017). In line, specific NK-cell depleting antibodies markedly increases the metastatic burden in immunocompetent mice upon inoculation with cancer cell lines. Likewise, inactivation of cytotoxic NK cell effector molecules (like IFN $\gamma$ ) by gene knockout renders mice more sensitive to metastatic disease (López-Soto et al., 2017). Trafficking of NK cells is an important determinant of their anti-metastatic functions. Profound alterations in trafficking of NK cells to peripheral organs were found in mice carrying an NK-cell-specific phosphatase and tensin homolog (*Pten*) deletion. Increased metastatic burden in lungs of mice has been documented upon B16F10 melanoma cells inoculation (Leong et al., 2015). Along these results, deletion of zinc finger E-box binding homeobox 2 (*Zeb2*) from NKp46<sup>+</sup> NK cells reduces the pool of NK cells in multiple organs, rendering the mice more susceptible to metastatic lung colonization by melanoma cells (van Helden et al., 2015). Several signaling pathways are involved in the regulation of NK cell functions. Studies could

show involvement of the JAK-STAT signaling pathway as for example the treatment with Ruxolitinib (a JAK1/2 inhibitor) has an impact on the metastatic burden of mice. Inoculation of E0771 or 4T1 mammary carcinoma cells in mice in combination with Ruxolitinib administration leads to increased metastatic burden (Bottos et al., 2016).

Additionally, observations in the clinics reveal an inverse correlation between high levels of circulating and tumor-infiltrating NK cells and the presence of metastasis at clinical presentation. This correlation was found in patients with gastrointestinal sarcoma (GIST) (Delahaye et al., 2011), gastric (Ishigami et al., 2000), colorectal (Coca et al., 1997), renal (Donskov and Von Der Maase, 2006) and prostate carcinomas (Gannon et al., 2009). Additionally, high expression of NK cell activating receptors on the cell surface or enhanced NK cell cytotoxicity were linked to good prognosis in different cohorts of cancer patients who suffered from a metastatic disease or were at risk of doing so. For example, patients suffering from primary prostate carcinoma infiltrated with NK cells that expressed high levels of NKG2D and NKp46 levels did not develop metastasis one year after surgery (Pasero et al., 2016).

Independent of MHC-mediated antigen presentation, NK cell activity in the control of metastasis is regulated via three pathways. They release pre-formed granules which contain the lytic enzymes perforin and granzyme B, secrete IFN $\gamma$  or they expose death receptor ligands, including FASLG and TRAIL (Morvan and Lanier, 2016). To get full NK cell activation, the intracellular phosphorylation-dependent signal cascade gets inhibited or activated by regulation of inhibitory and activating receptors at the plasma membrane. Inhibitory and activating receptors may also have overlapping ligand specificity, as e.g. the poliovirus receptor (PVR, also known as CD155) and NECTIN2 (CD112), which can bind DNAM-1 to stimulate NK cell effector functions or CD96, TIGIT or CD112R exerting inhibitory activity (Chan et al., 2014; Stanietsky et al., 2009; Zhu et al., 2016). Effector functions of NK cells are finely regulated, to allow rapid activation against infected, damaged, or malignant cells, but also signals to prevent autoimmune reactions against healthy tissues (López-Soto et al., 2017). Taken together, normal cells and some malignant cells express various inhibitory receptors (NKIRs), which suppress the activation of NK cells (Figure 20A). Potentially metastatic cancer cells and cells who underwent EMT, lose the expression of ligands for inhibitory receptors and upregulate ligands for activating receptors (NKARs) by which NK cells in turn get activated and mediate anti-metastatic effects (Figure 20B) (López-Soto et al., 2017).

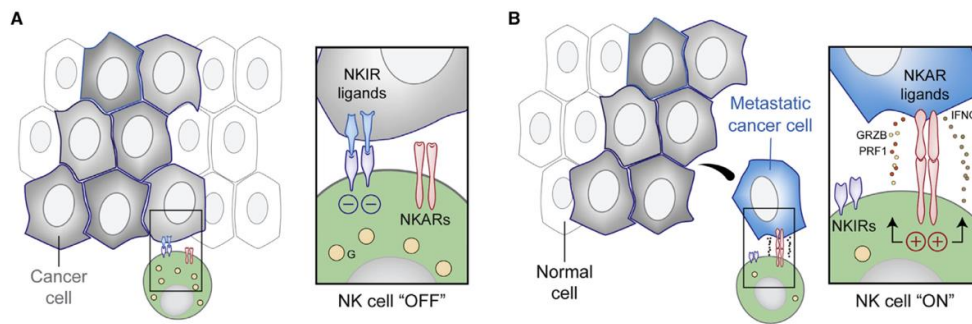


Figure 20: Immunoregulation of Metastasis by NK Cells.

(López-Soto et al., 2017) (Copyright permission obtained by Copyright Clearance Center, License number: 5240840529678).

In contrast, the precise role of NK cells in immunosurveillance of primary solid tumors is still unclear, demanding further research. In the control of hematological malignancies, including leukemia and lymphoma, NK cells reportedly have a prominent role (Ilander et al., 2017; Street et al., 2004). However, in primary solid tumor growth, the involvement of NK cells in physiological settings remains a matter of debate. *In vivo*, it was reported that in the absence of adaptive immunity, NK cells shape developing tumors (O'Sullivan et al., 2012). *In vitro*, different cancer cell lines are killed by NK cells including malignant cells with stem-cell like features, irrespective of their histological origin (primary tumor versus metastatic lesions) (Ames et al., 2015; Castriconi et al., 2009; Talerico et al., 2013). In immunological infiltrates of most solid tumors in humans, NK cells are a minor fraction and their presence is of limited prognostic value compared to those of other tumor-infiltrating lymphocytes (López-Soto et al., 2017; Senovilla et al., 2012). Current literature suggests a prominent part of NK cells in metastasis control and remains ambiguous regarding precise roles in the immunosurveillance of solid tumors.

## 2. Manuscripts

### 2.1. Prologue

The first indication for the oncogenic role of CDK8 came from colorectal cancer and was later extended to other cancer entities, including melanoma, breast cancer, pancreatic cancer and acute myeloid leukemia.

In the following study we found an essential role for CDK8 in triple-negative breast cancer (TNBC) cells, especially in regulating their invasiveness and metastatic capacity. Additionally, we observed CDK8 to be involved in driving cancer-intrinsic immune evasion mechanisms by regulating crucial immune checkpoints. We show that knockdown of CDK8 in murine TNBC cells impairs tumor regrowth after surgical removal and prevents metastasis formation *in vivo*. Differential gene expression analysis confirmed that CDK8 drives EMT in a kinase-independent manner and that it controls NK-cell-mediated immune evasion in TNBC cells. Our *in vitro* and *in vivo* experiments confirm this finding. On top, we pioneered and describe an axis between CDK8 and PD-L1 in mouse and human TNBC cells.

In summary, we identified CDK8 as a critical regulator of tumorigenesis and describe it as a novel immune checkpoint - providing a rationale for studying a CDK8-directed therapy for TNBC.

This research was originally published in Cell Death & Disease:

**Vanessa M. Knab**, Dagmar Gotthardt, Klara Klein, Reinhard Grausenburger, Gerwin Heller, Ingeborg Menzl, Daniela Prinz, Jana Trifinopoulos, Julia List, Daniela Fux, Agnieszka Witalisz-Siepracka, Veronika Sexl. **Triple-negative breast cancer cells rely on kinase-independent functions of CDK8 to evade NK-cell-mediated tumor surveillance.** *Cell Death & Disease* 12, 991 (2021) <https://www.nature.com/articles/s41419-021-04279-2.pdf>

#### Author contributions

V.S. and D.F. supervised the study. V.S., D.F. and D.G. provided reagents and material. V.M.K., K.K., D.G., and A.W.S. designed and analyzed the experiments; V.M.K., K.K., I.M., D.P., J.T., and J.L. performed the experiments. R.G. and G.H. performed bioinformatics analysis. V.M.K., K.K., D.G., A.W.S., and V.S. wrote the paper.

## 2.1.1. Triple-negative breast cancer cells rely on kinase-independent functions of CDK8 to evade NK-cell-mediated tumor surveillance

CDDpress

www.nature.com/cddis

ARTICLE OPEN



### Triple-negative breast cancer cells rely on kinase-independent functions of CDK8 to evade NK-cell-mediated tumor surveillance

Vanessa Maria Knab<sup>1</sup>, Dagmar Gotthardt<sup>1</sup>, Klara Klein<sup>1</sup>, Reinhard Grausenburger<sup>1</sup>, Gerwin Heller<sup>1,2,3</sup>, Ingeborg Menzl<sup>1</sup>, Daniela Prinz<sup>1</sup>, Jana Trifinopoulos<sup>1</sup>, Julia List<sup>1</sup>, Daniela Fux<sup>1</sup>, Agnieszka Witalisz-Siepracka<sup>1</sup> and Veronika Sexl<sup>1,3</sup>

© The Author(s) 2021

Triple-negative breast cancer (TNBC) is an aggressive malignant disease that is responsible for approximately 15% of breast cancers. The standard of care relies on surgery and chemotherapy but the prognosis is poor and there is an urgent need for new therapeutic strategies. Recent *in silico* studies have revealed an inverse correlation between recurrence-free survival and the level of cyclin-dependent kinase 8 (CDK8) in breast cancer patients. CDK8 is known to have a role in natural killer (NK) cell cytotoxicity, but its function in TNBC progression and immune cell recognition or escape has not been investigated. We have used a murine model of orthotopic breast cancer to study the tumor-intrinsic role of CDK8 in TNBC. Knockdown of CDK8 in TNBC cells impairs tumor regrowth upon surgical removal and prevents metastasis. In the absence of CDK8, the epithelial-to-mesenchymal transition (EMT) is impaired and immune-mediated tumor-cell clearance is facilitated. CDK8 drives EMT in TNBC cells in a kinase-independent manner. *In vivo* experiments have confirmed that CDK8 is a crucial regulator of NK-cell-mediated immune evasion in TNBC. The studies also show that CDK8 is involved in regulating the checkpoint inhibitor programmed death-ligand 1 (PD-L1). The CDK8–PD-L1 axis is found in mouse and human TNBC cells, underlining the importance of CDK8-driven immune cell evasion in these highly aggressive breast cancer cells. Our data link CDK8 to PD-L1 expression and provide a rationale for investigating the possibility of CDK8-directed therapy for TNBC.

*Cell Death and Disease* (2021)12:991; <https://doi.org/10.1038/s41419-021-04279-2>

#### INTRODUCTION

Triple-negative breast cancer (TNBC) cells lack the expression of estrogen and progesterone receptors, with normal human epidermal growth factor receptor type 2 (HER2) gene copy number and expression. TNBC accounts for approximately 15–20% of all breast cancers with high prevalence in young and African-American women. It is an aggressive disease with a high risk of relapse and mortality. Compared to other breast cancer subtypes, visceral metastasis formation is frequent and involves lung, bone, and brain [1–3]. Chemotherapy is the current standard-of-care treatment of TNBC in adjuvant, neoadjuvant, and metastatic settings. Although TNBCs are highly sensitive to chemotherapy, the frequent occurrence of relapse enforces the search and evaluation of novel therapeutic approaches [2].

*In silico* investigations of patient samples revealed an inverse correlation between recurrence-free survival and cyclin-dependent kinase 8 (CDK8) levels in various breast cancer types, however, a correlation separately for TNBC patients has not yet been reported [4–6]. CDK8 and its close homologue CDK19 are serine/threonine kinases and key players in transcriptional regulation. They form the kinase module of the Mediator complex, together with Cyclin C, MED12, and MED13 [7, 8]. The

CDK8 submodule has as well been described to directly phosphorylate signaling molecules, including members of the Janus kinase and signal transducer and activator of transcription (JAK-STAT) pathway [9], transforming growth factor- $\beta$  (TGF- $\beta$ ), and bone morphogenetic protein (BMP) receptor signaling [10]. By utilizing the JAK-STAT pathway, CDK8 can interfere and regulate immune responses [9]. A function of the CDK8-STAT1 axis was also reported in natural killer (NK) cells—showing that knockdown of CDK8 within NK cells enhances their cytotoxicity *in vitro* and *in vivo* by increasing the expression of lytic molecules [11]. Paradoxically, deletion of CDK8 in NK cells partially recapitulates the enhanced NK-cell-mediated cytotoxicity, but STAT1-S727 phosphorylation is unaltered in CDK8-deficient NK cells, presumably due to a compensatory function of CDK19 [12]. The use of a specific CDK8/CDK19 inhibitor showed supportive results that this effect is dependent on the kinase activity of CDK8 and the same study provides evidence that combination treatments with either anti-programmed death 1 (PD-1) monoclonal antibodies in a colorectal cancer model or SMAC mimetic in a breast cancer model increase the survival of mice [13].

In T cells, CDK8/CDK19 kinase inhibition induces the conversion of conventional T cells to regulatory T cells, enhancing antitumor

<sup>1</sup>Institute of Pharmacology and Toxicology, University of Veterinary Medicine, Vienna, Austria. <sup>2</sup>Department of Medicine I, Medical University of Vienna, Vienna, Austria. <sup>3</sup>Comprehensive Cancer Center, Vienna, Austria. ✉email: veronika.sexl@vetmeduni.ac.at  
Edited by Professor Hans-Uwe Simon

Received: 30 July 2021 Revised: 24 September 2021 Accepted: 4 October 2021  
Published online: 23 October 2021



2

surveillance and highlighting a role of CDK8/CDK19 in the repression of forkhead box protein P3 (FOXP3) [14].

Additionally, CDK8 has been identified as an oncogenic driver in a variety of cancer types including melanoma, colorectal cancer, and hematological malignancies [4, 6, 15, 16].

A recent study describes CDK8 as a potential therapeutic target in estrogen receptor (ER)-positive breast cancer cells, showing that

estrogen-induced transcription depends on CDK8 kinase activity. Chemical inhibition of CDK8/CDK19 or genetic knockdown of CDK8 impaired cell growth and progression of this breast cancer type in vitro and in vivo [17].

Moreover, it has been shown that CDK8 contributes to epithelial-to-mesenchymal transition (EMT), a process which plays

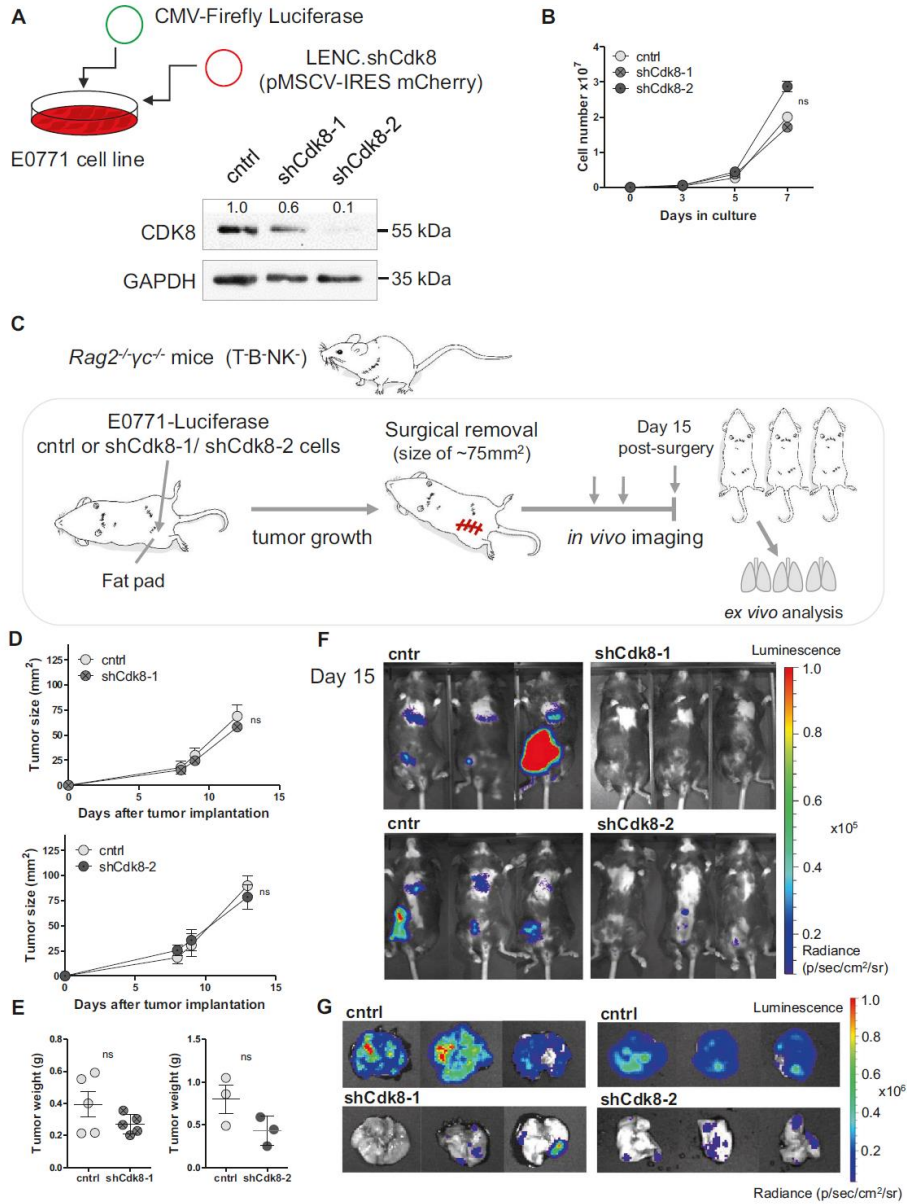




**Fig. 1** **CDK8 supports the regrowth of tumors and distant metastasis formation.** **A** TNBC E0771 cells were stably infected with a CMV-Firefly Luciferase construct and subsequently with two different CDK8-targeting shRNAs (shCdk8-1 and -2) or a control shRNA (cntrl), and the expression of CDK8 and GAPDH was analyzed by western blot. **B** Proliferation of E0771 cell lines infected with shCdk8-1, shCdk8-2 and the control cell line was assessed on day 3, 5, and 7 by flow cytometry. Symbols and error bars represent cell numbers in mean  $\pm$  SEM of  $n = 3$  technical replicates. **C** Experimental setup of experiments from (D–G) is shown. *Rag2*<sup>-/-</sup>*yc*<sup>-/-</sup> mice were orthotopically transplanted with E0771 control, shCdk8-1, or shCdk8-2 cells (in independent experiments) and monitored for primary tumor growth. Tumors were surgically removed and regrowth and distant metastasis of tumor cells was monitored with in vivo imaging. **D** Primary tumor growth of control vs. shCdk8-1 or shCdk8-2 implanted mice, and **E** tumor weight of mice at operation. Symbols and error bars represent tumor area (mm<sup>2</sup>) in mean  $\pm$  SEM. **F, G** Representative in vivo-imaging pictures of mice (**F**) and ex vivo lungs (**G**) of two independent experiments with either shCdk8-1 or shCdk8-2 compared to control, at day 15 post surgery ( $n = 3$ –5 mice per group).

an important role in invasion and metastasis of breast cancer cells [18–20].

We here show that tumor-intrinsic CDK8 regulates invasiveness and metastatic capacity of TNBC cells and shields the tumor cells from NK-cell-mediated recognition and killing in a kinase-independent manner. These data suggest that CDK8 not only represses perforin and granzyme production, and thereby hampers NK-cell cytotoxicity, but also drives cancer-intrinsic immune evasion by regulating crucial immune checkpoints. We describe a novel CDK8–PD-L1 (programmed death-ligand 1) axis, which might provide a mechanistic explanation for the CDK8-driven NK-cell evasion and is of utmost therapeutic relevance as PD-L1/PD-1 blocking antibodies show promising results in clinical trials of TNBC patients. In summary, we identify CDK8 as an important regulator of tumorigenesis and describe it as a novel immune checkpoint in TNBC.

## RESULTS

### CDK8 promotes regrowth of tumors and distant metastasis formation

To study the role of CDK8 in TNBC, we used shRNA-mediated knockdown of CDK8 in murine TNBC E0771 cells [21]. Immunoblotting confirmed the decreased CDK8 levels with two different hairpins to a varying extent (shCdk8-1 and shCdk8-2) (Fig. 1A). We did not detect any changes in proliferation (Fig. 1B), cell cycle distribution (Supplementary Fig. S1A), or survival upon CDK8 knockdown in vitro (Supplementary Fig. S1B).

To study primary tumor growth and metastasis formation in vivo, we used a well-established orthotopic breast cancer model [22] and transplanted Luciferase-expressing E0771 cells into the mammary fat pad of immunocompromised recombination activating gene 2 and interleukin 2 receptor gamma chain double knockout (*Rag2*<sup>-/-</sup>*yc*<sup>-/-</sup>) mice. When the primary tumor reached an area of 75 mm<sup>2</sup>, it was surgically removed and we followed disease progression by live imaging (Fig. 1C). In accordance with the unaltered cell proliferation in vitro, we did not observe any significant difference in primary tumor growth and weight irrespective of the expression of CDK8 (Fig. 1D, E). Persistent knockdown of CDK8 was confirmed in lysates from primary tumors (Supplementary Fig. S2A). CDK8-expressing cells gave rise to increasing Luciferase signals from day 9 to 15 post surgery at the site of injection, indicative of the regrowth of the tumor. In contrast, no Luciferase signals were detectable in mice that had received shCdk8-1 or shCdk8-2 knockdown cells (Fig. 1F and Supplementary Fig. S2B). At day 15 post surgery, the animals were sacrificed and analyzed for lung metastasis. Substantial metastatic spreading to the lungs had occurred upon injection with wild-type E0771 cells, while lung metastasis was significantly reduced in the absence of CDK8 (Fig. 1G and Supplementary Fig. S2C, D). This led us to conclude that tumor-intrinsic CDK8 promotes regrowth of tumors and distant metastasis formation in the orthotopic TNBC mouse model.

### Metastasis-related genes are deregulated upon CDK8 knockdown

To gain insights into how CDK8 promotes the metastatic potential of murine TNBC, we performed RNA sequencing (RNA-seq) and

compared gene expression of E0771 control (cntrl), shCdk8-1, and shCdk8-2 cells. We included cntrl cells treated with the CDK8/CDK19 inhibitor SnxB (SnxB) in the experimental setting. The efficiency of the SnxB treatment was confirmed by analyzing the CDK8 kinase substrate pSTAT1-S727 [9] by immunoblotting (Supplementary Fig. S3A). We identified 887 genes that were deregulated upon CDK8 knockdown by both shRNAs, whereas CDK8/CDK19 kinase inhibition by SnxB treatment resulted in only 25 deregulated genes (Fig. 2A and Supplementary Fig. S3B, C). Only nine genes were commonly deregulated by both CDK8 knockdowns and SnxB (Supplementary Fig. S3D). Differentially regulated genes between cntrl and shCdk8 cells included metastasis-related genes. We validated the downregulation of snail family transcriptional repressor 2 (*Snai2*), matrix metalloproteinase-9 (*Mmp9*), and chemokine (C-C motif) ligand 2 (*Ccl2*) in shCdk8 compared to cntrl cells, while expression of these genes was unaltered upon SnxB treatment (Fig. 2B). Besides qPCR in cell lines, we validated the altered expression of *Snai2* and *Mmp9* in cells derived from primary tumors (Supplementary Fig. S4A). Thus, we conclude that CDK8 is a crucial driver of metastasis in TNBC.

### CDK8 knockdown enhances NK-cell-mediated killing of TNBC cells in vitro

We used KEGG to identify pathways deregulated by CDK8 knockdown, which revealed “Natural killer cell-mediated cytotoxicity” among the top hits (Fig. 2C). This included 19 deregulated genes (7 genes upregulated, 12 genes downregulated) upon CDK8 knockdown, which was not mimicked by CDK8/CDK19 kinase inhibition upon SnxB treatment (Fig. 3A). NK cells are innate lymphoid cells that have been implicated in preventing metastatic outgrowth [11, 23–25]. NK-cell activity is regulated by activating and inhibitory ligands on the surface of target cells [26, 27]. Self-major histocompatibility complex (MHC) class I molecules represent the most important inhibitory ligands that allow the discrimination of “self” and “missing self” [28]. CDK8 loss was associated with reduced expression of the MHC I genes H2-K1 and H2-D1 (Fig. 3A), which was validated by flow cytometry (Fig. 3B). We also confirmed the reduced protein levels of the activating natural killer group 2 member D (NKG2D) ligand ribonucleic acid export 1 (RAE1) and upregulation of the intercellular adhesion molecule 1 (ICAM-1) in CDK8-deficient cells by flow cytometry (Fig. 3C, D). No changes in MHC I and RAE1 expression were detected upon SnxB treatment (Supplementary Fig. S4B). Our transcriptome analysis of CDK8-deficient E0771 cells also revealed diminished expression of *Cd274*, encoding for PD-L1—a ligand of PD-1 and an important immune checkpoint protein. We confirmed the reduced expression of PD-L1 on protein level upon loss of CDK8 in E0771 cells (Fig. 3E).

These data point to CDK8 as a regulator of NK-cell-mediated recognition of TNBC cells. We thus performed in vitro cytotoxicity assays with IL-2-expanded splenic NK cells. E0771 cell lines were more susceptible to NK-cell-mediated cytotoxicity upon CDK8 knockdown (Fig. 3F), whereas no changes in NK-cell-mediated killing of E0771 cells were detected upon CDK8/CDK19 kinase inhibition, as observed by treating E0771 cell lines with SnxB for 48 h (Supplementary Fig. S4C). This led us to conclude that CDK8

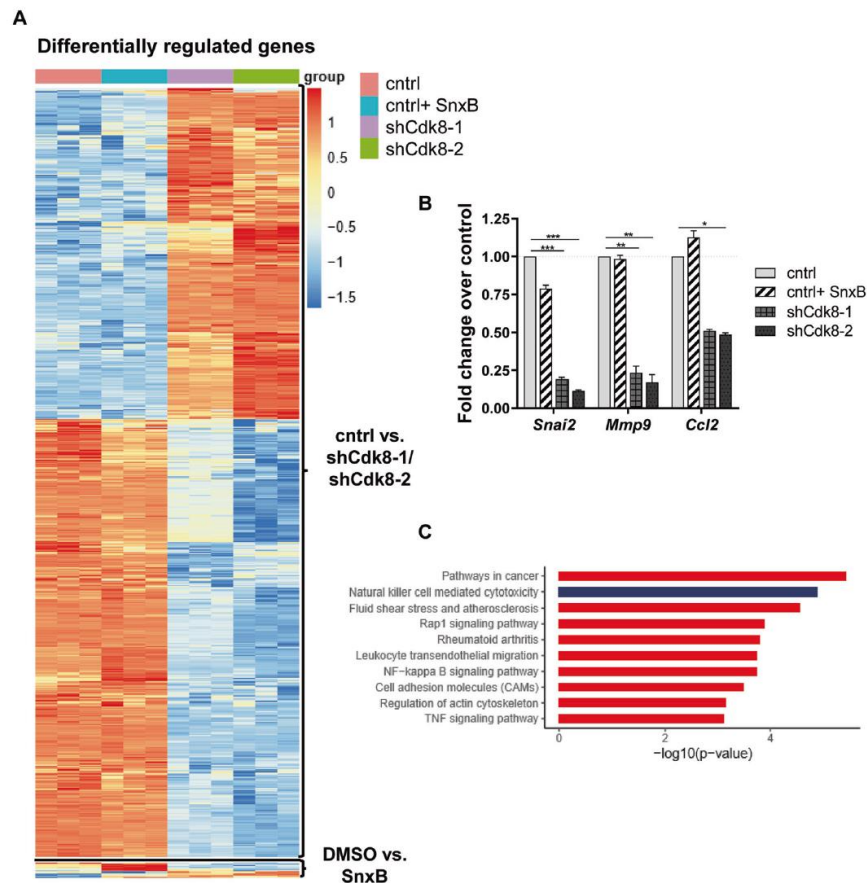


**Fig. 2** Loss of CDK8 regulates metastasis-related genes. **A** Heatmap of differentially expressed genes between untreated E0771 control or Senexin B (SnxB)-treated cells and shCdk8-1 or shCdk8-2 cell lines (RNA sequencing data;  $n = 3$  replicates). **B** Real-time quantitative PCR of RNA extracted from the different E0771 cell lines. Fold change expression of *Snai2*, *Mmp9*, and *Ccl2* over E0771 control, normalized to *Rplp0*. One out of two to three independent experiments with similar outcome is depicted. Bar graphs and error bars represent mean  $\pm$  SEM of technical triplicates. **C** Pathway analysis of 887 genes found to be differentially regulated by both CDK8-targeting shRNAs compared to control (overlap of cntrl vs. shCdk8-1 and cntrl vs. shCdk8-2) using KEGG pathway analysis.

in TNBC cells blocks NK-cell-mediated tumor recognition in a kinase-independent manner.

#### Loss of CDK8 in TNBC increases NK-cell-mediated tumor surveillance in vivo

To address the relevance of CDK8 in NK-cell-mediated recognition in an in vivo setting, we orthotopically injected CDK8-deficient and wild-type tumor cells into recombination activating gene 2 knockout (*Rag2*<sup>-/-</sup>) mice that rely on NK cells for tumor surveillance but lack T and B cells (Fig. 4A). Primary tumor growth was significantly delayed in mice transplanted with CDK8-knockdown cells (Fig. 4B), indicating an enhanced NK-cell-mediated tumor surveillance of the primary tumor. Surgical removal of the primary tumor was consistently performed at a tumor size of 75 mm<sup>2</sup> (Fig. 4A), and the persistent knockdown of CDK8 was confirmed (Supplementary Fig. S5A). Tumor weight (Supplementary Fig. S5B) and the numbers of tumor-infiltrating

NK cells (Fig. 4C) were comparable at the day of operation. In contrast to *Rag2*<sup>-/-</sup>*yc*<sup>-/-</sup> mice, no re-growing of the tumors post-surgery at the site of injection was observed in *Rag2*<sup>-/-</sup> mice (Supplementary Fig. S5C).

At day 23 post surgery, all mice were imaged, sacrificed, and analyzed for lung metastasis (Fig. 4A). In line with a role of NK cells in recognizing TNBC cells, radiance signals as a readout for lung metastasis were generally lower in *Rag2*<sup>-/-</sup> compared to *Rag2*<sup>-/-</sup>*yc*<sup>-/-</sup> mice (Supplementary Fig. S5D). These data confirm that NK cells are able to recognize and eliminate the metastatic spread of TNBC cells. The knockdown of CDK8 enhanced this effect; lung metastasis in *Rag2*<sup>-/-</sup> mice were almost absent upon transplantation with CDK8-knockdown tumors (Fig. 4D). The numbers of infiltrating NK cells were comparable between lungs of shCdk8-1 knockdown and control transplanted mice; however, there was a significant decrease in NK-cell numbers in the lungs of mice transplanted with shCdk8-2 knockdown cells (Fig. 4E). In line

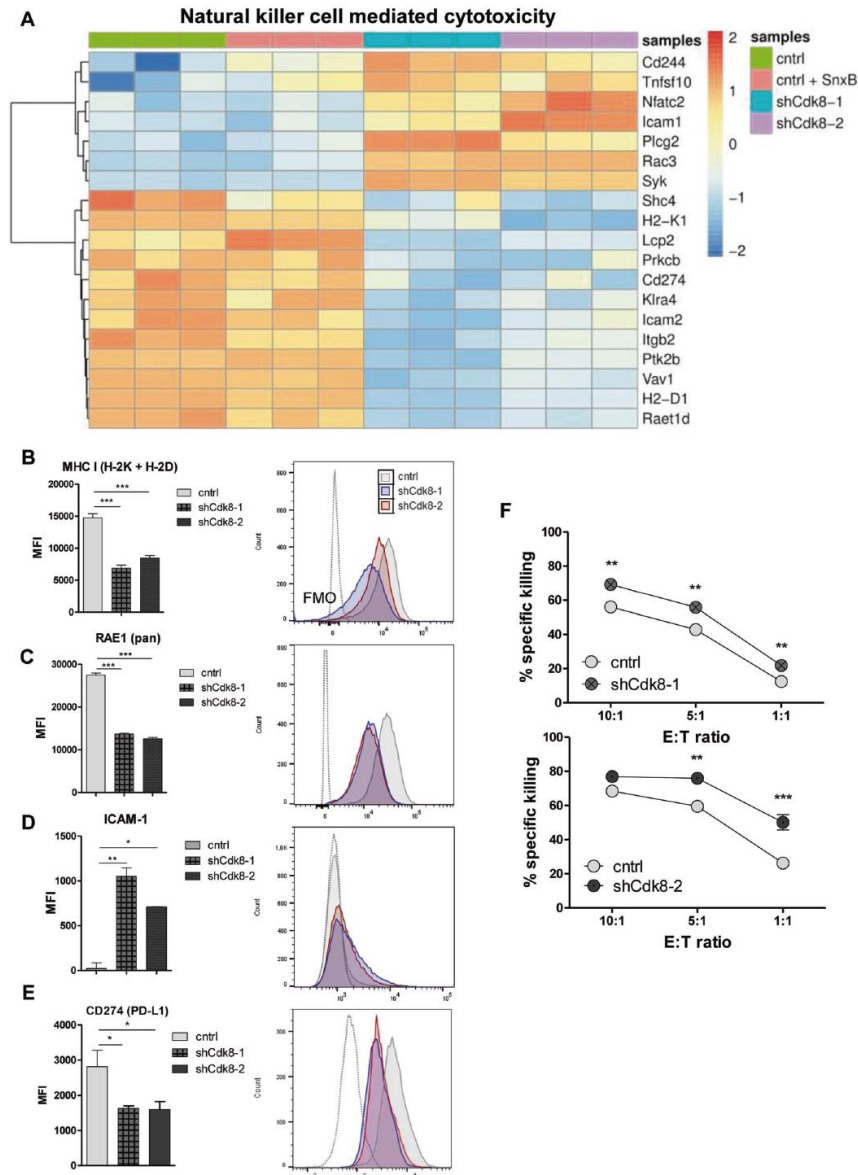


**Fig. 3** Loss of CDK8 enhances TNBC's visibility to NK cells. **A** Heatmap of differentially expressed genes between untreated or Senexin B-treated E0771 control cells and shCdk8-1 or shCdk8-2 cell lines in the KEGG pathway "Natural killer cell-mediated cytotoxicity" (RNA sequencing data;  $n = 3$  replicates). **B–E** Median fluorescence intensity (MFI) and representative histograms of **(B)** MHC I (H-2K + H-2D), **(C)** RAE1 (pan), **(D)** ICAM-1, and **(E)** CD274 (PD-L1) expression of E0771 control, shCdk8-1, and shCdk8-2 cells; expression levels of NK ligands were analyzed by flow cytometry. Bar graphs represent technical triplicates (mean  $\pm$  SEM). **F** IL-2-expanded C57BL/6 NK cells were incubated for 4 h with CFSE-labeled E0771 control or shCdk8-1/shCdk8-2 tumor cells in effector:target (E:T) ratio of 10:1, 5:1, and 1:1. The specific killing was assessed by flow cytometry. One representative experiment out of two to three independent experiments is shown. Symbols and error bars represent mean  $\pm$  SEM of technical duplicates.



6

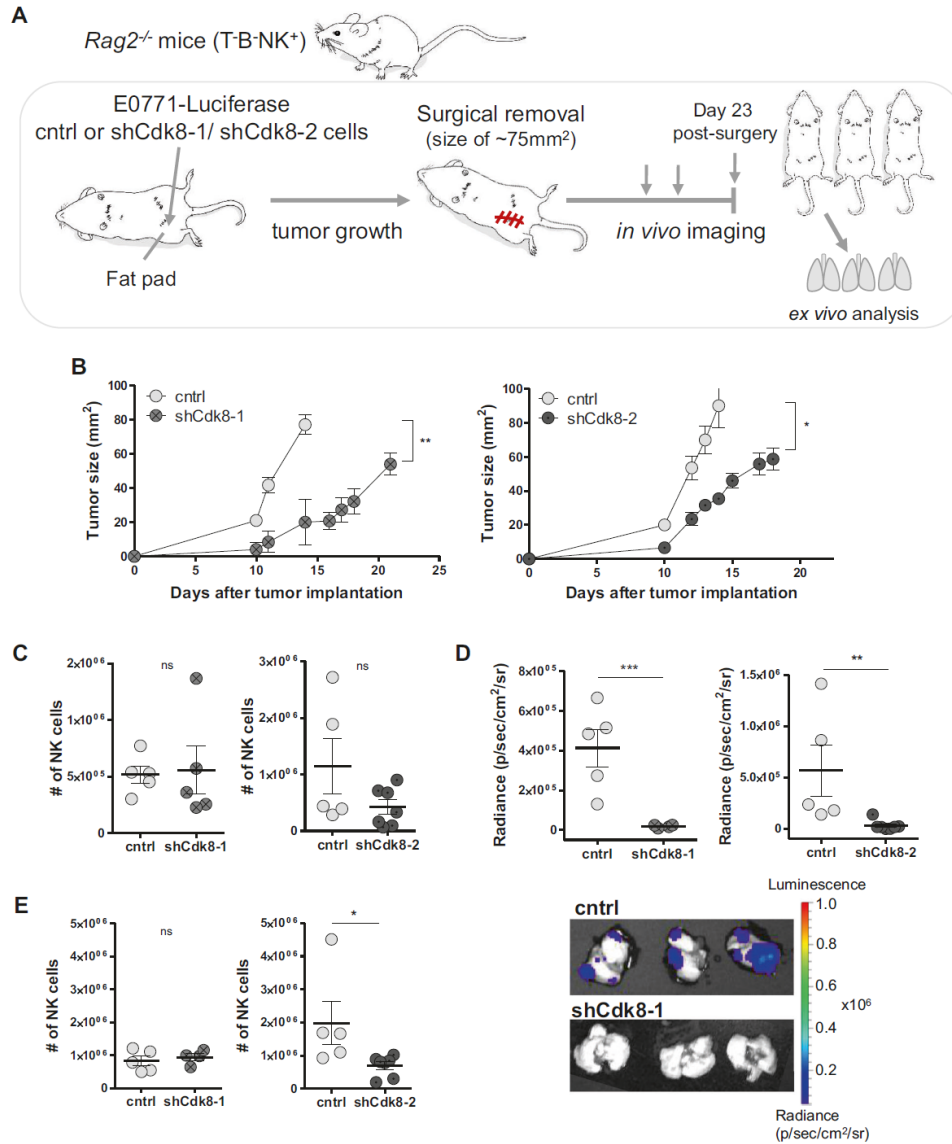


**Fig. 4** Loss of CDK8 in TNBC enhances NK-cell-mediated tumor surveillance. **A** Experimental setup of data shown in (B–E). *Rag2*<sup>-/-</sup> mice were orthotopically transplanted with E0771 control, shCdk8-1, or shCdk8-2 cells (in independent experiments) and monitored for primary tumor growth. Tumors were surgically removed and regrowth and distant metastasis formation of tumor cells was monitored with *in vivo* imaging. **B** *In vivo* primary tumor growth for control vs. shCdk8-1 or shCdk8-2 E0771 cells in the left and right panel, respectively. **C** Total infiltrating NK-cell numbers (CD45<sup>+</sup>NK1.1<sup>+</sup>NKp46<sup>+</sup>) of digested primary tumors at day of surgery. **D** Radiance signals of lungs ex *in vivo* measured by an *in vivo*-imaging system and representative pictures of lungs (lower panel) at the end of the experiment (day 23 post surgery). **E** Total numbers of infiltrating NK cells (CD45<sup>+</sup>NK1.1<sup>+</sup>NKp46<sup>+</sup>) of lung lysates were assessed. Symbols and error bars represent mean ± SEM ( $n = 4–9$  mice per group).

with the altered metastasis formation, we found that the lung weights were elevated in control mice, yet not reaching significance (Supplementary Fig. S5E).

To confirm that NK cells are the key players for tumor control of CDK8-deficient E0771 cells in *Rag2*<sup>-/-</sup> mice, we performed depletion experiments using an  $\alpha$ NK1.1 antibody. Mice were treated three times with the depletion antibody prior to tumor-cell implantation and subsequently treated twice a week (Fig. 5A). The successful depletion of CD3<sup>-</sup>NKp46<sup>+</sup> cells was confirmed (Supplementary Fig. S5F). Again, in the control setting, CDK8-knockdown tumors grew significantly slower in *Rag2*-deficient mice. This difference was lost upon depletion of NK cells (Fig. 5B, C), unequivocally assigning the differences to NK-cell-mediated tumor surveillance.

In summary, these data define a role of tumor-cell-intrinsic CDK8 as an immune checkpoint controlling NK-cell-mediated tumor recognition. Expression of CDK8 in E0771 cells facilitates evasion from NK-cell surveillance, validating the RNA-seq-based pathway analysis.

#### CDK8 contributes to IFN $\gamma$ -induced PD-L1 expression

The inhibitory PD-1/PD-L1 axis has recently also been implicated in the regulation of NK-cell cytotoxicity besides its important effects on cytotoxic T cells [29–31]. RNA-seq data indicated that PD-L1 (*Cd274*) expression is significantly impaired in E0771 cells upon CDK8 knockdown. We validated this finding on protein level by flow cytometry analysis (Fig. 3E). PD-L1 is regulated by interferon- $\gamma$  (IFN $\gamma$ ) signaling and displays interferon regulatory factor 1 (IRF1) binding at its promoter, as described in melanoma cells and other cancer entities [32]. As CDK8 has been reported to act downstream of IFN $\gamma$ , we stimulated E0771 cell lines with 100 U/ml IFN $\gamma$  for 48 h and analyzed PD-L1 surface levels. E0771 cells significantly induced PD-L1 levels upon IFN $\gamma$  treatment, which is impaired in E0771 shCdk8-1 and shCdk8-2 knockdown cells (Fig. 6A). These data suggest that regulation of PD-L1 by CDK8 might partially involve the IFN $\gamma$  signaling pathway.

#### CDK8 correlates with PD-L1 expression and survival in TNBC patients

To explore the human relevance of our findings, we analyzed publicly available data from large cohorts of breast cancer patients sub-filtered for TNBC patients ( $n = 113$ ; The Cancer Genome Atlas (TCGA) RNA sequencing data). In accordance with previous studies, focusing on breast cancer patients with molecular subtypes luminal A and B, basal, and HER2<sup>+</sup> [5], we extended the link of CDK8 expression to overall survival to a selected TNBC patient cohort (Fig. 6B). Analysis of correlations of CDK8 with genes identified by RNA sequencing of E0771 cells showed a significant association of CDK8 with PD-L1 in TNBC patients (Fig. 6C). These findings support the detrimental role of CDK8 in TNBC patients and link it to PD-L1 levels as potential immune evasion mechanism.

#### DISCUSSION

We here describe a role of CDK8 in controlling metastatic properties of TNBC cells and driving NK-cell immune evasion (Fig. 7). Whereas CDK8 is not required for cell proliferation or cell survival of TNBC, CDK8 promotes regrowth of primary tumors and subsequently the metastatic spread of TNBC cells in a murine orthotopic breast cancer model.

CDK8 has been implicated in the regulation of EMT in pancreatic, ovarian, and HER2-enriched breast cancer cell lines [20, 33] and promotes metastasis of colon cancer [34]. We confirmed the CDK8-dependent regulation of EMT markers such as *Snai2* in TNBC cells. Besides, CDK8 drives the expression of matrix metalloproteinase *Mmp9*, which contributes to the invasive character of several cancer cell types [34–36] and regulates *Ccl2* in TNBC cells, which has been found overexpressed in invasive breast

cancers and is suggested to support metastasis [37–39]. Taken together, CDK8 drives a pro-metastatic program in TNBC.

Serrao et al. [20] reported reduced EMT upon CDK8/CDK19 kinase inhibition in a murine breast cancer model using Py2T cells, mimicking HER2-enriched breast cancer [40]. Our study shows opposing results as we failed to detect any deregulation of the EMT-associated transcription factors *Snai2*, as well as *Mmp9* or *Ccl2* upon CDK8/CDK19 kinase inhibition, indicating a kinase-independent regulation.

In accordance, our global RNA-seq approach identified 887 CDK8-specific genes deregulated upon CDK8 knockdown in E0771 cell lines while only 25 genes were differentially expressed upon CDK8/CDK19 kinase inhibition. This further emphasizes that in TNBC, CDK8 controls several transcriptional programs in a kinase-independent manner. The close CDK8 paralog CDK19 cannot compensate for the loss of CDK8, suggesting that CDK8 and CDK19 have non-redundant roles in TNBC. This is also evidenced by others that assign mechanistically distinct functions to CDK8 and CDK19 [41, 42].

RNA sequencing of TNBC cells also uncovered modulators of NK-cell cytotoxicity as a major CDK8-dependent pathway. Enhanced NK-cell-mediated killing of CDK8-deficient murine TNBC cells was demonstrated in vitro and confirmed in an in vivo setting using NK-cell depletion. Our experiments further demonstrate that NK cells, in principle, possess the ability to control primary tumor growth in breast cancer, but that NK-cell-mediated tumor surveillance is blocked by the presence of CDK8 in E0771 tumor cells. When CDK8 is present, breast cancer cells are not killed by NK cells and escape tumor surveillance. This might explain why several reports show that NK cells control breast cancer metastasis, but have no impact on the growth of the primary tumor [11, 13, 23, 43]. Our data now shed new light on the role of NK cells in the control of the primary tumor growth. Loss of CDK8 allows to overcome immune evasion programs that counteract NK-cell-mediated recognition of the primary tumor.

As we observed equal numbers of tumor-infiltrating NK cells in control and shCdk8 tumor-bearing mice, we exclude that the enhanced surveillance is explained by a quantitative difference in NK cells. We rather hypothesize that CDK8 interferes with NK-cell-mediated tumor surveillance by regulating distinct checkpoints within TNBC cells as our transcriptome analysis revealed differential expression of crucial NK-cell-receptor ligands including the immune checkpoint protein PD-L1.

PD-L1 expression was significantly reduced on the transcriptional and translational level in E0771 cell lines lacking CDK8, identifying a new promising CDK8–PD-L1 axis in TNBC cells. PD-L1 (CD274) is a PD-1 ligand that is significantly higher expressed in TNBC compared to non-TNBC patients [2, 44]. Additionally, Phase 3 clinical trials combining chemotherapy with atezolizumab, a PD-L1 targeted antibody treatment, are promising and have given the largest overall survival benefit ever seen in patients with advanced or metastatic TNBC [45].

The consequences of PD-1 signaling for NK cells are incompletely understood, albeit there is accumulating evidence that in addition to T cells, NK cells contribute to the promising antitumor effects of PD-1/PD-L1 checkpoint inhibitors [29, 30, 46, 47]. Accordingly, we hypothesize that significantly lower levels of PD-L1 in Cdk8-knockdown cell lines are in part responsible for eliciting a stronger NK-cell-mediated antitumor response. Although a study [48] described only minimal PD-1 expression in mouse and human NK cells, we observe significant PD-1 expression on tumor-infiltrating NK cells in our model (data not shown). Our data are also supported by a positive correlation of CDK8 and PD-L1 in a dataset of human TNBC patients.

NK-cell cytotoxicity is the result of multiple influences of activating and inhibitory ligands. Thus, we believe that the reduced expression of MHC class I and NKG2D ligands, as well as the increased ICAM-1 expression contribute to the molecular

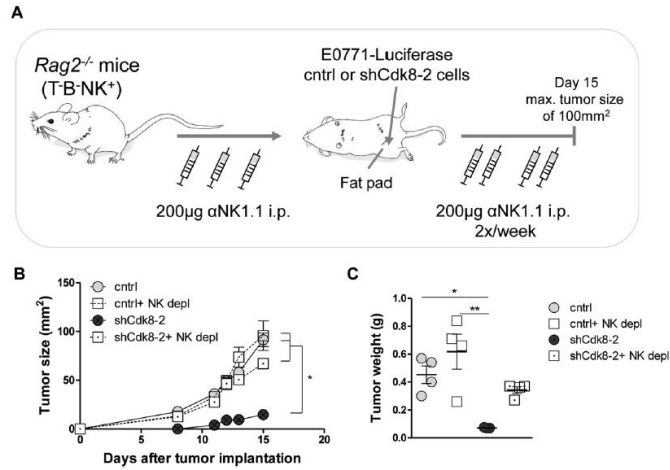


**Fig. 5** NK-cell depletion allows outgrowth of CDK8-deficient TNBC tumor cells. **A** Experimental setup of data shown in **(B, C)**. *Rag2*<sup>-/-</sup> mice were NK-cell depleted by i.p. injections of an αNK1.1 antibody (200 µg/mouse), three times prior to implantation of E0771 control or shCdk8-2 cells and subsequently twice per week. **B** Primary tumor growth of control vs. shCdk8-2 E0771 cells, of mice treated with αNK1.1 antibody (PBS injection served as control). Symbols and error bars represent tumor size (mm<sup>2</sup>) in mean ± SEM. **C** Tumor weight of mice at day 15 after tumor implantation at the endpoint of the experiment ±SEM (n = 4 mice per group).

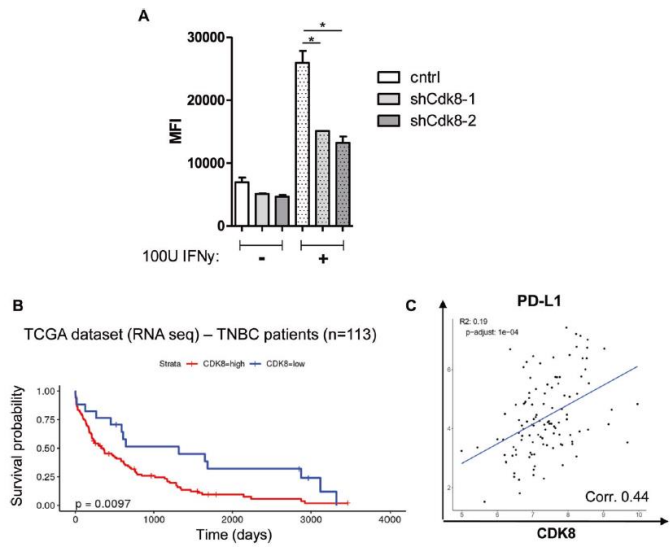


**Fig. 6** CDK8 correlates with poor prognosis and with PD-L1 expression in a human dataset. **A** Median fluorescence intensity (MFI) of PD-L1 expression of E0771 control, shCdk8-1, and shCdk8-2 cells, cultivated with or without 100 U/ml IFNγ for 48 h (indicated by “-” and “+” on the bottom of the graph); analyzed by flow cytometry. One representative experiment out of two is shown. Symbols and error bars represent mean ± SEM of technical duplicates. **B, C** Patient data from the TCGA database were sub-grouped in TNBC patients (n = 113) and analyzed for **(B)** overall survival comparing CDK8-high- and CDK8-low-expressing patients and **(C)** correlation between CDK8 and PD-L1 expression in this human dataset of TNBC patients.



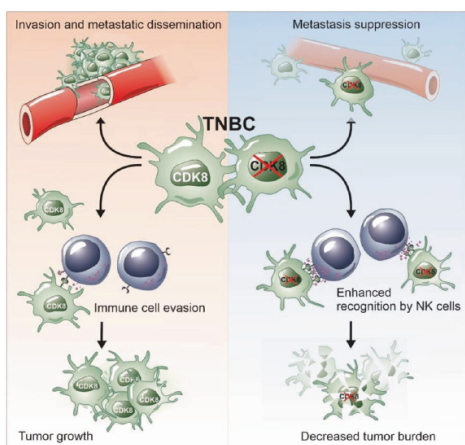


**Fig. 7** CDK8 controls metastatic properties of TNBC cells and drives NK-cell immune evasion. CDK8 in TNBC drives invasion and metastatic dissemination of tumor cells and immune evasion (left box). Loss of CDK8 in tumor cells on the one hand, dampens invasiveness and pro-metastatic behavior of tumor cells and on the other hand, enhances recognition by NK cells, thereby decreasing tumor burden (right box).

mechanisms how CDK8 drives immune evasion. Low MHC class I levels point to enhanced missing self-recognition [28]. ICAM-1 is an adhesion molecule that binds LFA-1 on NK cells and contributes to the formation of the NK-cell cytotoxic immunological synapse, and thereby induces the cytotoxic activity in NK cells [49]. Although NKG2D is an activating receptor, an upregulation of NKG2D ligands has been reported to occur during EMT in colorectal cancer [50], and high levels of NKG2D ligands are associated with poor prognosis in breast cancer [51].

Comparable to the kinase-independent role of CDK8 in EMT, enhanced NK-cell-mediated recognition and elimination of E0771 cells was not recapitulated upon inhibitor treatment of the tumor cells. This also indicates a kinase-independent function of CDK8 in immune cell evasion of TNBC. Additionally, kinase-independent effects of CDK8 have also been previously described in melanoma cells and hematologic malignancies [16, 52, 53], while the effect of CDK8 on ER<sup>+</sup> breast cancer progression is kinase dependent [17]. Thus, CDK8 clearly has divergent roles in different cancer entities.

In summary, we here identify CDK8 as a novel driver of immune evasion and demonstrate that targeting CDK8 in TNBC has therapeutic potential. Targeting CDK8 may be beneficial through different aspects; first, by dampening the invasive and pro-metastatic behavior of the breast cancer cells, and, second, by preventing evasion from NK cells. On top, previous studies described a suppressive effect of NK-cell-intrinsic CDK8 on NK-cell activity by regulating the lytic molecule perforin [12, 13]. Thus, targeting CDK8 in cancer patients could prevent tumor progression and immune evasion while enhancing NK-cell cytotoxicity.

As our data suggest that tumor-intrinsic CDK8 controls NK-cell immune evasion in a kinase-independent manner, CDK8/CDK19 kinase inhibitors would not suffice to reach a clinical benefit. The generation of small-molecule compounds degrading CDK8 could be a promising alternative for TNBC therapy. We believe that our data provide important mechanistic insights and pave the way for potential new options in the treatment of this fatal disease.

## MATERIALS AND METHODS

### Mice and cell lines

*Rag2*<sup>-/-</sup>*yc*<sup>-/-</sup> (C.Cg-Rag2<sup>tm1Fwa</sup>-Il2rg<sup>tm1Wj</sup>) [54], *Rag2*<sup>-/-</sup> [55], and C57BL/6J mice were in-house bred. All animals were age and gender matched (female, 9–13 weeks) for experiments and maintained at the University of Veterinary Medicine Vienna under specific pathogen-free (SPF) conditions according to Federation for Laboratory Animal Science Associations (FELASA) guidelines (2014). The animal experiments were approved by the Ethics and Animal Welfare Committee of the University of Veterinary Medicine Vienna and granted by the National Authority (Austrian Federal Ministry of Science and Research) according to Section 8ff of Law for Animal Experiments under license BMWFV-68.205/0093-WFV/3b/2015, and were conducted according to the guidelines of FELASA and ARRIVE.

The murine TNBC cell line E0771 [56] was kindly provided by Piotr Tymozuk (Medical University of Innsbruck) and maintained in Dulbecco's modified Eagle's medium (DMEM; Sigma) supplemented with 10% FCS (Bio & Sell), 100 U/ml penicillin, 100 µg/ml streptomycin (Sigma), 50 µM β-mercaptoethanol (Sigma), and 0.02 M HEPES (Sigma). Cells were cultured at 37 °C with 5% CO<sub>2</sub> and regularly tested for potential *mycoplasma* contamination. E0771 cells were lentivirally infected with a CMV-Firefly Luciferase construct with ~1 × 10<sup>7</sup> IFU/ml (Amsbio) and positively selected with 0.75 µg/ml puromycin (InvivoGen).

Next, E0771-Luciferase cells were transduced with CDK8-targeting shRNAs or a control shRNA (Ren.713) in a retroviral LENC (pMSCV-IRES mCherry) vector [57]. Sequences of shRNAs: Ren.713 (control): TGCT GTTGACAGTGAGCGCAGGAATTATA ATGCTATCTATAGTGAAGCCACAGATG TATAGATAAGCATTATAATTCCTATGCTACTGCCTCGGA; shCdk8-1: TGCTG TTGACAGTGAGCGAAGCAGATTATGTTAACAAAAT ATAGTGAAGCCACAGATGT ATATTTTGTAAACATAATCTGTGCTCTACTGCCTCGGA; shCdk8-2: TGCTGTT GACAGTGAGCGCTGGAGTTAGACTTGAATGAATAGTGAAGCCACAGATGTAT TCATT CAAAGCTAACTCCAATGCCTACTGCCTCGGA.

The Phoenix ecotropic (φNX Eco) packaging system was used to produce supernatant containing retroviral pseudoparticles. To increase the virus concentration, the Retro-X<sup>TM</sup> Concentrator (Clontech) was utilized according to the manufacturer's protocol. Phoenix cells were seeded 1 day before the transfection in 10 cm dishes and grown to 50–70% confluence. Plasmid DNA was diluted in DMEM containing 10 mM HEPES buffer pH 7.4 and Turbofect<sup>®</sup> Transfection Reagent (Qiagen) was added, vortexed, and incubated for 15 min at room temperature before the transfection mix was added dropwise to the cells. After harvesting and concentrating the virus supernatant, polybrene (Sigma) was added and E0771 cells were infected. Cells were sorted on a BD FACS Aria III based on mCherry expression, and CDK8 deletion was verified by western blot analysis.

### In vivo tumor models, NK-cell depletion, and imaging

To start with, 2 × 10<sup>5</sup> E0771 cells were injected into the 4th mammary fat pad of female *Rag2*<sup>-/-</sup> or *Rag2*<sup>-/-</sup>*yc*<sup>-/-</sup> mice, and tumor growth (length and width) was measured frequently using a caliper. At a tumor area of approximately 75 mm<sup>2</sup>, primary tumors were surgically removed. Starting 9 days after surgery, mice were live imaged using an IVIS Lumina S5 (Perkin Elmer) system. Mice were injected with 200 µl (3 mg) D-Luciferin Bioluminescent Substrate (Perkin Elmer) i.p., narcotized with 5% isoflurane, and continuously kept in 2% isoflurane throughout the imaging procedure. At day 15 post surgery (*Rag2*<sup>-/-</sup>*yc*<sup>-/-</sup> mice) or day 23 post surgery (*Rag2*<sup>-/-</sup> mice), experiments were terminated, mice were sacrificed, imaged, and lungs were additionally imaged ex vivo. Primary tumors and lungs were minced and digested using culture media containing 1 mg/ml collagenase D (Sigma/Roche) and 20 µg/ml DNase I (Fisher Scientific), on a gentleMACS<sup>™</sup> Octo Dissociator (Milteny Biotec). Single-cell suspensions were replated on 10 cm dishes and used for western blot or mRNA pellets.

In vivo-imaging data were analyzed using Living Image Software V 4.7.4 (Perkin Elmer).

For NK-cell depletion experiments, *Rag2*<sup>-/-</sup> mice were injected with 200 µg αNK1.1 (PK136) antibody i.p. two times per week, starting 1 week before tumor-cell inoculation. Tumor growth was measured over time, and twice a week mice were injected with αNK1.1 antibody until termination of the experiment. Successful NK-cell depletion was verified in the blood prior to tumor-cell implantation and was confirmed at the end of the experiment.

### NK-cell isolation, expansion, and cytotoxicity assay

NK cells were isolated from spleen single-cell suspensions using DX5-labeled MACS beads according to the manufacturer's instructions (Milteny Biotec). NK cells were expanded in RPMI1640 complete medium supplemented with 5000 U/ml rhIL2 (Proleukin, Novartis) for 7 days. The

purity was analyzed by flow cytometry and was 85–95% CD3<sup>+</sup>NK1.1<sup>+</sup>NKp46<sup>+</sup> of all living cells.

For in vitro cytotoxicity assays, 7 days expanded NK cells were mixed at indicated effector:target ratios with carboxyfluorescein diacetate succinimidyl ester (CFSE, Molecular Probes, CellTrace CFSE Cell Proliferation Kit) labeled E0771 cells. The specific target cell lysis was assessed by flow cytometry as previously described [58].

#### In vitro proliferation, flow cytometry, and cell sorting

To start with,  $2 \times 10^4$  E0771 cells were seeded in 6-well plates in triplicate for growth curves, and counted every 2 days by flow cytometry. Analysis of NK-cell ligands was performed by staining for ICAM-1, MHC class I, RAE1, and PD-L1. Analysis of apoptotic fractions was performed by staining with AnnexinV and 7-AAD in AnnexinV 10x Staining Buffer (ThermoFisher) according to the manufacturer's protocol. Cell cycle staining was performed using propidium iodide (Sigma).

The following antibodies (clones) were purchased from: eBioscience/Invitrogen™: CD3 (17A2), NK1.1 (PK136), NKp46 (29A1.4); BioLegend™: CD54/ICAM-1 (YN1/1.7.4), CD274/PD-L1 (10 F.9G2); BD Pharmingen™: H-2K[b] and H-2D[b] MHC class I (28-8-6); and from R&D Systems: RAE-1 (205001).

Flow cytometry experiments were performed on a BD FACSCanto II (BD Bioscience) or CytoFLEX (Beckman Coulter) and analyzed using BD FACSDiva V8.0, FlowJo V10 software and CytExpert Software V2.3.1.22. Sorting of mCherry-expressing E0771 was performed on a BD FACSAria III (BD Bioscience).

#### Western blot

Whole-cell extracts were lysed in RIPA buffer (50 mM Tris-HCl (pH 7.6), 150 mM NaCl, 1% NP-40, 0.25% sodium deoxycholate, 1 mM EDTA; 20 mM  $\beta$ -glycero-phosphate) including cOmplete protease inhibitor cocktail (Roche) or in SDS-sample buffer. Equal amounts of proteins were separated by SDS polyacrylamide gels and transferred to a PVDF blotting membrane (GE Life science). After blocking with 5% bovine serum albumin in pY-TBST buffer (10 mM Tris/HCl pH 7.4, 75 mM NaCl, 1 mM EDTA, 0.1% Tween-20), membranes were incubated with primary antibodies overnight at 4 °C. Immunoreactive bands were visualized after incubation with the secondary antibody and Clarity Western ECL Substrate (Bio-Rad) using the ChemiDoc™ Touch (Bio-Rad) and analyzed by Image Lab software (BioRad). Antibodies against CDK8 (#4106), GAPDH (#5174), pSTAT1-S727 (#9177), tSTAT1 (#9172), rabbit IgG (HRP linked, #7074 S), and mouse IgG (HRP linked, #7076 S) were purchased from Cell Signaling Technology.

#### RNA Isolation and qRT-PCR

Total RNA was isolated from stable E0771 cell lines or digested primary tumors of *Rag2<sup>-/-</sup>yc<sup>-/-</sup>* mice. RNA was extracted using the RNeasy Mini Kit (Qiagen) or peqGOLD TriFast (VWR) according to the protocols of the manufacturer. Reverse transcription was performed using the iScript cDNA Synthesis Kit following the manufacturer's instructions (Bio-Rad). All quantitative PCRs (qPCRs) were performed with Sso Advanced Universal SYBR Green Supermix (Bio-Rad) according to the instructions of the manufacturer. Expression of mRNA was normalized to *Rplp0* mRNA. The following primers were used: *Rplp0* fwd: GCTTCTGGAGGGTGTCC, rev: GCTTCAGCTTTGGCAGGG; *Snai2* fwd: TGTGTCTGCAAGATCTGTGGC, rev: TCCCCAGTGTGAGTTCTAATGTG; *Mmp9* fwd: TGTCTGGAGATTCGACTTGAAG, rev: ATAGGCTTTGTCTGGTACTGG; *Ccl2* fwd: TCAGCCAGATGCAGTAAAGCC, rev: GCTTCTTTGGACACCTGCTGCT.

#### RNA sequencing analysis

Libraries from untreated murine E0771 control or Senexin B (SnxB)-treated cells, and shCdk8-1 or shCdk8-2 cell lines in triplicate were prepared using the NEBNext Multiplex Oligos for Illumina (Dual Index Primers). Single-end, 50 bp sequencing was performed on an Illumina HiSeqV4 SR50 sequencer (Illumina, San Diego, CA, USA). After quality control of raw data with FastQC and removal of adapters and low-quality reads with Trimmomatic (version 0.36), reads were mapped to the GENCODE M13 genome using STAR (version 2.5.2b) with default parameters. Counts for union gene models were obtained using featureCounts from the Subread package (version 1.5.1). Differentially expressed (Benjamin-Hochberg corrected *p*-value (*p*-adjust) < 0.05 and fold change > 2) genes were identified using edgeR (version 3.30.3). Over-representation analysis was done using the STRING enrichment API

method (<https://string-db.org/cgi/help.pl?subpage=api%23getting-functional-enrichment>). The RNA-seq data reported in this article have been deposited in the Gene Expression Omnibus database (Accession ID: GSE161295).

#### Inhibitors

E0771 cells were incubated for 48 h with the CDK8/CDK19 inhibitor Senexin B (Gentaur GmbH/APEXBio) or DMSO as a control. Inhibitor concentrations were first titrated based on pSTAT1-S727 levels using western blotting. For NK-cell cytotoxicity assays, 1  $\mu$ M Senexin B was applied and kept in the medium throughout the assay. Treatment with 1500 U/ml IFN $\gamma$  (Merck) for 30 min was used to induce STAT1-S727 phosphorylation. For experiments analyzing surface expression of PD-L1 by flow cytometry, E0771 cells were treated with 100 U/ml IFN $\gamma$  for 48 h.

#### Human patient data

RNA-seq data from TNBC patients from TCGA was obtained from the R package MetaGxBreast by selecting for samples with an estrogen receptor, progesterone receptor, and HER2-negative status. Differences in overall survival between groups were calculated using the log-rank test and visualized by Kaplan-Meier curves using the ggsurvplot function from the same package. Pairwise correlations (Spearman) between the expression levels of CDK8 and genes found significantly regulated in CDK8-knockdown E0771 breast cancer cell lines (relative to control) of TNBC patients, and were calculated using the cor.test function from base R. Correction for multiple testing was done with the base R function p.adjust (method "BH"). Coefficient of determination ( $=R^2$ ) and Benjamini Hochberg corrected *p*-value are indicated in the plots. Values in the plots represent mRNA expression z-scores.

#### Statistical analysis

Kruskal-Wallis test (followed by Dunn's test), one-way analysis of variance (followed by Tukey's multiple comparison test), unpaired *t*-test, Mann-Whitney test and a linear regression model were performed with log transformed data using GraphPad Prism™ Software version 5.04 and R Studio version 1.2.1335. All data are shown as mean  $\pm$  SEM. Statistical significance is indicated for each experiment (\**p* < 0.05, \*\**p* < 0.01, \*\*\**p* < 0.001, \*\*\*\**p* < 0.0001).

#### DATA AVAILABILITY

The data that support the findings of this study are available from the corresponding author upon request. The RNA-seq data reported in this article are available in the Gene Expression Omnibus database under accession number GSE161295.

#### REFERENCES

- Aysola K, Desai A, Welch C, Xu J, Qin Y, Reddy V, et al. Triple negative breast cancer - an overview. *Hereditary Genet.* 2013;2013:001.
- Lebert JM, Lester R, Powell E, Seal M, McCarthy J. Advances in the systemic treatment of triple-negative breast cancer. *Curr Oncol.* 2018;25:142–50.
- Fabbri F, Salvi S, Bravaccini S. Know your enemy: genetics, aging, exposomic and inflammation in the war against triple negative breast cancer. *Semin Cancer Biol.* 2020;60:285–93.
- Philip S, Kumarasiri M, Teo T, Yu M, Wang S. Cyclin-dependent kinase 8: a new hope in targeted cancer therapy? *J Med Chem.* 2018;61:5073–92.
- Broude EV, Györfy B, Chumanevich AA, Chen M, McDermott MSJ, Shtutman M, et al. Expression of CDK8 and CDK8-interacting genes as potential biomarkers in breast cancer. *Curr Cancer Drug Targets.* 2015;15:739–49.
- Roninson IB, Györfy B, Mack ZT, Shtil AA, Shtutman MS, Chen M, et al. Identifying cancers impacted by CDK8/19. *Cells* 2019;8:821.
- Lim S, Kaldis P. Cdk8, cyclins and CK1s: roles beyond cell cycle regulation. *Development* 2013;140:3079–93.
- Malik S, Roeder RG. The metazoan mediator co-activator complex as an integrative hub for transcriptional regulation. *Nat Rev Genet.* 2010;11:761–72.
- Bancerek J, Poss ZC, Steinparzer I, Sedlyarov V, Pfaffenwimmer T, Mikulic I, et al. CDK8 kinase phosphorylates transcription factor STAT1 to selectively regulate the interferon response. *Immunity* 2013;38:250–62.
- Alarcón C, Zaromytidou AI, Xi Q, Gao S, Yu J, Fujisawa S, et al. Nuclear CDKs drive Smad transcriptional activation and turnover in BMP and TGF- $\beta$  pathways. *Cell* 2009;139:757–69.



11. Putz EM, Gotthardt D, Hoemann G, Csiszar A, Wirth S, Berger A, et al. CDK8-mediated STAT1-S727 phosphorylation restrains NK cell cytotoxicity and tumor surveillance. *Cell Rep.* 2013;4:437–44.
12. Witalisz-Siepracka A, Gotthardt D, Prchal-Murphy M, Didara Z, Menzl I, Prinz D, et al. NK cell-specific CDK8 deletion enhances antitumor responses. *Cancer Immunol Res.* 2018;6:458–66.
13. Hofmann MH, Mani R, Engelhardt H, Impagnatiello MA, Carotta S, Kerenyi M, et al. Selective and potent CDK8/19 inhibitors enhance NK-cell activity and promote tumor surveillance. *Mol Cancer Ther.* 2020;19:1018–30.
14. Guo Z, Wang G, Lv Y, Wan YY, Zheng J. Inhibition of Cdk8/Cdk19 activity promotes treg cell differentiation and suppresses autoimmune diseases. *Front Immunol.* 2019;10:1–10.
15. Menzl I, Witalisz-Siepracka A, Sexl V. CDK8-novel therapeutic opportunities. *Pharmaceuticals* 2019;12:92.
16. Menzl I, Berger-Becvar A, Zhang T, Grausenburger R, Prchal-Murphy M, Edlinger L, et al. A kinase-independent role for CDK8 in BCR-ABL1<sup>+</sup> leukemia. *Nat Commun.* 2019;10:4741.
17. McDermott MSJ, Chumanevich AA, Lim C, Chen M, Altilla S, Oliver D, et al. Inhibition of CDK8 mediator kinase suppresses estrogen dependent transcription and the growth of estrogen receptor positive breast cancer. *Oncotarget* 2017;8:12558–75.
18. Wang Y, Zhou BP. Epithelial-mesenchymal transition - a hallmark of breast cancer metastasis. *Cancer Hallm.* 2014;1:38–49.
19. Felipe Lima J, Nofech-Mozes S, Bayani J, Bartlett J. EMT in breast carcinoma - a review. *J Clin Med.* 2016;5:65.
20. Serrao A, Jenkins LM, Chumanevich AA, Horst B, Liang J, Gatza ML, et al. Mediator kinase CDK8/CDK19 drives YAP1-dependent BMP4-induced EMT in cancer. *Oncogene* 2018;37:4792–808.
21. Johnstone CN, Smith YE, Cao Y, Burrows AD, Cross RSN, Ling X, et al. Functional and molecular characterisation of E0771.LMB tumours, a new C57BL/6-mouse-derived model of spontaneously metastatic mammary cancer. *Dis Model Mech.* 2015;8:237–51.
22. Fantozzi A, Christofori G. Mouse models of breast cancer metastasis. *Breast Cancer Res.* 2006;8:212.
23. Bottos A, Gotthardt D, Gill JW, Gattelli A, Frei A, Tzankov A, et al. Decreased NK-cell tumour immunosurveillance consequent to JAK inhibition enhances metastasis in breast cancer models. *Nat Commun.* 2016;7:12258.
24. López-Soto A, Gonzalez S, Smyth MJ, Galluzzi L. Control of metastasis by NK cells. *Cancer Cell.* 2017;32:135–54.
25. Waldhauer I, Steinle A. NK cells and cancer immunosurveillance. *Oncogene* 2008;27:5932–43.
26. Koch J, Steinle A, Watzl C, Mandelboim O. Activating natural cytotoxicity receptors of natural killer cells in cancer and infection. *Trends Immunol.* 2013;34:182–91.
27. Raulet DH, Vance RE. Self-tolerance of natural killer cells. *Nat Rev Immunol.* 2006;6:520–31.
28. Vivier E, Tomasello E, Baratin M, Walzer T, Ugolini S. Functions of natural killer cells. *Nat Immunol.* 2008;9:503–10.
29. Hsu J, Raulet DH, Ardolino M. Contribution of NK cells to immunotherapy mediated by PD-1/PD-L1 blockade. *J Clin Invest.* 2018;128:4654–68.
30. Park JE, Kim SE, Keam B, Park HR, Kim S, Kim M, et al. Anti-tumor effects of NK cells and anti-PD-L1 antibody with antibody-dependent cellular cytotoxicity in PD-L1-positive cancer cell lines. *J Immunother cancer.* 2020;8:1–11.
31. Niu C, Li M, Zhu S, Chen Y, Zhou L, Xu D, et al. Pd-1-positive natural killer cells have a weaker antitumor function than that of pd-1-negative natural killer cells in lung cancer. *Int J Med Sci.* 2020;17:1964–73.
32. Garcia-Diaz A, Shin DS, Moreno BH, Saco J, Escuin-Ordinas H, Rodriguez GA, et al. Interferon receptor signaling pathways regulating PD-L1 and PD-L2 expression. *Cell Rep.* 2017;19:1189–201.
33. Xu W, Wang Z, Zhang W, Qian K, Li H, Kong D, et al. Mutated K-ras activates CDK8 to stimulate the epithelial-to-mesenchymal transition in pancreatic cancer in part via the Wnt/ $\beta$ -catenin signaling pathway. *Cancer Lett.* 2015;356:613–27.
34. Liang J, Chen M, Hughes D, Chumanevich AA, Altilla S, Kaza V, et al. CDK8 selectively promotes the growth of colon cancer metastases in the liver by regulating gene expression of TIMP3 and matrix metalloproteinases. *Cancer Res.* 2018;78:6594–606.
35. Mehner C, Hockla A, Miller E, Ran S, Radisky DC, Radisky ES. Tumor cell-produced matrix metalloproteinase 9 (MMP-9) drives malignant progression and metastasis of basal-like triple negative breast cancer. *Oncotarget* 2014;5:2736–49.
36. Aalinkel R, Nair BB, Reynolds JL, Sykes DE, Mahajan SD, Chadha KC, et al. Overexpression of MMP-9 contributes to invasiveness of prostate cancer cell line LNCaP. *Immunol Invest.* 2011;40:447–64.
37. Qian BZ, Li J, Zhang H, Kitamura T, Zhang J, Campion LR, et al. CCL2 recruits inflammatory monocytes to facilitate breast-tumour metastasis. *Nature* 2011;475:222–5.
38. Kitamura T, Qian BZ, Soong D, Cassetta L, Noy R, Sugano G, et al. CCL2-induced chemokine cascade promotes breast cancer metastasis by enhancing retention of metastasis-associated macrophages. *J Exp Med.* 2015;212:1043–59.
39. Bin FangW, Yao M, Brummer G, Acevedo D, Alhakamy N, Berkland C, et al. Targeted gene silencing of CCL2 inhibits triple negative breast cancer progression by blocking cancer stem cell renewal and M2 macrophage recruitment. *Oncotarget* 2016;7:49349–67.
40. Waldmeier L, Meyer-Schaller N, Diepenbruck M, Christofori G. Py2T murine breast cancer cells, a versatile model of TGF $\beta$ -induced EMT in vitro and in vivo. *PLoS ONE.* 2012;7:48651.
41. Steinparzer I, Sedlyarov V, Rubin JD, Eislmayr K, Galbraith MD, Levandowski CB, et al. Transcriptional responses to IFN- $\gamma$  require mediator kinase-dependent pause release and mechanistically distinct CDK8 and CDK19 functions. *Mol Cell.* 2019;76:1–15.
42. Nakamura A, Nakata D, Kakoi Y, Kunitomo M, Murai S, Ebara S, et al. CDK8/19 inhibition induces premature G1/S transition and ATR-dependent cell death in prostate cancer cells. *Oncotarget* 2018;9:13474–87.
43. Ohs I, Ducimetière L, Marinho J, Kulig P, Becher B, Tugues S. Restoration of natural killer cell antimetastatic activity by IL12 and checkpoint blockade. *Cancer Res.* 2017;77:7059–71.
44. Mittendorf EA, Phillips AV, Meric-Bernstam F, Qiao N, Wu Y, Harrington S, et al. PD-L1 expression in triple negative breast Cancer. *Immunol Res.* 2014;2:361–70.
45. Marra A, Viale G, Curigliano G. Recent advances in triple negative breast cancer: the immunotherapy era. *BMC Med.* 2019;17:1–9.
46. Quatrini L, Mariotti FR, Munari E, Tumino N, Vacca P, Moretta L. The immune checkpoint PD-1 in natural killer cells: expression, function and targeting in tumour immunotherapy. *Cancers (Basel).* 2020;12:1–21.
47. Liu Y, Cheng Y, Xu Y, Wang Z, Du X, Li C, et al. Increased expression of programmed cell death protein 1 on NK cells inhibits NK-cell-mediated anti-tumor function and indicates poor prognosis in digestive cancers. *Oncogene* 2017;36:6143–53.
48. Judge SJ, Dunai C, Aguilar EG, Vick SC, Sturgill IR, Khuat LT, et al. Minimal PD-1 expression in mouse and human NK cells under diverse conditions. *J Clin Invest.* 2020;130:3051–68.
49. Gross CC, Brzostowski JA, Liu D, Long EO. Tethering of ICAM on target cells is required for LFA-1- dependent NK cell adhesion and granule polarization. *J Immunol.* 2010;185:2918–26.
50. Lopez-Soto A, Huergo-Zapico L, Galvan JA, Rodrigo L, de Herrerros AG, Astudillo A, et al. Epithelial-mesenchymal transition induces an antitumor immune response mediated by NKG2D receptor. *J Immunol.* 2013;190:4408–19.
51. Madjd Z, Spendlove I, Moss R, Bevin S, Pinder SE, Watson NFS, et al. Upregulation of MICA on high-grade invasive operable breast carcinoma. *Cancer Immun.* 2007;7:1–10.
52. Kapoor A, Goldberg MS, Cumberland LK, Ratnakumar K, Segura MF, Emanuel PO, et al. The histone variant macroH2A suppresses melanoma progression through regulation of CDK8. *Nature* 2010;468:1105–11.
53. Poss ZC, Ebmeier CC, Odell AT, Tangpeerachaikul A, Lee T, Pelish HE, et al. Identification of mediator kinase substrates in human cells using cortistatin A and quantitative phosphoproteomics. *Cell Rep.* 2016;15:436–50.
54. Cao X, Shores EW, Hu-Li J, Anver MR, Kelsall BL, Russell SM, et al. Defective lymphoid development in mice lacking expression of the common cytokine receptor  $\gamma$  chain. *Immunity* 1995;2:223–38.
55. Shinkai Y, Gary Rathbun, Lam K-P, Oltz EM, Stewart V, Mendelsohn M, et al. RAG-2-deficient mice lack mature lymphocytes owing to inability to initiate V(D)J rearrangement. *Cell.* 1992;68:855–67.
56. Casey AE, Laster WR, Ross GL. Sustained enhanced growth of carcinoma EO771 in C57 black mice. *Exp Biol Med.* 1951;77:358–62.
57. Fellmann C, Hoffmann T, Sridhar V, Hopfgartner B, Muhar M, Roth M, et al. An optimized microRNA backbone for effective single-copy RNAi. *Cell Rep.* 2013;5:1704–13.
58. Mizutani T, Neugebauer N, Putz EM, Moritz N, Simma O, Zebadin-Brandl E, et al. Conditional IFNAR1 ablation reveals distinct requirements of type I IFN signaling for NK cell maturation and tumor surveillance. *Oncimmunology* . 2012;1:1027–37.

#### ACKNOWLEDGEMENTS

We want to thank S. Fajmann, P. Jodl, P. Kudweis, and the mouse facility team for all their help and C. Vogl for statistical support. This work was supported by the Austrian Science Fund FWF P 27248-B28, FWF P 28571-B21, PhD program, "Inflammation and Immunity" FWF W1212, FWF doc.funds DOC 32-B28, and the Stadt Wien Kultur MA7 Grant FA18020013.

**AUTHOR CONTRIBUTIONS**

V.S. and D.F. supervised the study. V.S., D.F. and D.G. provided reagents and material. V.M.K., K.K., D.G., and A.W.S. designed and analyzed the experiments; V.M.K., K.K., I.M., D.P., J.T., and J.L. performed the experiments. R.G. and G.H. performed bioinformatics analysis. V.M.K., K.K., D.G., A.W.S., and V.S. wrote the paper.

**COMPETING INTERESTS**

The authors declare no competing interests.

**ADDITIONAL INFORMATION**

**Supplementary information** The online version contains supplementary material available at <https://doi.org/10.1038/s41419-021-04279-2>.

**Correspondence** and requests for materials should be addressed to Veronika Sexl.

**Reprints and permission information** is available at <http://www.nature.com/reprints>

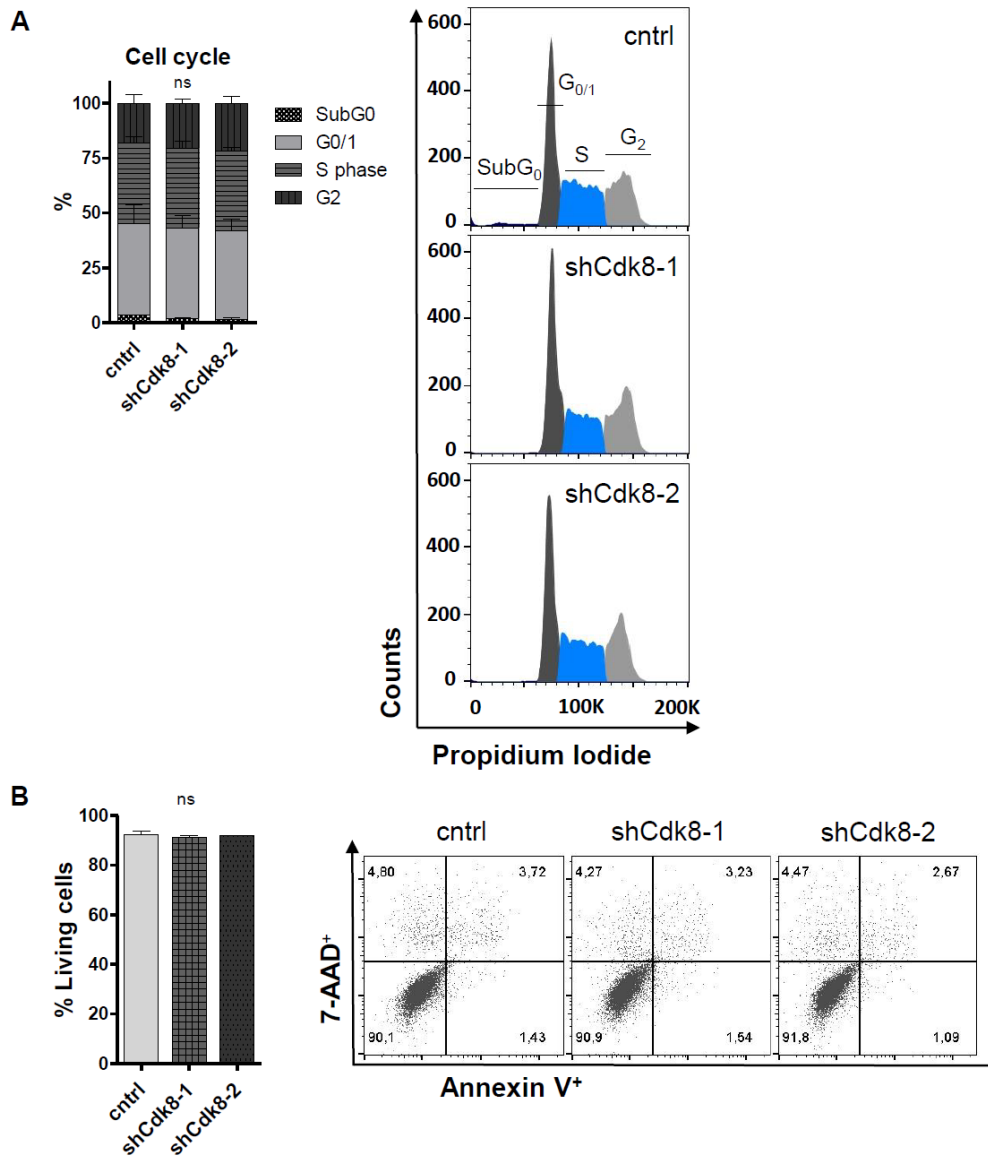
**Publisher's note** Springer Nature remains neutral with regard to jurisdictional claims in published maps and institutional affiliations.



**Open Access** This article is licensed under a Creative Commons Attribution 4.0 International License, which permits use, sharing, adaptation, distribution and reproduction in any medium or format, as long as you give appropriate credit to the original author(s) and the source, provide a link to the Creative Commons license, and indicate if changes were made. The images or other third party material in this article are included in the article's Creative Commons license, unless indicated otherwise in a credit line to the material. If material is not included in the article's Creative Commons license and your intended use is not permitted by statutory regulation or exceeds the permitted use, you will need to obtain permission directly from the copyright holder. To view a copy of this license, visit <http://creativecommons.org/licenses/by/4.0/>.

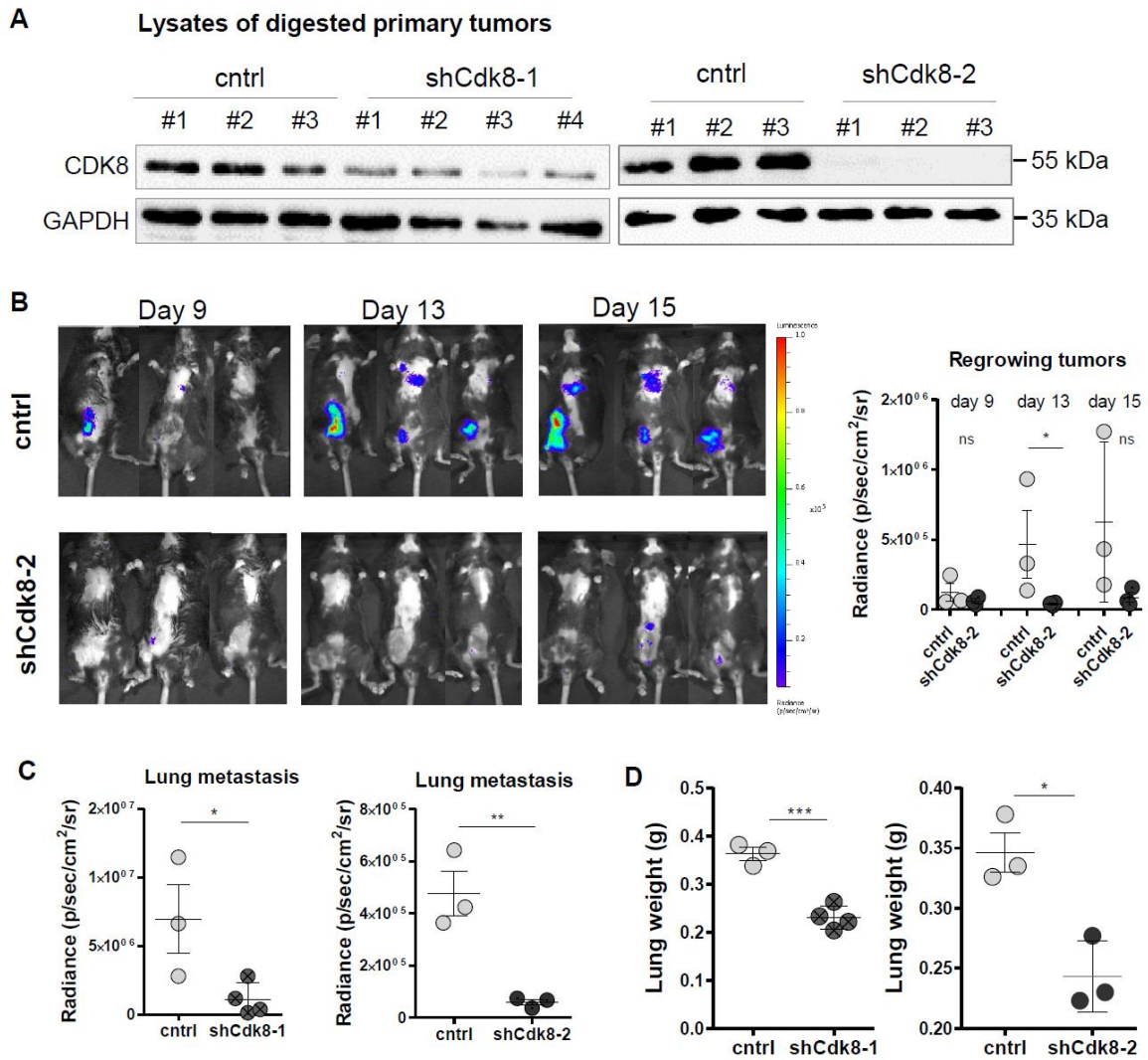
© The Author(s) 2021

## Supplementary Figures



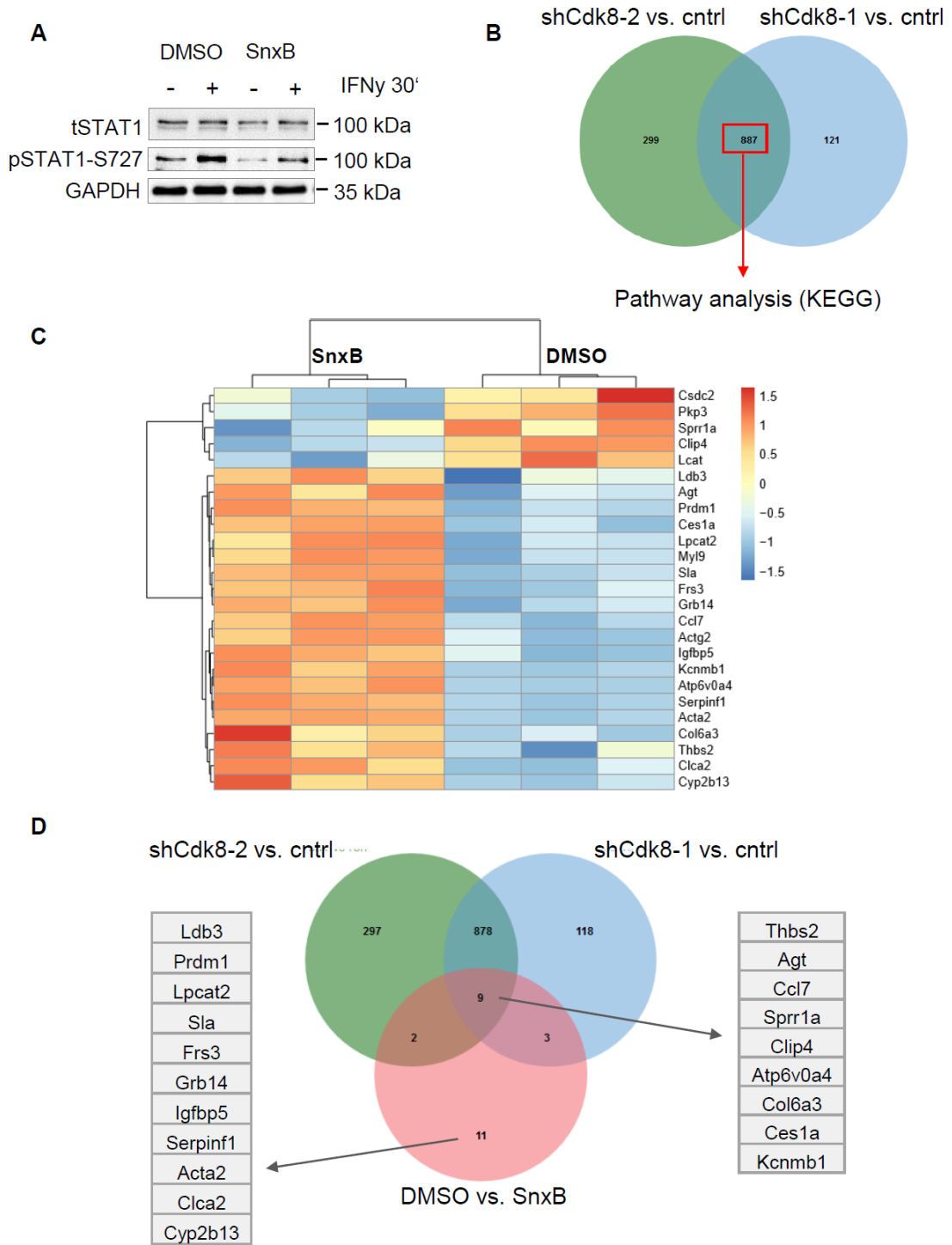
**Supplementary Figure S1. Loss of CDK8 does not alter survival or cell cycle progression of murine TNBC cells.**

(A) PI cell cycle staining and (B) Annexin V/ 7-AAD staining of control, shCdk8-1 and shCdk8-2 E0771 cells. Graphs show mean  $\pm$  SEM of two pooled independent experiments. Representative histograms (A) and FACS blots (B) are shown.



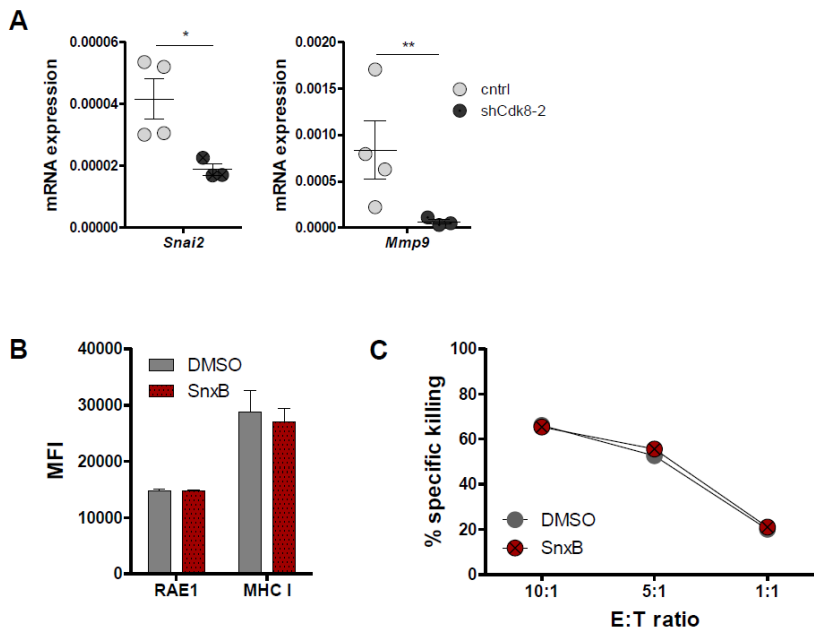
**Supplementary Figure S2. CDK8 supports the re-growth of tumors and distant metastasis formation.**

(A) Lysates of digested primary tumors were analyzed for CDK8 expression by western blotting. GAPDH was used as a loading control. (B) Representative *in vivo* imaging pictures of mice (left) and evaluation of measured radiance signals  $\pm$  SEM (right) of mice implanted with E0771 control versus shCdk8-2 cells. *In vivo* imaging was performed on day 9, day 13 and day 15 post-surgery (endpoint of the experiment). (C) Radiance signals of *ex vivo* lung metastasis and (D) lung weight  $\pm$  SEM of two independent experiments, at day 15 post-surgery.



**Supplementary Figure S3. CDK8/CDK19 inhibitor treatment does not mimic genetic knockdowns of CDK8.**

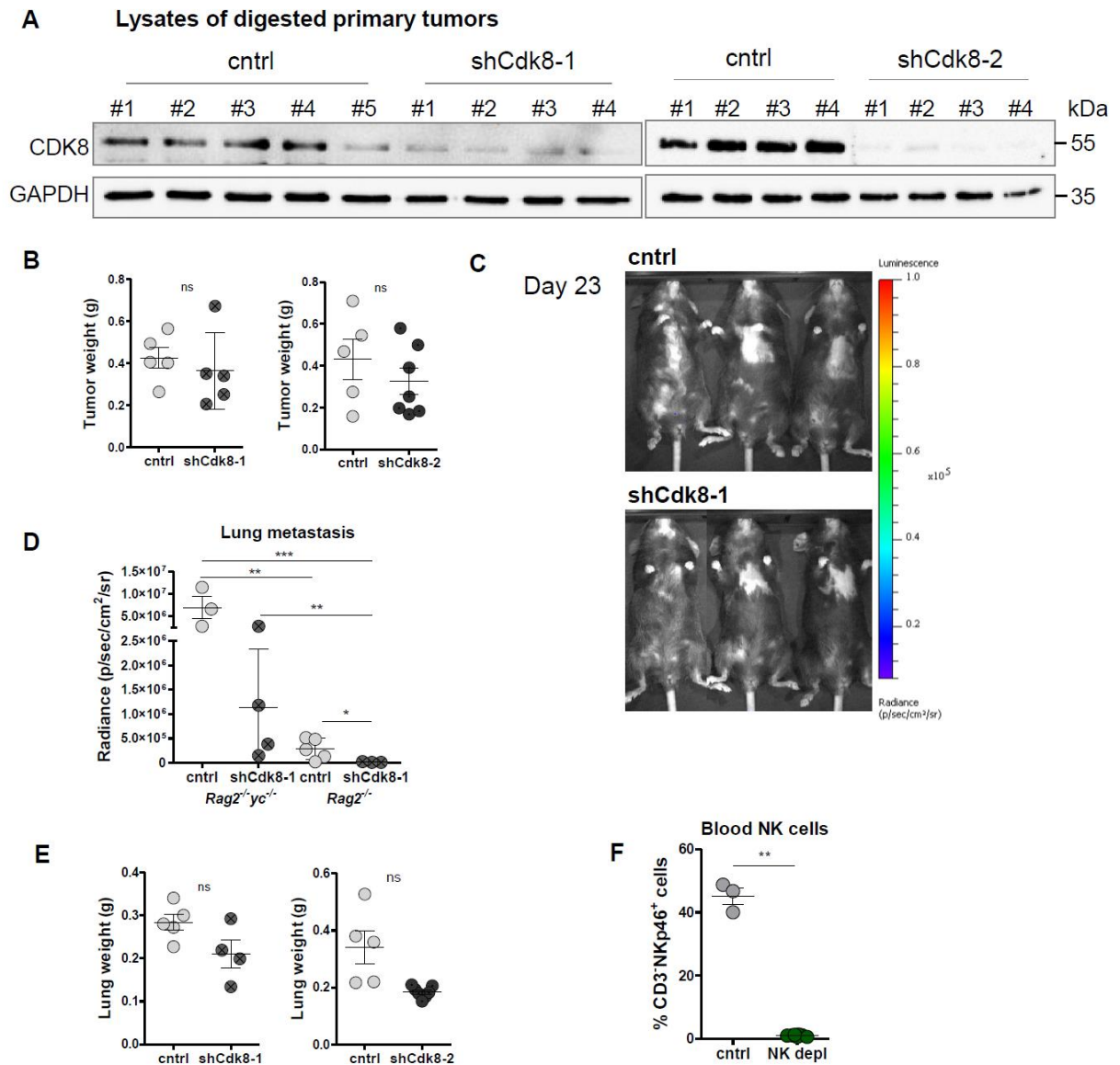
(A) E0771 control cells were treated with 1 $\mu$ M Senexin B (SnxB) or DMSO for 48 hours and incubated  $\pm$  IFN $\gamma$  for 30min and blotted for STAT1, pSTAT1-S727 and GAPDH expression. (B) Venn diagram depicting overlap of genes regulated by two different CDK8-targeting shRNAs (shCdk8-1 and -2). (C) Heatmap of 25 differentially expressed genes between E0771 control cells treated with 1 $\mu$ M Senexin B (SnxB) or DMSO for 48 hours (RNA-seq data; n=3 replicates). (D) Venn diagram depicting overlaps of genes regulated upon Senexin B treatment with genes regulated by two different CDK8-targeting shRNAs (shCdk8-1 and -2). Left table shows 11 genes solely regulated by Senexin B treatment and right table depicts 9 genes regulated upon Senexin B treatment and genetic CDK8 knockdowns.



**Supplementary Figure S4. CDK8/CDK19 inhibitor treatment of E0771 does not alter their killing by NK cells.**

(A) Real-time quantitative PCR of RNA extracted from digested primary tumors of control versus shCdk8-2 implanted *Rag2<sup>-/-</sup>yc<sup>-/-</sup>* mice  $\pm$  SEM. Expression levels of *Snai2* and *Mmp9* were normalized to the house keeping gene *Rplp0*. (B) MFI of RAE1 and MHC I (H-2K+ H-2D) expression of E0771 cells treated with 1 $\mu$ M Senexin B (SnxB) or DMSO as a cntrl; expression levels of NK ligands were analyzed by flow cytometry. Bar graphs represent technical triplicates (mean  $\pm$  SEM). (C) IL2-expanded C57BL/6 NK cells were incubated for 4 hours with CFSE-labelled E0771 control tumor cells pretreated with 1 $\mu$ M Senexin B (SnxB) or DMSO for 44 hours in effector:target (E:T) ratio of 10:1, 5:1 and 1:1. The specific killing was assessed by flow cytometry. One representative experiment out of two independent experiments is shown.





**Supplementary Figure S5. Loss of CDK8 in TNBC increases NK-cell mediated tumor surveillance.**

(A) Lysates of digested primary tumors were analyzed for CDK8 expression by western blotting. GAPDH was used as a loading control. (B) Tumor weight (g)  $\pm$  SEM of *Rag2<sup>-/-</sup>* mice shown in Figure 4B. (C) Representative *in vivo* imaging pictures of *Rag2<sup>-/-</sup>* mice on day 23 post surgery. (D) Comparison of radiance signals of lung metastasis  $\pm$  SEM of *Rag2<sup>-/-</sup>yc<sup>-/-</sup>* (on day 15 post-surgery) and *Rag2<sup>-/-</sup>* mice (on day 23 post-surgery) implanted with control versus shCdk8-1 TNBC cells. (E) Lung weight (g) of *Rag2<sup>-/-</sup>* mice  $\pm$  SEM. (F) Percentage of CD3<sup>+</sup>NKp46<sup>+</sup> NK cells  $\pm$  SEM in blood of control and NK-cell depleted mice, after three injections of  $\alpha$ NK1.1 antibody and prior to tumor cell implantation; percentage of NK cell numbers were analyzed by flow cytometry.

## 2.2. Prologue

In this study we report a novel essential function for CDK8 in BCR-ABL-driven leukemia and provide a potential therapeutic strategy for the treatment of ALL patients. Using *Mx1Cre* and *Vav-Cre* mouse models with a loss of CDK8, we observed an enhanced disease latency and prevention of disease maintenance. This we found associated with pronounced transcriptional changes, which could not be recapitulated with CDK8/CDK19 kinase inhibitors. Transcriptomic analysis revealed a connection of CDK8 with mTOR signaling, together with a significant correlation of CDK8 with mTOR pathway members, when analyzing human cohorts of ALL and AML patients.

That led us to apply a small molecule YKL-06-101, which inhibits mTOR and simultaneously degrades the CDK8 protein. We verified this molecule to significantly reduce viability of human leukemic cell lines and primary patient samples and thereby might represent a new promising treatment strategy.

This research was originally published in Nature Communications:

Ingeborg Menzl, Tinghu Zhang, Angelika Berger-Becvar, Reinhard Grausenburger, Gerwin Heller, Michaela Prchal-Murphy, Leo Edlinger, **Vanessa M. Knab**, Iris Z. Uras, Eva Grundschober, Karin Bauer, Mareike Roth, Anna Skucha, Yao Liu, John M. Hatcher, Yanke Liang, Nicholas P. Kwiatkowski, Daniela Fux, Andrea Hoelbl-Kovacic, Stefan Kubicek, Junia V. Melo, Peter Valent, Thomas Weichhart, Florian Grebien, Johannes Zuber, Nathanael S. Gray & Veronika Sexl. **A kinase-independent role for CDK8 in BCR-ABL1<sup>+</sup> leukemia.** *Nature Communications* 10, 4741 (2019)

<https://www.nature.com/articles/s41467-019-12656-x.pdf>

### Author contributions

V.S. was the principal investigator and takes primary responsibility for the article. V.S. and N.S.G. designed and supervised the study. I.M., A.B.-B., M.P.-M., L.E., V.M.K., I.Z.U., E.G., K.B., and A.S. performed and analyzed experiments. T.Z., Y.L., J.M.H., and Y.L. synthesized and characterized the degraders. R.G. and G.H. performed bioinformatics analysis. P.V. provided patient materials and human leukemic cell lines. J.V.M. provided the Z199 cell line. M.R., S.K., F.G., J.Z., D.F., A.H.K., N.P.K., and T.W. contributed to interpretation of the data and revised the manuscript with regard to critical intellectual content. I.M. and V.S. wrote the manuscript.



## 2.2.1. A kinase-independent role for CDK8 in BCR-ABL1<sup>+</sup> leukemia



ARTICLE

<https://doi.org/10.1038/s41467-019-12656-x>

OPEN

# A kinase-independent role for CDK8 in BCR-ABL1<sup>+</sup> leukemia

Ingeborg Menzl<sup>1</sup>, Tinghu Zhang<sup>2</sup>, Angelika Berger-Becvar<sup>1</sup>, Reinhard Grausenburger<sup>1</sup>, Gerwin Heller<sup>1,3,4</sup>, Michaela Prchal-Murphy<sup>1</sup>, Leo Edlinger<sup>1</sup>, Vanessa M. Knab<sup>1</sup>, Iris Z. Uras<sup>1</sup>, Eva Grundschober<sup>1</sup>, Karin Bauer<sup>5</sup>, Mareike Roth<sup>6</sup>, Anna Skucha<sup>7,8</sup>, Yao Liu<sup>2</sup>, John M. Hatcher<sup>2</sup>, Yanke Liang<sup>2</sup>, Nicholas P. Kwiatkowski<sup>2</sup>, Daniela Fux<sup>1</sup>, Andrea Hoelbl-Kovacic<sup>1</sup>, Stefan Kubicek<sup>8</sup>, Junia V. Melo<sup>9,10</sup>, Peter Valent<sup>5</sup>, Thomas Weichhart<sup>11</sup>, Florian Grebien<sup>7,12</sup>, Johannes Zuber<sup>6</sup>, Nathanael S. Gray<sup>2</sup> & Veronika Sexl<sup>1\*</sup>

Cyclin-dependent kinases (CDKs) are frequently deregulated in cancer and represent promising drug targets. We provide evidence that CDK8 has a key role in B-ALL. Loss of CDK8 in leukemia mouse models significantly enhances disease latency and prevents disease maintenance. Loss of CDK8 is associated with pronounced transcriptional changes, whereas inhibiting CDK8 kinase activity has minimal effects. Gene set enrichment analysis suggests that the mTOR signaling pathway is deregulated in CDK8-deficient cells and, accordingly, these cells are highly sensitive to mTOR inhibitors. Analysis of large cohorts of human ALL and AML patients reveals a significant correlation between the level of CDK8 and of mTOR pathway members. We have synthesized a small molecule YKL-06-101 that combines mTOR inhibition and degradation of CDK8, and induces cell death in human leukemic cells. We propose that simultaneous CDK8 degradation and mTOR inhibition might represent a potential therapeutic strategy for the treatment of ALL patients.

<sup>1</sup>Institute of Pharmacology and Toxicology, University of Veterinary Medicine, Vienna, Austria. <sup>2</sup>Department of Cancer Biology, Department of Biological Chemistry and Molecular Pharmacology, Dana-Farber Cancer Institute, Harvard Medical School, Boston, Massachusetts, USA. <sup>3</sup>Department of Medicine I, Medical University of Vienna, Vienna, Austria. <sup>4</sup>Comprehensive Cancer Center, Vienna, Austria. <sup>5</sup>Division of Hematology and Hemostaseology, Department of Internal Medicine I, Ludwig Boltzmann Institute for Hematology and Oncology, Medical University of Vienna, Vienna, Austria. <sup>6</sup>Research Institute of Molecular Pathology, Campus-Vienna-Biocenter 1, Vienna, Austria. <sup>7</sup>Ludwig Boltzmann Institute for Cancer Research, Vienna, Austria. <sup>8</sup>Research Center for Molecular Medicine of the Austrian Academy of Sciences, Vienna, Austria. <sup>9</sup>Faculty of Health and Medical Sciences, University of Adelaide, Adelaide, South Australia 5005, Australia. <sup>10</sup>Department of Hematology, Imperial College London, Kensington, London SW7 2AZ, UK. <sup>11</sup>Center of Pathobiochemistry and Genetics, Institute of Medical Genetics, Medical University of Vienna, Vienna, Austria. <sup>12</sup>Institute for Medical Biochemistry, University of Veterinary Medicine, Vienna, Austria. \*email: [veronika.sexl@vetmeduni.ac.at](mailto:veronika.sexl@vetmeduni.ac.at)

Cyclin-dependent kinases (CDKs) are serine/threonine kinases that are regulated by binding to cyclins<sup>1</sup>. CDKs were initially shown to play important roles in cell cycle control. Over time, their broad and diverse roles in many biological processes were uncovered and CDKs are now considered as important players in transcription, metabolism, neuronal differentiation, hematopoiesis, and stem cell self-renewal [reviewed in ref. 2]. CDKs comprise two major sub-groups; the first CDK family including CDK1, 2, 4, and 6 is predominantly involved in cell cycle control. The second group comprising CDKs 7 through 13 are modulators of transcriptional processes<sup>3</sup>. CDK6 unifies functions of both groups<sup>4–8</sup>. This dual function may underlie the great success of three independent CDK4/6 inhibitors (palbo-, ribo-, and abemaciclib), which were recently declared as therapeutic breakthrough by the FDA<sup>9</sup>. Besides CDK4/6, also CDK7 and CDK9 have drawn considerable attention as drug targets. Both CDK7 and CDK9 phosphorylate serine residues in the C-terminal tail of RNA Polymerase II. CDK9 regulates transcription of key genes in hematological cancers such as myeloid cell leukemia-1 (MCL-1), B-cell lymphoma extra-long (BCL-x<sub>L</sub>), or X-linked inhibitor of apoptosis protein (XIAP)<sup>10</sup>. CDK7 is considered to drive super-enhancer-(SE)-associated gene expression in neuroblastoma<sup>11</sup> and T-cell acute lymphoid leukemia (T-ALL)<sup>12</sup>. First-generation CDK inhibitors such as flavopiridol<sup>13</sup> and dinaciclib<sup>14</sup> are active in acute myeloid leukemia (AML)<sup>15</sup> and chronic myeloid leukemia (CML), but clinical benefit is limited due to adverse effects<sup>16,17</sup>.

CDK8 was initially reported to exert transcriptional repressive functions as part of the mediator complex, a core component of the basal transcription machinery. CDK8 and its paralog CDK19 bind to the mediator complex in a mutually exclusive way but both rely on binding of cyclin C (CCNC) for kinase activity<sup>3</sup>. Single knockout of *Cdk8* and *CCNC* results in embryonic lethality at E2.5–3 due to preimplantation defects<sup>18</sup>, whereas conditional deletion of CDK8 in adult mice is surprisingly well tolerated<sup>19</sup>. Recent studies have shown that CDK8 can exert activating functions as a co-regulator of p53<sup>20</sup> or hypoxia-induced gene expression<sup>21</sup>. STAT transcription factors are among the best-described targets of CDK8<sup>22,23</sup>. Phosphorylation of STAT1<sup>S727</sup> enhances transcriptional activity and results in interferon (IFN)-induced gene transcription<sup>24</sup>.

The role of CDK8 appears to be divergent and highly context-dependent. In colon cancer<sup>25,26</sup>, melanoma<sup>27</sup>, prostate<sup>28</sup>, and breast cancer<sup>29</sup>, CDK8 accelerates proliferation and migration. In contrast, it acts as a tumor suppressor in endometrial<sup>30</sup> and intestinal tumors<sup>19</sup>. In some AML cell lines, inhibition of CDK8 via steroidal alkaloid cortistatin A dramatically alters gene expression and blocks cell proliferation. These changes were due to the relief of CDK8-mediated repression of SE-driven transcription<sup>31</sup>.

The BCR-ABL1 fusion protein drives the development of CML and a subset of ALL cases, which are considered a particular therapeutic challenge. Albeit tyrosine kinase inhibitors (TKIs) for the BCR-ABL1 oncoprotein are available, further therapeutic improvement is required<sup>32</sup>. Resistance mechanisms towards TKIs demand the development of therapeutic strategies<sup>33</sup>. Our findings identify CDK8 as a key mediator of BCR-ABL1-driven leukemia. The role of CDK8 goes beyond its kinase activity, suggesting the development of therapeutic strategies towards its kinase-independent functions.

## Results

**CDK8 is essential for survival of BCR-ABL1<sup>P185+</sup> leukemic cells.** To investigate which CDKs are expressed in hematopoietic malignancies, we measured the levels of CDK6, CDK7, CDK8,

CDK9, and CDK19 in a panel of human leukemic cell lines by immunoblotting. Irrespective of the cells' origin, the levels of CDK6, CDK7, CDK8, CDK9, and CDK19 were dramatically increased in all cell lines compared with non-transformed human mononuclear lymphocytes (hMNL). CDK8 is part of the kinase submodule of the mediator complex, so we tested whether the other members of this complex are also upregulated and we found increased levels of MED12, MED13, and CCNC, which are part of the mediator kinase module (Fig. 1a). A comparable situation was found in murine leukemia cell lines transformed by the *v-ABL1<sup>P160+</sup>* or *BCR-ABL1<sup>P185+</sup>* oncogenes (Fig. 1b).

We tested which of the CDKs support viability and proliferation of mouse *BCR-ABL1<sup>P185+</sup>* B-ALL cells by using an inducible Tet-On RNAi system, in which short hairpin RNA (shRNA) expression is coupled to a dsRed reporter gene. DsRed<sup>+</sup> cells were detectable 2 days after doxycycline treatment and followed over time. Although knockdown of CDK6, 7, or 9 did not induce strong anti-proliferative responses, we found a pronounced reduction in the frequency of dsRed<sup>+</sup> cells upon knockdown of CDK8 comparable to MYC knockdown, a positive control (Fig. 1c). This prompted us to include CDK19, which has functional homology to CDK8, and the CDK8-binding partners CCNC and MED12, which regulate CDK8's kinase activity. Neither of these knockdown approaches fully recapitulated the effects of loss of CDK8, with the exception of MED12 (Fig. 1c). Efficiencies of CDK6, CDK7, CDK9, CDK19, MED12, and CCNC knockdown were verified by immunoblotting (Fig. 1d and Supplementary Fig. 1a). Downregulation of CDK8, MED12, or c-MYC was less pronounced, indicating that loss of either protein is incompatible with survival. Growth curves supported these observations (Fig. 1e).

Stable shRNA-mediated knockdown for CDK9, CDK19, MED12, MED13, or CCNC in four individually derived murine *BCR-ABL1<sup>P185+</sup>* cell lines gave similar effects to the inducible knockdowns. However, we failed to obtain lines deficient for CDK8 or CDK7 (Supplementary Fig. 1b). We have no explanation for the different effects of CDK7 deletion in short- and long-term knockdown experiments. Our failure to generate CDK8-deficient lines shows that loss of CDK8 is incompatible with survival of *BCR-ABL1<sup>P185+</sup>* cells.

## Steady-state hematopoiesis is not affected by loss of CDK8.

Efficient drug treatment requires a sufficiently large therapeutic window, which allows killing of tumor cells while sparing normal tissue. We therefore investigated the consequences of *Cdk8* deletion on normal, non-leukemic hematopoiesis using *Cdk8<sup>Δ/Δ</sup>Vav-Cre* mice. Bone marrow (BM) was isolated from 6-week-old mice. Efficient deletion of CDK8 was verified by immunoblotting (Fig. 2a). Overall, the loss of CDK8 was well tolerated, as white blood cell counts (WBCs), red blood cell counts (RBCs) and numbers of platelets were comparable to those of control mice (Fig. 2b). Detailed flow cytometric analyses revealed no significant differences in the frequencies of hematopoietic cells at various stages of differentiation, indicating that hematopoiesis remained largely unaffected under steady-state conditions (Fig. 2c). Importantly, percentages of LSK cells and stem cell sub-fractions were comparable (Fig. 2d–e). As *BCR-ABL1<sup>P185+</sup>* cells are of B-lymphoid origin, we closely investigated the consequences of CDK8 deficiency on early B-cell development. B-cell developmental stages can be distinguished by differential cell-surface expression of B220, CD43, CD19, BP-1, IgM, and IgD<sup>34,35</sup>. Frequencies of individual B-cell fractions were unaltered in BMs of *Cdk8<sup>Δ/Δ</sup>Vav-Cre* mice (Fig. 2f). Poly(I:C) treatment in *Cdk8<sup>Δ/Δ</sup>Mx1Cre* mice was used to challenge stress-induced hematopoiesis as it induces a type I IFN-triggered

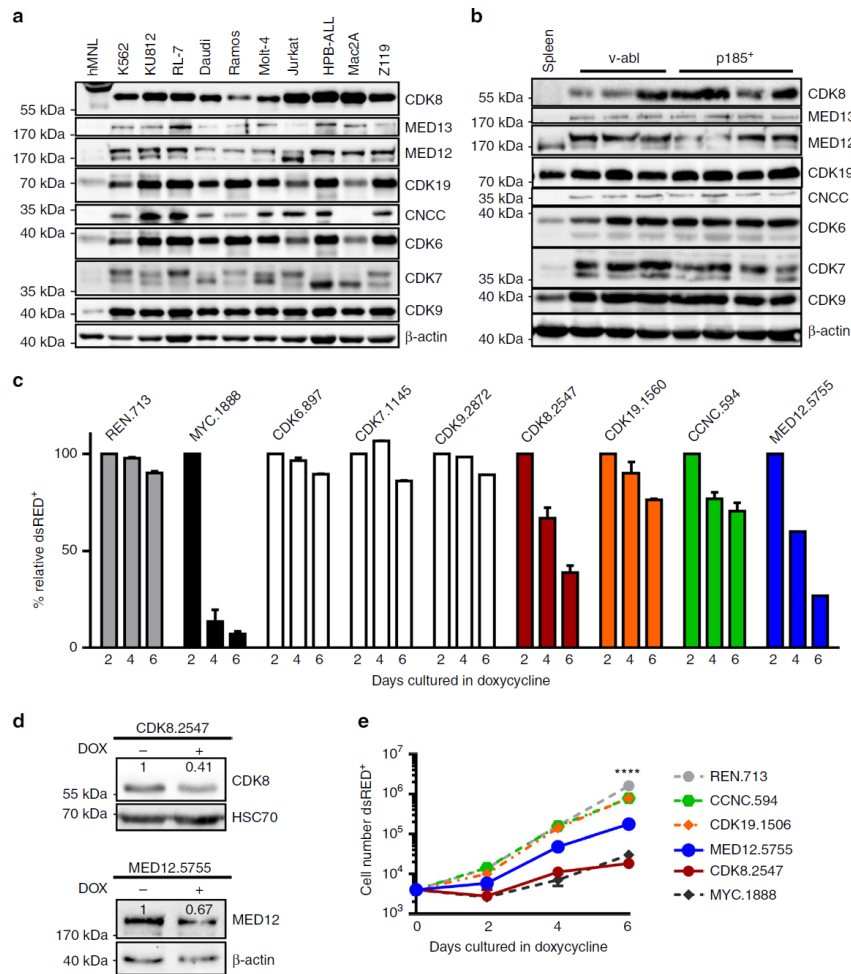
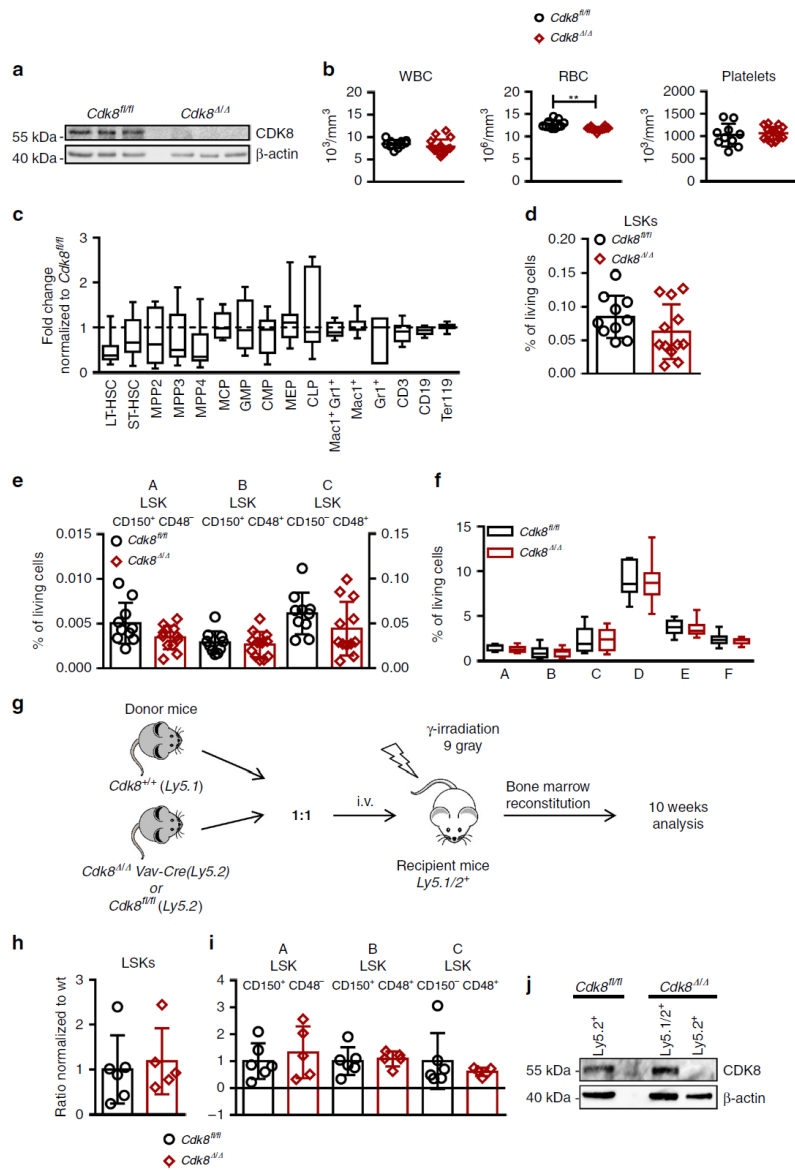


**Fig. 1** CDK8 is essential for survival of BCR-ABL1<sup>P185+</sup> leukemic cells. Immunoblotting: levels of CDK6, CDK7, CDK8, CDK9, CDK19, CCNC, MED12, and MED13 in leukemic human (**a**) and murine (**b**) cell lines. Levels of  $\beta$ -actin served as loading control. **c** Induction of shRNA-mediated knockdowns by doxycycline. Percentages of dsRED<sup>+</sup> BCR-ABL1<sup>P185+</sup> leukemic cells transduced with TRE3G-dsRED-shRNA-puro (Tet-On) targeting CDK6, CDK7, CDK8, CDK9, CDK19, CCNC, or MED12. Numbers indicate the starting point of shRNA sequence. Data represent frequencies of dsRED<sup>+</sup> BCR-ABL1<sup>P185+</sup> cells over time, normalized to the percentages of dsRED<sup>+</sup> cells after 2 days of doxycycline (DOX) administration. shRNAs directed against Renilla (REN) or MYC served as negative and positive controls. One representative experiment performed in duplicates out of three with similar outcome is shown. **d** Verification of shRNA-mediated knockdown of CDK8 and MED12 by immunoblotting (day 2 after doxycycline administration).  $\beta$ -Actin and HSC70 served as a loading control. Numbers refer to densitometric analysis of the blotted protein in reference to loading control levels. **e** Growth curves of shRNA-expressing (dsRED<sup>+</sup>) Tet-On BCR-ABL1<sup>P185+</sup> cells. One representative experiment performed in triplicates out of three with similar outcome is shown. Levels of significance were calculated using two-way ANOVA followed by Dunn's test; data represents means  $\pm$  SD (\*\*\*\* $p < 0.0001$ ). Source data are provided as a Source Data file

ubiquitous deletion of *Cdk8*. Poly(I:C) treatment in *Cdk8*<sup>f/f</sup> *Mx1Cre* mice reflected the observations in *Cdk8* <sup>$\Delta\Delta$</sup>  *Vav-Cre* mice; we did not detect significant changes in the frequencies of hematopoietic cell subsets in the BM or in the blood cells upon *Cdk8* deletion (Supplementary Fig. 2a-f). To explore the functionality of CDK8-deficient stem cells, we set up a competitive

transplant experiment. We mixed BM cells from *Cdk8* <sup>$\Delta\Delta$</sup>  *Vav-Cre* *Ly5.2*<sup>+</sup> or *Cdk8*<sup>f/f</sup> *Ly5.2*<sup>+</sup> mice with *CDK8*<sup>+/+</sup> *Ly5.1*<sup>+</sup> BM cells in a 1:1 ratio and injected them intravenously (i.v.) into lethally irradiated *Ly5.1/2*<sup>+</sup> mice (Fig. 2g). Ten weeks after transplantation, no differences in the repopulation capacity of stem cells of different genotypes were observed (Fig. 2h, i). The absence of



CDK8 was confirmed in sorted BM-derived *Cdk8<sup>Δ/Δ</sup>* Vav-Cre Ly5.2<sup>+</sup> cells (Fig. 2j). In summary, conditional and inducible loss of CDK8 in the hematopoietic system is well tolerated, underlining the potential of CDK8 as a therapeutic target.

**CDK8 is not required for initial BCR-ABL1<sup>P185+</sup> transformation.** To test the consequences of *Cdk8* deficiency for B-lymphoid transformation, we infected *Cdk8<sup>Δ/Δ</sup>* Vav-Cre-BM

cells with a retrovirus encoding pMSCV-Bcr-Abl1<sup>P185</sup>-IRES-eGFP or Ab-MuLV (encoding v-ABL1<sup>P160+</sup>). Infected cells were subsequently plated in growth factor-free methylcellulose. Irrespective of the genotype, comparable numbers of B-lymphoid colonies grew out (Fig. 3a and Supplementary Fig. 3a). Deficiency of CDK8 did not affect the levels of CDK19, MED12, MED13, or CNCC (Fig. 3b and Supplementary Fig. 3b). Transformation by BCR-ABL1<sup>P185+</sup> or v-ABL1<sup>P160+</sup> resulted in the outgrowth of



**Fig. 2** Steady-state hematopoiesis is not affected by loss of CDK8 (*Cdk8<sup>Δ/Δ</sup>Vav-Cre*). **a** Efficiency of CDK8 deletion in 6-week-old *Cdk8<sup>Δ/Δ</sup>Vav-Cre* mice. Immunoblotting of BM cells from *Cdk8<sup>fl/fl</sup>* and *Cdk8<sup>Δ/Δ</sup>Vav-Cre* mice ( $n = 3$  per genotype). **b** Analysis of white blood cell count (WBC), red blood cell count (RBC), and platelet count of *Cdk8<sup>fl/fl</sup>* ( $n = 10$ ) and *Cdk8<sup>Δ/Δ</sup>Vav-Cre* mice ( $n = 16$ ) are depicted. **c** Relative fold change of BM composition of *Cdk8<sup>Δ/Δ</sup>Vav-Cre* mice ( $n = 10$ ) normalized to mean of *Cdk8<sup>fl/fl</sup>* ( $n = 10$ ). Center value represents median, the box 25th to 75th percentiles, and whiskers min to max. **d** Bar diagram of Lin<sup>-</sup> Sca-1<sup>+</sup> c-kit<sup>+</sup> (LSK) frequencies in BMs of *Cdk8<sup>fl/fl</sup>* ( $n = 10$ ) and *Cdk8<sup>Δ/Δ</sup>Vav-Cre* ( $n = 12$ ) mice. **e** Frequencies of LSK subpopulations (fraction A, B, and C; *Cdk8<sup>fl/fl</sup>*  $n = 10$ , *Cdk8<sup>Δ/Δ</sup>Vav-Cre*  $n = 12$ ). **f** Frequencies of individual populations during early B-cell development according to Hardy nomenclature in pre-pro-B (B220<sup>+</sup>/CD43<sup>hi</sup>/CD19<sup>-</sup>/BP-1<sup>-</sup>; fraction A), early pro-B (B220<sup>+</sup>/CD43<sup>hi</sup>/CD19<sup>+</sup>/BP-1<sup>-</sup>; fraction B), late pro-B (B220<sup>+</sup>/CD43<sup>hi</sup>/CD19<sup>+</sup>/BP-1<sup>+</sup>; fraction C), pre-B (B220<sup>+</sup>/CD43<sup>lo</sup>/IgM<sup>-</sup>/IgD<sup>-</sup>; fraction D), immature (B220<sup>+</sup>/CD43<sup>lo</sup>/IgM<sup>+</sup>/IgD<sup>-</sup>; fraction E), and mature (B220<sup>+</sup>/CD43<sup>lo</sup>/IgM<sup>+</sup>/IgD<sup>+</sup>; fraction F) B cells<sup>34,35</sup> (*Cdk8<sup>fl/fl</sup>*  $n = 9$ , *Cdk8<sup>Δ/Δ</sup>Vav-Cre*  $n = 12$ ). Center value represents median, the box 25th to 75th percentiles and whiskers min to max. **g** Experimental setup of competition transplants data shown in **h**, **i**. **h** Bar graph displays LSK<sup>+</sup> cells analyzed for Ly5.1<sup>+</sup>/Ly5.2<sup>+</sup> composition in total BM. **i** Contributions of Ly5.1<sup>+</sup> and Ly5.2<sup>+</sup> cells in LSK subpopulations (fraction A, B, and C; *Cdk8<sup>fl/fl</sup>*  $n = 6$  and *Cdk8<sup>Δ/Δ</sup>Vav-Cre*  $n = 5$ ). **j** Immunoblot of sorted BM cells after competitive transplant. Detection of CDK8 in *Cdk8<sup>fl/fl</sup>* Ly5.2, *Cdk8<sup>fl/fl</sup>* Ly5.1, and *Cdk8<sup>Δ/Δ</sup>* Ly5.2 cells;  $\beta$ -actin served as loading control. Levels of significance were calculated using **b**, **d**, **e**, **f** unpaired *t*-test, **i** Mann-Whitney, and **c** Kruskal-Wallis test followed by Dunn's test; data represent means  $\pm$  SD (\*\* $p < 0.01$ ). Source data are provided as a Source Data file

pro-B cells that consistently stain positive for B220, CD19, and CD43, and negative for the maturation markers IgM and IgD (Fig. 3c). BCR-ABL1<sup>P185+</sup> and v-ABL1<sup>P160+</sup>-transduced *Cdk8<sup>Δ/Δ</sup>Vav-Cre* cell lines showed higher frequencies of apoptotic cells (Fig. 3d and Supplementary Fig. 3c) that were also evident in growth curves; the numbers of v-ABL1<sup>P160+</sup> *Cdk8<sup>Δ/Δ</sup>Vav-Cre* cells rose significantly slower than those of the control group (Supplementary Fig. 3d). Consistently, the number of cells in the SubG<sub>1</sub> phase increased upon loss of CDK8 (Fig. 3e and Supplementary Fig. 3e).

The enhanced apoptosis and reduced proliferation of CDK8-deficient cells in vitro may be compensated in vivo by the microenvironment. We transplanted BCR-ABL1<sup>P185+</sup> or v-ABL1<sup>P160+</sup> transformed *Cdk8<sup>Δ/Δ</sup>* cell lines into NSG mice. Leukemia latency of BCR-ABL1<sup>P185+</sup> and v-ABL1<sup>P160+</sup> transformed *Cdk8<sup>Δ/Δ</sup>* cells was significantly increased compared to wild-type cells (Fig. 3f and Supplementary Fig. 3f). Analysis of moribund animals unraveled slight differences in disease phenotypes; although the numbers of WBCs were comparable, the frequency of CD19<sup>+</sup> cells containing the transformed cell population in the BM was significantly increased upon CDK8 loss (BCR-ABL1<sup>P185+</sup>) (Fig. 3g and Supplementary Fig. 3g). The absence of CDK8 was confirmed by immunoblotting of ex vivo-isolated BCR-ABL1<sup>P185+</sup>- and v-ABL1<sup>P160+</sup>-transduced cells (Fig. 3h and Supplementary Fig. 3h). The prolonged disease latency of the *Cdk8<sup>Δ/Δ</sup>Vav-Cre*-transplanted cohort does not result from differences in homing to the BM, as there were no significant differences between BCR-ABL1<sup>P185+</sup> CDK8-expressing and BCR-ABL1<sup>P185+</sup> *Cdk8<sup>Δ/Δ</sup>Vav-Cre* cells (Fig. 3i). Expression of a CDK8 kinase-dead mutant (D173A) in leukemic *Cdk8<sup>Δ/Δ</sup>Vav-Cre* cells accelerated disease development, which indicates that CDK8 exerts its effect in a kinase-independent manner (Supplementary Fig. 3i, j). The data suggest that CDK8 is largely dispensable for the initiation of BCR-ABL1<sup>P185+</sup> or v-ABL1<sup>P160+</sup> B-ALL, but instead may play an important part in disease maintenance by controlling cell survival.

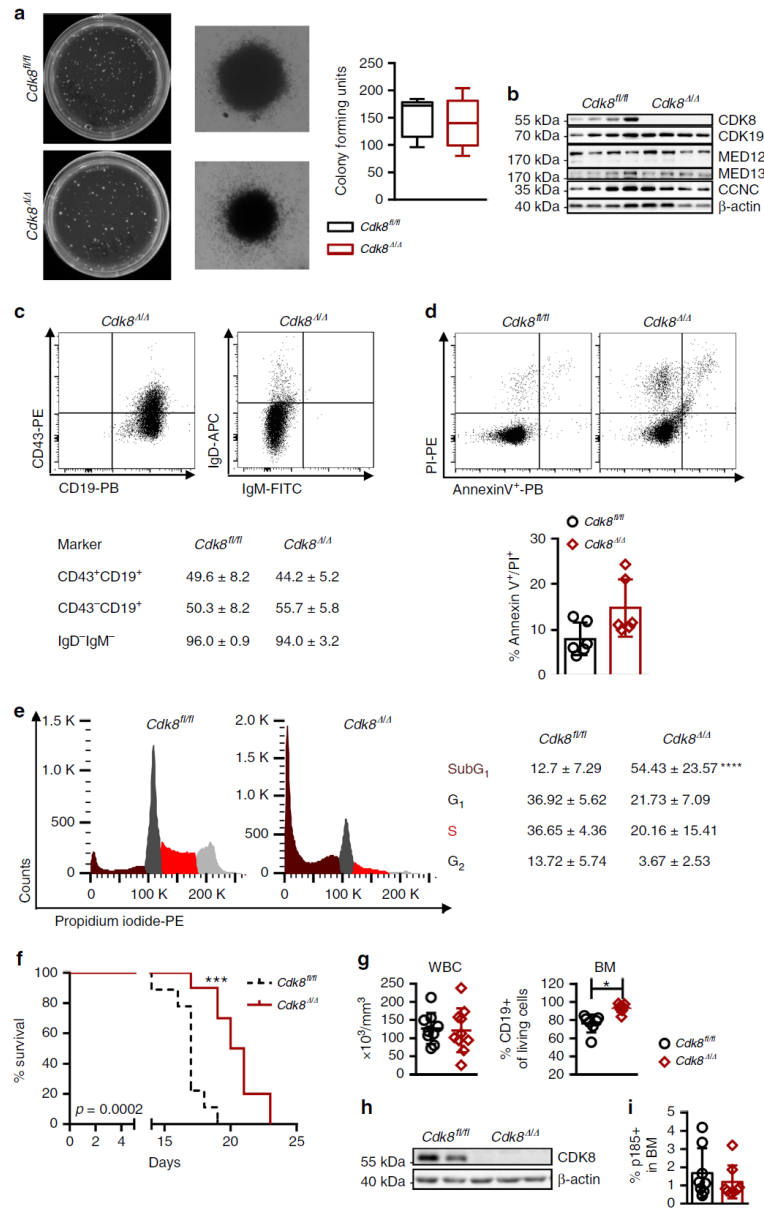
**CDK8 is required for maintenance of BCR-ABL1<sup>P185+</sup> leukemia.** To investigate the immediate consequence of CDK8 loss in leukemic cells, we created *Cdk8<sup>fl/fl</sup>Mx1Cre* BCR-ABL1<sup>P185+</sup> cell lines and deleted *Cdk8* at specific time points by IFN- $\beta$  (Fig. 4a). Immunoblotting confirmed that IFN- $\beta$  administration deleted *Cdk8* until day 7, after which multiplication of the few remaining *Cdk8*-positive (non-deleting) cells gave rise to a weak signal for CDK8 (Fig. 4b). Whereas wild-type BCR-ABL1<sup>P185+</sup> cells were only marginally affected by IFN- $\beta$  stimulation, the percentage of AnnexinV<sup>+</sup>-positive cells was significantly over 7 days upon loss of CDK8 (Fig. 4c). Cell cycle analysis on day 3 after addition of IFN- $\beta$  revealed a significant increase of cells in SubG<sub>1</sub> and a reduction of cells in the S- and G<sub>2</sub> phases (Fig. 4d). To test the effects of

deletion of *Cdk8* in vivo, we transplanted BCR-ABL1<sup>P185+</sup> wild type and *Cdk8<sup>fl/fl</sup>Mx1Cre* into NSG mice (Fig. 4e). Deletion of *Cdk8* resulted in a significant survival benefit (Fig. 4f). Immunoblotting of the leukemic cells ex vivo revealed residual CDK8 expression in the leukemic compartment, representing heterozygous deleters or repopulating BCR-ABL1<sup>P185+</sup> *Cdk8<sup>fl/fl</sup>Mx1Cre* cells that managed to avoid deletion (Fig. 4g). These non-deleters caused the fatal leukemia with a significant increase in circulating WBCs but a decreased frequency of CD19<sup>+</sup> cells in the spleen (SPL) (Fig. 4h, i). To follow the kinetics of leukemic cells, we again injected BCR-ABL1<sup>P185+</sup> *Cdk8<sup>fl/fl</sup>Mx1Cre* into NSG mice and found a pronounced decrease in the BM upon poly(I:C) treatment after 17 days. Leukemic cells increased again thereafter, indicating a selection of non-deleters that finally induce disease (Supplementary Fig. 4a, b). These experiments using inducible deletion led us to conclude that BCR-ABL1<sup>P185+</sup> cells depend on CDK8.

#### Kinase inhibition fails to mimic the effects of *Cdk8* deletion.

Various small-molecule inhibitors have been developed to target CDKs in cancer. To further investigate whether CDK8's kinase activity accounts for the substantial effects in leukemogenesis, we applied the CDK8/CDK19 inhibitors Senexin B and MSC (MSC2530818). The efficiency of the inhibitors was confirmed by reduction of STAT1<sup>S727</sup> phosphorylation, a known CDK8 kinase substrate (Fig. 5a)<sup>24</sup>. The reduced phosphorylation was accompanied by a lower induction of STAT1 target genes (*Mx1*, *Stat1*, *Tap1*, *Gbp2*, *Irf1*, and *Ido1*) upon IFN- $\beta$  stimulation (Supplementary Fig. 5a). Despite reduction of pSTAT1<sup>S727</sup> and its target genes, there was no significant change in the frequency of apoptotic cells in BCR-ABL1<sup>P185+</sup> *Cdk8<sup>fl/fl</sup>* and *Cdk8<sup>Δ/Δ</sup>Vav-Cre* cell lines upon treatment with inhibitor (Fig. 5b). The IC<sub>50</sub> values for Senexin B were almost identical, irrespective of the presence of CDK8 (Supplementary Fig. 5b). We investigated these differences by RNA sequencing (RNA-seq), comparing four individually derived BCR-ABL1<sup>P185+</sup> *Cdk8<sup>Δ/Δ</sup>Vav-Cre* cell lines with four BCR-ABL1<sup>P185+</sup> *Cdk8<sup>fl/fl</sup>* cell lines in the absence and in the presence of a kinase inhibitor (Senexin B). The absence of CDK8 protein resulted in 103 upregulated and 56 downregulated genes in BCR-ABL1<sup>P185+</sup> *Cdk8<sup>Δ/Δ</sup>Vav-Cre* compared with control cell lines. In contrast, Senexin B had only minor effects and affected the transcription of only six genes (Fig. 5c and Supplementary Fig. 5c). CDK8 deletion is thus not recapitulated by inhibition of CDK8 kinase activity in leukemogenesis.

**CDK8 regulates the mTOR pathway.** We used gene set enrichment analysis (GSEA) to identify pathways that are perturbed in the absence of CDK8 (*Cdk8<sup>Δ/Δ</sup>Vav-Cre*). GSEA analysis



identified downregulation of 14 pathways, including several prominent signaling pathways involved in BCR-ABL1-driven disease. Among the top hits, we found “tumor necrosis factor- $\alpha$  signaling via nuclear factor- $\kappa$ B (NF $\kappa$ B)”, “mammalian target of rapamycin complex 1 (mTORC1) signaling,” and “phosphoinositide 3-kinase (PI3K) AKT mTOR signaling” (Fig. 6a).

A complete list of deregulated pathways is provided in Supplementary Table 1. Confirmation was provided by the EnrichR program (Supplementary Fig. 6a and Supplementary Table 2), which validated the deregulation of 18 genes (Supplementary Fig. 6b). Phosphorylation of key players in the mTOR pathway (pS6<sup>S240/244</sup>, p4E-BP-1<sup>T37/46</sup>, and pAKT<sup>S473</sup>) was reduced in

**Fig. 3** CDK8 is not required for initial BCR-ABL1<sup>P185+</sup> transformation. **a** BCR-ABL1<sup>P185+</sup>-induced colony formation of *Cdk8<sup>fl/fl</sup>* and *Cdk8<sup>Δ/Δ</sup>Vav-Cre* BM cells in growth-factor-free methylcellulose. The second panel shows single-colony pictures of each phenotype. Summary of colony-formation assays. Center value represents median, the box 25th to 75th percentiles and whiskers min to max ( $n = 4$  per genotype; each performed in duplicates). **b** CDK8, CDK19, CCNC, MED12, and MED13 protein levels in BCR-ABL1<sup>P185+</sup> *Cdk8<sup>fl/fl</sup>* and BCR-ABL1<sup>P185+</sup> *Cdk8<sup>Δ/Δ</sup>Vav-Cre* cell lines (immunoblotting).  $\beta$ -Actin served as loading control. **c** Representative FACS blots of B-cell marker staining; B220<sup>+</sup> gated BCR-ABL1<sup>P185+</sup> *Cdk8<sup>Δ/Δ</sup>Vav-Cre* cells with CD43, CD19, IgD, and IgM. Table below indicates frequencies of indicated markers for BCR-ABL1<sup>P185+</sup> *Cdk8<sup>fl/fl</sup>* and BCR-ABL1<sup>P185+</sup> *Cdk8<sup>Δ/Δ</sup>Vav-Cre* cell lines ( $n = 4$  per genotype). **d** FACS profile of an AnnexinV/PI staining of BCR-ABL1<sup>P185+</sup> *Cdk8<sup>fl/fl</sup>* and BCR-ABL1<sup>P185+</sup> *Cdk8<sup>Δ/Δ</sup>Vav-Cre* cell lines ( $n = 6$  per genotype). **e** PI cell cycle staining of BCR-ABL1<sup>P185+</sup> *Cdk8<sup>fl/fl</sup>* and BCR-ABL1<sup>P185+</sup> *Cdk8<sup>Δ/Δ</sup>Vav-Cre* cell lines. The experiment was performed in technical duplicates; data from one out of three independent experiments are depicted. Table contains frequencies of cells in individual phases of the cell cycle ( $n = 3$  per genotype). **f** BCR-ABL1<sup>P185+</sup> *Cdk8<sup>fl/fl</sup>* and BCR-ABL1<sup>P185+</sup> *Cdk8<sup>Δ/Δ</sup>Vav-Cre* cells were injected intravenously (i.v.) into non-irradiated NSG mice (2500 cells/mouse,  $n = 9$  mice received BCR-ABL1<sup>P185+</sup> *Cdk8<sup>fl/fl</sup>* and 10 mice BCR-ABL1<sup>P185+</sup> *Cdk8<sup>Δ/Δ</sup>Vav-Cre* cells, 3 independent cell lines per genotype were injected). Survival curves of recipients are depicted (median survival of *Cdk8<sup>fl/fl</sup>* and *Cdk8<sup>Δ/Δ</sup>Vav-Cre* cohorts: 17 days and 21 days). **g** White blood cell count (WBC) ( $n = 9$  *Cdk8<sup>fl/fl</sup>*;  $n = 10$  *Cdk8<sup>Δ/Δ</sup>Vav-Cre*) cells and frequencies of CD19<sup>+</sup> cells in BM of diseased mice ( $n = 7$  BCR-ABL1<sup>P185+</sup> *Cdk8<sup>fl/fl</sup>*;  $n = 9$  BCR-ABL1<sup>P185+</sup> *Cdk8<sup>Δ/Δ</sup>Vav-Cre*). **h** Immunoblotting for CDK8 of ex vivo-derived BCR-ABL1<sup>P185+</sup> *Cdk8<sup>fl/fl</sup>* and BCR-ABL1<sup>P185+</sup> *Cdk8<sup>Δ/Δ</sup>Vav-Cre* cells. Levels of  $\beta$ -actin served as loading control. **i** Homing assay of BCR-ABL1<sup>P185+</sup> *Cdk8<sup>fl/fl</sup>* vs. BCR-ABL1<sup>P185+</sup> *Cdk8<sup>Δ/Δ</sup>Vav-Cre* cells. Bar diagram show percentages of BCR-ABL1<sup>P185+</sup> cells in the BM 18 h post injection. Asterisks denote statistical significances as determined by an **a, c, e, g** (WBC) unpaired t-test, **d, g** (BM), **i** Mann-Whitney, or a **f** log-rank test; data represent means  $\pm$  SD (\* $p < 0.05$ ; \*\* $p < 0.001$ ; \*\*\* $p < 0.001$ ). Source data are provided as a Source Data file

CDK8-deficient cells (Fig. 6b, c). We confirmed the involvement of CDK8 in the regulation of signaling pathways with commercially available inhibitors of the mTOR, PI3K, and NF $\kappa$ B pathways. IC<sub>50</sub> levels were determined in BCR-ABL1<sup>P185+</sup> *Cdk8<sup>fl/fl</sup>* and BCR-ABL1<sup>P185+</sup> *Cdk8<sup>Δ/Δ</sup>Vav-Cre* cell lines (Fig. 6d). Loss of CDK8 was associated with a >20-fold enhanced susceptibility to the two mTOR inhibitors Torin1 and Everolimus. The combined inhibition of PI3K and mTOR (by BEZ235) was threefold more effective in *Cdk8*-positive cell lines, presumably because of feedback loops. Sensitivity to inhibition of the NF $\kappa$ B pathway (by Bay11) was little altered by the loss of CDK8 and the effects of inhibition of PDK1/Akt, Flt3/PIM, JAK1, and JAK2 (by Ruxolitinib), and of PI3K $\delta$  (by Cal101) were also independent of the presence of CDK8. The absence of CDK8 renders cells slightly more susceptible to inhibition of CDK9 (NVP-2) or CDK7 (THZ-1), although the IC<sub>50</sub>'s are well above the published ranges for specific effects so the results presumably reflect general toxicity (Fig. 6d and Supplementary Fig. 6c). The findings confirm that CDK8 has a role in the mTOR signaling pathway.

**Chemical CDK8 degradation cooperates with mTOR inhibition.** We analyzed publicly available data from large cohorts of ALL ( $n = 203$ ; TARGET study) and AML ( $n = 179$ ; The Cancer Genome Atlas (TCGA) study) patients for a potential link between CDK8 and members of the mTOR pathway. Data on AML patients were included, as CDK8 has been implicated in the disease<sup>31</sup>. In both diseases, we found a significant correlation of CDK8 with members of the mTOR pathway including CREB1, TSC1, mTOR, PIK3CD, ZZZ1, DEPTOR, SOS1, RRAGB, LAMTOR5, PIK3CB, and PTEN (Fig. 7a, b). Furthermore, CDK8 and members of the mTOR pathway are correlated in a number of other cancers including thyroid carcinoma, thymoma, prostate adenocarcinoma, and liver hepatocellular carcinoma (Supplementary Fig. 7a).

To evaluate the therapeutic potential of our findings, we targeted CDK8 alone or in combination with mTOR inhibition in human leukemic cells (cell lines or primary samples). As inhibition of CDK8 kinase activity does not mimic the effects of CDK8 knockdown in mice, we used chemical-induced protein degradation strategy<sup>36</sup> to deplete the CDK8 protein in human leukemic cell lines. The CDK8 degrader JH-XI-10-02 selectively degrades CDK8<sup>37</sup>. In addition, medical chemistry optimization of Torin1, an inhibitor of mTOR, which also affects CDK8 kinase activity (IC<sub>50</sub> of 159 nM)<sup>38</sup>, resulted in the development of THZ-55, a more potent inhibitor of CDK8 (IC<sub>50</sub> = 5 nM). By linking THZ-55 with thalidomide, a ligand that can recruit the E3 ligase

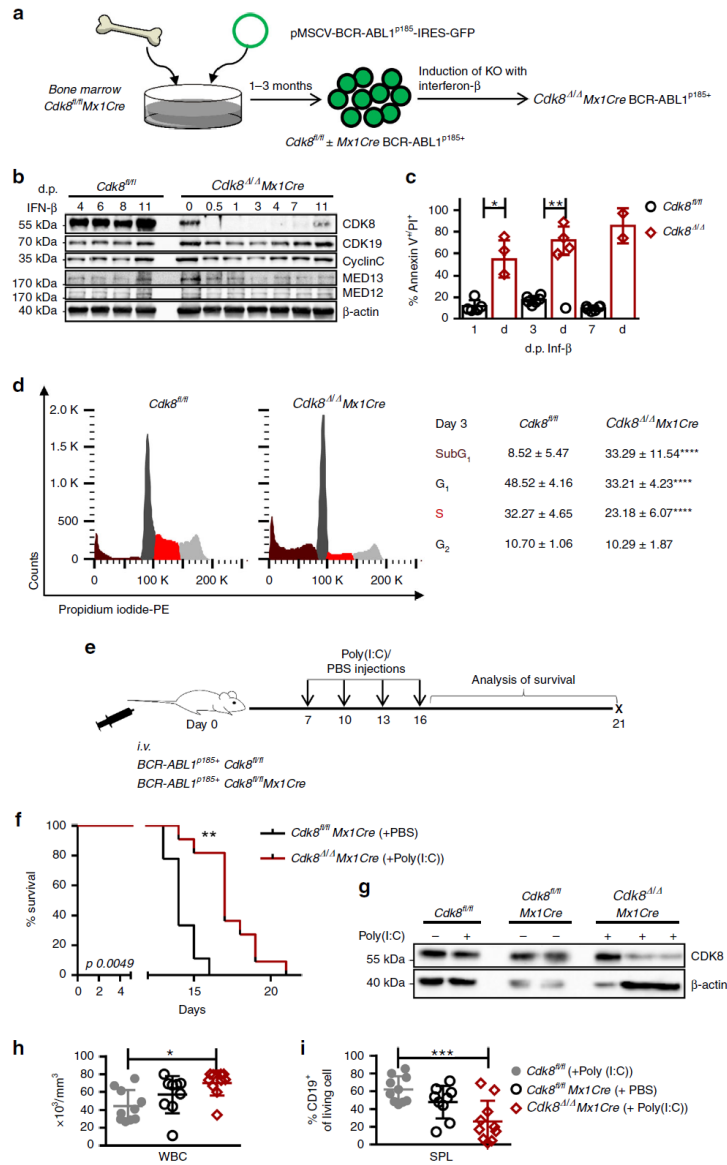
cereblon, we generated a bivalent CDK8 degrader, YKL-06-101, which can also inhibit mTOR (Fig. 7c). We tested Senexin B, JH-XI-10-02, and YKL-06-101 in human BCR-ABL1<sup>+</sup> (BV173, Nalm1, TOM-1, and Z119) and BCR-ABL1<sup>-</sup> (BL41, Raji, Ramos, and REH) cells. Degradation of JH-XI-10-02 and Senexin B treatment induces a proliferation arrest at IC<sub>50</sub> values above 10  $\mu$ M. In contrast, the bivalent degrader YKL-06-101 stops proliferation of BCR-ABL1<sup>+</sup> (Z119, BV173) and of BCR-ABL1<sup>-</sup> cells (REH) at concentrations below 1  $\mu$ M (Fig. 7d). Growth arrest is observed after 48 h (Fig. 7d) and is followed by induction of apoptosis and a significant increase in AnnexinV<sup>+</sup>/7AAD<sup>+</sup> cells (Fig. 7e, h and Supplementary Fig. 8a). Degradation of CDK8 but not of mTOR was verified by western blotting (Fig. 7f, g and Supplementary Fig. 8b). The reduced phosphorylation of S6<sup>S240/244</sup>, indicative of mTOR inhibition, confirms the dual function of the YKL-06-101 degrader (Fig. 7f, g and Supplementary Fig. 8b). Levels of CDK19, CCNC, MED12, and MED13 remained unaltered, irrespective of whether the CDK8 protein was degraded or its kinase activity was inhibited (Supplementary Fig. 8c, d). We verified the synergistic effects of CDK8 degradation and mTOR inhibition by treating cells simultaneously with the CDK8 degrader JH-XI-10-02 and Torin1. Incubation of BCR-ABL1<sup>+</sup> Z119 cells with 1  $\mu$ M JH-XI-10-02 and 10 nM Torin1 caused significantly more apoptosis than single treatments, confirming that the effects result from the simultaneous degradation of CDK8 and the inhibition of mTOR (Fig. 7i).

Treatment of primary ALL patient samples with JH-XI-10-02 and YKL-06-101 confirmed the efficacy of YKL-06-101 but not of JH-XI-10-02 alone to induce apoptosis. YKL-06-101 reduced cell viability in 5 out of 12 patient samples, whereas JH-XI-10-02 had no effect (Fig. 7j and Supplementary Table 3). The result strongly suggests that combining CDK8 degradation with mTOR inhibition may represent a therapeutic approach for a subset of ALL patients.

## Discussion

CDK8 has attracted much attention over the last years as potential target for cancer therapy<sup>39</sup>. Small-molecule inhibitors that block CDK8 kinase activity have been shown to be effective in AML<sup>31</sup>, melanoma<sup>27</sup>, breast<sup>29</sup>, prostate<sup>28</sup>, and colon cancer models<sup>39,40</sup>. We describe a kinase-independent function of CDK8 in hematopoietic tumors and suggest that the proteasome-induced degradation of CDK8 in combination with inhibition of mTOR might represent an addition to the therapeutic armory.

CDKs are present at high levels in hematopoietic neoplasms. Although murine leukemia cells (BCR-ABL1<sup>P185+</sup>) contain high



levels of CDK6, CDK7, CDK8, CDK9, and CDK19, knockdown of CDK6, CDK7, CDK9, or CDK19 has little effect on cell survival and proliferation in an inducible system. In contrast, deletion of CDK8 has a dramatic effect. Stable knockdown experiments recapitulated the results with inducible shRNAs, although we were not able to generate CDK7- or CDK8-deficient cell lines. The apparent discrepancy between the short- and long-term effects of CDK7 knockdown can be explained by speculating the

existence of a stable factor that depends on CDK7; further experiments will be required to test this notion. The pronounced anti-proliferative effects of *Cdk8* deletion in murine leukemia cells were unexpected and indicate the unique role of CDK8 downstream of BCR-ABL1<sup>P185+</sup> in murine B-ALL. The effect is at least partially independent of the mediator as the deletion of CCNC or MED13 was well tolerated. The pronounced effects of deleting MED12 may be explained by the requirement for MED12 in



**Fig. 4** CDK8 is required for maintenance of BCR-ABL1<sup>P185+</sup> leukemia. **a** Generation of stable BCR-ABL1<sup>P185+</sup> *Cdk8*<sup>fl/fl</sup> and BCR-ABL1<sup>P185+</sup> *Cdk8*<sup>fl/fl</sup>Mx1Cre cell lines. Scheme depicts experimental setup of data shown in **b-d**. **b** Efficiency of CDK8 deletion and protein levels of CDK19, CCNC, MED12, and MED13 at indicated time points post interferon- $\beta$  (IFN- $\beta$ ) administration (immunoblotting). Levels of  $\beta$ -actin served as a loading control. **c** Proportions of AnnexinV<sup>+</sup> cells in BCR-ABL1<sup>P185+</sup> *Cdk8*<sup>fl/fl</sup> or BCR-ABL1<sup>P185+</sup> *Cdk8* <sup>$\Delta$</sup>  Mx1Cre cell lines 1, 3, and 7 days after administration of IFN- $\beta$  (d.p. IFN- $\beta$ : days post IFN- $\beta$ ;  $n = 6$  BCR-ABL1<sup>P185+</sup> *Cdk8*<sup>fl/fl</sup>;  $n = 4$  BCR-ABL1<sup>P185+</sup> *Cdk8* <sup>$\Delta$</sup>  Mx1Cre, three independent experiments). **d** Representative PI cell cycle staining of BCR-ABL1<sup>P185+</sup> *Cdk8*<sup>fl/fl</sup> and BCR-ABL1<sup>P185+</sup> *Cdk8* <sup>$\Delta$</sup>  Mx1Cre cell lines. The experiment was performed in duplicates; one of three experiments is depicted. Table indicates frequencies of cells in individual phases of the cell cycle ( $n = 3$  per genotype, measured in duplicates). **e** Scheme depicting experimental setup of in vivo experiment. **f** Kaplan-Meier shows survival curves of non-irradiated NSG mice that have received BCR-ABL1<sup>P185+</sup> *Cdk8*<sup>fl/fl</sup> or BCR-ABL1<sup>P185+</sup> *Cdk8* <sup>$\Delta$</sup>  Mx1Cre cell lines (2500 cells/mouse,  $n = 9$  mice received BCR-ABL1<sup>P185+</sup> *Cdk8*<sup>fl/fl</sup> and  $n = 11$  BCR-ABL1<sup>P185+</sup> *Cdk8* <sup>$\Delta$</sup>  Mx1Cre cells, 3 independent cell lines per genotype were injected). **g** Immunoblotting for CDK8 of ex vivo-derived BCR-ABL1<sup>P185+</sup> cell lines ( $\pm$ poly(I:C) injections). Levels of HSC70 served as a loading control. **h** White blood cell count (WBC) of mice on day of terminal disease (analysis). **i** Summary of frequencies of CD19<sup>+</sup> cells in spleens (SPL) of diseased mice,  $n = 10$  per genotype. Asterisks denote statistical significances as determined by **d** unpaired *t*-test, **c, h** Mann-Whitney, **f** log-rank test, or **i** one-way ANOVA followed by Tukey's test; data represent means  $\pm$  SD (\* $p < 0.05$ ; \*\* $p < 0.01$ ; \*\*\* $p < 0.001$ ). Source data are provided as a Source Data file

hematopoietic stem cell homeostasis; *Med12*<sup>fl/fl</sup>*Vav1*-Cre animals die within 2 weeks of birth with severely reduced BM and thymus cellularity<sup>41</sup>.

CDK8 does not influence initial transformation by the BCR-ABL1<sup>P185+</sup> oncogene but is indispensable for the maintenance of established leukemic cell lines. This effect might stem at least in part from CDK8's role in the phosphorylation of STAT5, a key factor for leukemia maintenance<sup>22,24,42</sup>. Similar to STAT5, CDK8 is essential for the survival of leukemic cells, making it a potential therapeutic target. Deletion of *Cdk8* after disease onset is associated with reduced viability of leukemic cells in vitro and with prolonged survival of the mice in vivo. An additional benefit from targeting CDK8 might arise from the fact that CDK8 represses the natural killer (NK) cell-dependent surveillance of hematopoietic tumors<sup>23</sup>. Deletion of CDK8 in NK cells enhances their cytotoxicity and prolongs the survival of mice suffering from BCR-ABL1<sup>+</sup> leukemia<sup>43</sup>. Degrading CDK8 would thus kill two birds with one stone: it would inhibit the survival of leukemic cells, while enhancing NK cell cytotoxicity.

A pre-requisite for drug development is the existence of a sufficiently large therapeutic window—any therapeutic strategy must harm transformed cells, while sparing their healthy counterparts. Although CDK8 is absolutely required for the pre-implantation of the embryo, *Cdk8* deletion is well tolerated in adult mice. It does not seem to interfere with homeostasis of hematopoietic organs, irrespective of whether it is performed by means of Mx1Cre or by Vav-Cre, and has no impact on the viability or functionality of the HSC. Our findings are consistent with previous work, in which deletion of *Cdk8* in adult mice had no significant effect<sup>19</sup>. It is possible that CDK19, the paralog of CDK8, can compensate for the loss of CDK8 in the adult organism in non-transformed tissues, as proposed in NK<sup>43</sup> and prostate cancer cells<sup>28</sup>.

Despite its involvement in the transcription machinery (it associates with the mediator complex), CDK8 appears to have some functions that are context-specific. In AML cell lines, inhibition of CDK8/CDK19 kinase activity upregulates SE-associated genes with tumor suppressor and lineage-controlling functions, thereby exerting anti-leukemic effects<sup>31</sup>. No such effects were seen in HCT116 colon cancer cells<sup>31</sup> and we do not find them in B-ALL cells. Further studies are required to identify the precise mechanism by which CDK8 influences leukemogenesis. As knockdown of MED13 and CCNC is well tolerated, at least some of the effects are independent of the mediator complex.

Although CDK8 was initially discovered as a kinase that regulates transcription, we provide evidence that it has a function that is independent of its kinase activity: inhibition of the CDK8 kinase activity does not consistently mirror the effects of *Cdk8* gene knockdown. Kinase inhibition with Senexin B or MSC

causes only minor effects on transcription, whereas the deletion of CDK8 significantly affects transcriptional responses and critical signaling pathways in BCR-ABL1<sup>P185+</sup>-driven leukemia. This finding is consistent with work in HCT116 colon cancer cells, in which inhibition of CDK8 kinase activity induces weak anti-proliferative responses, whereas gene deletion has pronounced effects<sup>5,25,31,44</sup>. Deletion of *Cdk8* (but not inhibition of its kinase activity) leads to reduced levels of mTOR signaling, which has been implicated in BCR-ABL1<sup>+</sup> leukemia<sup>45</sup>. Although loss of CDK8 and mTOR inhibition has synergistic effects, not such interdependence is seen between the loss of CDK8 and PI3K inhibition. This apparently paradoxical result presumably stems from the complex feedback loops and crosstalk between the mTOR and other PI3K-dependent pathways. CDK8 has been suggested to interact with mTOR in the context of lipogenesis<sup>46</sup> but not in any form of cancer. An analysis of publicly available RNA-seq data from a range of human cancers suggests that CDK8 levels are highly correlated with the levels of members of the mTOR pathway. The mechanism for the interaction remains a matter for conjecture: we have no direct evidence for or against a physical interaction between CDK8 and mTOR.

TKIs have revolutionized leukemia therapy. Nevertheless, the prognosis for many types of cancer remains poor and patients face a high risk of acquiring resistance-mediating mutations. Specific protein degradation represents a recent mechanism to target proteins independent of their enzymatic activity. We have investigated the potential application of CDK8 degraders, testing the effects of two structurally distinct compounds in human leukemic cell lines. Both molecules cause the efficient degradation of CDK8 but only YKL-06-101 is able to block mTOR signaling. The combined effect of degrading CDK8 and inhibiting mTOR significantly increased apoptosis in three human leukemic cell lines. We believe that this strategy holds a great promise for the clinic, as targeting two unrelated signaling pathways will reduce the probability of developing resistance. Our preliminary investigations suggest that CDK8 interacts with the mTOR signaling pathway not only in a subset of leukemia patients but also in a range of solid cancers. We therefore propose that a combinatorial therapy could represent an approach to treat a range of human cancers.

## Methods

**Cell culture.** The following commercially available cell lines were obtained from American Type Culture Collection (ATCC). Established human B-lymphoid cell lines: RL-7 (ATCC no. CRL-2261), REH (ATCC no. CRL-8286), Daudi (ATCC no. CCL-213), and Ramos (ATCC no. CRL-1596). Transformed human T cell lines: Molt-4 (ATCC no. CRL-1582), Jurkat (ATCC no. TIB-152), Mac2A<sup>47</sup> (RRID: CVCL\_H637), and HPB-ALL<sup>48</sup>. K562 (ATCC no. CCL-243) is a well-defined human erythroid leukemia cell line transformed by the BCR-ABL1 oncogene. The following cell lines were kindly provided by Peter Valent and

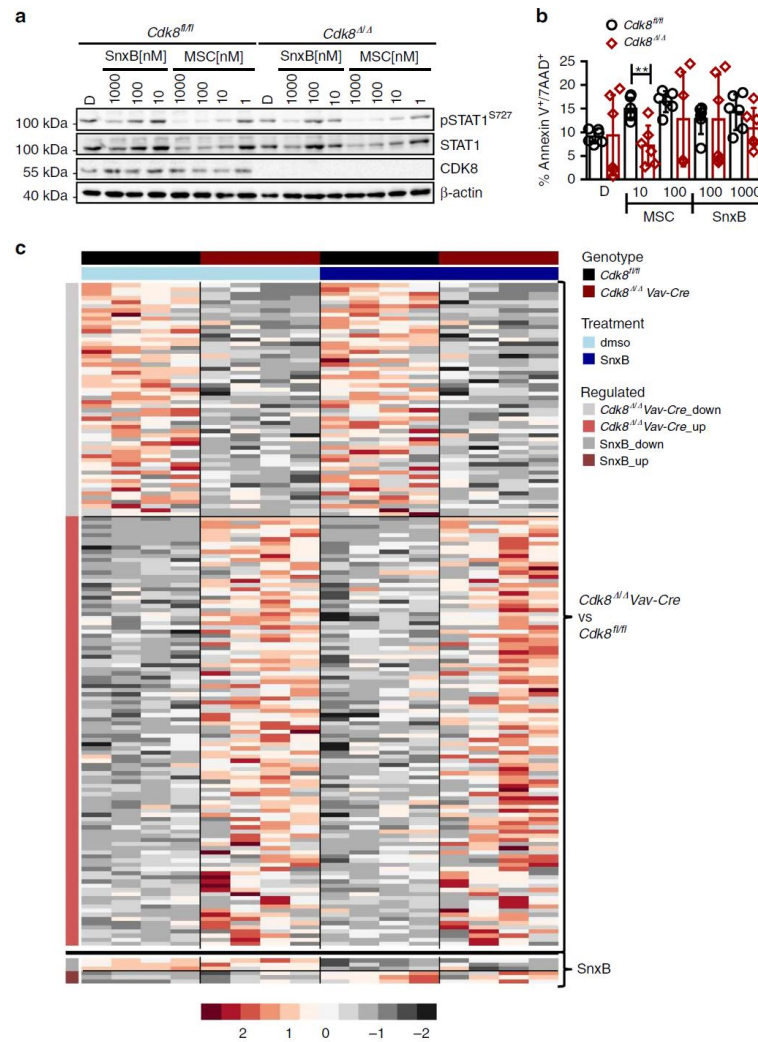


**Fig. 5** Kinase inhibition fails to mimic the effects of *Cdk8* deletion. **a** Immunoblotting of pSTAT1<sup>S727</sup> of BCR-ABL1<sup>p185+</sup> cells after 48 h incubation with increasing concentrations of MSC or Senexin B (SnxB). Induction of phosphorylation was induced by 30 min IFN- $\beta$  stimulation prior collection.  $\beta$ -Actin served as a loading control. **b** AnnexinV/PI staining (after 48 h) of BCR-ABL1<sup>p185+</sup> *Cdk8<sup>fl/fl</sup>* and BCR-ABL1<sup>p185+</sup> *Cdk8<sup>Δ/Δ</sup>Vav-Cre* cell lines in the presence of indicated Senexin B or MSC concentrations. DMSO (0.1%) served as solvent control. Bars represent means  $\pm$  SD from two independent experiments ( $n = 2$  per genotype, measure in triplicates). Asterisks denote statistical significances as determined by unpaired t-test ( $*p < 0.01$ ). **c** Heatmap of 159 differentially expressed genes between BCR-ABL1<sup>p185+</sup> *Cdk8<sup>fl/fl</sup>* and BCR-ABL1<sup>p185+</sup> *Cdk8<sup>Δ/Δ</sup>Vav-Cre* cell lines ( $n = 4$  per genotype). The black line separates the sets of genes, which are differentially regulated upon loss of the entire CDK8 protein (BCR-ABL1<sup>p185+</sup> *Cdk8<sup>Δ/Δ</sup>Vav-Cre* cell lines vs. BCR-ABL1<sup>p185+</sup> *Cdk8<sup>fl/fl</sup>*; above the black line) from those whose expressions change upon treatment with 1000 nM Senexin B for 48 h (of BCR-ABL1<sup>p185+</sup> *Cdk8<sup>fl/fl</sup>* cell lines) (FDR < 0.1). Colors display centered and scaled  $r$ -log counts ranging from red to gray (high to low expression). Source data are provided as a Source Data file

purchased from the Leibnitz Institute DSMZ-German Collection of Micro-organisms and Cell Cultures; Ph<sup>+</sup> cell lines: KU812 (RRID: CVCL\_0379), TOM-1 (RRID: CVCL\_1895), NALM1 (RRID: CVCL\_0091), BV173 (RRID: CVCL\_0181); Ph<sup>-</sup> cell lines: BL41 (RRID: CVCL\_1087) and Raji (RRID: CVCL\_0511) are Ph<sup>-</sup>. The Ph<sup>+</sup> Z119 (RRID: CVCL\_IU88) cell line was kindly provided to J. V. Melo by Zeev Estrov. hMNLs were isolated from peripheral

blood samples over a Ficoll gradient. Human leukemia cell lines and different v-ABL1<sup>p160+</sup>, BCR-ABL1<sup>p185+</sup> mouse cell lines were cultured in RPMI-1640 (Sigma) supplemented with heat-inactivated fetal calf serum (FCS), 50  $\mu$ M 2-mercaptoethanol, and 100 U/mL penicillin/streptomycin (Sigma). A010 cells (Ab-MuLV producer) and phoenix-ECO (ATCC<sup>®</sup> CRL-3214<sup>TM</sup>) packaging cells were cultured in Dulbecco's modified Eagle's medium (DMEM) (Sigma) medium

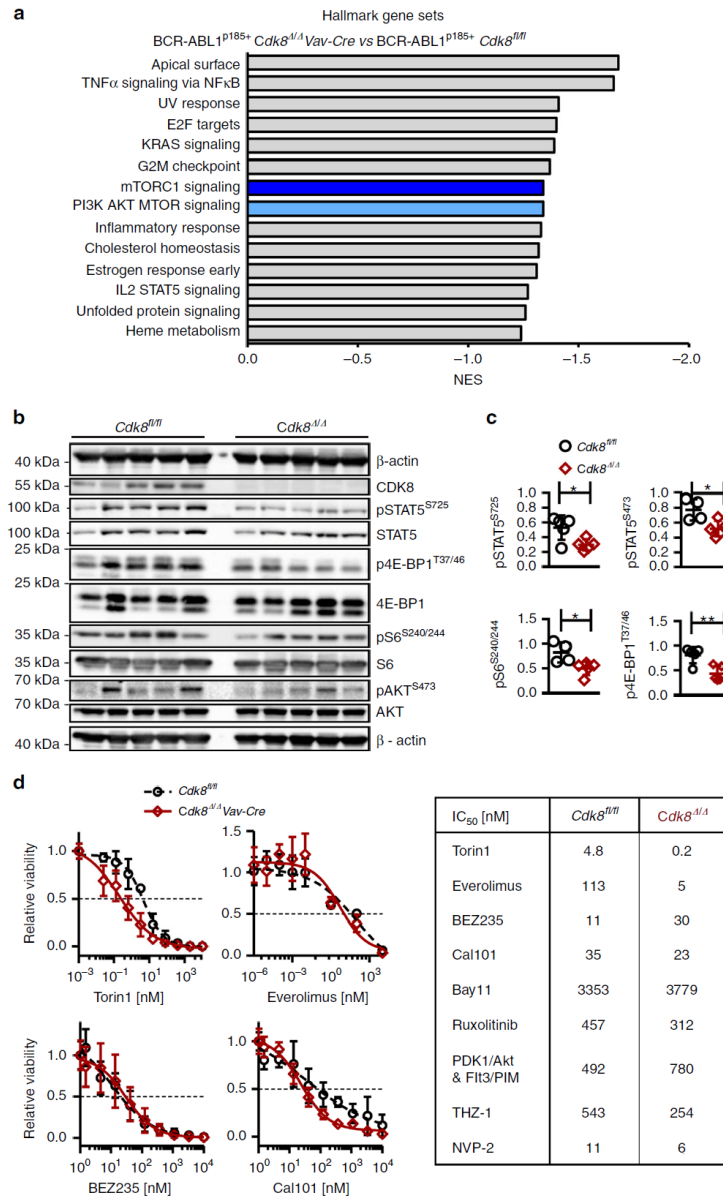
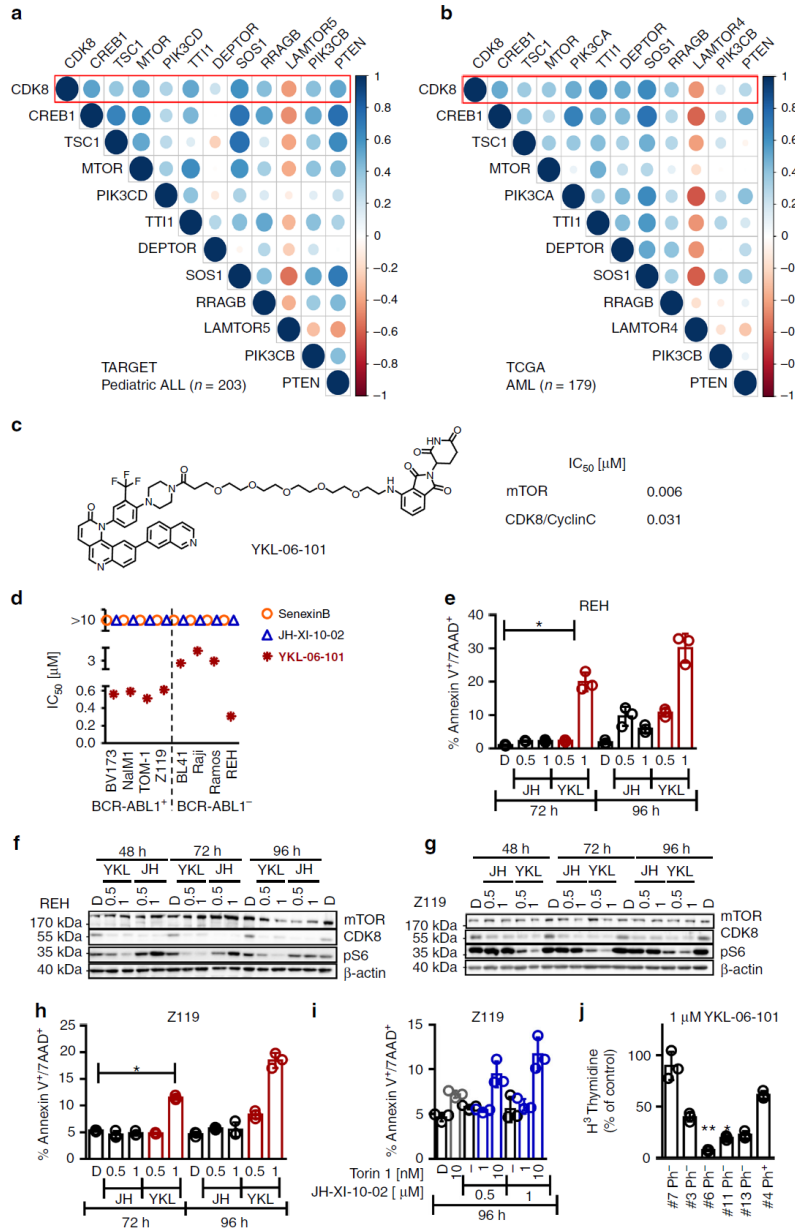


**Fig. 6** CDK8 regulates the mTOR pathway. **a** Gene set enrichment analysis (RNA-seq data) reveals 14 significantly downregulated pathways in BCR-ABL1<sup>P185+</sup> *Cdk8*<sup>fl/fl</sup> *Vav-Cre* cells. NES: normalized enrichment score. **b** Immunoblots of five independent cell lines per genotype were probed for pAKT<sup>S473</sup>, total AKT, pS6<sup>S240/244</sup>, total S6, p4E-BP<sup>T37/46</sup>, and total 4E-BP-1. In addition, pSTAT5<sup>S725</sup>, STAT5, and CDK8 were blotted. β-Actin served as loading control. **c** Bar diagrams depict densitometric analysis of signal intensities relative to the loading control (of western blottings shown in **b**). **d** Representative dose-response curves for Torin1, Everolimus, BEZ235, and Cal101; mean ± SD. Table includes IC<sub>50</sub> values of Torin1 (mTORC1 and mTORC2), Everolimus (mTORC1), BEZ235 (PI3K/ATM/ATR and mTOR), Cal101 (PI3Kdelta), Bay11 (NFκB), Ruxolitinib (JAK1 and JAK2), PDK1/Akt and FIt3/Pim dual inhibitor, THZ-1 (CDK7) and NVP-2 (CDK9) on BCR-ABL1<sup>P185+</sup> *Cdk8*<sup>fl/fl</sup>, and BCR-ABL1<sup>P185+</sup> *Cdk8*<sup>fl/fl</sup> *Vav-Cre* cell lines. Data represent the summary of one to three cell lines per genotype in technical triplicates. Asterisks denote statistical significances as determined by an unpaired *t*-test; mean ± SD (\**p* < 0.05; \*\**p* < 0.01). Source data are provided as a Source Data file



containing 10% FCS and 100 U/mL penicillin/streptomycin. Cell lines are maintained at 37 °C (5% CO<sub>2</sub>) and have been tested regularly for the absence of *Mycoplasma*.

**shRNA knockdowns.** For the inducible knockdown experiments, 20 bp shRNAs against mouse CDK8 (*Cdk8* mRNA (NM\_153599); starting position: 2547), CDK6

(*Cdk6* mRNA (NM\_009873) starting position: 897), CDK7 (*Cdk7* mRNA (NM\_009874) starting position: 1145), CDK9 (*Cdk9* mRNA (NM\_130860) starting position: 2872), CDK19 (*Cdk19* mRNA (NM\_198164) starting position 1560), CCNC (*Ccnc* mRNA (NM\_016746) starting position: 594), MED12 (*Med12* mRNA (NM\_021521) starting position: 5755), and MED13 (*Med13* mRNA (NM\_001080931) starting position: 9367) were designed based on improved design rules and cloned into microRNA stem (miR-E) in the pSIN-TRE3G-dsRED-miR-



**Fig. 7** Chemical CDK8 degradation cooperates with mTOR inhibition. **a** Co-expression matrix of CDK8 and members of mTOR/PI3K signaling pathways in samples of 203 pediatric ALL patients (TARGET cohort, RNA-seq) and **b** 179 AML patients (TCGA AML cohort, RNA-seq). The scale indicates Spearman's correlation coefficients ranging from -1 (red) to 1 (blue). **c** Structure of degrader YKL-06-101 and biochemically verified IC<sub>50</sub>'s for mTOR and CDK8/Cyclin C inhibition. **d** Thymidine incorporation assay based IC<sub>50</sub>'s of BCR-ABL1<sup>+</sup> (BV173, Nalm1, Tom1, Z119) and BCR-ABL1<sup>-</sup> (BL41, Raji, Ramos, REH) human leukemic cell lines after 48 h incubation with increasing concentrations of JH-XI-10-02, YKL-06-101, or Senexin B. **e** AnnexinV/7AAD staining of REH cells incubated with 0.5 μM and 1 μM of JH-XI-10-02 or YKL-06-101 for 72 and 96 h. DMSO was used as vehicle control (D: DMSO, n = 3). Immunoblots show mTOR, CDK8, and pS6 after incubation of **f** REH cells or **g** Z119 cells with 0.5 μM and 1 μM of JH-XI-10-02 or YKL-06-101 for 48, 72, and 96 h. DMSO (indicated as D) was used as vehicle control and β-actin served as loading control. **h** AnnexinV/7AAD staining of Z119 cells incubated with 0.5 μM and 1 μM of JH-XI-10-02 or YKL-06-101 for 72 and 96 h. DMSO was used as a vehicle control (D: DMSO, n = 3). **i** AnnexinV/7AAD staining of Z119 cells incubated with Torin1, JH-XI-10-02, or both in combination with indicated concentrations for 72 and 96 h. DMSO (indicated as D) was used as a vehicle control. One representative experiment out of three is depicted. **j** Bar diagram depicts relative thymidine incorporation of six primary B-ALL patient samples incubated for 48 h with 1 μM of YKL-06-101. Patient #1 represents a non-responder, patient #4 was BCR-ABL1<sup>+</sup> (Ph<sup>+</sup>), whereas the others were BCR-ABL1<sup>-</sup> (Ph<sup>-</sup>). Levels of significance were calculated using Kruskal-Wallis test followed by Dunn's test, data represents means ± SD (\*p < 0.05, \*\*p < 0.01). Source data are provided as a Source Data file

E-PGK-Neo (RT3GEN)-inducible retroviral vector<sup>49</sup>. Two vectors containing shRNA against *Renilla* (Ren713) and *MYC* (*Myc* mRNA (NM\_001177352) starting position 1888) served as controls. Exact shRNA sequences are available in the Supplementary Table 4.

BCR-ABL1<sup>P185+</sup> cell lines, modified to express rtTA3<sup>50</sup>, were cultured in RPMI-1640 as above with additional 2 μg/mL Puromycin (Invivogen/Eubio). Tet-On BCR-ABL1<sup>P185+</sup> cells were transduced with RT3GEN-based retroviral pseudoparticles supplemented with 7 μg/mL polybrene (Sigma). Transduced cells were selected for 2 weeks in 1 mg/mL G418 (Invitrogen). Positively selected cells were treated with 0.5 μg/mL doxycycline (Sigma) to induce expression of the dsRed-miR-E cassette. To monitor proliferation and dsRED expression, induced BCR-ABL1<sup>P185+</sup> cell lines were seeded in 48-well plates at a concentration of 4000 cells/well/mL. The cells were incubated at 37 °C, 5% CO<sub>2</sub>, were counted every 48 h, and were transferred to a plate with fresh media. The percentage of dsRED<sup>+</sup> cells was determined by flow cytometry (FACSCanto II BD Biosystems).

**Mouse strains.** Conditional C57Bl/6N-*Cdk8*<sup>fl/fl</sup> (*Cdk8*<sup>tm1a(EUCOMM)Hmg</sup>)<sup>43</sup> were bred to B6N-Tg(*Mx1Cre*)<sup>51</sup> and B6N-Tg(*Vav-Cre*)<sup>52</sup>. *Cdk8*<sup>fl/fl</sup>, *Cdk8*<sup>fl/fl</sup>*Mx1Cre*, *Cdk8*<sup>fl/fl</sup>*Vav-Cre*, *Ly5.1*<sup>+/+</sup>(*CD45.1*<sup>+</sup>), *Ly5.1/2*<sup>+</sup> (*CD45.1*<sup>+</sup> and *CD45.2*<sup>+</sup>), and NSG (NOD.Cg-Prkdc<sup>scid</sup>Il2rg<sup>tm1Wj/Sz</sup>; The Jackson Laboratory) were maintained under pathogen-free conditions at the University of Veterinary Medicine Vienna. Genotyping primers and detailed thermocycling conditions are available in the Supplementary Table 5.

**Generation of leukemic cell lines and in vitro deletion of endogenous Cdk8.** To generate stable leukemic cell lines, bones of *Cdk8*<sup>fl/fl</sup>*Mx1Cre* or *Cdk8*<sup>fl/fl</sup>*Vav-Cre* were flushed to isolate BM cells for transformation. The phoenix ectropic (pNX Eco) packaging system was used to produce supernatant containing pMSCV-IRES-GFP-based BCR-ABL1<sup>P185+</sup> retroviral pseudoparticles. Therefore, phoenix cells were transduced with retroviral vectors using Turbofect<sup>®</sup> Transfection Reagent (Qiagen). Cells were seeded 1 day before the transfection in six-well plates and grown to 50–70% confluence. Plasmid DNA (1.5 μg) was diluted in 100 μL DMEM containing 10 mM HEPES buffer pH 7.4, 10 μL Turbofect<sup>®</sup> Transfection Reagent was added, vortexed, and incubated 15 min at room temperature before the transfection mix was added dropwise to the cells. After 24 h, the transfection mix was replaced by RPMI-1640 supplemented with 10% FCS, 50 μM 2-mercaptoethanol, and 100 U/mL penicillin, 100 μg/mL streptomycin (Sigma). Another 24 h and 48 h later freshly collected BM cells were infected with the collected supernatant. A010 cells were used for the production of an ectropic replication-deficient form of the Abelson virus. To delete *Cdk8* in the BCR-ABL1<sup>P185+</sup> *Cdk8*<sup>fl/fl</sup>*Mx1Cre* lines, leukemic cells were incubated 24 h in 1000 U/mL recombinant IFN-β (MerckMillipore). *Cdk8* deletion was verified by immunoblot analysis.

**Colony-formation assay.** BM cells from 6-week-old donor mice were transduced with Abelson virus or BCR-ABL1<sup>P185+</sup> supernatants including 7 μg/mL polybrene (Sigma). After 24 h, cells were collected and equal numbers of cells were embedded into growth factor-free methylcellulose (MethoCult<sup>®</sup>). Colonies were counted after 10–14 days.

**In vivo leukemia studies.** A total of 2500 *Cdk8*<sup>fl/fl</sup> BCR-ABL1<sup>P185+</sup>, *Cdk8*<sup>Δ/Δ</sup>*Vav-Cre* BCR-ABL1<sup>P185+</sup>, or 1 × 10<sup>5</sup> *Cdk8*<sup>fl/fl</sup> v-ABL1<sup>P160+</sup> or *Cdk8*<sup>Δ/Δ</sup>*Vav-Cre* v-ABL1<sup>P160+</sup> cells were injected via the tail vein into non-irradiated NSG mice. Disease onset was traced by analyzing peripheral blood. Upon appearance of BCR-ABL1<sup>P185+</sup> cells in the peripheral blood, we initiated poly(I:C) injections (200 μg) to induce Cre recombinase expression and *Cdk8* deletion, specifically in the transplanted leukemic cells. Poly(I:C) injections were given intraperitoneally every 3 days (four times in total); subsequently, survival of the mice was monitored. BM,

SPL, and blood were collected, cells isolated in phosphate-buffered saline (PBS), and further analyzed by fluorescence-activated cell sorting (FACS).

**Homolog assay.** *Cdk8*<sup>Δ/Δ</sup>*Vav-Cre* *Ly5.2*<sup>+</sup> or *Cdk8*<sup>fl/fl</sup> *Ly5.2*<sup>+</sup> BM was mixed with *CDK8*<sup>+/+</sup> *Ly5.1*<sup>+</sup> BM cells in a 1:1 ratio (containing comparable numbers of LSKs) and injected them i.v. into lethally irradiated (9 Gy) *Ly5.1/2*<sup>+</sup> mice. Ten weeks after transplantation, composition of BM of recipient mice was analysed for repopulation of LSKs and stem cell populations by FACS staining.

For the noncompetitive setting, 1 × 10<sup>6</sup> BCR-ABL1<sup>P185+</sup> *Cdk8*<sup>fl/fl</sup> *Ly5.2*<sup>+</sup> or BCR-ABL1<sup>P185+</sup> *Cdk8*<sup>Δ/Δ</sup>*Vav-Cre* *Ly5.2*<sup>+</sup> cells were injected into lethally irradiated (9 Gy) *Cdk8*<sup>+/+</sup> *Ly5.1*<sup>+</sup> mice. After 18 h, mice were euthanized and the BM was analysed for the presence of BCR-ABL1<sup>P185+</sup> *Ly5.2*<sup>+</sup> cells by FACS.

**Flow cytometry.** Single-cell suspensions of the splenocytes, thymus, and BM were prepared. For blood analysis, the erythrocytes were lysed using BD FACS Lysing Solution according to the manufacturer's protocol (BD Bioscience). Hematopoietic stem cell fractions in the BM were identified according to Wilson et al.<sup>53</sup>. Hematopoietic progenitors were characterized by flow cytometry as follows: MCP (Lin<sup>-</sup>, CD127<sup>-</sup>, c-Kit<sup>+</sup>, Sca-1<sup>-</sup>), CMP (Lin<sup>-</sup>, CD127<sup>-</sup>, CD16/CD32<sup>-</sup>, CD34<sup>+</sup>), GMP (Lin<sup>-</sup>, CD127<sup>-</sup>, CD16/CD32<sup>+</sup>, CD34<sup>+</sup>), MEP (Lin<sup>-</sup>, CD127<sup>-</sup>, CD16/CD32<sup>-</sup>, CD34<sup>-</sup>), and CLP (Lin<sup>-</sup>, CD127<sup>+</sup>, c-kit<sup>mid</sup>, Sca-1<sup>mid</sup>). For cell cycle analysis, cells were stained with propidium iodide (PI) (50 μg/mL) in a hypotonic lysis buffer (0.1% sodium citrate, 0.1% Triton X-100, 100 μg/mL RNase) and incubated at 37 °C for 30 min. Analysis of apoptotic fractions was performed by staining with AnnexinV and 7AAD or PI in AnnexinV 10× Staining Buffer (eBiosciences) according to the manufacturer's protocol. Flow cytometry experiments were performed on a BD FACSCanto II (BD Bioscience) and analyzed using BD FACSDiva V8.0 or FlowJo V10 software. The detailed information to utilized antibodies are available in the Supplementary Table 6.

**RNA-seq analysis and GSEA.** RNA was isolated from immortalized BCR-ABL1<sup>P185+</sup> *Cdk8*<sup>fl/fl</sup> and *Cdk8*<sup>Δ/Δ</sup>*Vav-Cre* cells. Single-end, 50 bp sequencing of libraries prepared with the Lexogen SENSE mRNA-Seq library preparation kit was performed on an Illumina HiSeq-2500 sequencer. After quality control of raw data with FastQC and removal of adapters and low quality reads with Trimmomatic (version 0.36), reads were mapped to the GENCODE M13 genome using STAR (version 2.5.2b) with default parameters. Then, featureCounts from the Subread package (version 1.5.1) was used to obtain gene counts for union gene models. Differentially expressed (*p*-adjust < 0.05 and fold change > 2) treatment dependent (*Cdk8*<sup>fl/fl</sup> dimethyl sulfoxide (DMSO) vs. *Cdk8*<sup>fl/fl</sup> Senexin B; *Cdk8*<sup>Δ/Δ</sup>*Vav-Cre* DMSO vs. *Cdk8*<sup>Δ/Δ</sup>*Vav-Cre* Senexin B) and genotype-dependent (*Cdk8*<sup>fl/fl</sup> vs. *Cdk8*<sup>Δ/Δ</sup>*Vav-Cre*) genes were identified using DESeq2 (version 1.18.1). For the heatmap, centered and scaled regularized log-transformed<sup>54</sup> library size-normalized counts were visualized using the heatmap function of the R package NMF (version 0.20.6). The command-line version of GSEA was used for GSEA<sup>55</sup> and pathway analysis was performed with EnrichR<sup>56</sup> using either significant up- or downregulated genes (fold change > 2, padj < 0.1) of *Cdk8*<sup>fl/fl</sup> vs. *Cdk8*<sup>Δ/Δ</sup>*Vav-Cre* cell lines.

**Co-expression matrix.** Publicly available datasets of the TARGET pediatric ALL cohort and of 19 TCGA cohorts were obtained from the cBioPortal for Cancer Genomics database<sup>57,58</sup>. RNA-seq RPKM values of CDK8 and various members of the mTOR/PI3K signaling pathways were extracted from these datasets and were used for co-expression analyses. Spearman's correlation was calculated using the cor function of R software (v3.5.1) and the resulting correlation matrix was visualized using the corrplot package.

**Immunoblotting.** Whole-cell extracts were lysed in RIPA buffer (50 mM Tris-HCl (pH 7.6), 150 mM NaCl, 1% NP-40, 0.25% sodium deoxycholate, 1 mM EDTA; 20 mM  $\beta$ -glycero-phosphate, 1 mM sodium vanadate, 1 mM sodium fluoride, 1 mg/mL aprotinin, 1 mg/mL leupeptin, and 1 mM phenylmethylsulfonyl fluoride) or in SDS-sample buffer. Equal amounts of proteins were separated by SDS polyacrylamide gels and were transferred to nitrocellulose membranes (Whatman<sup>®</sup>Protran<sup>®</sup>). After blocking with 5% bovine serum albumin in pY-TBST buffer (10 mM Tris/HCl pH 7.4, 75 mM NaCl, 1 mM EDTA, 0.1% Tween-20), membranes were probed with primary antibodies (Supplementary Table 7) overnight at 4 °C. Immunoreactive bands were visualized after incubation with the secondary antibody and Clarity Western ECL Substrate (Bio-Rad) using the ChemiDoc<sup>™</sup> Touch (Bio-Rad).

**RNA isolation and qRT-PCR.** Total RNA was isolated from stable BCR-ABL1<sup>P185+</sup> cell lines. RNA was extracted using the RNeasy Mini Kit (Qiagen). Reverse transcription was performed using the iSCRIPT cDNA synthesis kit following the manufacturer's instructions (Bio-Rad). All quantitative PCRs (qPCRs) were performed in triplicates with So Advanced Universal SYBR Green Supermix (Bio-Rad) according to the instructions of the manufacturer. Levels of mRNAs were normalized to hypoxanthine guanine phosphoribosyltransferase (HRPT),  $\beta$ -actin, or Ube2d2a mRNA. Primer information are available in the Supplementary Table 8.

**Inhibitors.** For dose-response curves, BCR-ABL1<sup>P185+</sup> *Cdk8<sup>fl/fl</sup>* or *Cdk8<sup>ΔVav-Cre</sup>* cells were plated in triplicates in 96-well plates. Four thousand cells per well in 100  $\mu$ L of media were incubated 48 h with inhibitors (Senexin B: Gentaur GmbH/APEXBio; MSC2530818, THZ-1, Torin1, and Everolimus: Selleck Chemicals; Cal101, PDK1/Akt/Htt dual pathway inhibitor, and BAY11-7085: Calbiochem; NVP-2, SEL120-34A: MedChemExpress; Ruxolitinib: Chemietek). Cell viability was assessed using CellTiterGlo (Promega) according to the manufacturer's instructions. Data for each cell line were normalized to the negative control (DMSO, set to 100% viability) and 50% inhibitor concentration (IC<sub>50</sub>) was determined by using GraphPad Prism<sup>®</sup> version 5.00. REH, Z119, BV173, BCR-ABL1<sup>P185+</sup> *Cdk8<sup>fl/fl</sup>*, or *Cdk8<sup>ΔVav-Cre</sup>* cells were seeded in a six-well dish at a concentration of 10<sup>6</sup> cells/mL. Senexin B, MSC2530818, or SEL120-34A was added and after 48 h incubation cells were collected. Cells (10<sup>6</sup>) were washed with ice-cold phosphate-buffered saline (PBS) and were boiled (95 °C) for 20 min in 100  $\mu$ L SDS-sample buffer consisting of 5% SDS (Biomol), 5% glycerol (Merck), 2.5% 2-mercaptoethanol, and a trace amount of bromophenol blue sodium salt (Merck) in 375 mM Tris/HCl (pH 6.8). The remaining cells were analyzed by FACS (cell cycle and viability).

**Degraders.** Synthesis details of YKL-06-101 and JH-XI-10-02 are provided in Supplementary Notes 1 and 2. Proliferation of degrader-exposed human leukemic cell lines and primary ALL patient cells were examined by measuring 3H-thymidine uptake after 48 h. For immunoblotting and FACS analysis, cells were incubated with the indicated concentrations of the degraders up to 96 h.

**Statistical analysis.** Kruskal-Wallis test (followed by Dunn's test), one-way analysis of variance (followed by Tukey's multiple comparison test), log-rank (Mantel-Cox) test, Wilcoxon-Mann-Whitney test, and assessment of half maximal inhibitory concentration values were performed using GraphPad Prism<sup>®</sup> Software version 5.04 and 6.02. All data are shown as mean  $\pm$  SD or otherwise as described in the figure legends. The significance is indicated for each experiment (\**p* < 0.05, \*\**p* < 0.01, \*\*\**p* < 0.001, \*\*\*\**p* < 0.0001).

**Study approvals.** All animal experiments were approved by the institutional ethics committee and were granted by the national authority (Austrian Federal Ministry of Science and Research) according to Section 8ff of Law for Animal Experiments under license BMWF-68.205/0218-II/3b/2012, and were conducted according to the guidelines of FELASA and ARRIVE.

The ethics committee of the Medical University of Vienna approved the study on human leukemic cells (approval number: 011-2005). All patients gave their written informed consent to participate before BM or blood cells were examined.

**Reporting summary.** Further information on research design is available in the Nature Research Reporting Summary linked to this article.

#### Data availability

The RNA sequencing data have been deposited in the Gene Expression Omnibus (GEO) database under the accession code [GSE136923](https://www.ncbi.nlm.nih.gov/geo/query/acc.cgi?acc=GSE136923). The source data and uncropped gel pictures underlying Figs. 1a–e, 2a–f, h–j, 3a–i, 4b–d, f–i, 5a–b, 6b–d, and 7d–j, and Supplementary Figs. 1a, 2a–f, 3a–h, 4a–b, 5a–b, 6b–c, and 8a–d are provided as a source data file. Data that support the findings of this study are available from the authors upon reasonable request.

Received: 12 January 2019; Accepted: 20 September 2019;

Published online: 18 October 2019

#### References

- Cao, L. et al. Phylogenetic analysis of CDK and cyclin proteins in premetazoan lineages. *BMC Evol. Biol.* **14**, 10 (2014).
- Lim, S. & Kaldis, P. Cdks, cyclins and CKIs: roles beyond cell cycle regulation. *Development* **140**, 3079–3093 (2013).
- Malumbres, M. et al. Cyclin-dependent kinases. *Genome Biol.* **15**, 122 (2014).
- Malumbres, M. et al. Mammalian cells cycle without the D-type cyclin-dependent kinases Cdk4 and Cdk6. *Cell* **118**, 493–504 (2004).
- Kollmann, K. et al. A kinase-independent function of CDK6 links the cell cycle to tumor angiogenesis. *Cancer Cell* **24**, 167–181 (2013).
- Kollmann, K. et al. c-JUN promotes BCR-ABL-induced lymphoid leukemia by inhibiting methylation of the 5' region of Cdk6. *Blood* **117**, 4065–4075 (2011).
- Scheicher, R. et al. CDK6 as a key regulator of hematopoietic and leukemic stem cell activation. *Blood* **125**, 90–101 (2015).
- Uras, I. Z. et al. Palbociclib treatment of FLT3-ITD+ AML cells uncovers a kinase-dependent transcriptional regulation of FLT3 and PIM1 by CDK6. *Blood* **127**, 2890–2902 (2016).
- Laderian, B. & Fojo, T. CDK4/6 inhibition as a therapeutic strategy in breast cancer: palbociclib, ribociclib, and abemaciclib. *Semin. Oncol.* **44**, 395–403 (2017).
- Thomas, D. et al. Targeting acute myeloid leukemia by dual inhibition of PI3K signaling and Cdk9-mediated Mcl-1 transcription. *Blood* **122**, 738–748 (2013).
- Chipumuro, E. et al. CDK7 inhibition suppresses super-enhancer-linked oncogenic transcription in MYCN-driven cancer. *Cell* **159**, 1126–1139 (2014).
- Kwiatkowski, N. et al. Targeting transcription regulation in cancer with a covalent CDK7 inhibitor. *Nature* **511**, 616–620 (2014).
- Arguello, B. F. et al. Flavopiridol induces apoptosis of normal lymphoid cells, causes immunosuppression, and has potent antitumor activity in vivo against human leukemia and lymphoma xenografts. *Blood* **91**, 2482–2490 (2016).
- Kumar, S. K. et al. Dinaciclib, a novel CDK inhibitor, demonstrates encouraging single-agent activity in patients with relapsed multiple myeloma. *Blood* **125**, 443–448 (2015).
- Baker, A. et al. The CDK9 inhibitor dinaciclib exerts potent apoptotic and antitumor effects in preclinical models of MLL-rearranged acute myeloid leukemia. *Cancer Res.* **76**, 1158–1169 (2016).
- Bose, P. et al. Phase I trial of the combination of flavopiridol and imatinib mesylate in patients with Bcr-Abl+ hematological malignancies. *Cancer Chemother. Pharmacol.* **69**, 1657–1667 (2012).
- Morales, F. & Giordano, A. Overview of CDK9 as a target in cancer research. *Cell Cycle* **15**, 519–527 (2016).
- Westerling, T., Kuuluvainen, E. & Mäkelä, T. P. Cdk8 is essential for preimplantation mouse development. *Mol. Cell. Biol.* **27**, 6177–6182 (2007).
- McClelland, M. L. et al. Cdk8 deletion in the ApcMin murine tumour model represses EZH2 activity and accelerates tumorigenesis. *J. Pathol.* **237**, 508–519 (2015).
- Donner, A. J., Szostek, S., Hoover, J. M. & Espinosa, J. M. CDK8 is a stimulus-specific positive coregulator of p53 target genes. *Mol. Cell* **27**, 121–133 (2007).
- Galbraith, M. D. et al. HIF1A employs CDK8-mediator to stimulate RNAPII elongation in response to hypoxia. *Cell* **153**, 1327–1339 (2013).
- Rzyski, T. et al. SEL120-34A is a novel CDK8 inhibitor active in AML cells with high levels of serine phosphorylation of STAT1 and STAT5 transactivation domains. *Oncotarget* **8**, 33779–33795 (2017).
- Putz, E. M. et al. CDK8-mediated STAT1-S727 phosphorylation restrains NK cell cytotoxicity and tumor surveillance. *Cell Rep.* **4**, 437–444 (2013).
- Bancerek, J. et al. CDK8 kinase phosphorylates transcription factor STAT1 to selectively regulate the interferon response. *Immunity* **38**, 250–262 (2013).
- Firestein, R. et al. CDK8 is a colorectal cancer oncogene that regulates  $\beta$ -catenin activity. *Nature* **455**, 547–551 (2008).
- Firestein, R., Shima, K., Noshko, K., Irahara, N. & Baba, Y. CDK8 expression in 470 colorectal cancers in relation to  $\beta$ -catenin activation, other molecular alterations and patient survival. *Int. J. Cancer* **126**, 2863–2873 (2011).
- Kapoor, A. et al. The histone variant macroH2A suppresses melanoma progression through regulation of CDK8. *Nature* **468**, 1105–1109 (2010).
- Nakamura, A., Nakata, D., Kakoi, Y. & Kunitomo, M. CDK8/19 inhibition induces premature G1/S transition and ATR-dependent cell death in prostate cancer cells. *Oncotarget* **9**, 13474–13487 (2018).
- McDermott, M. S. J. et al. Inhibition of CDK8 mediator kinase suppresses estrogen dependent transcription and the growth of estrogen receptor positive breast cancer. *Oncotarget* **8**, 12558–12575 (2017).
- Gu, W. et al. Tumor-suppressive effects of CDK8 in endometrial cancer cells. *Cell Cycle* **12**, 987–999 (2013).
- Pelish, H. E. et al. Mediator kinase inhibition further activates super-enhancer-associated genes in AML. *Nature* **526**, 273–276 (2015).
- Piccaluga, P. P., Paolini, S. & Martinelli, G. Tyrosine kinase inhibitors for the treatment of Philadelphia chromosome-positive adult acute lymphoblastic leukemia. *Cancer* **110**, 1178–1186 (2007).

33. Yang, K. & Fu, L. W. Mechanisms of resistance to BCR-ABL TKIs and the therapeutic strategies: a review. *Crit. Rev. Oncol. Hematol.* **93**, 27–292 (2015).
34. Hardy, R. R. et al. Immunological reviews B-cell commitment, development and selection. *Immunol. Rev.* **175**, 23–32 (2000).
35. Hardy, R. R. B-cell commitment: deciding on the players. *Curr. Opin. Immunol.* **15**, 158–165 (2003).
36. Winter, G. E. et al. Phthalimide conjugation as a strategy for in vivo target protein degradation. *Science* **348**, 1376–1381 (2015).
37. Hatcher, J. M. et al. Development of highly potent and selective steroidal inhibitors and degraders of CDK8. *ACS Med. Chem. Lett.* **9**, 540–545 (2018).
38. Thoreen, C. C. et al. An ATP-competitive mammalian target of rapamycin inhibitor reveals rapamycin-resistant functions of mTORC1. *J. Biol. Chem.* **284**, 8023–8032 (2009).
39. Philip, S., Kumarasiri, M., Teo, T., Yu, M. & Wang, S. Cyclin-dependent kinase 8: a new hope in targeted cancer therapy? *J. Med. Chem.* **61**, 5073–5092 (2017).
40. Clarke, P. A. et al. Assessing the mechanism and therapeutic potential of modulators of the human mediator complex-associated protein kinases. *Elife* **5**, e20722 (2016).
41. Aranda-Orgilles, B. et al. MED12 regulates HSC-specific enhancers independently of mediator kinase activity to control hematopoiesis. *Cell Stem Cell* **19**, 784–799 (2016).
42. Berger, A. et al. PAK-dependent STAT5 serine phosphorylation is required for BCR-ABL-induced leukemogenesis. *Leukemia* **28**, 629–641 (2014).
43. Witalisz-Siepracka, A. et al. NK cell-specific CDK8 deletion enhances antitumor responses. *Cancer Immunol. Res.* **6**, 458–466 (2018).
44. Koehler, M. F. T. et al. Development of a potent, specific CDK8 kinase inhibitor which phenocopies CDK8/19 knockout cells. *ACS Med. Chem. Lett.* **7**, 223–228 (2016).
45. Carayol, N. et al. Critical roles for mTORC2- and rapamycin-insensitive mTORC1-complexes in growth and survival of BCR-ABL-expressing leukemic cells. *Proc. Natl Acad. Sci. USA* **107**, 12469–12474 (2010).
46. Feng, D. et al. mTORC1 down-regulates cyclin-dependent kinase 8 (CDK8) and cyclin C (CycC). *PLoS ONE* **10**, e0126240 (2015).
47. Marti, R. M., Wasik, M. A. & Kadin, M. E. Constitutive secretion of GM-CSF by three different cell lines derived from a single patient with a progressive cutaneous lymphoproliferative disorder. *Cytokine* **8**, 323–329 (1996).
48. Morikawa, S., Tatsumi, E., Baba, M., Harada, T. & Yasuhira, K. Two E-rosette-forming lymphoid cell lines. *Int. J. Cancer* **21**, 166–170 (1978).
49. Fellmann, C. et al. An optimized microRNA backbone for effective single-copy RNAi. *Cell Rep.* **5**, 1704–1713 (2013).
50. Zuber, J. et al. RNAi screen identifies Brd4 as a therapeutic target in acute myeloid leukaemia. *Nature* **478**, 524–528 (2011).
51. Kühn, R., Schwenk, F., Aguet, M. & Rajewsky, K. Inducible gene targeting in mice. *Science* **269**, 1427–1429 (1995).
52. Georgiades, P. et al. *vavCre* transgenic mice: a tool for mutagenesis in hematopoietic and endothelial lineages. *Genesis* **34**, 251–256 (2002).
53. Wilson, A., Laurenti, E. & Trumpp, A. Balancing dormant and self-renewing hematopoietic stem cells. *Curr. Opin. Genet. Dev.* **19**, 461–468 (2009).
54. Love, M. I., Huber, W. & Anders, S. Moderated estimation of fold change and dispersion for RNA-seq data with DESeq2. *Genome Biol.* **15**, 550 (2014).
55. Subramanian, A. et al. Gene set enrichment analysis: a knowledge-based approach for interpreting genome-wide expression profiles. *Proc. Natl Acad. Sci. USA* **102**, 15545–15550 (2005).
56. Kuleshov, M. V. et al. Enrichr: a comprehensive gene set enrichment analysis web server 2016 update. *Nucleic Acids Res.* **44**, W90–W97 (2016).
57. Gao, J. et al. Integrative analysis of complex cancer genomics and clinical profiles using the cBioPortal. *Sci. Signal.* **6**, pl1 (2013).
58. Cerami, E. et al. The cBio cancer genomics portal: an open platform for exploring multidimensional cancer genomics data. *Cancer Discov.* **2**, 401–404 (2012).

## Acknowledgements

We thank the European Conditional Mouse Mutagenesis Consortium and Mohammed Selloum (Yann Herault Group) for providing the *Cdk8<sup>tm1c(EUCOMM)Hmgu</sup>* mouse strain. We are grateful to Thomas Ruelicke and Thomas Kolbe for their help in acquiring the mice and to all members of the mouse facility. Z119 cells were kindly provided to J. V. Melo by Zeey Estrov. For technical support, we want to thank Sabine Fajmann and Philipp Jodl. We are deeply indebted to Graham Tebb for critical discussions and editing of the manuscript. This work was supported by grants from Austrian Science Foundation (FWF) SFB 4701-B20 to P.V., F4704-B20 to P.V., F4706-B20 to V.S., P28571-B21 to V.S., P27248-B28 to D.F., and SFB6107 to V.S.

## Author contributions

V.S. was the principal investigator and takes primary responsibility for the article. V.S. and N.S.G. designed and supervised the study. I.M., A.B.-B., M.P.-M., L.E., V.M.K., I.Z.U., E.G., K.B., and A.S. performed and analyzed experiments. T.Z., Y.L., J.M.H., and Y.L. synthesized and characterized the degraders. R.G. and G.H. performed bioinformatics analysis. P.V. provided patient materials and human leukemic cell lines. J.V.M. provided the Z199 cell line. M.R., S.K., F.G., J.Z., D.F., A.H.K., N.P.K., and T.W. contributed to interpretation of the data and revised the manuscript with regard to critical intellectual content. I.M. and V.S. wrote the manuscript.

## Competing interests

N.S.G. is a founder, science advisory board member (SAB), and equity holder in Gatekeeper, Syros, Petra, C4, B2S, and Soltego. The Gray lab receives or has received research funding from Novartis, Takeda, Astellas, Taiho, Janssen, Kinogen, Voronoi, Her2Lc, Deerfield, and Sanofi. N.P.K., N.S.G., T.Z., and Y.L. are inventors on the patent WO2017/185034 that covers degrader YKL-06-101. N.S.G. and J.M.H. are inventors on a patent that covers JH-XI-10-02. The remaining authors declare no competing interests.

## Additional information


Supplementary information is available for this paper at <https://doi.org/10.1038/s41467-019-12656-x>.

Correspondence and requests for materials should be addressed to V.S.

Peer review information *Nature Communications* thanks Jonathan Schatz and the other, anonymous, reviewer(s) for their contribution to the peer review of this work.

Reprints and permission information is available at <http://www.nature.com/reprints>

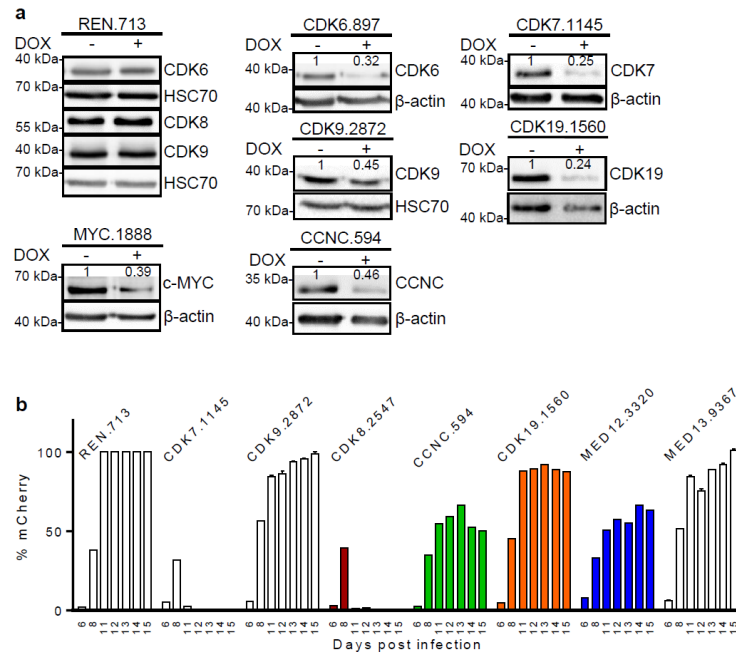
Publisher's note Springer Nature remains neutral with regard to jurisdictional claims in published maps and institutional affiliations.

 Open Access This article is licensed under a Creative Commons Attribution 4.0 International License, which permits use, sharing, adaptation, distribution and reproduction in any medium or format, as long as you give appropriate credit to the original author(s) and the source, provide a link to the Creative Commons license, and indicate if changes were made. The images or other third party material in this article are included in the article's Creative Commons license, unless indicated otherwise in a credit line to the material. If material is not included in the article's Creative Commons license and your intended use is not permitted by statutory regulation or exceeds the permitted use, you will need to obtain permission directly from the copyright holder. To view a copy of this license, visit <http://creativecommons.org/licenses/by/4.0/>.

© The Author(s) 2019

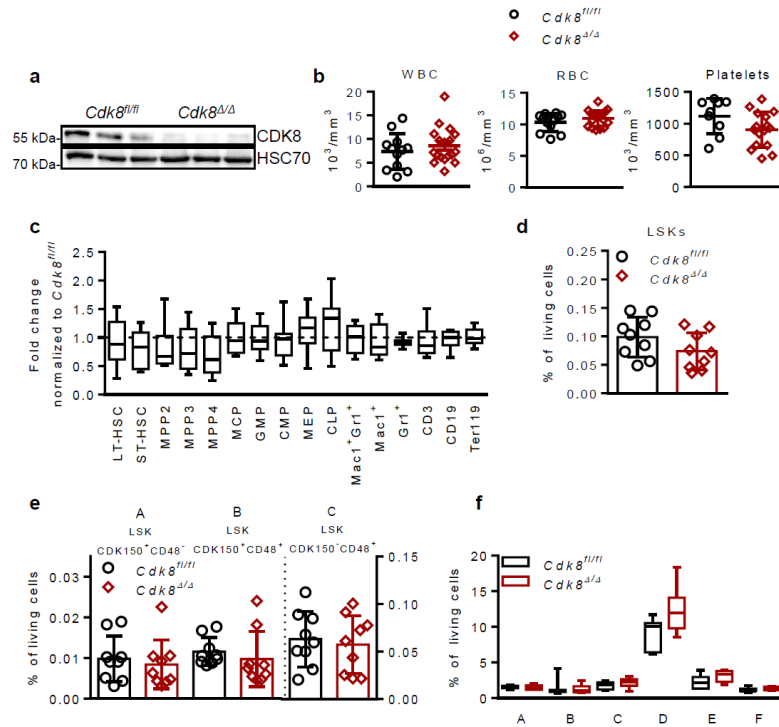


## Supplementary Figures

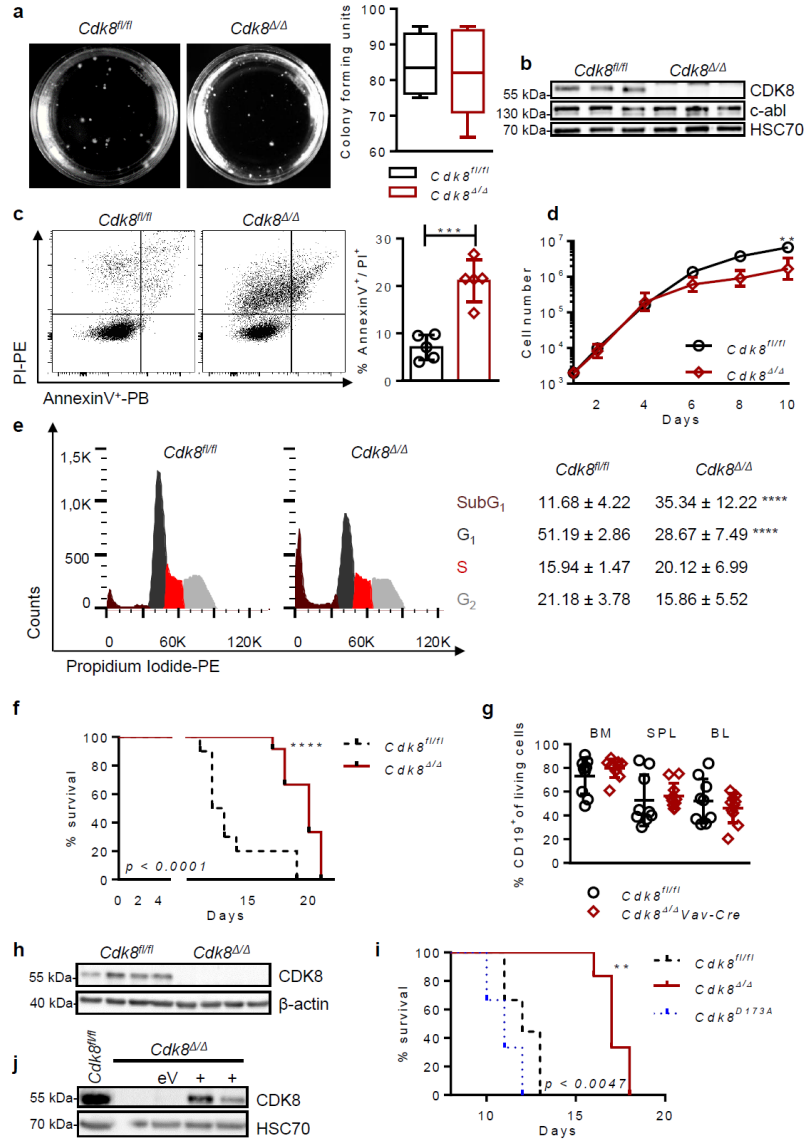


**Supplementary Figure 1:** CDK8 is essential for survival of BCR-ABL1<sup>p185+</sup> leukemic cells. **a** Verification of shRNA mediated knockdown in Tet-On BCR-ABL1<sup>p185+</sup> cell lines. ShREN-expression served as negative and shRNA against MYC served as positive control. Data derived from one representative set of hairpins (directed against REN, MYC, CDK6, CDK7, CDK9, CCNC or CDK19) are depicted. HSC70 or β-actin served as loading controls. **b** Bar diagram shows percentages of mCherry<sup>+</sup> BCR-ABL1<sup>p185+</sup> leukemic cells expressing stable shRNAs targeting CDK7, CDK9, CDK8, CCNC, CDK19, MED12 and MED13. Data represents outgrowth of mCherry<sup>+</sup> BCR-ABL1<sup>p185+</sup> cells over time. ShRNA directed against Renilla (REN) served as negative control, bars represent mean ± SD. Source data are provided as a Source Data file

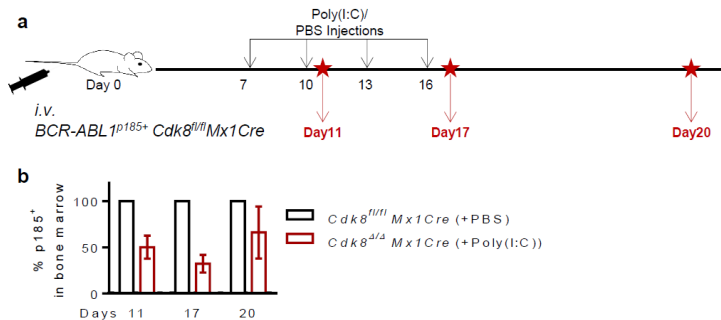




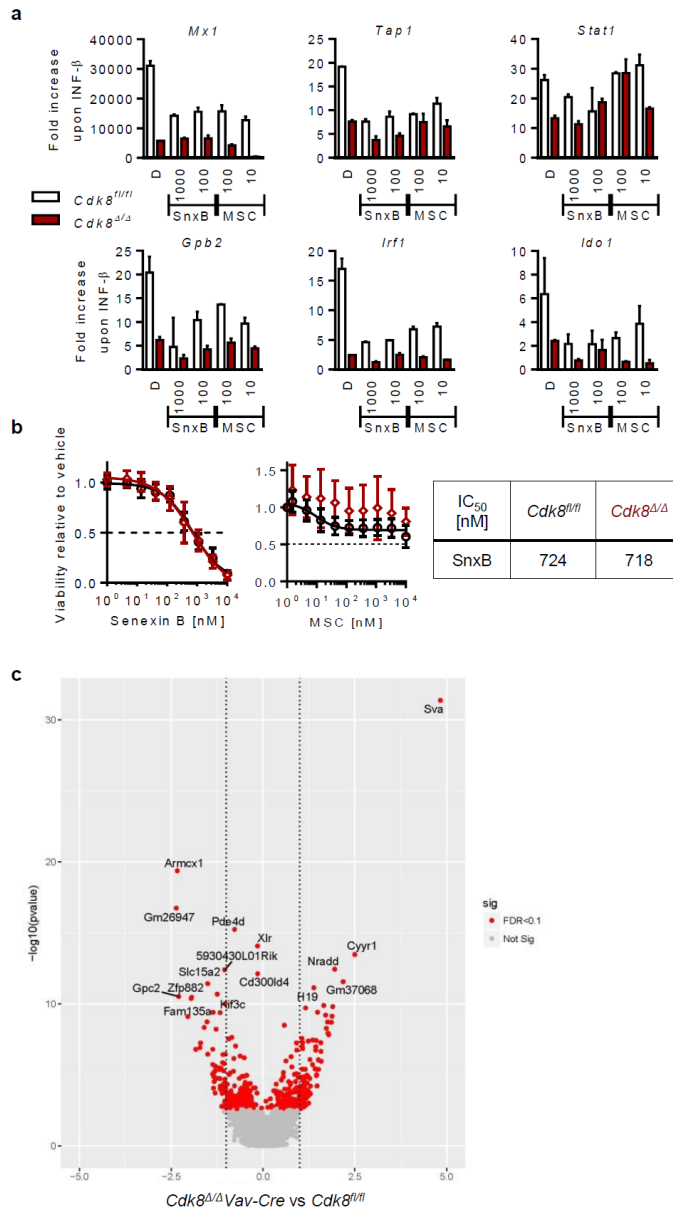
**Supplementary Figure 2:** Steady-state hematopoiesis is not affected by loss of CDK8 (*Cdk8<sup>ΔΔ/Δ</sup>Mx1Cre*). **a** Efficiency of *Cdk8* deletion in *Cdk8<sup>ΔΔ/Δ</sup>Mx1Cre* mice after four intraperitoneal poly(I:C) injections. Immunoblot of BM cells from *Cdk8<sup>fl/fl</sup>* and *Cdk8<sup>ΔΔ/Δ</sup>Mx1Cre* mice ( $n = 3$  per genotype). **b** Analysis of white blood cell count (WBC), red blood cell count (RBC) (*Cdk8<sup>fl/fl</sup>*  $n = 12$  and *Cdk8<sup>ΔΔ/Δ</sup>Mx1Cre* mice  $n = 18$ ) and platelets count of *Cdk8<sup>fl/fl</sup>* ( $n = 9$ ) and *Cdk8<sup>ΔΔ/Δ</sup>Mx1Cre* mice ( $n = 16$ ). **c** Relative fold change of BM composition normalized to mean of *Cdk8<sup>fl/fl</sup>* BM population frequencies (*Cdk8<sup>fl/fl</sup>*  $n = 11$ , *Cdk8<sup>ΔΔ/Δ</sup>Mx1Cre*  $n = 10$ ). Center value represents median, the box 25<sup>th</sup> to 75<sup>th</sup> percentiles and whiskers min to max. **d** Bar diagram of Lin<sup>-</sup> Sca-1<sup>+</sup> c-kit<sup>+</sup> (LSK) frequencies in BM of *Cdk8<sup>fl/fl</sup>* ( $n = 9$ ) and *Cdk8<sup>ΔΔ/Δ</sup>Mx1Cre* ( $n = 9$ ) mice. **e** Frequencies of LSK subpopulations (fraction A, B and C;  $n = 9$  per genotype). **f** Frequencies of individual populations during early B-cell development according to Hardy nomenclature in pre-pro-B (B220<sup>+</sup>/CD43<sup>hi</sup>/CD19<sup>+</sup>/BP-1<sup>-</sup>; fraction A), early pro-B (B220<sup>+</sup>/CD43<sup>hi</sup>/CD19<sup>+</sup>/BP-1<sup>-</sup>; fraction B), late pro-B (B220<sup>+</sup>/CD43<sup>hi</sup>/CD19<sup>+</sup>/BP-1<sup>+</sup>; fraction C), pre-B (B220<sup>+</sup>/CD43<sup>lo</sup>/IgM<sup>+</sup>/IgD<sup>-</sup>; fraction D), immature (B220<sup>+</sup>/CD43<sup>lo</sup>/IgM<sup>+</sup>/IgD<sup>-</sup>; fraction E) and mature (B220<sup>+</sup>/CD43<sup>lo</sup>/IgM<sup>+</sup>/IgD<sup>+</sup>; fraction F) B cells (*Cdk8<sup>fl/fl</sup>*  $n = 7$  and *Cdk8<sup>ΔΔ/Δ</sup>Mx1Cre* mice  $n = 6$ )<sup>1,2</sup>. Center value represents median, the box 25<sup>th</sup> to 75<sup>th</sup> percentiles and whiskers min to max. Levels of significance were calculated using **b** (WBC), **e** (A and B) Mann-Whitney, **c**, **f** Kruskal-Wallis test followed by Dunn's test and **b** (RBC, Platelets), **d**, **e** (C) unpaired *t*-test, data represents means  $\pm$  SD. Source data are provided as a Source Data file



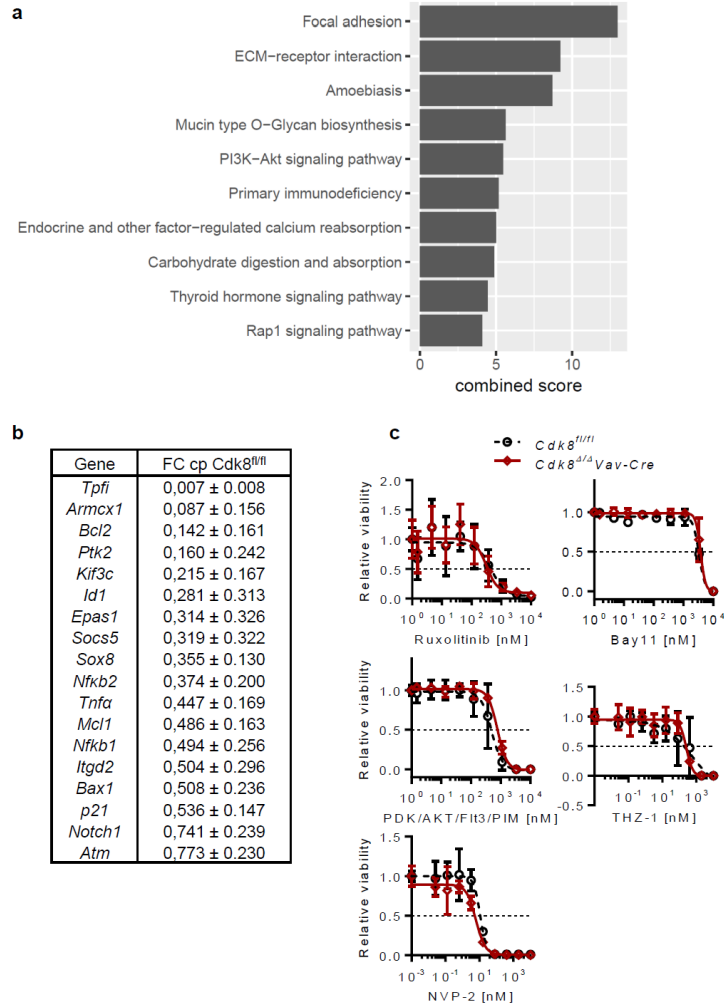
**Supplementary Figure 3:** CDK8 is not required for initial v-ABL<sup>p160+</sup> transformation. **a** v-ABL<sup>p160+</sup>-induced colony formation of *Cdk8<sup>fl/fl</sup>* and *Cdk8<sup>Δ/Δ</sup> Vav-Cre* BM cells in growth-factor free methylcellulose. Summary of colony formation assays (*Cdk8<sup>fl/fl</sup>* n = 2 and *Cdk8<sup>Δ/Δ</sup> Vav-Cre* n = 4 per genotype in duplicates). Center value represents median, the box 25<sup>th</sup> to 75<sup>th</sup> percentiles and whiskers min to max. **b** CDK8 and c-ABL protein levels in v-ABL<sup>p160+</sup> cell lines. HSC70 served as loading control. **c** Representative FACS profile of an AnnexinV/PI staining of v-ABL<sup>p160+</sup> *Cdk8<sup>fl/fl</sup>* and v-ABL<sup>p160+</sup> *Cdk8<sup>Δ/Δ</sup>Vav-Cre* cell lines and summary of the data (n = 3 per genotype, measured in duplicates). **d** Growth curve of v-ABL<sup>p160+</sup> *Cdk8<sup>fl/fl</sup>* and v-ABL<sup>p160+</sup> *Cdk8<sup>Δ/Δ</sup>Vav-Cre* cell lines. Experiment was performed in triplicates (n = 2 per genotype). **e** PI cell cycle staining of v-ABL<sup>p160+</sup> *Cdk8<sup>fl/fl</sup>* and v-ABL<sup>p160+</sup> *Cdk8<sup>Δ/Δ</sup>Vav-Cre* cell lines. Table indicates frequencies of cells in individual phases. **f** v-ABL<sup>p160+</sup> *Cdk8<sup>fl/fl</sup>* and v-ABL<sup>p160+</sup> *Cdk8<sup>Δ/Δ</sup>Vav-Cre* cells were injected intravenously into non-irradiated NSG mice (100000 cells/mouse, n = 10 mice received v-ABL<sup>p160+</sup> *Cdk8<sup>fl/fl</sup>* and 12 mice v-ABL<sup>p160+</sup> *Cdk8<sup>Δ/Δ</sup>Vav-Cre* cells, 3 independent cell lines per genotype). Survival curves of recipients (median survival of *Cdk8<sup>fl/fl</sup>* and *Cdk8<sup>Δ/Δ</sup>Vav-Cre* cohorts: 12.5 and 20 days). **g** Summary of CD19<sup>+</sup> cell distribution in diseased mice. **h** Immunoblotting for CDK8 of ex vivo derived v-ABL<sup>p160+</sup> *Cdk8<sup>fl/fl</sup>* and v-ABL<sup>p160+</sup> *Cdk8<sup>Δ/Δ</sup>Vav-Cre* cells. Levels of β-actin served as loading controls. **i** v-ABL<sup>p160+</sup> *Cdk8<sup>D173A</sup>*, v-ABL<sup>p160+</sup> *Cdk8<sup>fl/fl</sup>* and v-ABL<sup>p160+</sup> *Cdk8<sup>Δ/Δ</sup>Vav-Cre* cells were injected intravenously into non-irradiated NSG mice (100000 cells/mouse, n = 9 mice received v-ABL<sup>p160+</sup> *Cdk8<sup>D173A</sup>* and 6 mice v-ABL<sup>p160+</sup> *Cdk8<sup>D173A</sup>* or v-ABL<sup>p160+</sup> *Cdk8<sup>Δ/Δ</sup>Vav-Cre* cells, 2 independent cell lines per genotype). Survival curves of recipients are depicted (median survival of *Cdk8<sup>D173A</sup>*, *Cdk8<sup>fl/fl</sup>* and *Cdk8<sup>Δ/Δ</sup>Vav-Cre* cohorts: 11, 12 and 17 days). **j** Immunoblotting for CDK8 of v-ABL<sup>p160+</sup> *Cdk8<sup>fl/fl</sup>*, v-ABL<sup>p160+</sup> *Cdk8<sup>Δ/Δ</sup>Vav-Cre*, v-ABL<sup>p160+</sup> *Cdk8<sup>Δ/Δ</sup>Vav-Cre* + empty Vector (eV) and v-ABL<sup>p160+</sup> *Cdk8<sup>Δ/Δ</sup>Vav-Cre* reconstituted with CDK8 kinase-dead mutant *Cdk8<sup>D173A</sup>* cells. HSC70 served as loading control. Levels of significance were calculated using **d**, **g** (BM) Mann-Whitney, **a**, **c**, **e** and **g** (SPL, BL) unpaired *t*-test and **f**, **i** long-rank test, data represents means ± SD (\*\*p < 0.01; \*\*\*p < 0.001; \*\*\*\*p < 0.0001). Source data are provided as a Source Data file



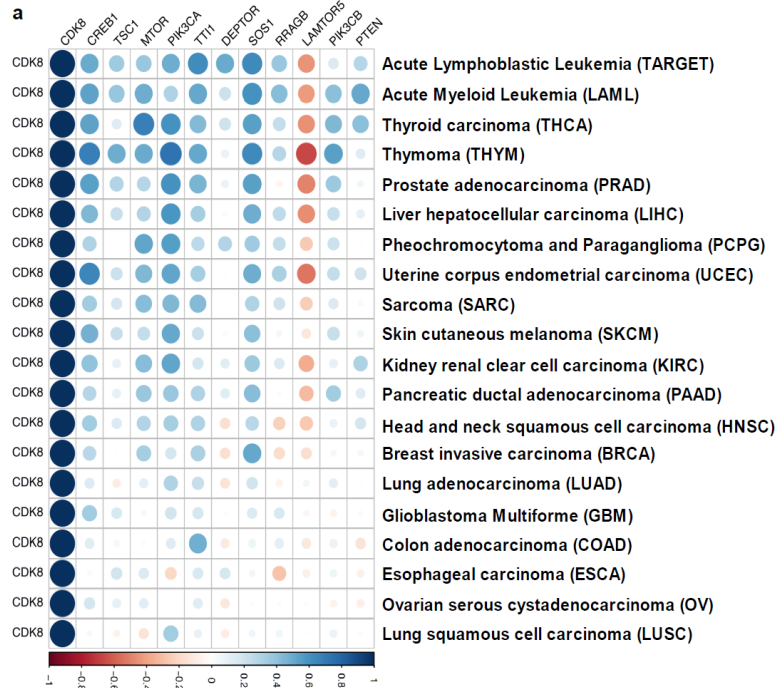
**Supplementary Figure 4:** CDK8 is required for maintenance of BCR-ABL1<sup>p185+</sup> **a** Experimental setup of in vivo time course experiment. Non-irradiated NSG mice received BCR-ABL1<sup>p185+</sup> *Cdk8<sup>fl/fl</sup> Mx1Cre* cell lines and were analysed at the indicated time point for BCR-ABL1<sup>p185+</sup> cell in the BM (2500 cells/mouse, n = 3 received PBS as vehicle control and n = 9 received intraperitoneal poly (I:C) (200 μg) injections, 3 independent cell lines were used). **b** Bar diagram depicts percentages of BCR-ABL1<sup>p185+</sup> cells in the bone marrow on days 11, 17 and 20. Data represents means ± SD



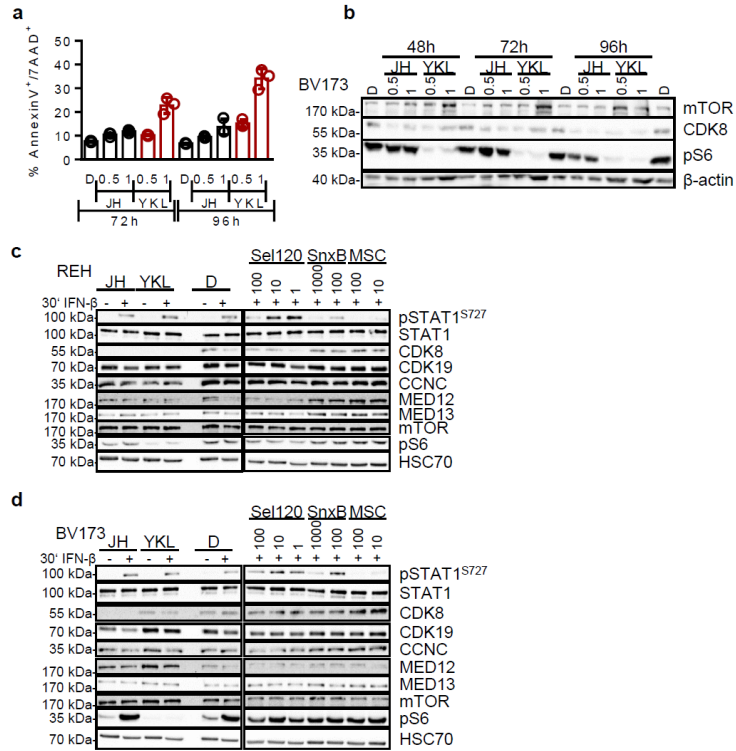
**Supplementary Figure 5:** CDK8 kinase-inhibition fails to mimic the effects of *Cdk8* deletion in BCR-ABL1<sup>p185+</sup> cell lines. **a** RT-qPCRs of STAT1 target genes *Mx1*, *Stat1*, *Tap1*, *Gpb2*, *Irf1* and *Ido1*. BCR-ABL1<sup>p185+</sup> *Cdk8*<sup>fl/fl</sup> were incubated 48 hours with 1000 nM or 100 nM SenexinB (SnxB) or 100 nM or 10nM MSC and stimulated 24 hours with interferon- $\beta$ . Fold increase is relative to unstimulated gene expression. Bars depict mean  $\pm$  SD. **b** Dose-response curves of BCR-ABL1<sup>p185+</sup> *Cdk8*<sup>fl/fl</sup> and BCR-ABL1<sup>p185+</sup> *Cdk8*<sup>Δ/Δ</sup> Vav-Cre cell lines (sum of MSC n = 2 and SnxB n = 5 cell lines per genotype, measured in quadruplicates (MSC) or triplicates (SnxB); mean  $\pm$  SD). IC<sub>50</sub>'s for Senexin B of BCR-ABL1<sup>p185+</sup> *Cdk8*<sup>fl/fl</sup> and BCR-ABL1<sup>p185+</sup> *Cdk8*<sup>Δ/Δ</sup> Vav-Cre are listed in the table. **c** Volcano Blot of the 159 differentially expressed genes of BCR-ABL1<sup>p185+</sup> *Cdk8*<sup>Δ/Δ</sup> Vav-Cre vs BCR-ABL1<sup>p185+</sup> *Cdk8*<sup>fl/fl</sup> cell lines. Source data are provided as a Source Data file



**Supplementary Figure 6: CDK8 regulates the mTOR pathway.** **a** Top 10 enriched KEGG pathways of genes down-regulated in BCR-ABL1<sup>P185+</sup> *Cdk8*<sup>Δ/Δ</sup>*Vav-Cre* vs. BCR-ABL1<sup>P185+</sup> *Cdk8*<sup>fl/fl</sup> cell lines. Top 10 KEGG pathways obtained by Enrichr ranked by the combined score (log (Fisher exact test p-value) \* z-score). For p-values and z-scores, see Supplementary Table 2. **b** Table shows fold changes in gene expression BCR-ABL1<sup>P185+</sup> *Cdk8*<sup>Δ/Δ</sup>*Vav-Cre* compare to BCR-ABL1<sup>P185+</sup> *Cdk8*<sup>fl/fl</sup> of a set of genes that were found to be differentially expressed (RNA-seq) by qRT-PCR. Values display mean ± SD of n = 4 per genotype measured in triplicates. **c** Dose-response curves for Ruxolitinib, Bay11, PDK/AKT/FIT3/PIM, THZ-1 and NVP-2; mean ± SD. Source data are provided as a Source Data file



**Supplementary Figure 7:** Co-expression matrix of *Cdk8* and members of the mTOR pathway. **a** Co-expression of *Cdk8* and members of mTOR/PI3K signaling pathways in a pediatric ALL dataset (TARGET cohort, RNA-seq) and in 19 TCGA RNA-seq datasets. The scale indicates Spearman correlation coefficients ranging from -1 (red) to 1 (blue).



**Supplementary Figure 8:** Chemical CDK8 degradation cooperates with mTOR inhibition. **a** AnnexinV/7AAD<sup>+</sup> staining of BV173 cells incubated with 0.5  $\mu$ M and 1  $\mu$ M of JH-XI-10-02 or YKL-06-101 for 72 and 96 hours. DMSO was used as vehicle control (D: DMSO, n = 3). **b** Immunoblotting of mTOR, CDK8 and pS6<sup>S240/244</sup> of BV173 cell line incubated with 0.5  $\mu$ M and 1  $\mu$ M of JH-XI-10-02 or YKL-06-101 for 48, 72 and 96 hours. DMSO (indicated as D) served as vehicle control and  $\beta$ -actin as loading control. REH **c** or BV173 **d** incubated with 1  $\mu$ M of JH-XI-10-02 or YKL-06-101 or indicated concentrations [nM] of Sel120, SnxB or MSC for 48 hours. Plus (+) indicates samples treated 30 min with interferon- $\beta$  (IFN- $\beta$ ) before harvesting. Blots were probed for pSTAT1<sup>S727</sup>, total STAT1, CDK8, CDK19, CCNC, MED12, MED13, mTOR and pS6<sup>S240/244</sup>. DMSO (indicated as D) served as vehicle control and HSC as loading control. Levels of significance were calculated using Kruskal-Wallis test followed by Dunn's test, data represents means  $\pm$  SD. Source data are provided as a Source Data file

## Supplementary Tables

Supplementary Table 1: Genes set enrichment analysis.

Gene set enrichment analysis – Hallmarks					
Gene sets	ES	NES	NOM p-val	FDR q-val	FWER p-val
Apical surface	-0.50	-1.68	0.000	0.010	0.004
TNF $\alpha$ signaling via NF $\kappa$ B	-0.42	-1.66	0.000	0.014	0.010
UV response	-0.36	-1.41	0.004	0.132	0.147
E2F targets	-0.36	-1.40	0.000	0.099	0.147
KRAS signaling	-0.35	-1.39	0.004	0.096	0.173
G2M Checkpoint	-0.35	-1.37	0.004	0.093	0.197
MTORC1 signaling	-0.33	-1.34	0.000	0.109	0.253
PI3K AKT MTOR signaling	-0.36	-1.34	0.022	0.097	0.258
Inflammatory response	-0.34	-1.33	0.007	0.100	0.296
Cholesterol homeostasis	-0.38	-1.32	0.041	0.091	0.298
Estrogen response early	-0.33	-1.31	0.008	0.092	0.327
IL2 STAT5 signaling	-0.31	-1.27	0.004	0.128	0.456
Unfolded protein response	-0.34	-1.26	0.037	0.130	0.488
Heme metabolism	-0.31	-1.24	0.017	0.139	0.541
Spermatogenesis	-0.32	-1.22	0.034	0.161	0.623
Allograft rejection	-0.30	-1.21	0.037	0.178	0.684
Oxidative phosphorylation	-0.30	-1.20	0.043	0.174	0.703
Hedgehog signaling	-0.36	-1.14	0.243	0.285	0.874
p53 pathway	-0.36	-1.14	0.243	0.285	0.874
Angiogenesis	-0.36	-1.13	0.243	0.284	0.900
IL6 JAK-STAT3 signaling	-0.32	-1.11	0.248	0.317	0.929
Hypoxia	-0.28	-1.10	0.159	0.33	0.945
Apoptosis	-0.28	-1.10	0.195	0.325	0.950
Interferon gamma response	-0.28	-1.10	0.129	0.313	0.951
Estrogen response late	-0.27	-1.07	0.208	0.367	0.974
Adipogenesis	-0.27	-1.07	0.207	0.360	0.975
Pancreas beta cells	-0.35	-1.06	0.325	0.377	0.982
Reactive oxygen species pathway	-0.31	-1.06	0.316	0.372	0.985
Apical junction	-0.26	-1.05	0.280	0.402	0.994

ES: enrichment score; NES: normalized enrichment score; NOM p-val: nominal p-value; FDR q-val: False discovery rate q-value; FWER p-val: familywise-error rate p-value



**Supplementary Table 2:** EnrichR pathway analysis.

Term	Overlap	P-value	Z-score	Combined score	Genes
Focal adhesion	7/202	0,0011	-1,922	12,9539	LAMA5;ACTN1;SPP1;PTK2;THBS3;IGF1R;ITGA9
ECM-receptor interaction	4/82	0,0041	-1,6821	9,2221	LAMA5;SPP1;THBS3;ITGA9
Amaeociasis	4/100	0,0083	-1,8183	8,6999	LAMA5;ACTN1;PLCB2;PTK2
Mucin type O-Glycan biosynthesis	2/31	0,0251	-1,524	5,6147	GALNT6;GALNT10
PI3K-Akt signaling pathway	6/341	0,0552	-1,8856	5,4591	LAMA5;SPP1;PTK2;THBS3;IGF1R;ITGA9
Primary immunodeficiency	2/37	0,0348	-1,538	5,1612	RAG2;RAG1
Endocrine and other factor-regulated calcium reabsorption	2/47	0,0537	-1,7135	5,0078	ATP1A3;PLCB2
Carbohydrate digestion and absorption	2/45	0,0497	-1,625	4,8755	ATP1A3;PLCB2
Thyroid hormone signaling pathway	3/118	0,0679	-1,6469	4,4274	RCAN1;ATP1A3;PLCB2
Rap1 signaling pathway	4/211	0,088	-1,685	4,0946	ID1;PLCB2;RAP1GAP;IGF1R

Results from EnrichR pathway analysis using significant downregulated genes (fold change > 2, padjust < 0.1) between BCR-ABL1<sup>P185+</sup> *Cdk8<sup>Δ/Δ</sup>Vav-Cre* vs. BCR-ABL1<sup>P185+</sup> *Cdk8<sup>fl/fl</sup>* cell lines.

**Supplementary Table 3:** Patient information.

Pat. No No#	Gender (f/m)	Age (years)	Diagnosis	WBC (g/l)	Blasts (%) BM	Blasts (%) PB	BCR-ABL1 (variant)	sample	JH-XI-10-02 IC <sub>50</sub>	YKL-06-101 IC <sub>50</sub>
#1	f	41	T-ALL	2.66	94	n.a.	-	BM	> 10 μM	> 10 μM
#3	m	72	c-ALL	2.42	80-85	18	-	BM	> 10 μM	0.9 μM
#4	m	69	prā B-ALL	17.04	71	46	+(p190)	BM	> 10 μM	> 10 μM
#6	f	22	T-ALL	56.65	90	61	-	PB	> 10 μM	0.1 μM
#7	m	333	T-ALL	14.53	40	n.a.	-	BM	> 10 μM	> 10 μM
#8	f	71	c-ALL	69.58	85	73	-	PB	> 10 μM	> 10 μM
#9	f	73	c-ALL	11.98	90-95	23	-	BM	> 10 μM	9 μM
#11	m	51	c-ALL	2.79	88	19	-	BM	> 10 μM	0.4 μM
#12	f	76	pro B-ALL	14.88	95	67	-	PB	> 10 μM	> 10 μM
#13	m	36	T-ALL	6.44	22	n.a.	-	BM	> 10 μM	0.3 μM
#14	m	39	T-ALL	19.83	80	56	-	BM	> 10 μM	> 10 μM
#15	f	50	prā B-ALL	94.01	80	92	-	BM	> 10 μM	10 μM

Pat. No: patient number; WBC: white blood cell count; f: female, m: male; G/l: 10<sup>9</sup> cells per liter; BM: bone marrow, PB: peripheral blood; -: negative for BCR-ABL1; +: positive for BCR-ABL1, n.a.: not available

### 3. Discussion and Conclusion

Our studies identify novel oncogenic functions of CDK8 in triple-negative breast cancer and BCR-ABL<sup>+</sup> leukemia. We provide first insights into the underlying molecular mechanisms and define CDK8 as a promising drug target.

Triple-negative breast cancer (TNBC) is an aggressive disease with a high risk of relapse and metastasis formation. The standard of care relies on surgery and chemotherapy. As no targeted therapies are available (Aysola et al., 2013; Fabbri et al., 2019; Lebert et al., 2018), we set out to identify new therapeutic angles. Our studies were initiated by *in silico* studies that reveal an inverse correlation between recurrence-free survival and the levels of CDK8 in various types of breast cancer (Broude et al., 2015; Lim and Kaldis, 2013; Roninson et al., 2019). CDK8 was reported to be involved in EMT, an important process for invasion and metastasis of breast cancer cells (Serrao et al., 2018; Wang and Zhou, 2014).

These observations encouraged us to focus on the role of CDK8 in highly metastatic TNBC. We found that CDK8 is not required for cell proliferation or survival of murine TNBC cells. CDK8 was required to allow the regrowth of primary tumors after their surgical removal and metastatic spreading. These observations are drawn from our studies in a murine orthotopic breast cancer model. In line, we detected a CDK8-dependent regulation of the EMT-associated TF *Snai2* in TNBC cells, which is in accordance with previous reports, that had implicate CDK8 in the regulation of EMT TFs in ovarian, pancreatic and HER2-enriched breast cancer cell lines and in the promotion of metastasis of colon cancer (Liang et al., 2018; Serrao et al., 2018). Similarly, the expression levels of *Mmp9* and *Ccl2* were significantly higher when CDK8 was present. The matrix metalloproteinase *Mmp9* controls the invasiveness of different cancer cell types (Aalinkeel et al., 2011; Liang et al., 2018; Mehner et al., 2014) while *Ccl2* is overexpressed in invasive breast cancers and is postulated to support metastasis (Fang et al., 2016; Kitamura et al., 2015; Qian et al., 2011). One recent study (Serrao et al., 2018) reported reduced EMT upon CDK8/CDK19 kinase inhibition in a murine breast cancer model, which contrasts our observation. We failed to detect any deregulation of the EMT-associated TF *Snai2*, as well as *Ccl2* or *Mmp9* upon CDK8/CDK19 inhibitor treatment. We therefore propose a kinase-independent regulation.

RNA sequencing of TNBC cells highlighted the regulation of modulators of NK-cell cytotoxicity as a major CDK8-dependent pathway. Extensive preclinical literature and observations from the clinics point at a pivotal role of NK cells during metastatic dissemination (Cerwenka and Lanier, 2016; Guilleroy et al., 2016; Peinado et al., 2017). With respect to the immune-

surveillance of primary solid tumors, the involvement of NK cells is less clear and remains a matter of debate.

*In vitro*, NK cells kill cancer cell lines irrespective of whether they derive from a primary tumor or a metastatic lesion (Ames et al., 2015; Castriconi et al., 2009; Tallero et al., 2013). *In vivo*, the situation is more complex and less clear. NK cells appear to shape the developing tumor in the absence of adaptive immunity (O'Sullivan et al., 2012). NK cells represent a minor fraction of the immunological infiltrate in most solid tumors (López-Soto et al., 2017; Senovilla et al., 2012). The precise role of NK cells in the surveillance of primary solid tumors remained elusive. To shed new light onto the function of NK cells in the control of the primary tumor and of metastasis we used a murine orthotopic breast cancer model and NK depletion experiments. We demonstrate that NK cells have the ability to control primary tumor growth. Intriguingly, NK-mediated surveillance is counteracted when CDK8 is present in the tumor cells – in our E0771 model primary tumor cells are not killed by NK cells and hence escape surveillance. This might explain the observation of a NK cell-mediated control of metastasis in breast cancer while failing to see effects on primary tumor growth (Bottos et al., 2016; Hofmann et al., 2020; Ohs et al., 2017; Putz et al., 2013). Our data indicate that NK cells control primary tumor growth and that loss of CDK8 renders tumor cells “visible” for NK cells. We therefore characterize CDK8 as a novel player of immune evasion in TNBC.

We found PD-L1 (a PD-1 ligand) to be deregulated by CDK8 on a transcriptional and translational level in E0771 cells. This observation is supported by a dataset from TNBC patients, where the levels of expression of PD-L1 and CDK8 positively correlate. PD-L1 is significantly higher expressed in TNBC compared to non-TNBC patients. A Phase 3 clinical trial combined chemotherapy with PD-L1-targeted antibody treatment and yielded first promising results (Lebert et al., 2018; Marra et al., 2019; Mittendorf et al., 2014). Accumulating evidence points at a relevant role of PD-1 signaling in NK cells. This nourishes the hope that PD-1/PD-L1 checkpoint inhibitors may attack the tumor from two angles: from the T- and the NK-cell side (Hsu et al., 2018; Liu et al., 2017; Park et al., 2020; Quatrini et al., 2020). We hypothesize that the CDK8-PD-L1 axis – within the tumor cell – contributes to the evasion from NK cells and that CDK8 provides further lines of defense against NK-cell cytotoxicity by influencing a panel of inhibitory and activating NK ligands. Our data suggest a CDK8-mediated regulation of MHC class I, NKG2D ligands and ICAM-1. Together with PD-L1 they all contribute to the molecular mechanism how CDK8 drives immune evasion.

In summary, we propose that targeting CDK8 in TNBC has therapeutic potential. It may be beneficial as it dampens the invasive and pro-metastatic behavior of TNBC cells. Secondly it

may prevent tumor cells from evading NK cells. On top, a suppressive effect of NK-cell-intrinsic CDK8 on the activity of NK cells was described using mice with conditional ablation of CDK8 in Nkp46<sup>+</sup> cells. CDK8 did so by regulating the lytic molecule perforin (Witalisz-Siepracka et al., 2018). This study explains a cytotoxicity enhancing effect of CDK8 blockage.

We could not recapitulate our findings using a CDK8/CDK19 kinase inhibitor (Senexin B). With kinase-inhibition we failed to see effects on NK cell-mediated recognition or elimination of E0771 cells. These data again indicate a kinase-independent role for CDK8 in NK-cell immune evasion. This hypothesis is supported by independent studies describing mechanistically distinct transcriptional functions of CDK8 and its paralogue CDK19 (Steinparzer et al., 2019). CDK8 kinase-independent functions were also found in melanoma cells and hematologic malignancies (Kapoor et al., 2010; Menzl et al., 2019b; Poss et al., 2016). In contrast, the effect of CDK8 on ER<sup>+</sup> breast cancer progression seems to be kinase-dependent (McDermott et al., 2017), assigning divergent roles to CDK8 in different cancer entities. We assume that a small-molecule compound degrading only CDK8 is a promising alternative for therapy of TNBC.

In addition, we identified CDK8 as a key mediator of BCR-ABL-driven leukemia. Using an inducible system, we show that deletion of CDK8 but not of CDK6, CDK7, CDK9 or CDK19 has a dramatic effect on cell survival and proliferation of murine BCR-ABL<sup>1p185+</sup> cells. This indicates a unique role of CDK8 downstream of BCR-ABL<sup>1p185+</sup> in murine B-ALL. As all of these proteins were present at significantly elevated levels in the tumor cells, it was rather unexpected that only the knockdown of CDK8 affected cell viability and growth. CDK6 has been shown to exert tumor-promoting functions by enhancing proliferation and stimulating angiogenesis in BCR-ABL-induced leukemia (Bellutti et al., 2018; Kollmann et al., 2013), but did not show major effects in this setting. We speculate that our inducible experimental system only identifies essential players which cannot be compensated by other signaling pathways. We observed that the initial transformation by the oncogene is not influenced, but CDK8 is indispensable for the maintenance of our established leukemic cell lines.

STAT5 is a known target of CDK8 and a key factor for leukemia maintenance (Bancerek et al., 2013; Berger et al., 2013; Rzymiski et al., 2017). We thus hypothesize that the effects of CDK8 on cell viability and growth stem in part from the role of CDK8 as an upstream-kinase for the STAT5<sup>S725</sup> phosphorylation in BCR-ABL-driven leukemia.

*Cdk8* knockout mice are embryonically lethal, therefore we employed *Mx1Cre* and *VavCre* mouse models, to delete CDK8 inducible or within the hematopoietic compartment (Georgiades et al., 2002; Kühn et al., 1995). Once we deleted *Cdk8* after disease onset using

the inducible *Mx1Cre* system, we observe reduced viability of cells *in vitro* and prolonged survival of mice *in vivo*. Under physiological settings, CDK8 is required for embryonic development, however deletion of *Cdk8* in adult mice has no significant effect (McClelland et al., 2015). Our data are in accordance with this observation. The deletion of *Cdk8* in adult *Mx1Cre* or *Vav-Cre* mice is well tolerated. This opens a therapeutic window as healthy cells appear to be spared upon deletion of *Cdk8* while tumor cells might be efficiently targeted.

Our global RNA sequencing approach identified critical CDK8-dependent signaling pathways in BCR-ABL1<sup>p185+</sup>-driven leukemia, among them being the mTOR signaling pathway. The mTOR inhibitor Everolimus has already been discussed as a therapeutic strategy in BCR-ABL-induced ALL in combination with Imatinib to overcome resistance to Imatinib (Kuwatsuka et al., 2011). We tested the potential link of CDK8 and mTOR signaling in human ALL cells. Analysis of human RNA sequencing datasets from ALL and AML patients suggested a highly significant correlation between the levels of expression of CDK8 and members of the mTOR pathway. This finding is entirely new in the setting of a hematologic disease. The interaction of CDK8 with mTOR was suggested in the context of lipogenesis but not in any form of cancer to date (Feng et al., 2015).

Our data point at a kinase-independent role of CDK8. Senexin B treatment, that inhibited CDK8's kinase activity, had only minor effects on differential gene expression. It affected transcription of only six genes and we failed to detect any interaction of CDK8 with members of the mTOR signaling pathway when analyzing our RNA sequencing approach.

We used molecules for specific protein degradation – “proteolysis targeting chimeras” - to target CDK8 independent of its enzymatic activity. We tested two distinct compounds in human leukemic cell lines, one compound specifically degrading CDK8 (JH-XI-10-02) (Hatcher et al., 2018) and the other degrading CDK8 paralleled by the ability to block mTOR signaling (YKL-101-06). Only the combined effect of degrading CDK8 and inhibiting mTOR significantly increased apoptosis in three human leukemic cell lines. We verified these data in human patient samples where 5 out of 12 primary patients' samples reacted with a pronounced and statistically significant reduction of cell viability.

In summary, we found a connection between CDK8 and the mTOR signaling pathway in a subset of leukemic cells. We provide evidence that CDK8 interferes with BCR-ABL-driven leukemia and propose a new therapeutic strategy in their treatment. Targeting two unrelated signaling pathways holds a great promise as it will reduce the probability of resistance and may represent an approach to treat not only B-ALL but also a range of other human cancers.

Taken together our studies identified novel functions of CDK8 in triple-negative breast cancer and BCR-ABL-driven leukemia. They contribute to a better understanding on how CDK8 drives tumorigenesis and tumor immune surveillance.

In the future it will be of great therapeutic interest to learn whether tumor-intrinsic CDK8 drives NK-cell-mediated tumor surveillance in BCR-ABL<sup>+</sup> leukemia. In leukemia and lymphoma, NK cells are critical players of these immune responses (Carlsten and Järås, 2019; Ilander et al., 2017; Street et al., 2004) and high numbers and activation status of NK cells correlate with good prognosis in various leukemia types (Gonzalez-Rodriguez et al., 2019). In line, post treatment of BCR-ABL<sup>+</sup> leukemia with TKI the probability of relapse correlates with the number and activity of NK cells (Yoshimoto et al., 2014) and the use of TKIs lowers the levels of NK-cell-activating ligands on the surface of leukemic cells (Salih et al., 2010).

A second key future question is to explore whether the “dual degrader” (degrading CDK8 while inhibiting mTOR signaling) is a reasonable therapeutic strategy for TNBC. The majority of TNBC cases overexpress EGFR and therefore exhibit constitutive activation of EGFR-dependent signaling pathways, in particular the PI3K/AKT/mTOR pathway. Molecular alteration affecting key components of this pathway are frequently seen in TNBC as well. Loss of *PTEN* expression and the presence of activating mutations in the gene encoding PI3K (*PIK3CA*) constitutively activate downstream effectors such as mTOR. Additionally, studies provide evidence that an approach of co-targeting mTOR and EGFR could be a potential therapeutic strategy in TNBC (El Guerrab et al., 2020). So we believe that co-targeting mTOR and CDK8 represents a treatment approach in TNBC.

In summary, we were able to extend the knowledge of CDK8's function in triple-negative breast cancer and BCR-ABL<sup>+</sup> leukemia, which might help in the future to cure these aggressive diseases. Still, a lot of exiting research questions remain to be investigated.

## 4. References

- Aalinkeel, R., Nair, B.B., Reynolds, J.L., Sykes, D.E., Mahajan, S.D., Chadha, K.C., and Schwartz, S.A. (2011). Overexpression of MMP-9 contributes to invasiveness of prostate cancer cell line LNCaP. *Immunol. Invest.* *40*, 447–464.
- Abe, O., Abe, R., Enomoto, K., Kikuchi, K., Koyama, H., Masuda, H., Nomura, Y., Ohashi, Y., Sakai, K., Sugimachi, K., et al. (2011). Relevance of breast cancer hormone receptors and other factors to the efficacy of adjuvant tamoxifen: Patient-level meta-analysis of randomised trials. *Lancet* *378*, 771–784.
- Aguirre-Ghiso, J.A. (2007). Models, mechanisms and clinical evidence for cancer dormancy. *Nat. Rev. Cancer* *7*, 834–846.
- Alarcón, C., Zaromytidou, A., Xi, Q., Gao, S., Fujisawa, S., Barlas, A., Miller, A.N., Manovattodorova, K., Macias, J., Sapkota, G., et al. (2010). CDK8/9 drive Smad transcriptional action, turnover and YAP interactions in BMP and TGF $\beta$  pathways. *Cell* *139*, 757–769.
- Albain, K., Anderson, S., Arriagada, R., Barlow, W., Bergh, J., Bliss, J., Buyse, M., Cameron, D., Carrasco, E., Clarke, M., et al. (2012). Comparisons between different polychemotherapy regimens for early breast cancer: Meta-analyses of long-term outcome among 100 000 women in 123 randomised trials. *Lancet* *379*, 432–444.
- Allen, B.L., and Taatjes, D.J. (2015). The Mediator complex: A central integrator of transcription. *Nat. Rev. Mol. Cell Biol.* *16*, 155–166.
- Ames, E., Canter, R.J., Grossenbacher, S.K., Mac, S., Chen, M., Smith, R.C., Hagino, T., Perez-Cunningham, J., Sckisel, G.D., Urayama, S., et al. (2015). NK Cells Preferentially Target Tumor Cells with a Cancer Stem Cell Phenotype. *J. Immunol.* *195*, 4010–4019.
- Aragón, E., Goerner, N., Zaromytidou, A.I., Xi, Q., Escobedo, A., Massagué, J., and Macias, M.J. (2011). A smad action turnover switch operated by WW domain readers of a phosphoserine code. *Genes Dev.* *25*, 1275–1288.
- Asghar, U., Witkiewicz, A.K., Turner, N.C., and Knudsen, E.S. (2015). The history and future of targeting cyclin-dependent kinases in cancer therapy. *Nat. Rev. Drug Discov.* *14*, 130–146.
- Avelino, K.Y.P.S., Silva, R.R., da Silva Junior, A.G., Oliveira, M.D.L., and Andrade, C.A.S. (2017). Smart applications of bionanosensors for BCR/ABL fusion gene detection in leukemia. *J. King Saud Univ. - Sci.* *29*, 413–423.

- Aysola, K., Desai, A., Welch, C., Xu, J., Qin, Y., Reddy, V., Matthews, R., Owens, C., Okoli, J., Beech, D.J., et al. (2013). Triple Negative Breast Cancer-An Overview. *Hered. Genet.*
- Bancerek, J., Poss, Z.C., Steinparzer, I., Sedlyarov, V., Pfaffenwimmer, T., Mikulic, I., D??lken, L., Strobl, B., M??ller, M., Taatjes, D.J., et al. (2013). CDK8 Kinase Phosphorylates Transcription Factor STAT1 to Selectively Regulate the Interferon Response. *Immunity* **38**, 250–262.
- Beckers, R.K., Selinger, C.I., Vilain, R., Madore, J., Wilmott, J.S., Harvey, K., Holliday, A., Cooper, C.L., Robbins, E., Gillett, D., et al. (2016). Programmed death ligand 1 expression in triple-negative breast cancer is associated with tumour-infiltrating lymphocytes and improved outcome. *Histopathology* **69**, 25–34.
- Bellutti, F., Tigan, A.S., Nebenfuehr, S., Dolezal, M., Zojer, M., Grausenburger, R., Hartenberger, S., Kollmann, S., Doma, E., Prchal-Murphy, M., et al. (2018). CDK6 Antagonizes p53-Induced Responses during Tumorigenesis. *Cancer Discov.* **8**, 884–897.
- Berger, A., Hoelbl-Kovacic, A., Bourgeais, J., Hoefling, L., Warsch, W., Grundschober, E., Uras, I.Z., Menzl, I., Putz, E.M., Hoermann, G., et al. (2013). PAK-dependent STAT5 serine phosphorylation is required for BCR-ABL-induced leukemogenesis. *Leuk.* **2014** **283** **28**, 629–641.
- Bienz, M., and Clevers, H. (2000). Linking colorectal cancer to Wnt signaling. *Cell* **103**, 311–320.
- Blais, A., and Dynlacht, B.D. (2007). E2F-associated chromatin modifiers and cell cycle control. *Curr. Opin. Cell Biol.* **19**, 658–662.
- Blum, J.L., Flynn, P.J., Yothers, G., Asmar, L., Geyer, C.E., Jacobs, S.A., Robert, N.J., Hopkins, J.O., O’Shaughnessy, J.A., Dang, C.T., et al. (2017). Anthracyclines in early breast Cancer: The ABC Trials—USOR 06-090, NSABP B-46-I/USOR 07132, and NSABP B-49 (NRG Oncology). *J. Clin. Oncol.* **35**, 2647–2655.
- Bottino, C., Castriconi, R., Moretta, L., and Moretta, A. (2005). Cellular ligands of activating NK receptors. *Trends Immunol.* **26**, 221–226.
- Bottos, A., Gotthardt, D., Gill, J.W., Gattelli, A., Frei, A., Tzankov, A., Sexl, V., Wodnar-Filipowicz, A., and Hynes, N.E. (2016). Decreased NK-cell tumour immunosurveillance consequent to JAK inhibition enhances metastasis in breast cancer models. *Nat. Commun.* **7**, 12258.



- Broude, E. V., Gyorffy, B., Chumanevich, A.A., Chen, M., McDermott, M.S.J., Shtutman, M., Catroppo, J.F., and Roninson, I.B. (2015). Expression of CDK8 and CDK8-interacting Genes as Potential Biomarkers in Breast Cancer. *Curr. Cancer Drug Targets* 15, 739–749.
- Bryceson, Y.T., March, M.E., Ljunggren, H.G., and Long, E.O. (2006). Activation, coactivation, and costimulation of resting human natural killer cells. *Immunol. Rev.* 214, 73–91.
- Burstein, M.D., Tsimelzon, A., Poage, G.M., Covington, K.R., Contreras, A., Fuqua, S.A.W., Savage, M.I., Osborne, C.K., Hilsenbeck, S.G., Chang, J.C., et al. (2015). Comprehensive genomic analysis identifies novel subtypes and targets of triple-negative breast cancer. *Clin. Cancer Res.* 21, 1688–1698.
- Byun, J.M., Koh, Y., and Dong-Yeop, S. (2017). BCR-ABL translocation as a favorable prognostic factor in elderly patients with acute lymphoblastic leukemia in the era of potent tyrosine kinase inhibitors. *Haematologica* 9, 898–900.
- Carlsten, M., and Järås, M. (2019). Natural Killer Cells in Myeloid Malignancies: Immune Surveillance, NK Cell Dysfunction, and Pharmacological Opportunities to Bolster the Endogenous NK Cells. *Front. Immunol.* 10.
- Castriconi, R., Daga, A., Dondero, A., Zona, G., Poliani, P.L., Melotti, A., Griffiero, F., Marubbi, D., Spaziante, R., Bellora, F., et al. (2009). NK Cells Recognize and Kill Human Glioblastoma Cells with Stem Cell-Like Properties. *J. Immunol.* 182, 3530–3539.
- Cee, V.J., Chen, D.Y.K., Lee, M.R., and Nicolaou, K.C. (2009). Cortistatin A is a high-affinity ligand of protein kinases ROCK, CDK8, and CDK11. *Angew. Chemie - Int. Ed.* 48, 8952–8957.
- Cerwenka, A., and Lanier, L.L. (2016). Natural killer cell memory in infection, inflammation and cancer. *Nat. Rev. Immunol.* 16, 112–123.
- Chaix, J., Tessmer, M.S., Hoebe, K., Fuséri, N., Ryffel, B., Dalod, M., Alexopoulou, L., Beutler, B., Brossay, L., Vivier, E., et al. (2008). Cutting Edge: Priming of NK Cells by IL-18. *J. Immunol.* 181, 1627–1631.
- Chan, C.J., Martinet, L., Gilfillan, S., Souza-Fonseca-Guimaraes, F., Chow, M.T., Town, L., Ritchie, D.S., Colonna, M., Andrews, D.M., and Smyth, M.J. (2014). The receptors CD96 and CD226 oppose each other in the regulation of natural killer cell functions. *Nat. Immunol.* 15, 431–438.
- Chang, R.B., and Beatty, G.L. (2020). The interplay between innate and adaptive immunity in cancer shapes the productivity of cancer immunosurveillance. *J. Leukoc. Biol.* 108, 363–376.

- Cheang, M.C.U., Martin, M., Nielsen, T.O., Prat, A., Voduc, D., Rodriguez-Lescure, A., Ruiz, A., Chia, S., Shepherd, L., Ruiz-Borrego, M., et al. (2015). Defining Breast Cancer Intrinsic Subtypes by Quantitative Receptor Expression. *Oncologist* 20, 474–482.
- Chou, J., Quigley, D.A., Robinson, T.M., Feng, F.Y., and Ashworth, A. (2020). Transcription-associated cyclin-dependent kinases as targets and biomarkers for cancer therapy. *Cancer Discov.* 10, 351–370.
- Coca, S., Perez-Piqueras, J., Martinez, D., Colmenarejo, A., Saez, M.A., Vallejo, C., Martos, J.A., and Moreno, M. (1997). The prognostic significance of intratumoral natural killer cells in patients with colorectal carcinoma. *Cancer* 79, 2320–2328.
- Compe, E., and Egly, J.M. (2012). TFIIH: When transcription met DNA repair. *Nat. Rev. Mol. Cell Biol.* 13, 343–354.
- Curtis, C., Shah, S.P., Chin, S.F., Turashvili, G., Rueda, O.M., Dunning, M.J., Speed, D., Lynch, A.G., Samarajiwa, S., Yuan, Y., et al. (2012). The genomic and transcriptomic architecture of 2,000 breast tumours reveals novel subgroups. *Nature* 486, 346–352.
- Cutler, J.A., Tahir, R., Sreenivasamurthy, S.K., Mitchell, C., Renuse, S., Nirujogi, R.S., Patil, A.H., Heydarian, M., Wong, X., Wu, X., et al. (2017). Differential signaling through p190 and p210 BCR-ABL fusion proteins revealed by interactome and phosphoproteome analysis. *Leukemia* 31, 1513–1524.
- Daniels, D.L., Ford, M., Schwinn, M.K., and Benink, H. (2013). Mutual Exclusivity of MED12/MED12L, MED13/13L, and CDK8/19 Paralogs Revealed within the CDK-Mediator Kinase Module. *J. Proteomics Bioinform.* 01.
- Degnim, A.C., Brahmabhatt, R.D., Radisky, D.C., Hoskin, T.L., Stallings-Mann, M., Laudenschlager, M., Mansfield, A., Frost, M.H., Murphy, L., Knutson, K., et al. (2014). Immune cell quantitation in normal breast tissue lobules with and without lobulitis. *Breast Cancer Res. Treat.* 144, 539–549.
- Delahaye, N.F., Rusakiewicz, S., Martins, I., Ménard, C., Roux, S., Lyonnet, L., Paul, P., Sarabi, M., Chaput, N., Semeraro, M., et al. (2011). Alternatively spliced NKp30 isoforms affect the prognosis of gastrointestinal stromal tumors. *Nat. Med.* 17, 700–707.
- DeNardo, D.G., and Coussens, L.M. (2007). Inflammation and breast cancer. Balancing immune response: Crosstalk between adaptive and innate immune cells during breast cancer progression. *Breast Cancer Res.* 9, 1–10.

- Dent, R., Trudeau, M., Pritchard, K.I., Hanna, W.M., Kahn, H.K., Sawka, C.A., Lickley, L.A., Rawlinson, E., Sun, P., and Narod, S.A. (2007). Triple-negative breast cancer: Clinical features and patterns of recurrence. *Clin. Cancer Res.* *13*, 4429–4434.
- Diefenbach, A., and Raulet, D.H. (2002). The innate immune response to tumors and its role in the induction of T-cell immunity. *Immunol. Rev.* *188*, 9–21.
- Donskov, F., and Von Der Maase, H. (2006). Impact of immune parameters on long-term survival in metastatic renal cell carcinoma. *J. Clin. Oncol.* *24*, 1997–2005.
- Dranoff, G. (2004). Cytokines in cancer pathogenesis and cancer therapy. *Nat. Rev. Cancer* *4*, 11–22.
- Druker, B.J., Tamura, S., Buchdunger, E., Ohno, S., Segal, G.M., Fanning, S., Zimmermann, O.R.G., and Lydon, N.B. (1996). Effects of a selective inhibitor of the Abl tyrosine kinase on the growth of Bcr-Abl positive cells. *Nat. Med.* *2*, 561–566.
- Duarte, S., Baber, J., Fujii, T., and Coito, A.J. (2015). Matrix metalloproteinases in liver injury, repair and fibrosis. *Matrix Biol.* *44–46*, 147–156.
- Dunn, G.P., Bruce, A.T., Ikeda, H., Old, L.J., and Schreiber, R.D. (2002). Cancer Immunoediting: from Surveillance to Escape. *Nat. Immunol.* *3*, 85–99.
- Ebmeier, C.C., and Taatjes, D.J. (2010). Activator-mediator binding regulates mediator-cofactor interactions. *Proc. Natl. Acad. Sci. U. S. A.* *107*, 11283–11288.
- Emens, L.A., Adams, S., Barrios, C.H., Diéras, V., Iwata, H., Loi, S., Rugo, H.S., Schneeweiss, A., Winer, E.P., Patel, S., et al. (2021). First-line atezolizumab plus nab-paclitaxel for unresectable, locally advanced, or metastatic triple-negative breast cancer: IMpassion130 final overall survival analysis. *Ann. Oncol.* *32*, 983–993.
- Ernard, B., Isher, F., Nderson, T.A., Ohn, J., Ryant, B., Argolese, I.G.M., Eutsch, E.D., Isher, D.R.F., Ong -H Yeon, J., Eong, J., et al. (2002). Twenty-year follow-up of a randomized trial comparing total mastectomy, lumpectomy, and lumpectomy plus irradiation for the treatment of invasive breast cancer.
- Fabbri, F., Salvi, S., and Bravaccini, S. (2019). Know your enemy: Genetics, aging, exposomic and inflammation in the war against triple negative breast cancer. *Semin. Cancer Biol.* *1–9*.
- Fang, W. Bin, Yao, M., Brummer, G., Acevedo, D., Alhakamy, N., Berkland, C., and Cheng, N. (2016). Targeted gene silencing of CCL2 inhibits triple negative breast cancer progression by

blocking cancer stem cell renewal and M2 macrophage recruitment. *Oncotarget* 7, 49349–49367.

Fant, C.B., and Taatjes, D.J. (2019). Regulatory functions of the Mediator kinases CDK8 and CDK19. *Transcription* 10, 76–90.

Feng, D., Youn, D.Y., Zhao, X., Gao, Y., Quinn, W.J., Xiaoli, A.M., Sun, Y., Birnbaum, M.J., Pessin, J.E., and Yang, F. (2015). mTORC1 Down-Regulates Cyclin-Dependent Kinase 8 (CDK8) and Cyclin C (CycC). *PLoS One* 10, e0126240.

Finn, R.S., Martin, M., Rugo, H.S., and Jones, S. (2016). Palbociclib and Letrozole in Advanced Breast Cancer. *N Engl J Med* 375, 1925–1961.

Firestein, R., Bass, A.J., Kim, S.Y., Dunn, I.F., Silver, S.J., Guney, I., Freed, E., Ligon, A.H., Vena, N., Ogino, S., et al. (2008). CDK8 is a colorectal cancer oncogene that regulates beta-catenin activity. *Nature* 455, 547–551.

Firestein, R., Shima, K., Nosho, K., Irahara, N., Baba, Y., Bojarski, E., Giovannucci, E.L., Hahn, W.C., Fuchs, C.S., and Ogino, S. (2010). CDK8 expression in 470 colorectal cancers in relation to  $\beta$ -catenin activation, other molecular alterations and patient survival. *Int. J. Cancer* 126, 2863–2873.

Fryer, C.J., White, J.B., and Jones, K.A. (2004). Mastermind recruits CycC:CDK8 to phosphorylate the Notch ICD and coordinate activation with turnover. *Mol. Cell* 16, 509–520.

Galbraith, M.D., Andrysik, Z., Pandey, A., Hoh, M., Bonner, E.A., Hill, A.A., Sullivan, K.D., and Espinosa, J.M. (2017). CDK8 Kinase Activity Promotes Glycolysis. *Cell Rep.* 21, 1495–1506.

Gambacorti-Passerini, C., Le Coutre, P., Mologni, L., Fanelli, M., Bertazzoli, C., Marchesi, E., Di Nicola, M., Biondi, A., Corneo, G.M., Belotti, D., et al. (1997). Inhibition of the ABL kinase activity blocks the proliferation of BCR/ABL+ leukemic cells and induces apoptosis. *Blood Cells, Mol. Dis.* 23, 380–394.

Gannon, P.O., Poisson, A.O., Delvoye, N., Lapointe, R., Mes-Masson, A.M., and Saad, F. (2009). Characterization of the intra-prostatic immune cell infiltration in androgen-deprived prostate cancer patients. *J. Immunol. Methods* 348, 9–17.

Georgiades, P., Ogilvy, S., Duval, H., Licence, D.R., Charnock-Jones, D.S., Smith, S.K., and Print, C.G. (2002). VavCre transgenic mice: a tool for mutagenesis in hematopoietic and endothelial lineages. *Genesis* 34, 251–256.

- Ghebeh, H., Mohammed, S., Al-Omair, A., Qattan, A., Lehe, C., Al-Qudaihi, G., Elkum, N., Alshabanah, M., Amer, S. Bin, Tulbah, A., et al. (2006). The B7-H1 (PD-L1) T lymphocyte-inhibitory molecule is expressed in breast cancer patients with infiltrating ductal carcinoma: Correlation with important high-risk prognostic factors. *Neoplasia* 8, 190–198.
- Goetz, M.P., Toi, M., Campone, M., Trédan, O., Bourayou, N., Sohn, J., Park, I.H., Paluch-Shimon, S., Huober, J., Chen, S.C., et al. (2017). MONARCH 3: Abemaciclib as initial therapy for advanced breast cancer. *J. Clin. Oncol.* 35, 3638–3646.
- Goldhirsch, A., Winer, E.P., Coates, A.S., Gelber, R.D., Piccart-Gebhart, M., Thürlimann, B., Senn, H.J., Albain, K.S., André, F., Bergh, J., et al. (2013). Personalizing the treatment of women with early breast cancer: Highlights of the st gallen international expert consensus on the primary therapy of early breast Cancer 2013. *Ann. Oncol.* 24, 2206–2223.
- Gonzalez-Rodriguez, A.P., Villa-Álvarez, M., Sordo-Bahamonde, C., Lorenzo-Herrero, S., and Gonzalez, S. (2019). NK Cells in the Treatment of Hematological Malignancies. *J. Clin. Med.* 8.
- Grebien, F., Hantschel, O., Wojcik, J., Kaupe, I., Kovacic, B., Wyrzucki, A.M., Gish, G.D., Cerny-Reiterer, S., Koide, A., Beug, H., et al. (2011). Targeting the SH2-kinase interface in Bcr-Abl inhibits leukemogenesis. *Cell* 147, 306–319.
- El Guerrab, A., Bamdad, M., Bignon, Y.J., Penault-Llorca, F., and Aubel, C. (2020). Co-targeting EGFR and mTOR with gefitinib and everolimus in triple-negative breast cancer cells. *Sci. Rep.* 10.
- Guia, S., Cognet, C., De Beaucoudrey, L., Tessmer, M.S., Jouanguy, E., Berger, C., Filipe-Santos, O., Feinberg, J., Camcioglu, Y., Levy, J., et al. (2008). A role for interleukin-12/23 in the maturation of human natural killer and CD56+ T cells in vivo. *Blood* 111, 5008–5016.
- Guillerey, C., Huntington, N.D., and Smyth, M.J. (2016). Targeting natural killer cells in cancer immunotherapy. *Nat. Immunol.* 17, 1025–1036.
- Gumuskaya, B., Alper, M., Hucumenoglu, S., Altundag, K., Uner, A., and Guler, G. (2010). EGFR expression and gene copy number in triple-negative breast carcinoma. *Cancer Genet. Cytogenet.* 203, 222–229.
- Guo, Z., Wang, G., Lv, Y., Wan, Y.Y., and Zheng, J. (2019). Inhibition of Cdk8/Cdk19 Activity Promotes Treg Cell Differentiation and Suppresses Autoimmune Diseases. *Front. Immunol.* 10, 1–10.

- Hammond, M.E.H., Hayes, D.F., Wolff, A.C., Mangu, P.B., and Temin, S. (2010). American Society of Clinical Oncology/College of American Pathologists guideline recommendations for immunohistochemical testing of estrogen and progesterone receptors in breast cancer. *J. Oncol. Pract.* *6*, 195–197.
- Hanahan, D., and Weinberg, R.A. (2011). Hallmarks of cancer: The next generation. *Cell* *144*, 646–674.
- Hatcher, J.M., Wang, E.S., Johannessen, L., Kwiatkowski, N., Sim, T., and Gray, N.S. (2018). Development of Highly Potent and Selective Steroidal Inhibitors and Degradable of CDK8.
- Hehlmann, R. (2020). Chronic Myeloid Leukemia in 2020. *HemaSphere* *4*.
- van Helden, M.J., Goossens, S., Daussy, C., Mathieu, A.L., Faure, F., Marçais, A., Vandamme, N., Farla, N., Mayol, K., Viel, S., et al. (2015). Terminal NK cell maturation is controlled by concerted actions of T-bet and Zeb2 and is essential for melanoma rejection. *J. Exp. Med.* *212*, 2015–2025.
- Hofmann, M.H., Mani, R., Engelhardt, H., Impagnatiello, M.A., Carotta, S., Kerenyi, M., Lorenzo-Herrero, S., Böttcher, J., Scharn, D., Arnhof, H., et al. (2020). Selective and Potent CDK8/19 Inhibitors Enhance NK-Cell Activity and Promote Tumor Surveillance. *Mol. Cancer Ther.* *19*, 1018–1030.
- Hortobagyi, G.N., Stemmer, S.M., Burris, H.A., and Yap, Y.-S. (2016). Ribociclib as First-Line Therapy for HR-Positive, Advanced Breast Cancer.
- Howlander, N., Altekruze, S.F., Li, C.I., Chen, V.W., Clarke, C.A., Ries, L.A.G., and Cronin, K.A. (2014). US incidence of Breast cancer Subtypes Defined by Joint Hormone receptor and Her2 Status.
- Hsu, J., Raulet, D.H., and Ardolino, M. (2018). Contribution of NK cells to immunotherapy mediated by PD-1/PD-L1 blockade. *J. Clin. Invest.* *128*, 4654–4668.
- Hughes, T., Becknell, B., Freud, A.G., McClory, S., Briercheck, E., Yu, J., Mao, C., Giovenzana, C., Nuovo, G., Wei, L., et al. (2010). Interleukin-1 $\beta$  selectively expands and sustains interleukin-22+ immature human natural killer cells in secondary lymphoid tissue. *Immunity* *32*, 803–814.
- Ilander, M., Olsson-Strömberg, U., Schlums, H., Guilhot, J., Brück, O., Lähteenmäki, H., Kasanen, T., Koskenvesa, P., Söderlund, S., Höglund, M., et al. (2017). Increased proportion of mature NK cells is associated with successful imatinib discontinuation in chronic myeloid

leukemia. *Leukemia* 31, 1108–1116.

Inamdar, K. V., and Bueso-Ramos, C.E. (2007). Pathology of chronic lymphocytic leukemia: an update. *Ann. Diagn. Pathol.* 11, 363–389.

Ishigami, S., Natsugoe, S., Tokuda, K., Nakajo, A., Che, X., Iwashige, H., Aridome, K., Hokita, S., and Aikou, T. (2000). Prognostic value of intratumoral natural killer cells in gastric carcinoma. *Cancer* 88, 577–583.

Jasin, M., and Rothstein, R. (2013). Repair of strand breaks by homologous recombination. *Cold Spring Harb. Perspect. Biol.* 5.

Jeronimo, C., Bataille, A.R., and Robert, F. (2013). The writers, readers, and functions of the RNA polymerase II C-terminal domain code. *Chem. Rev.* 113, 8491–8522.

Jeronimo, C., Collin, P., and Robert, F. (2016). The RNA Polymerase II CTD: The Increasing Complexity of a Low-Complexity Protein Domain. *J. Mol. Biol.* 428, 2607–2622.

Johnson, J.R., Bross, P., Cohen, M., Rothmann, M., Chen, G., Zajicek, A., Gobburu, J., Rahman, A., Staten, A., and Pazdur, R. (2003). Approval summary: Imatinib mesylate capsules for treatment of adult patients with newly diagnosed Philadelphia chromosome-positive chronic myelogenous leukemia in chronic phase. *Clin. Cancer Res.* 9, 1972–1979.

Joshi, H., and Press, M.F. (2018). Molecular Oncology of Breast Cancer. *Breast Compr. Manag. Benign Malig. Dis.* 282-307.e5.

Kapoor, A., Goldberg, M.S., Cumberland, L.K., Ratnakumar, K., Segura, M.F., Emanuel, P.O., Menendez, S., Vardabasso, C., LeRoy, G., Vidal, C.I., et al. (2010). The histone variant macroH2A suppresses melanoma progression through regulation of CDK8. *Nature* 468, 1105–1111.

Kitamura, T., Qian, B.Z., Soong, D., Cassetta, L., Noy, R., Sugano, G., Kato, Y., Li, J., and Pollard, J.W. (2015). CCL2-induced chemokine cascade promotes breast cancer metastasis by enhancing retention of metastasis-associated macrophages. *J. Exp. Med.* 212, 1043–1059.

Knuesel, M.T., Meyer, K.D., Bernecky, C., and Taatjes, D.J. (2009). The human CDK8 subcomplex is a molecular switch that controls Mediator coactivator function. *Genes Dev.* 23, 439–451.

Koboldt, D.C., Fulton, R.S., McLellan, M.D., Schmidt, H., Kalicki-Veizer, J., McMichael, J.F., Fulton, L.L., Dooling, D.J., Ding, L., Mardis, E.R., et al. (2012). Comprehensive molecular



portraits of human breast tumours. *Nature* 490, 61–70.

Kollmann, K., Heller, G., Schneckenleithner, C., Warsch, W., Scheicher, R., Ott, R., Schäfer, M., Fajmann, S., Schleder, M., Schiefer, A.I., et al. (2013). A kinase-independent function of CDK6 links the cell cycle to tumor angiogenesis - Suppl. *Cancer Cell* 24, 167–181.

Komorowski, L., Fidy, K., Patkowska, E., and Firczuk, M. (2020). Philadelphia Chromosome-Positive Leukemia in the Lymphoid Lineage—Similarities and Differences with the Myeloid Lineage and Specific Vulnerabilities. *Int. J. Mol. Sci.* 2020, Vol. 21, Page 5776 21, 5776.

Kopan, R. (2012). Notch Signaling. *Cold Spring Harb. Perspect. Biol.* 4.

Kühn, R., Schwenk, F., Aguet, M., and Rajewsky, K. (1995). Inducible gene targeting in mice. *Science* 269, 1427–1429.

Kuwatsuka, Y., Minami, M., Minami, Y., Sugimoto, K., Hayakawa, F., Miyata, Y., Abe, A., Goff, D.J., Kiyoi, H., and Naoe, T. (2011). The mTOR inhibitor, everolimus (RAD001), overcomes resistance to imatinib in quiescent Ph-positive acute lymphoblastic leukemia cells. *Blood Cancer J.*

Lakshmikanth, T., Burke, S., Ali, T.H., Kimpfler, S., Ursini, F., Ruggeri, L., Capanni, M., Umansky, V., Paschen, A., Sucker, A., et al. (2009). NCRs and DNAM-1 mediate NK cell recognition and lysis of human and mouse melanoma cell lines in vitro and in vivo. *J. Clin. Invest.* 119, 1251–1263.

Lebert, J.M., Lester, R., Powell, E., Seal, M., and McCarthy, J. (2018). Advances in the systemic treatment of triple-negative breast cancer. *Curr. Oncol.* 25, 142–150.

Lehmann, B.D., Bauer, J.A., Chen, X., Sanders, M.E., Chakravarthy, A.B., Shyr, Y., and Pietenpol, J.A. (2011). Identification of human triple-negative breast cancer subtypes and preclinical models for selection of targeted therapies. *J. Clin. Invest.* 121, 2750–2767.

Lehmann, B.D., Jovanović, B., Chen, X., Estrada, M. V., Johnson, K.N., Shyr, Y., Moses, H.L., Sanders, M.E., and Pietenpol, J.A. (2016). Refinement of triple-negative breast cancer molecular subtypes: Implications for neoadjuvant chemotherapy selection. *PLoS One* 11, 1–22.

Leong, J.W., Schneider, S.E., Sullivan, R.P., Parikh, B.A., Anthony, B.A., Singh, A., Jewell, B.A., Schappe, T., Wagner, J.A., Link, D.C., et al. (2015). PTEN regulates natural killer cell trafficking in vivo. *Proc. Natl. Acad. Sci. U. S. A.* 112, E700–E709.

- Li, N., Fassi, A., Chick, J., Inuzuka, H., Li, X., Mansour, M.R., Wang, H., King, B., Shaik, S., Gutierrez, A., et al. (2014). Cyclin C is a haploinsufficient tumor suppressor. *Nat Cell Biol* *16*, 1080–1091.
- Li, Y., Hofmann, M., Wang, Q., Teng, L., Chlewicki, L.K., Pircher, H., and Mariuzza, R.A. (2009). Structure of Natural Killer Cell Receptor KLRG1 Bound to E-Cadherin Reveals Basis for MHC-Independent Missing Self Recognition. *Immunity* *31*, 35–46.
- Liang, J., Chen, M., Hughes, D., Chumanevich, A.A., Altilla, S., Kaza, V., Lim, C.U., Kiaris, H., Mythreye, K., Pena, M.M., et al. (2018). CDK8 selectively promotes the growth of colon cancer metastases in the liver by regulating gene expression of TIMP3 and matrix metalloproteinases. *Cancer Res.* *78*, 6594–6606.
- Lim, S., and Kaldis, P. (2013). Cdks, cyclins and CKIs: roles beyond cell cycle regulation. *Development* *140*, 3079–3093.
- Lin, H., Zhang, Y., Wang, H., Xu, D., Meng, X., Shao, Y., Lin, C., Ye, Y., Qian, H., and Wang, S. (2012). Tissue inhibitor of metalloproteinases-3 transfer suppresses malignant behaviors of colorectal cancer cells. *Cancer Gene Ther.* *19*, 845–851.
- Linderholm, B.K., Hellborg, H., Johansson, U., Elmberger, G., Skoog, L., Lehtiö, J., and Lewensohn, R. (2009). Significantly higher levels of vascular endothelial growth factor (VEGF) and shorter survival times for patients with primary operable triple-negative breast cancer. *Ann. Oncol.* *20*, 1639–1646.
- Litton, J.K., Rugo, H.S., and Ettl, J. (2018). Talazoparib in Patients with Advanced Breast Cancer and a Germline BRCA Mutation. *N Engl J Med* *379*, 753–763.
- Liu, Y., Cheng, Y., Xu, Y., Wang, Z., Du, X., Li, C., Peng, J., Gao, L., Liang, X., and Ma, C. (2017). Increased expression of programmed cell death protein 1 on NK cells inhibits NK-cell-mediated anti-tumor function and indicates poor prognosis in digestive cancers. *Oncogene* *36*, 6143–6153.
- Lopes Da Silva, J., Cristina, N., Nunes, C., Izetti, P., Gomes De Mesquita, G., and Cristina De Melo, A. (2020). Triple negative breast cancer: A thorough review of biomarkers. *Crit. Rev. Oncol. Hematol.* *145*.
- Lopez-Soto, A., Huergo-Zapico, L., Galvan, J.A., Rodrigo, L., de Herreros, A.G., Astudillo, A., and Gonzalez, S. (2013). Epithelial-Mesenchymal Transition Induces an Antitumor Immune Response Mediated by NKG2D Receptor. *J. Immunol.* *190*, 4408–4419.

- López-Soto, A., Gonzalez, S., Smyth, M.J., and Galluzzi, L. (2017). Control of Metastasis by NK Cells. *Cancer Cell* 32, 135–154.
- Lucas, M., Schachterle, W., Oberle, K., Aichele, P., and Diefenbach, A. (2007). Dendritic Cells Prime Natural Killer Cells by trans-Presenting Interleukin 15. *Immunity* 26, 503–517.
- Lund, M.J., Trivers, K.F., Porter, P.L., Coates, R.J., Leyland-Jones, B., Brawley, O.W., Flagg, E.W., O'Regan, R.M., Gabram, S.G.A., and Eley, J.W. (2009). Race and triple negative threats to breast cancer survival: A population-based study in Atlanta, GA. *Breast Cancer Res. Treat.* 113, 357–370.
- Malik, S., and Roeder, R.G. (2005). Dynamic regulation of pol II transcription by the mammalian Mediator complex. *Trends Biochem. Sci.* 30, 256–263.
- Malumbres, M. (2014). Cyclin-dependent kinases. *Genome Biol.* 15.
- Malumbres, M., and Barbacid, M. (2009). Cell cycle, CDKs and cancer: A changing paradigm. *Nat. Rev. Cancer* 9, 153–166.
- Malumbres, M., Harlow, E., Hunt, T., Hunter, T., Lahti, J.M., Manning, G., Morgan, D.O., Tsai, L.H., and Wolgemuth, D.J. (2009). Cyclin-dependent kinases: A family portrait. *Nat. Cell Biol.* 11, 1275–1276.
- Mariotti, F.R., Quatrini, L., Munari, E., Vacca, P., and Moretta, L. (2019). Innate lymphoid cells: Expression of PD-1 and other checkpoints in normal and pathological conditions. *Front. Immunol.* 10, 1–9.
- Marra, A., Viale, G., and Curigliano, G. (2019). Recent advances in triple negative breast cancer: The immunotherapy era. *BMC Med.* 17, 1–9.
- Martín-Fontecha, A., Thomsen, L.L., Brett, S., Gerard, C., Lipp, M., Lanzavecchia, A., and Sallusto, F. (2004). Induced recruitment of NK cells to lymph nodes provides IFN- $\gamma$  for TH1 priming. *Nat. Immunol.* 5, 1260–1265.
- Martin, M., Holmes, F.A., Ejlersen, B., Delaloge, S., Moy, B., Iwata, H., von Minckwitz, G., Chia, S.K.L., Mansi, J., Barrios, C.H., et al. (2017). Neratinib after trastuzumab-based adjuvant therapy in HER2-positive breast cancer (ExteNET): 5-year analysis of a randomised, double-blind, placebo-controlled, phase 3 trial. *Lancet Oncol.* 18, 1688–1700.
- Massagué, J. (2012). TGF $\beta$  signalling in context. *Nat. Rev. Mol. Cell Biol.* 13, 616–630.
- Masuda, N., Lee, S.-J., and Ohtani, S. (2017). Adjuvant Capecitabine for Breast Cancer after

Preoperative Chemotherapy. *N. Engl. J. Med.* 376, 2147–2159.

Maughan, K.L., Lutterbie, M.A., and Ham, P.S. (2010). Treatment of Breast Cancer.

McClelland, M.L., Soukup, T.M., Liu, S.D., Esensten, J.H., De Sousa E Melo, F., Yaylaoglu, M., Warming, S., Roose-Girma, M., and Firestein, R. (2015). Cdk8 deletion in the ApcMin murine tumour model represses EZH2 activity and accelerates tumourigenesis. *J. Pathol.* 237, 508–519.

McDermott, M.S.J., Chumanevich, A.A., Lim, C., Chen, M., Altilla, S., Oliver, D., Rae, J.M., Kiaris, H., Györfy, B., Roninson, I.B., et al. (2017). Inhibition of CDK8 mediator kinase suppresses estrogen dependent transcription and the growth of estrogen receptor positive breast cancer. *Oncotarget* 8, 12558–12575.

Mehner, C., Hockla, A., Miller, E., Ran, S., Radisky, D.C., and Radisky, E.S. (2014). Tumor cell-produced matrix metalloproteinase 9 (MMP-9) drives malignant progression and metastasis of basal-like triple negative breast cancer. *Oncotarget* 5, 2736–2749.

Melo, J. V. (1996). The diversity of BCR-ABL fusion proteins and their relationship to leukemia phenotype. *Blood* 88, 2375–2384.

Menzl, I., Witalisz-Siepracka, A., and Sexl, V. (2019a). CDK8-Novel Therapeutic Opportunities. *Pharmaceuticals* 12, 92.

Menzl, I., Berger-Becvar, A., Zhang, T., Grausenburger, R., Prchal-Murphy, M., Edlinger, L., Knab, V.M., Uras, I.Z., Grundschober, E., Bauer, K., et al. (2019b). A kinase-independent role for CDK8 in BCR-ABL1+ leukemia. *Nat. Commun.* 10, 4741.

Miller, K., Wang, M., Gralow, J., Dickler, M., Cobleigh, M., Perez, E.A., Shenkier, T., Cella, D., and Davidson, N.E. (2007). Paclitaxel plus Bevacizumab versus Paclitaxel Alone for Metastatic Breast Cancer. *N. Engl. J. Med.* 357, 2666–2676.

Von Minckwitz, G., Du Bois, A., Schmidt, M., Maass, N., Cufer, T., De Jongh, F.E., Maartense, E., Zielinski, C., Kaufmann, M., Bauer, W., et al. (2009). Trastuzumab beyond progression in human epidermal growth factor receptor 2-positive advanced breast cancer: A German Breast Group 26/Breast International Group 03-05 study. *J. Clin. Oncol.* 27, 1999–2006.

Von Minckwitz, G., Procter, M., and de Azambuja, E. (2018). Adjuvant Pertuzumab and Trastuzumab in Early HER2-Positive Breast Cancer. *N. Engl. J. Med.* 377, 122–131.

Mittendorf, E.A., Phillips, A. V., Meric-Bernstam, F., Qiao, N., Wu, Y., Harrington, S., Su, X.,

- Wang, Y., Gonzalez-Angulo, A.M., Akcakanat, A., et al. (2014). PD-L1 Expression in Triple Negative Breast Can. *Cancer Immunol Res* 2, 361–370.
- Moffett-King, A. (2002). Natural killer cells and pregnancy. *Nat. Rev. Immunol.* 2, 656–663.
- Mook, S., Schmidt, M.K., Rutgers, E.J., van de Velde, A.O., Visser, O., Rutgers, S.M., Armstrong, N., van't Veer, L.J., and Ravdin, P.M. (2009). Calibration and discriminatory accuracy of prognosis calculation for breast cancer with the online Adjuvant! program: a hospital-based retrospective cohort study. *Lancet Oncol.* 10, 1070–1076.
- Morigi, C. (2017). Tailored Treatments for Patients With Early Breast Cancer. *Ecancer* 11, 1–12.
- Mortier, E., Advincula, R., Kim, L., Chmura, S., Barrera, J., Reizis, B., Malynn, B.A., and Ma, A. (2009). Macrophage- and Dendritic-Cell-Derived Interleukin-15 Receptor Alpha Supports Homeostasis of Distinct CD8+ T Cell Subsets. *Immunity* 31, 811–822.
- Morvan, M.G., and Lanier, L.L. (2016). NK cells and cancer: you can teach innate cells new tricks. *Nat. Rev. Cancer* 16, 7–19.
- Mughal, T.I., Radich, J.P., Deininger, M.W., Apperley, J.F., Hughes, T.P., Harrison, C.J., Gambacorti-Passerini, C., Saglio, G., Cortes, J., and Daley, G.Q. (2016). Chronic myeloid leukemia: Reminiscences and dreams. *Haematologica* 101, 541–558.
- National Institutes of Health, N.C.I. Surveillance, Epidemiology, and End Results Program. Cancer stat facts: female breast cancer.
- Nitulescu, I.I., Meyer, S.C., Wen, Q.J., Crispino, J.D., Lemieux, M.E., Levine, R.L., Pelish, H.E., and Shair, M.D. (2017). Mediator Kinase Phosphorylation of STAT1 S727 Promotes Growth of Neoplasms With JAK-STAT Activation. *EBioMedicine* 26, 112–125.
- O'Sullivan, T., Saddawi-Konefka, R., Koebel, W.V., Arthur, C., White, J.M., Uppaluri, R., Andrews, D.M., Ngiow, S.F., Teng, M.W.L., Smyth, M.J., et al. (2012). Cancer immunoediting by the innate immune system in the absence of adaptive immunity. *J. Exp. Med.* 209, 1869–1882.
- Ohs, I., Ducimetière, L., Marinho, J., Kulig, P., Becher, B., and Tugues, S. (2017). Restoration of Natural Killer Cell Antimetastatic Activity by IL12 and Checkpoint Blockade. *Cancer Res.* 77, 7059–7071.
- Olson, C.M., Liang, Y., Leggett, A., Park, W.D., Li, L., Mills, C.E., Elsarrag, S.Z., Ficarro, S.B.,

Zhang, T., Düster, R., et al. (2019). Development of a Selective CDK7 Covalent Inhibitor Reveals Predominant Cell-Cycle Phenotype. *Cell Chem. Biol.* **26**, 792-803.e10.

Park, J.E., Kim, S.E., Keam, B., Park, H.R., Kim, S., Kim, M., Kim, T.M., Doh, J., Kim, D.W., and Heo, D.S. (2020). Anti-tumor effects of NK cells and anti-PD-L1 antibody with antibody-dependent cellular cytotoxicity in PD-L1-positive cancer cell lines. *J. Immunother. Cancer* **8**, 1–11.

Pasero, C., Gravis, G., Guerin, M., Granjeaud, S., Thomassin-Piana, J., Rocchi, P., Paciencia-Gros, M., Poizat, F., Bentobji, M., Azario-Cheillan, F., et al. (2016). Inherent and Tumor-Driven Immune Tolerance in the Prostate Microenvironment Impairs Natural Killer Cell Antitumor Activity. *Cancer Res.* **76**, 2153–2165.

Peinado, H., Zhang, H., Matei, I.R., Costa-Silva, B., Hoshino, A., Rodrigues, G., Psaila, B., Kaplan, R.N., Bromberg, J.F., Kang, Y., et al. (2017). Pre-metastatic niches: organ-specific homes for metastases. *Nat. Rev. Cancer* **17**, 302–317.

Pelish, H.E., Liau, B.B., Nitulescu, I.I., Tangpeerachaikul, A., Poss, Z.C., Da Silva, D.H., Caruso, B.T., Arefolov, A., Fadeyi, O., Christie, A.L., et al. (2015). Mediator kinase inhibition further activates super-enhancer-associated genes in AML. *Nature* **526**, 273–276.

Perou, C.M., Sùrlie, T., Eisen, M.B., Rijn, M. Van De, Jeffrey, S.S., Rees, C.A., Pollack, J.R., Ross, D.T., Johnsen, H., Akslen, L.A., et al. (2000). Molecular portraits of human breast tumours. *Nature* **533**, 747–752.

Piccart-Gebhart, M.J., Procter, M., Sci, M., Leyland-Jones, B., Goldhirsch, A., Untch, M., Smith, I., Gianni, L., Baselga, J., Bell, R., et al. (2005). Trastuzumab after Adjuvant Chemotherapy in HER2-Positive Breast Cancer. *N Engl J Med* **353**, 1659–1672.

Porter, D.C., Farmaki, E., Altília, S., Schools, G.P., West, D.K., Chen, M., Chang, B.-D., Puzyrev, A.T., Lim, C., Rokow-Kittell, R., et al. (2012). Cyclin-dependent kinase 8 mediates chemotherapy-induced tumor-promoting paracrine activities. *Proc. Natl. Acad. Sci.* **109**, 13799–13804.

Poss, Z.C., Ebmeier, C.C., Odell, A.T., Tangpeerachaikul, A., Lee, T., Pelish, H.E., Shair, M.D., Dowell, R.D., Old, W.M., and Taatjes, D.J. (2016). Identification of Mediator Kinase Substrates in Human Cells using Cortistatin A and Quantitative Phosphoproteomics. *Cell Rep.* **15**, 436–450.

Prat, A., Carey, L.A., Adamo, B., Vidal, M., Tabernero, J., Cortés, J., Parker, J.S., Perou, C.M.,

- and Baselga, J. (2014). Molecular features and survival outcomes of the intrinsic subtypes within HER2-positive breast cancer. *J. Natl. Cancer Inst.* *106*, 1–8.
- Putz, E.M., Gotthardt, D., Hoermann, G., Csiszar, A., Wirth, S., Berger, A., Straka, E., Rigler, D., Wallner, B., Jamieson, A., et al. (2013). CDK8-mediated STAT1-S727 phosphorylation restrains NK cell cytotoxicity and tumor surveillance. *Cell Rep.* *4*, 437–444.
- Putz, E.M., Gotthardt, D., and Sexl, V. (2014). STAT1-S727 - the license to kill. *Oncoimmunology* *3*, e955441.
- Putz, E.M., Guillerey, C., Kos, K., Stannard, K., Miles, K., Delconte, R.B., Takeda, K., Nicholson, S.E., Huntington, N.D., and Smyth, M.J. (2017). Targeting cytokine signaling checkpoint CIS activates NK cells to protect from tumor initiation and metastasis. *Oncoimmunology* *6*.
- Qian, B.Z., Li, J., Zhang, H., Kitamura, T., Zhang, J., Campion, L.R., Kaiser, E.A., Snyder, L.A., and Pollard, J.W. (2011). CCL2 recruits inflammatory monocytes to facilitate breast-tumour metastasis. *Nature* *475*, 222–225.
- Quatrini, L., Mariotti, F.R., Munari, E., Tumino, N., Vacca, P., and Moretta, L. (2020). The immune checkpoint PD-1 in natural killer cells: Expression, function and targeting in tumour immunotherapy. *Cancers (Basel)*. *12*, 1–21.
- Raulet, D.H., and Guerra, N. (2009). Oncogenic stress sensed by the immune system: Role of natural killer cell receptors. *Nat. Rev. Immunol.* *9*, 568–580.
- Reckel, S., Hamelin, R., Georgeon, S., Armand, F., Jolliet, Q., Chiappe, D., Moniatte, M., and Hantschel, O. (2017). Differential signaling networks of Bcr-Abl p210 and p190 kinases in leukemia cells defined by functional proteomics. *Leukemia* *31*, 1502–1512.
- Remsing Rix, L.L., Rix, U., Colinge, J., Hantschel, O., Bennett, K.L., Stranzl, T., Müller, A., Baumgartner, C., Valent, P., Augustin, M., et al. (2009). Global target profile of the kinase inhibitor bosutinib in primary chronic myeloid leukemia cells. *Leukemia* *23*, 477–485.
- Robert, N.J., Diéras, V., Glaspy, J., Brufsky, A.M., Bondarenko, I., Lipatov, O.N., Perez, E.A., Yardley, D.A., Chan, S.Y.T., Zhou, X., et al. (2011). RIBBON-1: Randomized, double-blind, placebo-controlled, phase III trial of chemotherapy with or without bevacizumab for first-line treatment of human epidermal growth factor receptor 2-negative, locally recurrent or metastatic breast cancer. *J. Clin. Oncol.* *29*, 1252–1260.
- Robson, M., Im, S.A., and Senkus, E. (2017). Olaparib for Metastatic Breast Cancer in Patients



with a Germline BRCA Mutation. *N Engl J Med* 377, 523–533.

Romond, E.H., Perez, E.A., Bryant, J., Suman, V.J., and Geyer, C.E. (2005). Trastuzumab plus Adjuvant Chemotherapy for Operable HER2-Positive Breast Cancer From the National Surgical Adjuvant Breast and Bowel Project, Pittsburgh. *N Engl J Med* 16, 1673–1684.

Roninson, I.B., Győrffy, B., Mack, Z.T., Shtil, A.A., Shtutman, M.S., Chen, M., and Broude, E. V. (2019). Identifying Cancers Impacted by CDK8/19. *Cells* 8, 821.

Rowley, J.D. (1973). A New Consistent Chromosomal Abnormality in Chronic Myelogenous Leukaemia identified by Quinacrine Fluorescence and Giemsa Staining. *Nature* 243, 290–293.

Rzymiski, T., Mikula, M., Wiklik, K., and Brzózka, K. (2015). CDK8 kinase—An emerging target in targeted cancer therapy. *Biochim. Biophys. Acta - Proteins Proteomics* 1854, 1617–1629.

Rzymiski, T., Mikula, M., Żyłkiewicz, E., Dreas, A., Wiklik, K., Gołas, A., Wójcik, K., Masiejczyk, M., Wróbel, A., Dolata, I., et al. (2017). SEL120-34A is a novel CDK8 inhibitor active in AML cells with high levels of serine phosphorylation of STAT1 and STAT5 transactivation domains. *Oncotarget* 8, 33779–33795.

Salih, J., Hilpert, J., Placke, T., Grünebach, F., Steinle, A., Salih, H.R., and Krusch, M. (2010). The BCR/ABL-inhibitors Imatinib, Nilotinib and Dasatinib differentially affect NK cell reactivity. *Int. J. Cancer* 127, 2119–2128.

Salvaris, R., and Fedele, P.L. (2021). Targeted therapy in acute lymphoblastic leukaemia. *J. Pers. Med.* 11.

Sathe, P., Delconte, R.B., Souza-Fonseca-Guimaraes, F., Seillet, C., Chopin, M., Vandenberg, C.J., Rankin, L.C., Mielke, L.A., Vikstrom, I., Kolesnik, T.B., et al. (2014). Innate immunodeficiency following genetic ablation of Mcl1 in natural killer cells. *Nat. Commun.* 5.

Sattler, M., and Griffin, J.D. (2003). Molecular mechanisms of transformation by the BCR-ABL oncogene. *Semin. Hematol.*

Sawyers, C.L. (1999). Chronic myeloid leukemia. *N Engl J Med.*

Schalper, K.A., Velcheti, V., Carvajal, D., Wimberly, H., Brown, J., Puzstai, L., and Rimm, D.L. (2014). In Situ Tumor PD-L1 mRNA Expression Is Associated with Increased TILs and Better Outcome in Breast Carcinomas. *Clin. Cancer Res.* 20, 2773–2782.

Schmid, P., Adams, S., and Rugo, H.S. (2018). Atezolizumab and Nab-Paclitaxel in Advanced Triple-Negative Breast Cancer. *N Engl J Med* 379, 2108–2121.

- Schmidt, M., Böhm, D., Von Törne, C., Steiner, E., Puhl, A., Pilch, H., Lehr, H.-A., Hengstler, J.G., Kölbl, H., and Gehrmann, M. (2008). The Humoral Immune System Has a Key Prognostic Impact in Node-Negative Breast Cancer. *Cancer Res.* *68*, 5405–5413.
- Schreiber, R.D., Old, L.J., and Smyth, M.J. (2011). Cancer immunoediting: Integrating immunity's roles in cancer suppression and promotion. *Science (80-. )*. *331*, 1565–1570.
- Senovilla, L., Vacchelli, E., Galon, J., Adjemian, S., Eggermont, A., Fridman, W.H., Sautès-Fridman, C., Ma, Y., Tartour, E., Zitvogel, L., et al. (2012). Trial watch: Prognostic and predictive value of the immune infiltrate in cancer. *Oncoimmunology* *1*, 1323–1343.
- Seo, J.-O., Han, S.I., and Lim, S.-C. (2010). Role of CDK8 and  $\beta$ -catenin in colorectal adenocarcinoma. *Oncol. Rep.* *24*, 285–291.
- Serrao, A., Jenkins, L.M., Chumanevich, A.A., Horst, B., Liang, J., Gatza, M.L., Lee, N.Y., Roninson, I.B., Broude, E. V., and Myhre, K. (2018). Mediator kinase CDK8/CDK19 drives YAP1-dependent BMP4-induced EMT in cancer. *Oncogene* *37*, 4792–4808.
- Shah, N.P., Tran, C., Lee, F.Y., Chen, P., Norris, D., and Sawyers, C.L. (2004). Overriding imatinib resistance with a novel ABL kinase inhibitor. *Science (80-. )*. *305*, 399–401.
- Shankaran, V., Ikeda, H., Bruce, A.T., White, J.M., Swanson, P.E., Old, L.J., and Schreiber, R.D. (2001). IFN $\gamma$  and lymphocytes prevent primary tumour development and shape tumour immunogenicity. *Nature* *410*, 1107–1111.
- Sharma, P., Klemp, J.R., Bruce, •, Kimler, F., Mahnken, J.D., Geier, L.J., Qamar, •, Khan, J., Manana, •, Carol, E. •, et al. (2014). Germline BRCA mutation evaluation in a prospective triple-negative breast cancer registry: implications for hereditary breast and/or ovarian cancer syndrome testing. *Breast Cancer Res. Treat.* *145*, 707–714.
- Slamon, D., Eiermann, W., Robert, N., Pienkowski, T., Martin, M., Press, M., Mackey, J., Glaspy, J., Chan, A., Pawlicki, M., et al. (2011). Adjuvant Trastuzumab in HER2-Positive Breast Cancer. *N Engl J Med* *14*, 1273–1283.
- Slamon, D.J., Clark, G.M., Wong, S.G., Levin, W.J., Ullrich, A., and McGuire, W.L. (1987). Human breast cancer: Correlation of relapse and survival with amplification of the HER-2/neu oncogene. *Science (80-. )*. *235*, 182–191.
- Smyth, M.J., Hayakawa, Y., Takeda, K., and Yagita, H. (2002). New Aspects of Natural-Killer-Cell Surveillance and Therapy of Cancer. *Nat. Rev. Cancer* *2*, 850–861.

- Soverini, S., Martinelli, G., Lacobucci, I., and Baccarani, M. (2008). Imatinib mesylate for the treatment of chronic myeloid leukemia. *Expert Rev. Anticancer Ther.* *8*, 853–864.
- Soverini, S., Mancini, M., Bavaro, L., Cavo, M., and Martinelli, G. (2018). Chronic myeloid leukemia: The paradigm of targeting oncogenic tyrosine kinase signaling and counteracting resistance for successful cancer therapy. *Mol. Cancer* *17*, 1–15.
- Staab, J., Herrmann-Lingen, C., and Meyer, T. (2013). CDK8 as the STAT1 serine 727 kinase? *Jak-Stat* *2*, e24275.
- Stanietsky, N., Simic, H., Arapovic, J., Toporik, A., Levy, O., Novik, A., Levine, Z., Beiman, M., Dassa, L., Achdout, H., et al. (2009). The interaction of TIGIT with PVR and PVRL2 inhibits human NK cell cytotoxicity. *Proc. Natl. Acad. Sci. U. S. A.* *106*, 17858–17863.
- Steinparzer, I., Sedlyarov, V., Rubin, J.D., Eislmayr, K., Galbraith, M.D., Levandowski, C.B., Vcelkova, T., Sneezum, L., Wascher, F., Amman, F., et al. (2019). Transcriptional Responses to IFN- $\gamma$  Require Mediator Kinase-Dependent Pause Release and Mechanistically Distinct CDK8 and CDK19 Functions. *Mol. Cell* *76*, 1–15.
- Street, S.E.A., Hayakawa, Y., Zhan, Y., Lew, A.M., MacGregor, D., Jamieson, A.M., Diefenbach, A., Yagita, H., Godfrey, D.I., and Smyth, M.J. (2004). Innate immune surveillance of spontaneous B cell lymphomas by natural killer cells and gammadelta T cells. *J. Exp. Med.* *199*, 879–884.
- Swann, J.B., and Smyth, M.J. (2007). Immune surveillance of tumors. *J. Clin. Invest.* *117*, 1137–1146.
- Tallerico, R., Todaro, M., Di Franco, S., Maccalli, C., Garofalo, C., Sottile, R., Palmieri, C., Tirinato, L., Pangigadde, P.N., La Rocca, R., et al. (2013). Human NK cells selective targeting of colon cancer-initiating cells: a role for natural cytotoxicity receptors and MHC class I molecules. *J. Immunol.* *190*, 2381–2390.
- Tan, P.H., Ellis, I., Allison, K., Brogi, E., Fox, S.B., Lakhani, S., Lazar, A.J., Morris, E.A., Sahin, A., Salgado, R., et al. (2020). The 2019 World Health Organization classification of tumours of the breast. *Histopathology* *77*, 181–185.
- Tassan, J.P., Jaquenoud, M., Léopold, P., Schultz, S.J., and Nigg, E.A. (1995). Identification of human cyclin-dependent kinase 8, a putative protein kinase partner for cyclin C. *Proc. Natl. Acad. Sci. U. S. A.* *92*, 8871–8875.
- Telli, M.L., Timms, K.M., Reid, J., Hennessy, B., Mills, G.B., Jensen, K.C., Szallasi, Z., Barry,

- W.T., Winer, E.P., Tung, N.M., et al. (2016). Homologous Recombination Deficiency (HRD) Score Predicts Response to Platinum-Containing Neoadjuvant Chemotherapy in Patients with Triple-Negative Breast Cancer. *Clin. Cancer Res.* 22, 3764–3773.
- Terwilliger, T., and Abdul-Hay, M. (2017). Acute lymphoblastic leukemia: a comprehensive review and 2017 update. *Blood Cancer J.* 7, e577.
- Tsai, K.L., Sato, S., Tomomori-Sato, C., Conaway, R.C., Conaway, J.W., and Asturias, F.J. (2013). A conserved Mediator-CDK8 kinase module association regulates Mediator-RNA polymerase II interaction. *Nat. Struct. Mol. Biol.* 20, 611–619.
- Tsang, J.Y.S., and Tse, G.M. (2020). Molecular Classification of Breast Cancer. *Adv. Anat. Pathol.* 27, 27–35.
- Underhill, C., Toulmonde, M., and Bonnefoi, H. (2011). A review of PARP inhibitors: From bench to bedside. *Ann. Oncol.* 22, 268–279.
- Veronesi, U., Boyle, P., Goldhirsch, A., Orecchia, R., and Viale, G. (2005). Breast cancer. *Lancet* 365, 1727–1741.
- Vesely, M.D., and Schreiber, R.D. (2013). Cancer immunoediting: Antigen, mechanisms, and implications to cancer immunotherapy. *Ann. N. Y. Acad. Sci.* 1284, 1–5.
- Vesely, M.D., Kershaw, M.H., Schreiber, R.D., and Smyth, M.J. (2011). Natural innate and adaptive immunity to cancer. *Annu. Rev. Immunol.* 29, 235–271.
- Viale, G., Regan, M.M., and Mastropasqua, M.G. (2008). Predictive Value of Tumor Ki-67 Expression in Two Randomized Trials of Adjuvant Chemoendocrine Therapy for Node-Negative Breast Cancer. *J Natl Cancer Inst* 100, 207–212.
- Vivier, E., Nunès, J.A., and Vély, F. (2004). Natural killer cell signaling pathways. *Science (80- )*. 306, 1517–1519.
- Vivier, E., Raulet, D.H., Moretta, A., Caligiuri, M.A., Zitvogel, L., Lanier, L.L., Yokoyama, W.M., and Ugolini, S. (2011). Innate or Adaptive Immunity? The Example of Natural Killer Cells. *Science (80- )*. 331, 44–49.
- Waks, A.G., and Winer, E.P. (2019). Breast Cancer Treatment: A Review. *JAMA - J. Am. Med. Assoc.* 321, 288–300.
- Walzer, T., Dalod, M., Robbins, S.H., Zitvogel, L., and Vivier, E. (2005). Natural-killer cells and dendritic cells: “L’union fait la force.” *Blood* 106, 2252–2258.

- Wang, S., and Fischer, P.M. (2008). Cyclin-dependent kinase 9: a key transcriptional regulator and potential drug target in oncology, virology and cardiology. *Trends Pharmacol. Sci.* **29**, 302–313.
- Wang, Y., and Zhou, B.P. (2014). Epithelial-mesenchymal Transition-A Hallmark of Breast Cancer Metastasis. *Cancer Hallm* **1**, 38–49.
- Wei, R., Kong, L., Xiao, Y., Yuan, H., Song, Y., Wang, J., Yu, H., Mao, S., and Xu, W. (2018). CDK8 regulates the angiogenesis of pancreatic cancer cells in part via the CDK8- $\beta$ -catenin-KLF2 signal axis. *Exp. Cell Res.* **369**, 304–315.
- Weisberg, E., Manley, P., Mestan, J., Cowan-Jacob, S., Ray, A., and Griffin, J.D. (2006). AMN107 (nilotinib): A novel and selective inhibitor of BCR-ABL. *Br. J. Cancer* **94**, 1765–1769.
- Weiss, A., Chavez-MacGregor, M., Lichtensztajn, D.Y., Yi, M., Tadros, A., Hortobagyi, G.N., Giordano, S.H., Hunt, K.K., and Mittendorf, E.A. (2018). Validation study of the American joint committee on cancer eighth edition prognostic stage compared with the anatomic stage in breast cancer. *JAMA Oncol.* **4**, 203–209.
- Westerling, T., Kuuluvainen, E., and Mäkelä, T.P. (2007). Cdk8 Is Essential for Preimplantation Mouse Development. *Mol. Cell. Biol.* **27**, 6177–6182.
- Whittaker, S.R., Mallinger, A., Workman, P., and Clarke, P.A. (2017). Inhibitors of cyclin-dependent kinases as cancer therapeutics. *Pharmacol. Ther.* **173**, 83–105.
- Winter, S.S., Greene, J.M., McConnell, T.S., and Willman, C.L. (1999). Pre-B acute lymphoblastic leukemia with b3a2 (p210) and e1a2 (p190) BCR-ABL fusion transcripts relapsing as chronic myelogenous leukemia with a less differentiated b3a2 (p210) clone. *Leukemia* **13**, 2007–2011.
- Witalisz-Siepracka, A., Gotthardt, D., Prchal-Murphy, M., Didara, Z., Menzl, I., Prinz, D., Edlinger, L., Putz, E.M., and Sexl, V. (2018). NK Cell-Specific CDK8 Deletion Enhances Antitumor Responses. *Cancer Immunol. Res.* **6**, 458–466.
- Wu, D., Zhang, Z., Chen, X., Yan, Y., and Liu, X. (2021). Angel or Devil ? - CDK8 as the new drug target. *Eur. J. Med. Chem.* **213**, 113043.
- Wylie, A.A., Schoepfer, J., Jahnke, W., Cowan-Jacob, S.W., Loo, A., Furet, P., Marzinzik, A.L., Pelle, X., Donovan, J., Zhu, W., et al. (2017). The allosteric inhibitor ABL001 enables dual targeting of BCR-ABL1. *Nature* **543**, 733–737.

- Xu, D., Li, C.F., Zhang, X., Gong, Z., Chan, C.H., Lee, S.W., Jin, G., Rezaeian, A.H., Han, F., Wang, J., et al. (2015a). Skp2-MacroH2A1-CDK8 axis orchestrates G2/M transition and tumorigenesis. *Nat. Commun.* 6.
- Xu, W., Wang, Z., Zhang, W., Qian, K., Li, H., Kong, D., Li, Y., and Tang, Y. (2015b). Mutated K-ras activates CDK8 to stimulate the epithelial-to-mesenchymal transition in pancreatic cancer in part via the Wnt/??-catenin signaling pathway. *Cancer Lett.* 356, 613–627.
- Yemelyanova, A., Vang, R., Kshirsagar, M., Lu, D., Marks, M.A., Shih, I.M., and Kurman, R.J. (2011). Immunohistochemical staining patterns of p53 can serve as a surrogate marker for TP53 mutations in ovarian carcinoma: an immunohistochemical and nucleotide sequencing analysis. *Mod. Pathol.* 24, 1248–1253.
- Yoshimoto, T., Mizoguchi, I., Katagiri, S., Tauchi, T., Furusawa, J., Chiba, Y., Mizuguchi, J., Ohyashiki, J., and Ohyashiki, K. (2014). Immunosurveillance markers may predict patients who can discontinue imatinib therapy without relapse. *Oncoimmunology*.
- Zhou, T., Commodore, L., Huang, W.S., Wang, Y., Thomas, M., Keats, J., Xu, Q., Rivera, V.M., Shakespeare, W.C., Clackson, T., et al. (2011). Structural Mechanism of the Pan-BCR-ABL Inhibitor Ponatinib (AP24534): Lessons for Overcoming Kinase Inhibitor Resistance. *Chem. Biol. Drug Des.* 77, 1–11.
- Zhu, Y., Paniccia, A., Schulick, A.C., Chen, W., Koenig, M.R., Byers, J.T., Yao, S., Bevers, S., and Edil, B.H. (2016). Identification of CD112R as a novel checkpoint for human T cells. *J. Exp. Med.* 213, 167–176.
- Zitvogel, L., Tesniere, A., and Kroemer, G. (2006). Cancer despite immunosurveillance: Immunoselection and immunosubversion. *Nat. Rev. Immunol.* 6, 715–727.